The role of the sea breeze and synoptic conditions in severe storm formation in Brisbane

by

Joss Kirk

Submitted in partial fulfilment of the requirements for the degree of
Bachelor of Science with Honours
in the Fenner School of Environment and Society,
Australian National University
October 2016

Candidate's Declaration

This thesis contains no material which has been accepted for the award of any other degree or diploma in any university. To the best of the author’s knowledge, it contains no material previously published or written by another person, except where due reference is made in the text.

Joss Kirk Date:

Acknowledgements

I would like to thank my primary supervisor Professor Janette Lindesay for her guidance and feedback throughout the research process, as well as my secondary supervisor Dr Nicholas Engerer for his assistance with technical questions and the editing process. I would also like to acknowledge Joshua Soderholm from the University of Queensland for his extensive assistance in planning my analysis, providing data and answering a multitude of technical questions. Thanks also must go to my fellow honours students, family and friends for their support. Finally, I would like to express my gratitude to the Australian Research Council Centre of Excellence for Climate System Science for providing mentoring opportunities and financial assistance throughout the year.

ARC CENTRE OF EXCELLENCE FOR CLIMATE SYSTEM SCIENCE

Abstract

This thesis assesses the role of the sea breeze and synoptic meteorological conditions in severe storm formation in Brisbane, southeast Queensland. Previous studies suggest that a causal link exists between severe storm initiation and the sea breeze in many regions, including a possible link in southeast Queensland. Numerous thunderstorm climatologies exist that describe Brisbane as a thunderstorm hotspot. The vast majority of these, however, focus on event-based sampling, radar data, reanalysis data or remotely-sensed data. Therefore, a significant knowledge gap exists in radiosonde-based thunderstorm climatologies for Brisbane. This analysis addresses this gap by considering three key radiosonde indicators of atmospheric stability (convective available potential energy, convective inhibition and effective storm relative helicity) for the 16 year period 2000-2015 and comparing these indicators between sea breeze days, non-sea breeze days and non-storm days.

The analysis determined that an existing algorithm derived by Soderholm *et al*. (2015) for identifying the sea breeze in near-coastal inland areas of southeast Queensland was inapplicable to a locality within the ocean-modified coastal environment. Instead, this thesis presents a new algorithm that identifies days in which onshore flow increased whilst also remaining within a particular directional range. This approach has greater applicability to the ocean-modified coastal environment, successfully identifying 60% of a list of manually verified sea breeze days and only 20% of a list of manually verified non-sea breeze days over the 15-year period considered. Analysis of a list of severe storm events from the volumetric radar dataset derived from the dataset of Soderholm *et al*. (2015) shows that 54% of the severe storm events in this period coincided with either a sea breeze day or a day that exhibited increasing onshore flow. The relationship between storm severity and the rate of increase in onshore flow is not proportional. In general, the sea breeze lowered the threshold value of convective available potential energy required for severe storm initiation and allowed higher convective inhibition values to be overcome. No clear relationship between effective storm relative helicity and the sea breeze is evident.

The synoptic-scale circulation conditions over Brisbane for all the storm days over the 16-year period are also analysed. Wind shear, vector wind and geopotential height at various pressure levels are considered, along with surface pressure. This analysis demonstrates that the "conducive storm conditions" reflected in these variables are indeed associated with severe storm formation but are not strictly necessary for all severe storm days, as they are not identified for all storm days. Therefore, instead of creating an idealised set of conditions that describe a severe storm day, these "conducive storm conditions" are ranked according to their relative usefulness in predicting severe storm formation.

Table of Contents

Candidate's Declaration **2**

Acknowledgements **3**

Abstract **4**

Table of Contents **5**

List of Tables **9**

List of Figures **10**

Glossary, Terms and Abbreviations **12**

Chapter 1: Introduction **15**

1.1 The impact of severe weather 15

1.2 The climate of Brisbane 16

1.3 Research motivations 21

1.4 Research question and hypothesis 24

1.5 Thesis overview 24

Chapter 2: Literature Review **26**

2.1 Key drivers of rainfall variability and thunderstorms in Queensland 26

2.1.1 A trend towards more extreme rain events 27

2.2 The sea breeze and other localised forcings on thunderstorm initiation and severe weather 27

2.2.1 Topography and urban heat islands 28

2.2.2 The sea breeze 29

2.3 The effect of the sea breeze on wind direction in Brisbane 33

2.4 Selecting a climatological method 38

2.4.1 Event-based sampling 38

2.4.2 Radiosonde soundings 39

2.4.3 Reanalysis datasets 39

2.4.4 Remote sensing 40

2.4.5 Radar 40

Chapter 3: Methodology **43**

3.1 Detecting past occurrences of the sea breeze 43

3.1.1 Limitations of existing detection method 44

3.1.2 Adaptation of existing algorithm 45

3.1.3 A new algorithm 47

3.2 Detecting past occurrences of severe weather and correlating these to the sea breeze 47

3.3 Comparing indicators of atmospheric stability between sea breeze storm days, non-sea breeze storm days and non-storm days 49

3.4 Assessing the relative importance of various synoptic patterns 49

Chapter 4: Sea breeze analysis **51**

4.1 Initial results – complications in applying the algorithm of Soderholm et al. (2015) 51

4.2 Identifying sea breeze days through strengthening onshore wind 53

4.3 Comparing sea breeze events with storm events 56

Chapter 5: Vertical profile of the atmosphere and synoptic conditions analysis **60**

5.1 January 66

5.2 February 70

5.3 October 72

5.4 November 74

5.5 December 77

Chapter 6: Discussion and Conclusions **81**

6.1 Sea breeze analysis 81

6.1.1 Inapplicability of the algorithm of Soderholm et al. (2015) to the ocean-modified coastal environment 81

6.1.2 Applicability of detecting the sea breeze through increasing onshore flow 81

6.2 Storm analysis 82

6.2.1 Comparing the occurrence of onshore flow events to severe storm events 82

6.2.2 Key indicators of atmospheric stability 82

6.2.3 Regional synoptic conditions analysis 83

6.3 Synthesis: project outcomes, limitations and recommendations 85

6.3.1 Outcomes 85

6.3.2 Limitations 85

6.3.3 Recommendations for future analysis 86

6.4 Implications 87

References **88**

Appendix 1: January 99
Sea breeze storms 99
Non-sea breeze storms 99
Non-storm days 100
31/1/2015 101
6/1/2006 104
25/1/2004 104
24/1/2004 109
18/1/2011 113
3/1/2011 113
6/1/2008 117
Appendix 2: February 122
Sea breeze storms 122
Non-sea breeze storms 122
Non-storm days 122
19/2/2003 123
21/2/2011 124
Appendix 3: October 129
Sea breeze storms 129
Non-sea breeze storms 129
Non-storm days 130
27/10/2014 131
15/10/2011 131
19/10/2004 135
26/10/2003 138
Appendix 4: November 143
Sea breeze storms 143
Non-sea breeze storms 144
Non-storm days 144
27/11/2014 145
18/11/2012 145
15/11/2006 149
29/11/2005 152
24/11/2013 155
17/11/2012 160
29/11/2009 161
17/11/2009 166
9/11/2004 166

Appendix 5: December 172

Sea breeze storms 172

Non-sea breeze storms 172

Non-storm days 173

9/12/2004 174

29/12/2013 174

16/12/2010 178

22/12/2009 181

13/12/2004 184

Appendix 6: Scripts used to perform the analysis 189

6.5 Scripts created by the author 189

6.5.1 For implementing the algorithm of Soderholm et al. (2015) 189

6.6 For implementing the increasing onshore flow algorithm 193

6.6.1 Gradient script 193

6.7 Scripts created by Halbert (2015) and modified by the author 194

6.7.1 Calculating indices of atmospheric stability (and writing to csv) 194

6.7.2 Producing skew-t plots 199

List of Tables

Table 1: A summary of Statistics for Brisbane Airport weather station (values averaged from 1950 to 2000) (Bureau of Meteorology, 2016). 20
Table 2: A list of known storm days for eastern Brisbane in the period 2000-2015. 54% of the events occurred on days in which a sea breeze or increasing onshore flow occurred. ‘Number of storm cell instances’ describes the number of 10 minute instances of a storm cell remaining within the lat-lon box described in the methodology. 58
Table 3 : (continued next page) – Description of synoptic conditions, geopotential height and vector wind conditions for storm events in January. 68
Table 4: Description of synoptic conditions, geopotential height and vector wind conditions for storm events in February. 71
Table 5: Description of synoptic conditions, geopotential height and vector wind conditions for storm events in October. 73
Table 6: (continued next page) - Description of synoptic conditions, geopotential height and vector wind conditions for storm events in November. 75
Table 7: (continued next page) - Description of synoptic conditions, geopotential height and vector wind conditions for storm events in December. 78
Table 8: Atmospheric conditions for severe storms on sea breeze days for January 99
Table 9: Atmospheric conditions for severe storms on non-sea breeze days for January 99
Table 10: Atmospheric conditions for non-storm days for January 100
Table 11: Atmospheric conditions for severe storms on sea breeze days for February 122
Table 12: Atmospheric conditions for severe storms on non-sea breeze days for February 122
Table 13: Atmospheric conditions for non-storm days for February 122
Table 14: Atmospheric conditions for severe storms on sea breeze days for October 129
Table 15: Atmospheric conditions for severe storms on non-sea breeze days for October 129
Table 16: Atmospheric conditions for non-storm days for October 130
Table 17: Atmospheric conditions for severe storms on sea breeze days for November 143
Table 18: Atmospheric conditions for severe storms on non-sea breeze days for November 144
Table 19: Atmospheric conditions for non-storm days for November 144
Table 20: Atmospheric conditions for severe storms on non-sea breeze days for December 172
Table 21: Atmospheric conditions for severe storms on sea breeze days for December 172
Table 22: Atmospheric conditions for non-storm days for December 173

List of Figures

Figure 1 : The Pinkenba region of Brisbane (which contains both Brisbane Airport and Port of Brisbane) can be used as an example of the drastic effect of rising sea levels on the Brisbane region in general. The maps are based on a simple 'bucket fill' approach, present the water level at predicted astronomical high tide and do not account for sea walls, storm surges, erosion or other local factors. Three scenarios are modelled: a low scenario of 50cm sea level rise by 2100 (a), a medium scenario of 80cm by 2100 (b) and a high scenario of 110cm (c). The figures are mainly distinguished by their shallow inundation levels (shown in darker blue) (OzCoasts, 2016). 17
Figure 2 : Koppen climate classification map. Brisbane is in the Cfa grouping (dark green on the east coast of Australia). Analogous climates occur in eastern Asia, the northern Mediterranean, the Pampas region of South America and the southeast United States (Kottek et al., 2006) 18
Figure 3: – Brisbane Aero (Station 040842) is located in eastern Brisbane, which is itself located in Southeast Queensland (Bureau of Meteorology, 2016). 19
Figure 4: Supercell storm in Brisbane on November 27 2014 (Jimenez, 2014). 21
Figure 5: Brisbane Airport represents a unique environmental setting amongst Australia's airports. Its close proximity to the coast and its low altitude make it susceptible to flooding events (Passmore, 2013). 22
Figure 6: The standard sea breeze conceptual model is as shown above. Moist marine air flows inland and interacts with warmer inland air. The actual behaviour of the sea breeze at different localities is significantly more complex than this standard model (The University Corporation for Atmospheric Research, 2016). 31
Figure 7: Schematic of sea breeze propagation across a weather station transect. These stations include Gatton (G), Amberley (AB) and Archerfield (AF). Most common arrival times (UTC) at each station are shown in black numbers. Topography elevation is shown in 100 m intervals above mean sea level. The towns of Boonah (B) and Esk (E) are also marked. Arrows indicate onshore flow of sea breeze at the surface (Soderholm et al., 2016). 33
Figure 8 : Figure 8a shows the annual wind direction before the onset of the sea breeze in the morning. It can be seen that the wind direction is fairly scattered, with a large portion being southwesterly. In Figure 8b the afternoon wind directions are represented, showing the period during which the sea breeze is having a significant impact. The largest portion of winds during this time are easterly or northeasterly. The effect of the sea breeze is more marked during summer, given that the differential heating between the land and ocean is more pronounced. This can be seen in Figure 8c and 8d. Figure 8c shows 1500m during winter, and the northeasterly wind direction characteristic of the Brisbane sea breeze is conspicuously absent. In Figure 8d, however, showing 1500 during summer, the effect of the sea breeze is very pronounced (Bureau of Meteorology, 2016). 37
Figure 9: Annual cumulative MESH swaths (sum of all MESH values averaged by the number of years in the climatology) for 21 mm threshold for (9a) all days. (9b) Sea breeze days (9c) Non-sea breeze days. Towns marked include Brisbane (BNE), Archerfield (AF), Boonah (BNH) and Esk (ESK). Marburg radar location marked with black diamond and range rings shown at 16 km, 40 km and 80 km. MESH values are discussed in detail in the Methodology. MESH can be treated as a proxy for severe storm occurrence, so the higher values in 9b compared to 9a suggest a significant relationship between the sea breeze and severe storms for much of southeast Queensland (Soderholm et al., 2015). 41
Figure 10: Flow diagram showing filters applied to identify sea breeze (SB) days based on a single surface weather station dataset at Archerfield by Soderholm et al. (2015). This approach was formulated by Azorin-Molina et al. (2011). 46
Figure 11: The region considered for storm identification is shown. The region comprises a 40km by 30km grid with a total area of 1 188 km^2. The region was selected so as to include Brisbane Airport but to exclude as much of Moreton Bay as possible, given that storms weaken significantly over water. The region is contained within the latitudes -27.362114° and -27.634977° and between the longitudes 153.202320° and 152.806812° (Google Maps, 2016). .48
Figure 12: Three randomly selected manually verified sea breeze days are shown above. Each of the three days exhibits an increase in wind speed from 0900 to 1500. 53
Figure 13: Number of days of increasing onshore flow per year. 55
Figure 14: Number of days of increasing flow per month from Jan 2001 to Dec 2015. 55
Figure 15: A comparison of MESH values with the rate of increasing onshore flow shows that there is not a proportional relationship between this rate and the severity of the storm. The red line is the threshold MESH value for severe storms for this analysis (21mm). 57
Figure 16: Monthly (October-February) CAPE and CIN for sea breeze storm days, non-sea breeze storm days and non-storm days. This figure demonstrates that CAPE values tend to be the highest on non-sea breeze storm days and the lowest on non-storm days. The figure also suggests that the sea breeze allowed severe storms to develop despite the occurrence of high levels of CIN. 63

Figure 17: Monthly (October-February) effective storm relative helicity for sea breeze storm days, non-sea breeze storm days and non-storm days. Although ESRH appears to be the highest on sea breeze days, more data must be used to allow for this conclusion to drawn more rigorously. 64
Figure 18: The 850 mb-200 mb wind shear charts (left) and the 200 mb vector wind chart (right) for two storm days showing that the 200 mb vector wind is similar to, but cannot be used as a proxy for, 850 mb-200 mb wind shear. 65
Figure 19: Ranking of 'storm conducive criteria' according to their usefulness in severe storm prediction. Although all of the criteria shown in this figure were conducive to severe storm formation, they are shown here in order of decreasing importance, as determined using the results presented in Chapter 4 and Chapter 5. Examples of each of the conducive criteria (with regards to Brisbane) are shown, drawn from the appendices of this thesis. 84
Figure 20: A guide for interpreting the skew-t plots provided in the appendices. The horizontal axis (as demonstrated using the temperature gradations) is temperature (in degrees Celsius) and the vertical axis (as demonstrated using the pressure gradients) is pressure (in hectopascals or millibars). 98

Glossary, Terms and Abbreviations

Bunkers' storm motion right/left mover

The predicted movement of a supercell storm according to Bunkers (2000). On the hodographs in this analysis (in the appendices), this value is presented either as left mover or right mover and as a blue dot or red dot respectively.

Convective available potential energy (CAPE)

The amount of energy a parcel of air will have if lifted a certain distance through the atmosphere, making it effectively a descriptor of the positive buoyancy of the air parcel and an indicator of atmospheric instability (Moncrieff and Miller, 1976). Variants of CAPE exist, based on calculating the energy from different altitudes. These include mixed layer CAPE (MLCAPE), most unstable CAPE (MUCAPE), and surface based CAPE (SBCAPE). This thesis primarily considers SBCAPE, which will be referred to as CAPE.

Convective inhibition (CIN)

A measure that indicates the amount of energy that will prevent an air parcel from rising to the level of free convection (Colby and Frank, 1984). Variants of CIN exist, based on calculating the energy from different altitudes. These include mixed layer CIN (MLCIN), most unstable (MUCAPE), and surface based CAPE (SBCAPE). This thesis primarily considers SBCIN, which will be referred to as CIN.

Effective bulk wind difference (EBWD)

The magnitude of the bulk vector shear from the "effective inflow base" upward to 50% of the equilibrium level height based on the must unstable parcel in the lowest 300 mb. This allows for identification of both surface based and elevated supercell environments (Thompson, 2016).

Effective inflow layer

The first layer in a sounding where all contiguous lifted parcels have CAPE greater than 100 J/kg and CIN greater than -250 J/kg. This layer represents the inflow layer for a thunderstorm (Thompson, 2016).

Equilibrium level (EL)

The level at which a lifted parcel becomes cooler than the environmental temperature and is no longer buoyant (Thompson, 2016). The equilibrium layer can be based on CAPE values calculated from various altitudes. This includes mixed layer EL (MLEL), most unstable EL (MUEL), and surface based EL (SBEL).

Hodograph

A diagram that gives a vectorial visual representation of the movement of a body or a fluid. In meteorology, a hodograph is used to plot winds at various altitudes using a polar diagram (American Meteorological Society, 2015). Hodographs have been included in the upper right hand corner of all skew-t plots for this analysis. They have been provided in this thesis in order to produce a ‘snapshot’ of each storm environment throughout the appendices, but are not referenced throughout the results.

K index

A measure of thunderstorm potential, based on vertical temperature lapse rate, moisture content of the lower atmosphere and the vertical extent of the moist layer (George, 1960).

Level of free convection (LFC)

The level at which a lifted parcel begins a free acceleration upward to the equilibrium level. The level of free convection can be based on CAPE values calculated from various altitudes, including mixed layer LFC (MLLFC), most unstable LFC (MULFC) and surface based LFC (SBLFC).

Lifted condensation level (LCL)

The level at which a lifted parcel becomes saturated, and is a reasonable estimate of cloud base height when air parcels experience forced ascent (Thompson, 2016). The lifted condensation level can be based on CAPE values calculated from various altitudes, including mixed layer LCL (MLLCL), most unstable LCL (MULCL) and surface based LCL (SBLCL).

MESH

Maximum Expected Size of Hail (MESH) is a descriptor of the expected size of hail for a storm and can be used a proxy for storm severity.

Significant hail parameter (SHIP)

An index used to delineate between significant and non-significant hail environments, based on multiple parameters, including most unstable CAPE (Storm Prediction Center, 2016).

Significant tornado parameter

An index that includes 0-6 km bulk wind difference, 0-1 km storm-relative helicity, surface based CAPE and surface based LCL (Thompson, 2004).

Skew-T log-P diagram

A thermodynamical diagram used in weather analysis and forecasting for the plotting of radiosonde soundings, giving a vertical profile of the temperature and dew point through the atmosphere (Iribarne and Godson, 1981).

Storm relative helicity 0-1km (SRH0-1), Storm relative helicity 0-3km (SRH0-3), Effective storm relative helicity (ESRH)

A measure of the potential for cyclonic updraft rotation in supercells, calculated for the lowest 1km layer and the lowest 3km layer above ground level. “Effective” SRH calculates SRH based on threshold values of lifted parcel CAPE (100 J/kg) and CIN (-250 J/kg), confining the SRH layer calculation to the part of a sounding where lifted parcels are buoyant, but not strongly capped (Thompson *et al*., 2004).

Supercell composite parameter (SCP)

An index that includes effective storm relative helicity based on Bunkers right supercell motion, most unstable CAPE, and effective bulk wind difference. In Australia, where left mover storms are more common, this parameter is less useful (Thompson, 2004).

Chapter 1: Introduction

1.1 The impact of severe weather

Severe weather refers to any meteorological phenomena that have the potential to cause injuries, deaths and significant economic losses through their impact on infrastructure and agriculture. One of the more common forms of severe weather is severe convective storms, produced primarily by intense heating of the land surface and high atmospheric moisture levels and often characterised by hail, high winds and even tornadoes. The probability of severe convective storms occurring in a given location is dependent on many factors, including climate, topography and the occurrence of atmospheric instability.

The combination of these factors in some regions means that severe storms play a greater role in the meteorology of those regions. Hail is the most commonly damaging phenomenon associated with severe storms, and typically occurs in continental interiors at mid-latitudes. The presence of mountain ranges can also promote severe storms, meaning that, although severe storms are prolific, they occur most often in specific climatic and topographic settings. These settings include northern India, China, central Europe, the Rocky Mountains of the United States, southern Australia and regions along the Great Dividing Range of Australia (Hand and Cappelluti, 2011).

In Australia, severe storms have been estimated to cost approximately $284 million per year, accounting for more than a quarter of the average cost of natural disasters each year in Australia (BTE, 2001). The effects of severe weather, however, are felt around the world. The cost of hailstorms can be enormous, with damages often reaching hundreds of millions of dollars and in some cases greater than a billion dollars: for example, in Germany in 2013 (Skywarn Deutschland, 2013), and in Texas in 2012 (National Weather Service, 2013).

Southeast Queensland is particularly susceptible to severe storms, especially during the months of November, December and January (Geoscience Australia, 2007), and Brisbane has been characterised as a ‘thunderstorm hotspot’ (Soderholm *et al*., 2015). Of particular note is the convective storm of 16 November 2008, which caused tremendous damage in the city’s inland suburbs, resulting in hundreds of felled trees and significant damage to housing and infrastructure, cutting power to 230 000 homes. A more recent severe thunderstorm occurred on 27 November 2014 and impacted the city centre, causing hail damage to skyscraper windows and flash flooding throughout the CBD. This storm produced peak recorded wind gusts of 141 km/h, severely damaging housing, vehicles and infrastructure in some areas (Australian Broadcasting Corporation, 2014).

1.2 The climate of Brisbane

To understand the factors that make Brisbane a thunderstorm hotspot, it is necessary to first consider its climate. Brisbane has a topography that is hilly but which also has regions that are on a low-lying floodplain, with creeks present in the city that can exacerbate the damage caused by flooding. This has resulted in three major flooding events in the last 150 years, in February 1893, January 1974 and January 2011. Climate change projections by Geoscience Australia indicate that the risk of flooding in Brisbane will increase as global mean surface temperatures increase (OzCoasts, 2016). In Figure 1, it can be seen that rising sea levels may inundate much of Brisbane.

Brisbane is east of the Great Dividing Range and is bounded to the east by Moreton Bay (see Figure 3). Brisbane is generally considered to have a humid subtropical climate, in what is classed as a C*fa* climate region according to the Köppen climate classification system (Kottek *et al*., 2006) (see Figure 2 for analogous regions around the world). Similarly, Hutchinson *et al*. (1992) described Brisbane as being an F4 region, characterised by warm and wet conditions, comparable to the east coast of South America and the highlands of Kenya and Ethiopia. Despite its reputation of being a warm, sunny city, Brisbane averages only 124 clear days per year, less than Perth’s 144, but still greater than Sydney’s 107. Much of Brisbane’s reputation for being a hot city can be attributed to its consistently high summer dew-point temperatures (averaging 20°C), resulting in an apparent temperature above 30°C for most summer days (Bureau of Meteorology, 2016). For a more detailed description of Brisbane’s climatic averages, refer to Table 1.

A B C

Figure 1 : *The Pinkenba region of Brisbane (which contains both Brisbane Airport and Port of Brisbane) can be used as an example of the drastic effect of rising sea levels on the Brisbane region in general. The maps are based on a simple 'bucket fill' approach, present the water level at predicted astronomical high tide and do not account for sea walls, storm surges, erosion or other local factors. Three scenarios are modelled: a low scenario of 50cm sea level rise by 2100 (a), a medium scenario of 80cm by 2100 (b) and a high scenario of 110cm (c). The figures are mainly distinguished by their shallow inundation levels (shown in darker blue) (OzCoasts, 2016).*

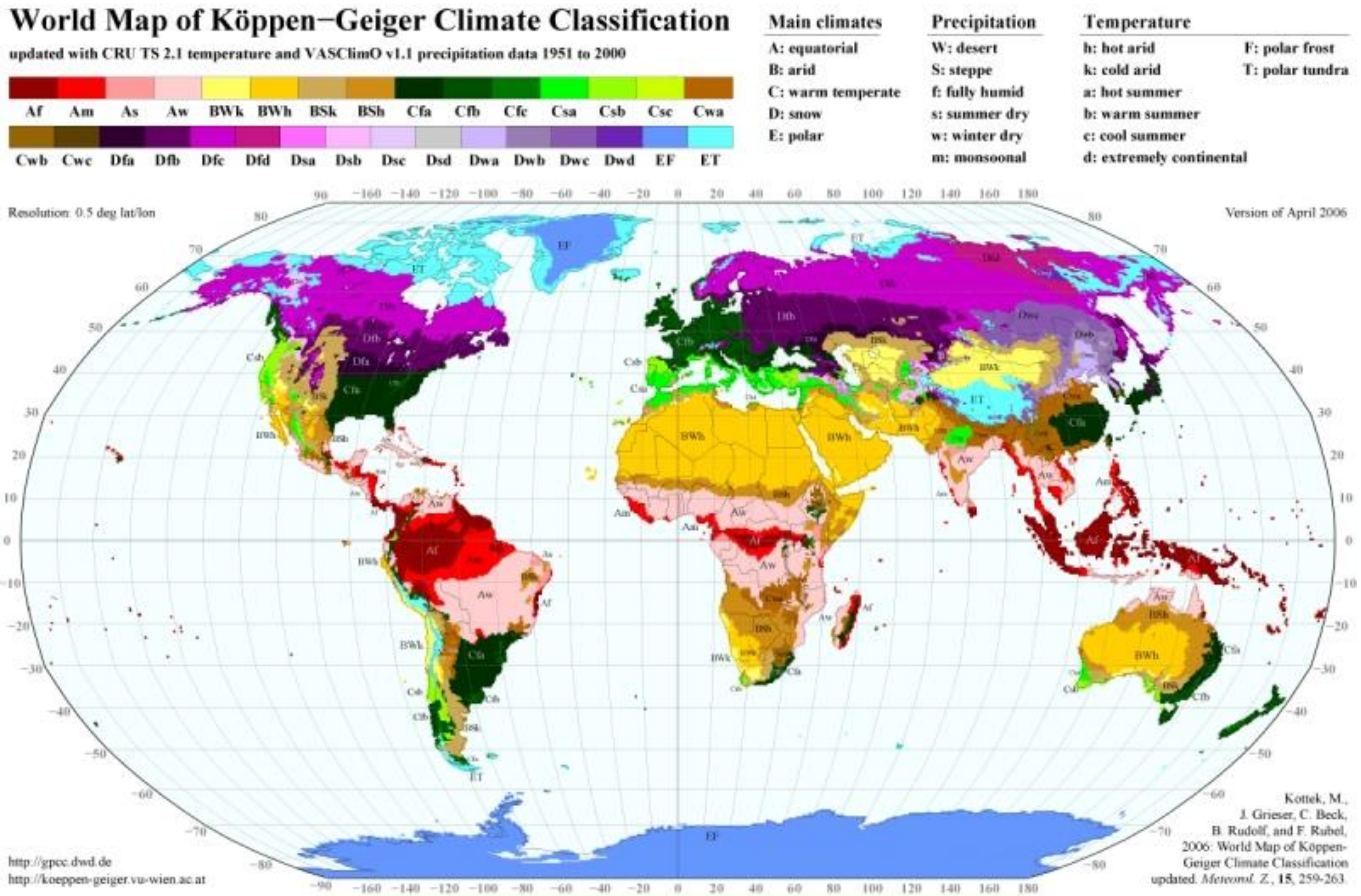

Figure 2 : *Koppen climate classification map. Brisbane is in the Cfa grouping (dark green on the east coast of Australia). Analogous climates occur in eastern Asia, the northern Mediterranean, the Pampas region of South America and the southeast United States (Kottek et al., 2006)*

Figure 3: – *Brisbane Aero (Station 040842) is located in eastern Brisbane, which is itself located in Southeast Queensland (Bureau of Meteorology, 2016).*

Table 1: *A summary of Statistics for Brisbane Airport weather station (values averaged from 1950 to 2000) (Bureau of Meteorology, 2016).*

Statistics	Jan	Feb	Mar	Apr	May	Jun	Jul	Aug	Sep	Oct	Nov	Dec	Annual
Mean maximum temperature (°C)	29	29	28	26	23.6	21.2	20.9	21.9	24.2	25.5	26.8	28.2	25.4
Mean minimum temperature (°C)	21.3	21.1	19.6	16.4	12.9	10.7	9.1	9.7	12.7	15.7	18.3	20	15.6
Mean rainfall (mm)	139.4	123.2	98.5	79.2	104.2	69.7	28.9	40.1	32.6	71.3	94.8	127.1	1059.5
Decile 5 (median) rainfall (mm)	98.5	118.9	78.6	51.2	57.2	55.2	20.8	25.6	25.2	50.2	90.9	102.9	1081
Mean number of days of rain ≥ 1 mm	9	8.9	9	7.7	7.1	5.8	4	4	4.4	5.7	8.6	9.1	83.3
Mean daily sunshine (hours)	8.4	8	7.6	7.8	7.7	6.5	7.7	8.6	9	8.9	9	8.4	8.1
Mean number of clear days	4.7	5.5	7.5	10.4	13.6	10.6	16.5	18.6	16	13.5	8.6	7.9	133.4
Mean number of cloudy days	11.3	10.7	9.5	7.6	6.4	8.5	6.5	5	4.6	7.1	10.3	11.4	98.9

1.3 Research motivations

In Australia, severe thunderstorms account for the greatest insured losses among all natural disasters (Australian Emergency Management Institute, 2014). In the past 20 years, high impact thunderstorms have caused significant damages in metropolitan areas, such as the 1999 Sydney Hailstorm, the 2008 Gap microburst in Brisbane, numerous hailstorm events in Perth and Melbourne in 2010 and in Melbourne on Christmas day 2011. Severe thunderstorms in Australia can produce extremely damaging wind gusts (Geerts, 2001), large hail (Schuster *et al*., 2005) and tornadoes. Yet, despite this danger to urban and regional coastal communities, and the fact that 45% of the global population lives within 150km of the coast (UN, 2010), thunderstorm 'hotspot activity' (Soderholm, 2015) has thus far only been documented in a few regions such as Florida and the Iberian Peninsula. In the interest of guarding the communities and economic interests of coastal regions, a better understanding of the processes that drive severe storm activity is vital.

Figure 4: *Supercell storm in Brisbane on November 27 2014 (Jimenez, 2014).*

Given the need to better understand the drivers of severe storm formation and mitigate their damaging impact on coastal populations, this thesis considers severe storms in Brisbane. Brisbane as the focus of analysis not only allows for a novel contribution to thunderstorm science, but is also a city with a clear economic and social imperative to minimise severe storm damage. In terms of novel research, similar studies have considered more inland locations, but not a locality so close to the ocean-modified costal environment, an environment which complicates the effect of key mesoscale processes such as the sea breeze. Economically, the specific location chosen for analysis, Brisbane Airport, also represents an important hub for the region. Brisbane Airport is the principal international and domestic gateway to Queensland and handles more than 21 million passengers annually. To more effectively process these passengers and to alleviate Brisbane's peak period congestion, over $2.5 billion worth of infrastructure is being developed over the next decade (Prasad, 2012), such as the New Parallel Runway (Brisbane Airport Corporation, 2016). This new project and the location in general is vulnerable to the impacts of severe weather and flooding. Figure 5 illustrates Brisbane Airport's low elevation. It is therefore imperative that an improved understanding of severe convective weather drivers for this location be established.

Figure 5: *Brisbane Airport represents a unique environmental setting amongst Australia's airports. Its close proximity to the coast and its low altitude make it susceptible to flooding events (Passmore, 2013).*

Given the key role that severe convective weather plays in Brisbane, this thesis explores the atmospheric conditions and processes that are conducive to severe convective storms, specifically the role of the sea breeze, which has been demonstrated in other studies to contribute to atmospheric instability (Soderholm *et al*., 2015). A list of sea breeze dates will be created using weather station data. Specifically, this analysis will test the applicability of existing algorithms which detect the passage of the sea breeze front (from Soderholm *et al*., 2015) to a locality within the ocean-modified coastal environment. Accompanying this analysis is the creation of an algorithm that identifies sea breezes through detecting a strengthening of onshore flow, allowing for a comparison between the efficacy of these two different approaches. Sea breeze and severe storm occurrences near Brisbane Airport will be compared in order to examine the role of the sea breeze and of strengthening onshore flow in the initiation of storms. Through an analysis of radiosonde soundings from Brisbane Airport, the atmospheric conditions that are conducive to storms on both sea breeze days and non-sea breeze days will be determined. Synoptic scale circulation patterns will then be analysed using regional synoptic meteorological charts and NCEP-NCAR reanalysis data. The goal of this analysis is to provide new insights into the interaction between the sea breeze and severe convective storms in Brisbane using local surface meteorological observations and radiosonde data and to ultimately frame this analysis in terms of the broader meteorological environment of Brisbane. The results may contribute to improving the predictive capacity of local forecasters with respect to regional synoptic data, local weather data and radiosonde data.

1.4 Research question and hypothesis

Given the damaging impact severe weather has on Brisbane, this thesis seeks to understand the key processes that produce the atmospheric instability necessary for large, sustained thunderstorms. As will be discussed in the literature review, one of the key mesoscale contributors to atmospheric instability is the sea breeze. Therefore, the primary research question posed by this analysis is: does the sea breeze affect key indicators of atmospheric stability for eastern Brisbane? The hypothesis concerning this question is that the sea breeze will have a clear impact on key indicators of atmospheric instability for eastern Brisbane. A secondary question addressed in this analysis is: what is the relative importance of skew-t plots and various synoptic charts for predicting the occurrence of severe weather? The hypothesis concerning this secondary question is that conventional surface-based synoptic charts will be demonstrated to be the most useful forecasting tool for predicting severe weather, followed by vertical atmospheric profiles in skew-t plots. The relative importance of skew-t plots will be greater for early to mid-summer (December and January).

1.5 Thesis overview

This thesis considers the analysis questions through six chapters. The role of each chapter will be:

Chapter 1: Introduction

Introduces the thesis, describing the research and economic motivations for the analysis, along with providing a summary of the thesis's key research questions.

Chapter 2: Literature Review

Details the existing literature that describes the climate and severe weather of Brisbane. This includes a review of the region's key drivers of rainfall variability, the localized phenomena that can trigger thunderstorms (with a focus on the sea breeze), and a review of existing thunderstorm climatologies for the region.

Chapter 3: Methodology

Describes the methodology used in this thesis. A description of the datasets and tools (e.g. algorithms) used to analyse the data is given, along with an in-depth justification for the method of analysis.

Chapter 4: Sea Breeze Analysis

Presents the results of the sea breeze analysis, describing the relationship between atmospheric stability indicators and the sea breeze.

Chapter 5: Vertical Profile of the Atmosphere and Synoptic Conditions Analysis

Presents the analysis of what conditions characterise storm days in the region, broken down into a month-by-month basis. This chapter references the appendices of this thesis, which provide skew-t plots (vertical atmospheric profiles), synoptic charts and reanalysis data in order to characterise storm days and assess which of these analysis tools is most useful for forecasting.

Chapter 6: Discussion and Conclusions

Presents the conclusions of the analysis, summarising the key results and discussing their significance and implications for the Brisbane region and other regions.

Chapter 2: Literature Review

This chapter revises existing knowledge about severe weather in Queensland, specifically Brisbane, and the role of the sea breeze, including a discussion of what climatological tools exist for analyzing storms and their relevance for this analysis.

2.1 Key drivers of rainfall variability and thunderstorms in Queensland

The dry season for southeast Queensland roughly comprises April-October and the wet season (through which most of the region's annual precipitation takes place) is November-March. However, the region departs significantly from the standard wet/dry season regime experienced further north. Mid-latitude cyclones bring frontal systems into Southeast Queensland, causing rainfall. Additionally, mid-latitude cyclones can also form off the coast of eastern Australia, bringing sustained and strong winds during the dry season (Hopkins and Holland, 1997). Conversely, during the wet season precipitation patterns are predominantly caused by the influx of moisture brought by trade winds as they travel to the monsoon trough. The likelihood of thunderstorm formation in the region is determined principally by the position of the inland trough and the subtropical ridge. It is common for these storms to form over mountain ranges and then move towards the coast (Peter *et al*., 2015).

Many studies such as Klingaman (2012) describe the key synoptic drivers of rainfall variability in Queensland as trade winds, east-coast cyclones, atmospheric blocking and the accompanying cut-off lows. Other studies such as Lyons and Bonnel (1992), Risbey *et al*. (2009), Lough (1993), Vecchi and Soden (2007) and Flay and Nott (2007) describe more factors that influence rainfall, however, these tend to affect dry season rainfall as opposed to severe weather or are associated with tropical cyclones and are not examined in detail within this thesis.

Queensland rainfall variability is affected by the Madden-Julian Oscillation on an intra-seasonal time scale, providing at most half of the intra-seasonal variance during the summer monsoon and affecting the placement of blocking anticyclones in spring and autumn (Wheeler and McBride, 2005, and Wheeler *et al*., 2009). This is more likely to affect the tropics and not subtropical regions such as southeast Queensland, due to the latitudinally narrow impact of the Madden-Julian Oscillation.

On inter-annual timescales the El Niño Southern Oscillation (ENSO) plays a significant role in Queensland rainfall variability, one which has strengthened since 1950. El Niño events generally result in negative rainfall anomalies in Queensland, while La Niña events tend to produce positive anomalies. The strength of either event does not necessarily produce a proportionate rainfall signal (Klingaman, 2012). Sea surface temperature anomalies in the central Pacific Ocean have a greater effect than those in the east Pacific Ocean (Wang and Hendon, 2007). Strong Inter-decadal Pacific Oscillation phases have also been associated with periods of weak ENSO variability (Cai *et al*, 2001), lower spatial coherence in Queensland rainfall (Lough, 1991) and fewer Coral Sea tropical cyclones (Grant and Walsh, 2001).

One study suggests that, unlike ENSO, the Southern Annular Mode plays a small role in Queensland rainfall while the Indian Ocean Dipole has no discernible impact (Risbey *et al*., 2009), but further research is required before the role of these two climatic drivers is better understood.

2.1.1 A trend towards more extreme rain events

From 1910 to 1990, coastal Queensland displayed an increase in the frequency of heavy rain events and the amount of rain that fell during those events, suggesting that annual rainfall was growing increasingly dependent upon the occurrence of a few high-rainfall events (Suppiah and Hennessy, 1998, and Haylock and Nicholls, 2000). These conclusions are supported by many general circulation models in the IPCC Fourth Assessment Report, which simulated a higher frequency of extreme rainfall events in a warming world (Tebaldi *et al*., 2006). These models, however, do not capture mesoscale events such as the sea breeze, introducing uncertainty into these conclusions.

These studies show that, although there are many factors at play, severe weather is playing an increasingly important role in the rainfall of coastal Queensland. Therefore, it is imperative that we understand the key drivers of severe weather in the region, such as the sea breeze.

2.2 The sea breeze and other localised forcings on thunderstorm initiation and severe weather

Numerous environmental features, including topography, urban heat islands, low-level jets (see Coniglio *et al*, 2011, Kamburova and Ludlam, 1966, Srivastava, 1985, and Proctor, 1989) and sea breezes have been associated with the initiation and modification of the deep convection required for severe thunderstorms (Doswell, 2001). All of these environmental factors, that is, topography, urban heat islands, and the sea breeze are present in Brisbane, leading to the area's reputation as a thunderstorm hotspot. This thesis seeks to explore the effects of increasing onshore flow, specifically the sea breeze, on severe storm occurrence in Brisbane.

2.2.1 Topography and urban heat islands

The dominant factors that lead to convective storm initiation, include convergence lines (e.g. sea breezes), irregular orographic heating and capping inversions (Peter *et al*., 2015). Two-dimensional radar composites have shown that topography plays a huge role for thunderstorms in Germany, with convective storms formed preferentially over mountains and then being strongly regulated by diurnal heating (Weckwerth *et al*., 2011). Radar observations of vertically integrated liquid water content allow for similar conclusions to be drawn (Bellon and Zawadzki, 2003). A similar study of convective storms in Belgium produced similar results (Goudenhoofdt and Delobbe, 2013). Further confirmation of these results can be seen in south China, where the windward slopes of mountains exhibit increased convective activity (Chen *et al*., 2014). Radar data from 12 thunderstorm days in the Sydney area shows that convective storms also form preferentially over mountain topography for that region (Potts *et al*., 2000). Topography plays a key role in determining rainfall distribution in Australia, with extreme rainfall often being closely aligned with topography (Johnson *et al.*, 2015). Bordering ranges in south-east Queensland (the Scenic Rim ranges and the western Great Dividing Range) especially contribute to the development of severe thunderstorms through increased boundary layer shear and moisture (Callaghan, 1996).

Urban areas modify regional precipitation maxima inside the city and also downwind of the city (Haberlie *et al*., 2015). This is believed to result from localized areas of enhanced instability and convergence induced by the urban heat island effect. The resulting change to the localized climate system is analogous to those produced by natural land-cover discontinuities such as vegetation and soil moisture boundaries.

2.2.2 The sea breeze

The sea breeze system is a coastal phenomenon in which cool marine air propagates inland as a result of a decreasing mesoscale pressure gradient from the ocean to the land, which itself results from daytime differential heating. This effect is reversed at nighttime as the land cools more rapidly than the ocean and the pressure gradient is reversed. In regions where the ocean current is warmer, such as those adjacent to the East Australian Current, the sea breeze typically occurs less frequently and with lower wind speeds than other regions in Australia such as Fremantle, where the ocean is typically cooler (Linacre and Geerts, 1997). The following describes the sea breeze front, the effect of the El Niño Southern Oscillation on the sea breeze, and also the impact of the sea breeze on atmospheric stability.

The sea breeze front

The sea breeze is characterised by a sea breeze front which produces rising air currents, along with a seaward flow aloft that produces diffuse sinking air currents well out to sea (Miller *et al*., 2003). The sea breeze front moves inland as continued heating of the land takes place during the day, at a speed significantly lower than the sea breeze wind speed itself, although the front usually accelerates during the day. The front is characterised by a switch of wind to the onshore direction, a drop of temperature and of the air's wet-bulb depression and a rise of surface pressure by about one hectopascal. These changes are sometimes accompanied by an increase in wind speed and turbulence, especially when the ground is not moist and has a low specific heat capacity (to enable rapid heating) (Linacre and Geerts, 1997).

The effect of the El Niño Southern Oscillation on the sea breeze

The frequency of the sea breeze is affected by the El Niño Southern Oscillation. During La Niña events, the zonal Walker Circulation shifts westward, resulting in the strengthening of trade winds in the southwest Pacific Ocean (Oort and Yienger, 1996, Garcia and Kayano, 2007). This in turn results in an increase in the flow of stable maritime air across southeastern Queensland, reducing the temperature gradient between the sea and land required for sea breeze circulations (Simpson *et al*., 1977). Additionally, synoptic ridges that result from the strengthening trade flows can cap the convective environment while also stabilizing the boundary layer (Yeo, 2005). El Niño conditions have the opposite effect, increasing the frequency of sea breeze days in southeastern Queensland.

Impact of the sea breeze on atmospheric stability

Buoyancy and shear

The sea breeze can increase buoyancy and shear, which are fundamental to deep convection. In southeast Queensland, the sea breeze is considered cool, moist and stable. However, Simpson *et al*. (1977) demonstrated that the sea breeze can entrain warming near-surface air during overland flow, thereby increasing buoyancy. This is referred to as the leading edge effect (Oke, 1978). The sea breeze can therefore engender subtle changes in boundary layer stability, which can in turn change the likelihood of thunderstorm initiation. This can also augment the magnitude of near surface vertical shear normal to the coastline, which tends to oppose in direction shear generated by the cold pool forward flank for storms moving under prevailing westerly flow (Weckwerth *et al*, 2008; Weckwerth, 2000). The net tendency of these opposing shear profiles is to promote deeper lifting along the cold pool interface (Soderholm *et al*., 2015), especially when these environments lack existing low-level environmental shear (Rotunno *et al*, 1988). Additionally, Karan and Knupp (2009), May (1999) and Wilson and Megenhardt (1997) observed that enhanced convection can take place as a result of colliding gravity currents such as the sea breeze.

Interaction between deep convection and the coastal plains sea breeze leads to the development of severe thunderstorms through increased boundary layer shear and moisture (Callaghan, 1996). Southeasterly changes have a history of prolonging, enhancing or sustaining severe thunderstorms in southeast Queensland (Callaghan, 1996). This is evidenced by a number of case studies: a tornadic storm through Brisbane city in 1973 (Holcombe and Moynihan, 1978), a hailstorm in 1985 (Callaghan, 1996) which resulted in insurance losses of approximately AU$2.1 billion (Insurance Council of Australia, 2015), a storm event in Brisbane in 2008 (Richter *et al*., 2014) and a 2014 thunderstorm which produced approximately 10 centimetre hail in Brisbane (Parackal *et al*., 2015).

Case studies such as that by Peter *et al.* (2015) have linked sea breezes to particular storms. The storms they analysed were characterised by a strong storm-relative low-level flow layer of very moist near surface air, while the storm-relative winds aloft were weak.

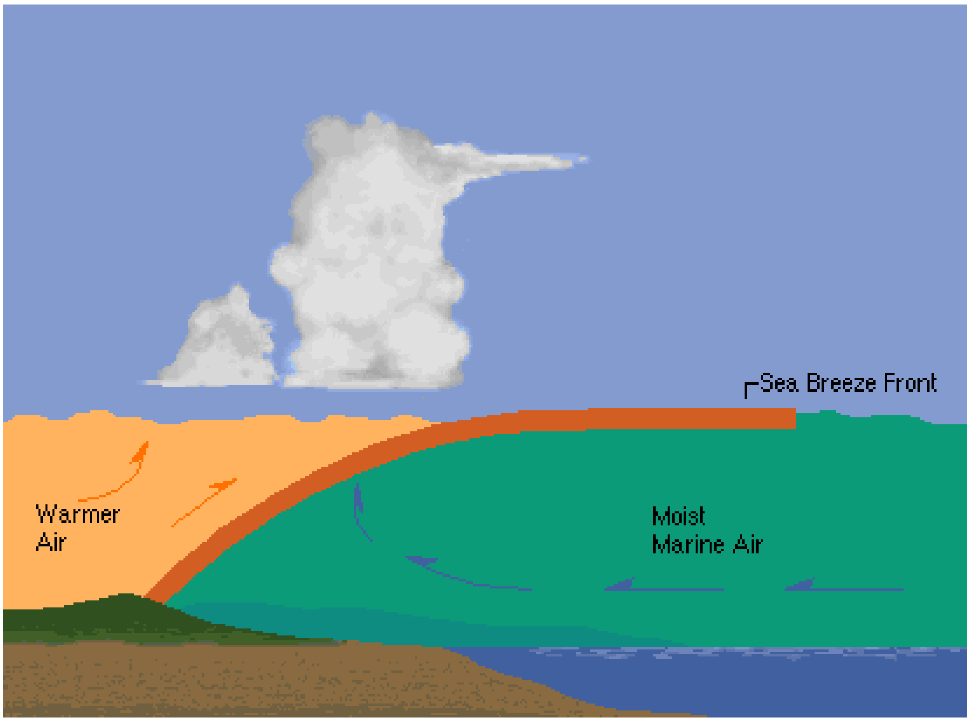

Figure 6: *The standard sea breeze conceptual model is as shown above. Moist marine air flows inland and interacts with warmer inland air. The actual behaviour of the sea breeze at different localities is significantly more complex than this standard model (The University Corporation for Atmospheric Research, 2016).*

Mesocyclones and supercells

Environmental wind shear plays a pivotal effect on storm morphology, as evidenced by numerical modelling studies that have explored the sensitivity of storm evolution to changes in the shear profile (Kirkpatrick and McCaul, 2008; Weisman and Klemp, 1982; Droegemeier *et al*., 1993; Adlerman and Droegemeier, 2005). An increase in low-level wind shear generally produces stronger mesocyclones (McCaul and Weisman, 2001), with this effect being more pronounced when "the greatest shears are confined to the shallowest depths" (Adlerman and Droegemeier, 2005). Vector shear magnitude (for 0-6km) allows for discrimination between tornadic and non-tornadic supercells (Thompson *et al*., 2003). Specifically, with a fixed storm motion, increasing the low-level shear corresponds to an increase in storm-relative helicity (Davies-Jones *et al*., 1990). This result was similar to that of Kerr and Darkow (1996), who also found that storm relative low-level flow was stronger in cases in which violent tornadoes occurred. Although less pivotal to the production of low-level vorticity and not linked to the sea breeze, middle and upper-level storm relative winds play a significant role in influencing the storm's precipitation distribution (Rasmussen and Straka, 1998).

This significant role of the sea breeze applies even for supercell storms, the most severe type of local storms. The standard supercell model was developed for the Great Plains of the USA, as described in case studies such as those by Weckwerth (2008), with environmental wind shear playing a pivotal role in establishing storm organization and longevity (Weisman and Rotunno, 2000, and Rotunno and Weisman, 2003). A sea breeze can provide some of the necessary shear required for supercell thunderstorm development. Although the standard supercell model has some applicability for Brisbane, significant complexities have been observed within sea breeze and thunderstorm circulations for southeast Queensland (Soderholm *et al*., 2015), and this limits the application of standard concepts for idealised gravity current interactions, and suggests that further work is needed to establish the exact role of the sea breeze.

Initiation of deep convection

The sea breeze front convergence zone can initiate deep convection (Miller *et al*., 2003, and Fovell, 2005), and this phenomenon has been explored in detail in Florida by extensive field programs (e.g. Atkins *et al*, 1995). Despite this wealth of knowledge, concepts developed for Florida have little potential for application in southeast Queensland. Florida is characterised as a low-lying peninsula, commonly producing converging sea breezes from the west and east coasts, while southeast Queensland is characterised as having significant inland topography that commonly initiates deep convection. Prevailing upper-level westerly steering flows tend to produce deep convection over the Great Dividing Range and lesser coastal ranges, and the resulting storms then move onto the coastal plains and are strengthened by interaction with sea breeze fronts and post frontal air masses. This interaction between the sea breeze, mountain ranges and prevailing westerlies has been documented in numerous reports for the Sydney and Brisbane regions and has been associated with many of the highest impact thunderstorm events (Holcombe and Moynihan, 1978; Harper and Callaghan, 1998; Richter *et al*., 2014; Callaghan, 1996). Complex physical settings such as urbanization, topography and a complex coastline can produce periodic maxima in the wind speed of the sea breeze (i.e. pulsation), which introduces further complications in determining its effect on the initiation of convection (Puygrenier *et al*., 2005 and Soderholm *et al.,* 2015).

2.3 The effect of the sea breeze on wind direction in Brisbane

The primary method for sea breeze detection will be via its effect on wind direction. The sea breeze causes a shift in the wind directions such that onshore winds are favoured. In the case of Brisbane, this causes winds to align between 10 degrees and 110 degrees true, resulting primarily in northeasterly winds (Figure 7).

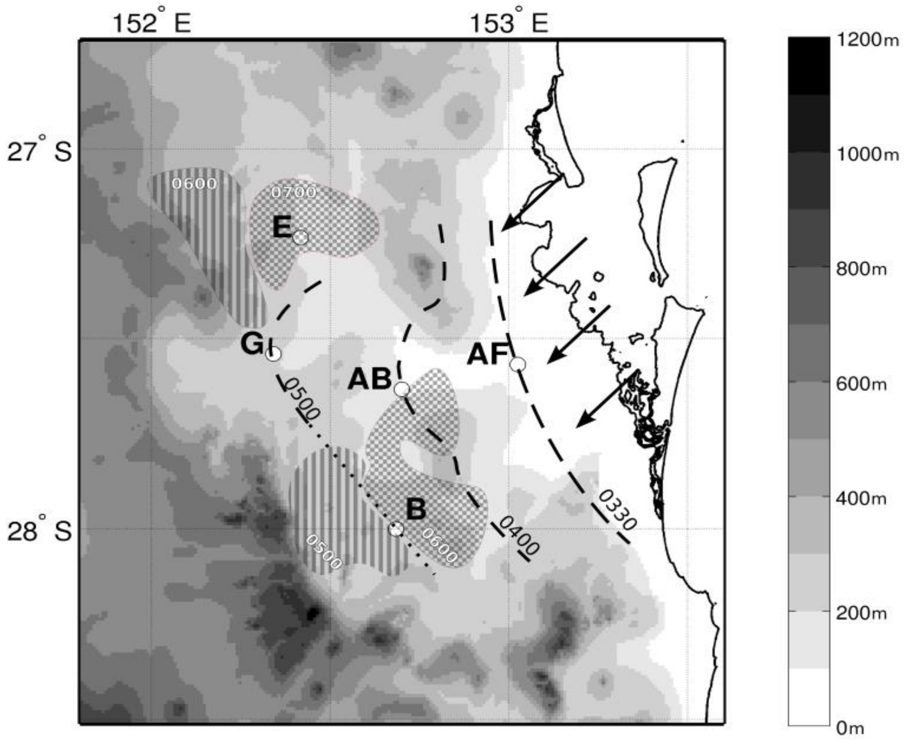

Figure 7: *Schematic of sea breeze propagation across a weather station transect. These stations include Gatton (G), Amberley (AB) and Archerfield (AF). Most common arrival times (UTC) at each station are shown in black numbers. Topography elevation is shown in 100 m intervals above mean sea level. The towns of Boonah (B) and Esk (E) are also marked. Arrows indicate onshore flow of sea breeze at the surface (Soderholm et al., 2016).*

An effective way of graphically representing the average distribution of wind directions (and illustrating sea breeze occurrence) at a location is using wind roses. Note that there are other meteorological factors at play in the following wind roses but that the sea breeze is one of the key factors, causing strengthening onshore wind during the day, especially during late-spring, summer and early autumn.

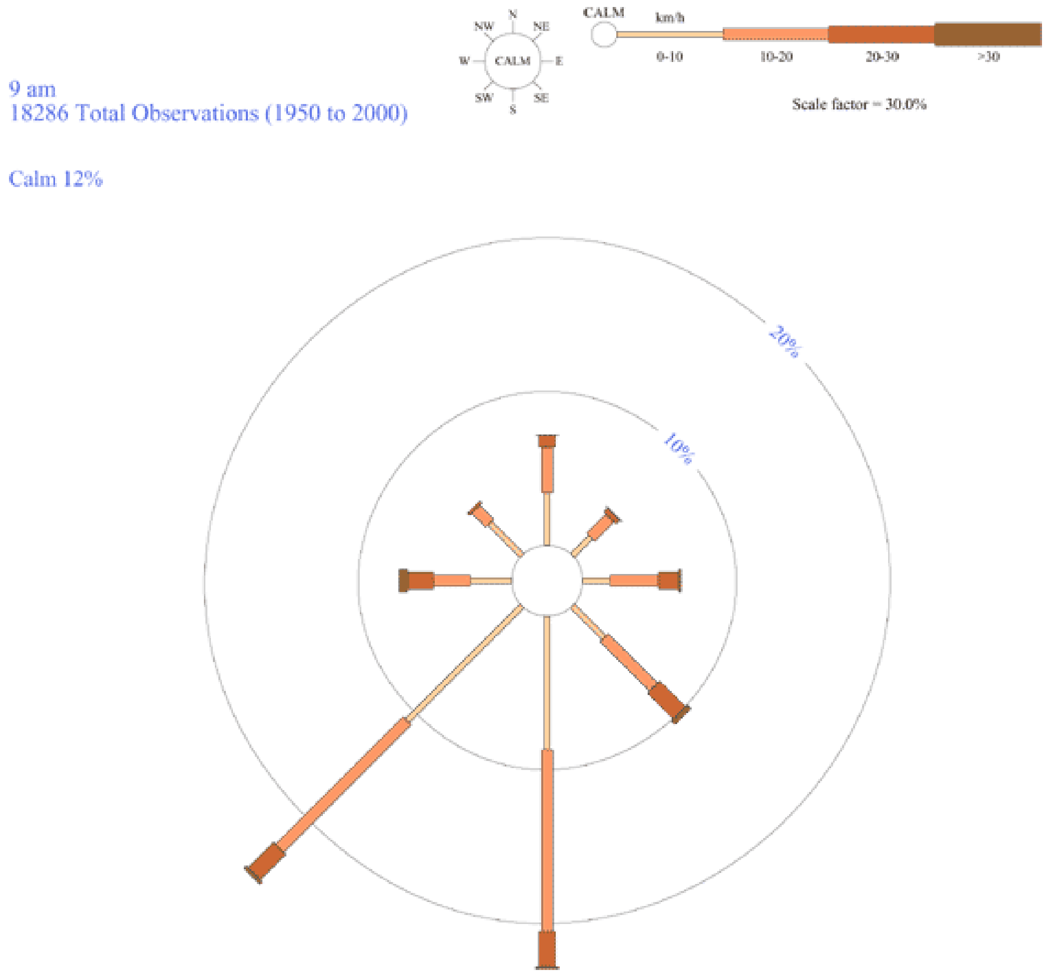

A.

Figure 8A (Bureau of Meteorology, 2016)

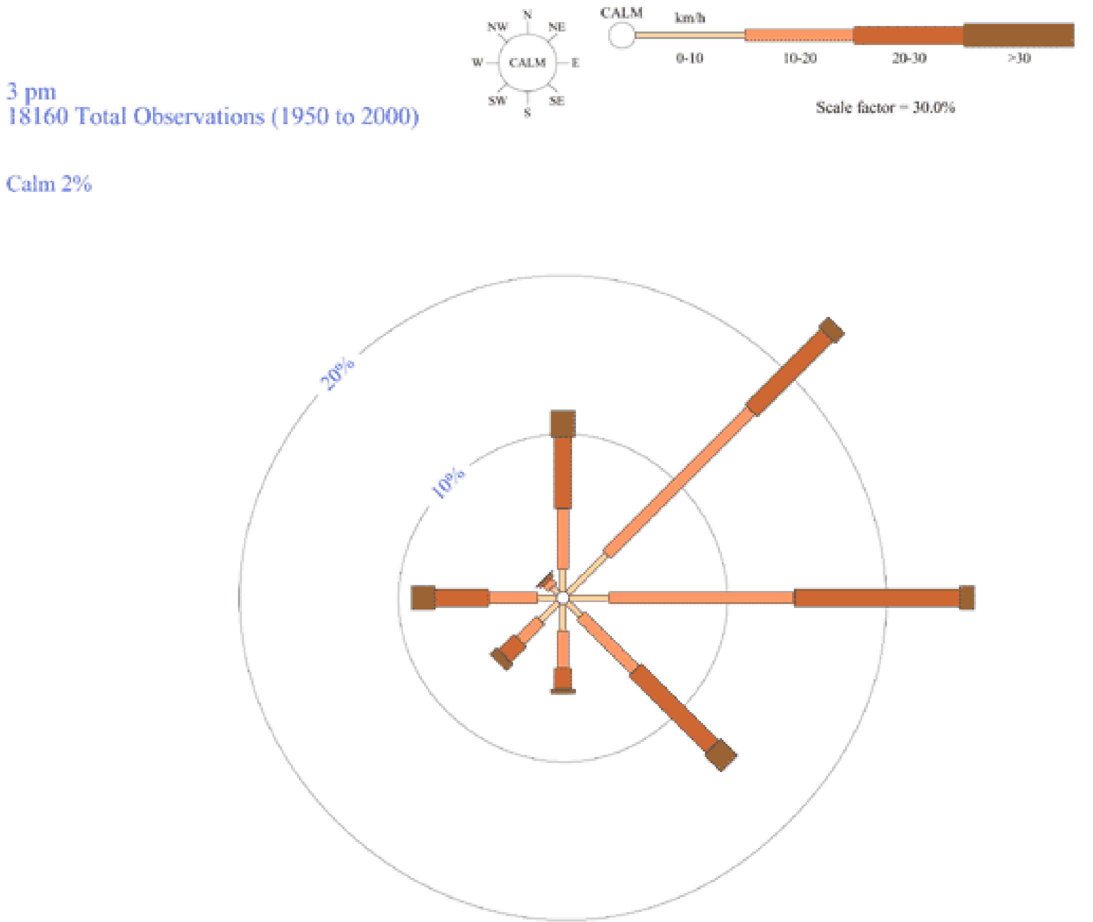

B.

Figure 8B (Bureau of Meteorology, 2016)

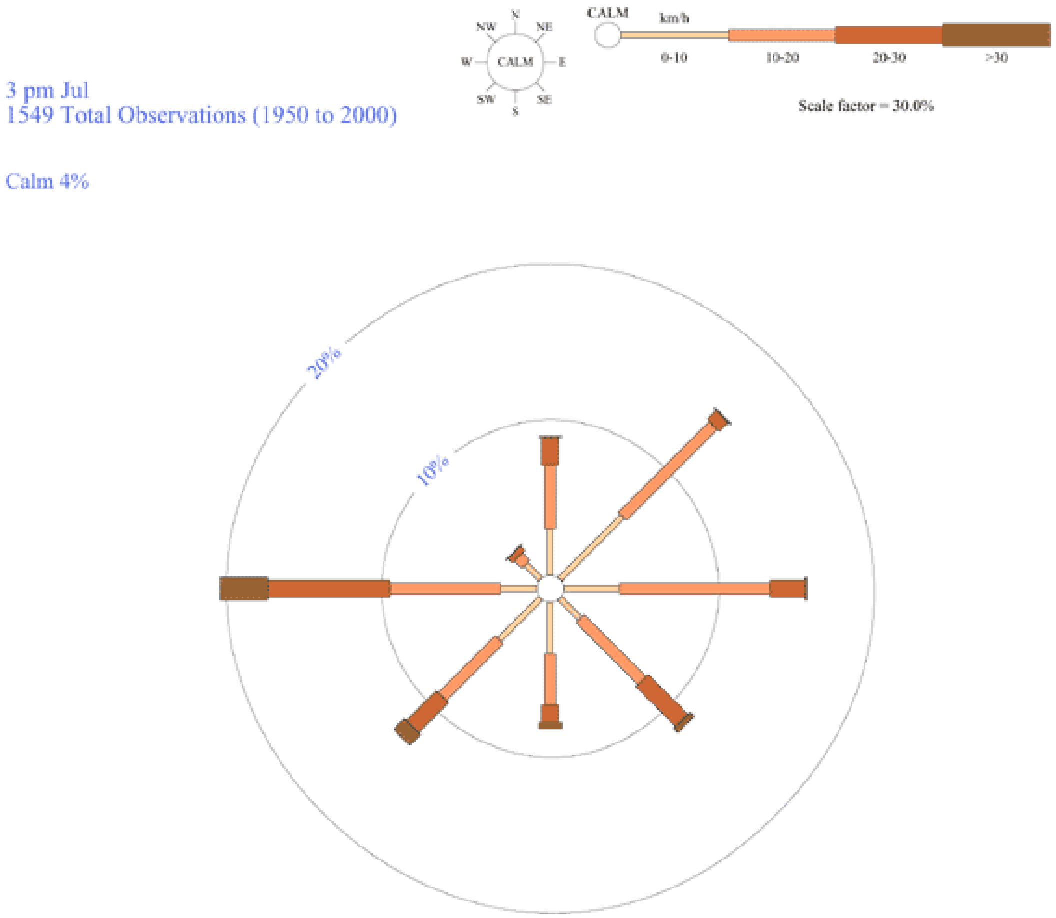

C.

Figure 8C (Bureau of Meteorology, 2016

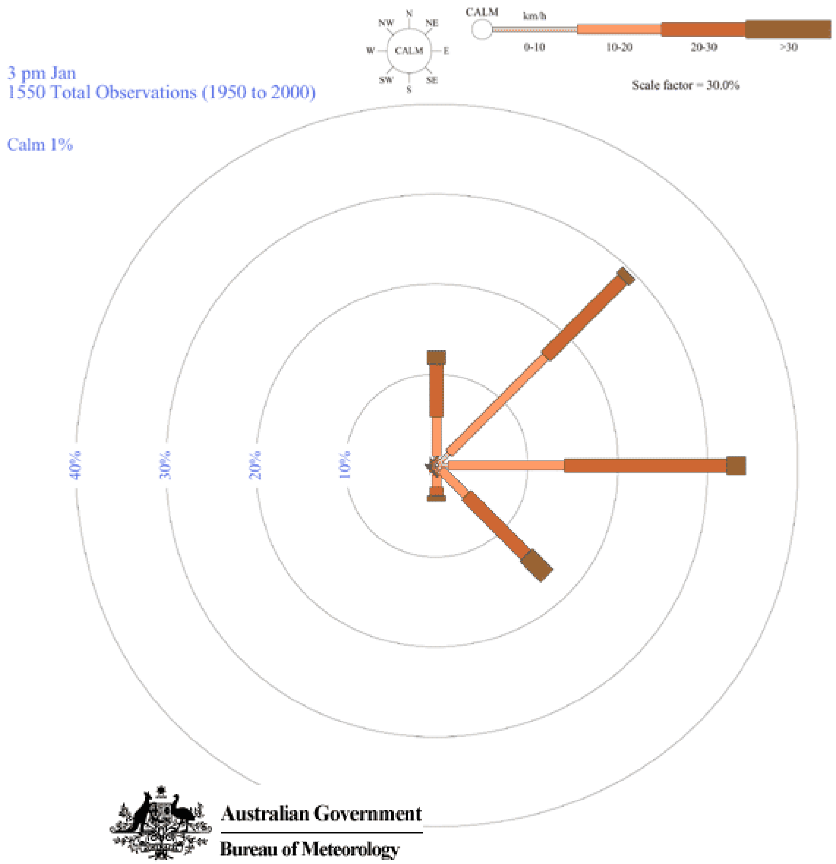

D.

Figure 8 : *Figure 8a shows the annual wind direction before the onset of the sea breeze in the morning. It can be seen that the wind direction is fairly scattered, with a large portion being southwesterly. In Figure 8b the afternoon wind directions are represented, showing the period during which the sea breeze is having a significant impact. The largest portion of winds during this time are easterly or northeasterly. The effect of the sea breeze is more marked during summer, given that the differential heating between the land and ocean is more pronounced. This can be seen in Figure 8c and 8d. Figure 8c shows 1500m during winter, and the northeasterly wind direction characteristic of the Brisbane sea breeze is conspicuously absent. In Figure 8d, however, showing 1500 during summer, the effect of the sea breeze is very pronounced (Bureau of Meteorology, 2016).*

2.4 Selecting a climatological method

Given that one of the goals of this analysis is to create a short-term severe storm climatology, it is necessary to review and assess existing climatologies for the region. Thunderstorm climatologies can be developed from a variety of datasets, spanning scales from the globe to individual cities. The various methods for creating a climatology are presented below and assessed in terms of their usefulness for this analysis.

2.4.1 Event-based sampling

Thunderstorm event-based reports provided by forecasters, the media and the public predate all standard meteorological instrumentation used today, and have even formed the basis for some thunderstorm climatologies. Yeo (2005) and Allen and Karoly (2013) sourced reports from the Australian Bureau of Meteorology Severe Storms Archive (BOM, 2016) to investigate correlations with climate oscillations and severe thunderstorm environments.

On a seasonal scale, El Niño Southern Oscillation (ENSO) has a guiding influence on the background synoptic patterns that can either inhibit or enhance severe thunderstorm development (Yeo, 2005). For data post-1977, Yeo determined that severe thunderstorms days were 23 percent more likely to occur during years in which the Southern Oscillation Index was neutral compared to years in which the index was positive (La Niña). Allen and Karoly (2013) also determined that ENSO has a significant impact on the spatial distribution of severe thunderstorms.

Event-based report sampling is sparse in both space and time, limiting the identification of recurring behaviour, especially on meso-gamma scales (2 to 20 km) (Soderholm, 2015). Event-based report sampling is also biased due to its inherent subjectivity, for example, Allen and Karoly (2013) described how a bias exists in severe thunderstorm observations, with more being documented in highly populated areas. Even some populated areas have many gaps in their observational record (such as lack of detail or missing storms) especially over climatically useful time periods (Griffiths *et al*., 1993).

2.4.2 Radiosonde soundings

In order to address this observational inadequacy a method is required that is not solely dependent on event-based reporting, necessitating a consideration of the common ingredients for thunderstorm events. These are generally considered to be the presence of instability, moisture, lift and environmental winds (Doswell *et al*., 1996; Doswell, 2001). Convective available potential energy (CAPE) and 0-6 km magnitude of the shear difference of horizontal wind (S06) are commonly used to describe these thunderstorm conducive environments, with the shear allowing for storm organization and sustained updraft (Rasmussen and Blanchard, 1998).

These indicators of atmospheric stability are usually measured using radiosonde soundings. Radiosonde soundings generally need to be recorded within 200 km of a storm and also within a few hours of a storm occurrence in order to be considered representative of that storm's environment. Australian radiosonde stations are further than 200 km apart in most cases (Ryan, 1992). Soundings in Australia are generally taken at 0000GMT (1000 for Brisbane) and in some cases at 1200GMT (2200 for Brisbane). These timings and spatial distributions are not ideal as storm proximity soundings because local meteorological processes can produce rapid modification of sounding environments.

2.4.3 Reanalysis datasets

Many studies (e.g. Allen and Karoly, 2013) sought to offset these difficulties using profiles produced from models or spatially interpolated reanalysis data. Interestingly, a comparison with soundings derived from reanalysis data for the contiguous US by Lee (2002) suggested that Australian significant severe thunderstorms occur in environments with lower CAPE than analogous storms in the US. Sixty per cent of US cases have CAPE values lower than 2000 J/kg, compared to 75 per cent for Australia. However, the vertical profiles produced by this method have reduced vertical resolution, with differences of up to 500 J/kg between the actual value and the reanalysis value for thermodynamic quantities such as CAPE (Allen *et al*., 2011). The limitations of the radiosonde network described by Allen and Karoly (2013) do not apply when the analysis considers only a single locality. In other words, for an analysis of a particular area such as metropolitan Brisbane, reanalysis data are not as useful given that high quality radiosonde data exist for this particular locality. This thesis, therefore, will favour actual radiosonde data over reanalysis data.

2.4.4 Remote sensing

To overcome these sampling issues, thunderstorm climatologies are often constructed from remotely sense datasets. For example, Dowdy and Kuleshov (2014) constructed an 18-year lightning dataset derived from two satellite instruments in order to produce lightning density maps for Australia. This particular approach towards establishing a thunderstorm climatology is made more difficult by the complicated relationship between lightning and convective intensity (Rudlosky and Fuelberg, 2013).

2.4.5 Radar

Recent economic imperatives such as water scarcity have prompted the creation of more exhaustive climatologies for southeast Queensland, such as the Queensland Cloud Seeding Research Project (Tessendorf *et al*., 2012) in conjunction with a study by the Bureau of meteorology that focussed on convective storms in southeast Queensland. This culminated in the Thunderstorms Identification, Tracking, Analysis and Nowcasting (TITAN) package developed by the National Center for Atmospheric Research (Dixon and Wiener, 1993) being used to explore the deep convective properties of southeast Queensland (Peter *et al*., 2015). However, the limited time series prevented development of a high resolution spatial thunderstorm climatology. The TITAN tracking algorithm was a key tool used by Soderholm *et al*. (2015) in verifying storm occurrences using volumetric radar data. Their results indicated that severe weather is indeed linked to sea breeze occurrences for parts of Brisbane (see Figure 9). Data from Soderholm *et al.* (2015) are used in this thesis, so the derivation of their methods (especially the derivation of Maximum Expected Size of Hail, MESH, a descriptor of storm severity) is discussed further in the methodology.

Given the limitations of event based reporting and reanalysis data described above, the key motivation of this paper is to improve the understanding of the relationship between key indicators of atmospheric stability such as CAPE and severe storm initiation, specifically with respect to eastern Brisbane. It will also be necessary to consider the effect of the sea breeze and avoid the limitations of event-based reporting and the reduced vertical resolutions associated with reanalysis data. In contrast to the volumetric radar data climatology of Soderholm *et al*. (2015), an analysis of radiosonde soundings has a greater focus on improving the predictive capability of forecasters for severe weather.

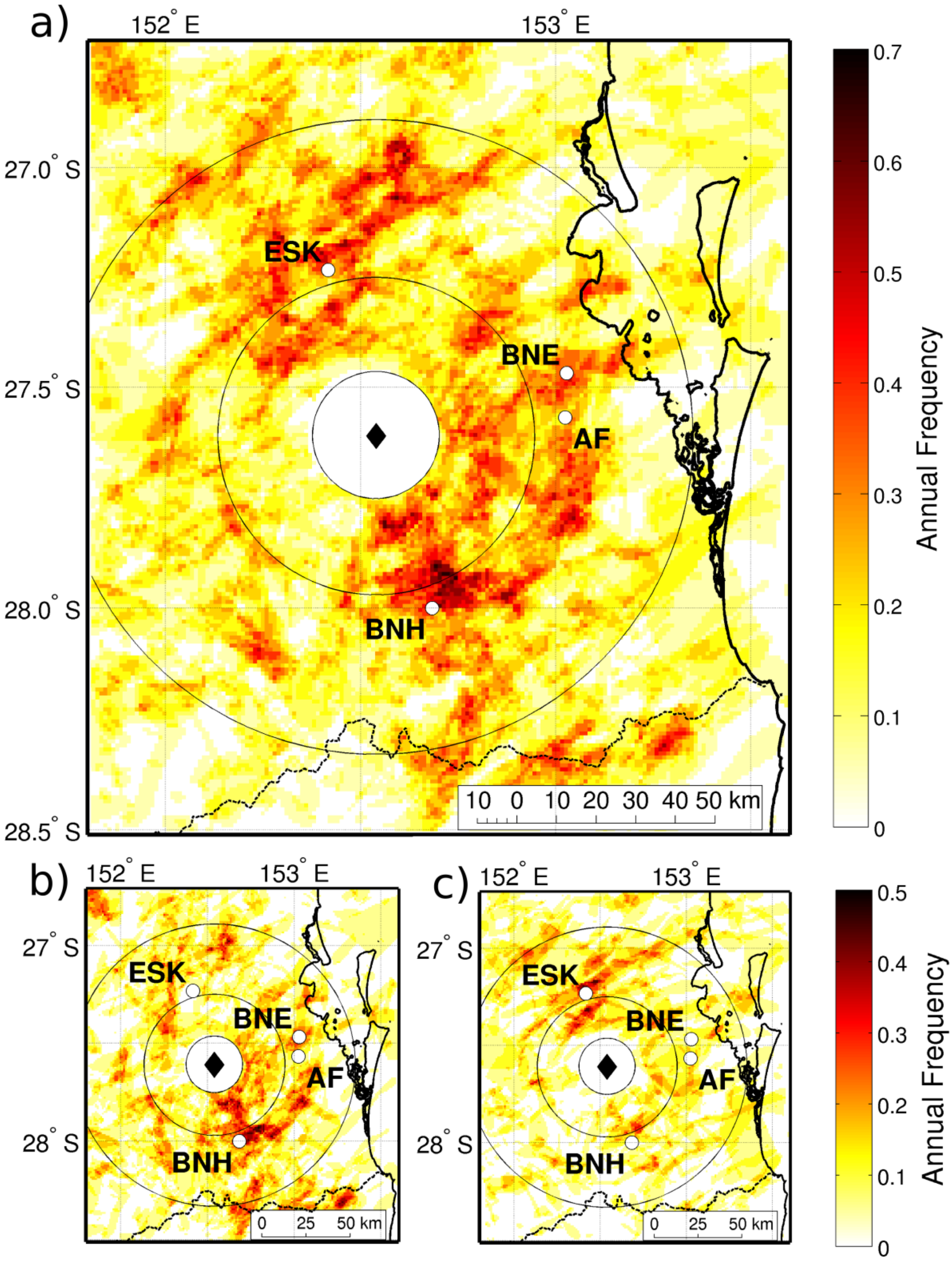

Figure 9: *Annual cumulative MESH swaths (sum of all MESH values averaged by the number of years in the climatology) for 21 mm threshold for (9a) all days. (9b) Sea breeze days (9c) Non-sea breeze days. Towns marked include Brisbane (BNE), Archerfield (AF), Boonah (BNH) and Esk (ESK). Marburg radar location marked with black diamond and range rings shown at 16 km, 40 km and 80 km. MESH values are discussed in detail in the Methodology. MESH can be treated as a proxy for severe storm occurrence, so the higher values in 9b compared to 9a suggest a significant relationship between the sea breeze and severe storms for much of southeast Queensland (Soderholm et al., 2015).*

The next chapter, Methodology, describes and justifies the algorithms and approaches used for this analysis, explaining how a list of sea breeze dates will be derived, and with which tools radiosonde data will be analysed. The next chapter also discusses the synoptic graphs that will be used to describe severe storm days.

Chapter 3: Methodology

In order to address the research questions described in Chapter 1, this chapter details the steps that will be undertaken to identify sea breeze days and storm events, together with a description of the tools used to describe atmospheric conditions for both storm days and non-storm days. These steps are justified with reference to a probative analysis of the dataset and previous analyses conducted for the region such as that by Soderholm et al. (2015). A description of the synoptic maps that will be used to describe severe storm days is also presented.

This thesis will use three main datasets to determine the relationship between the sea breeze and thunderstorm initiation in the Brisbane region during the period 2000-2015. These three datasets are: upper air soundings from Brisbane Airport radiosondes (BOM, 2016), meteorological observation data from the Brisbane Airport weather station (BOM, 2016) and volumetric radar data for the Brisbane region (Soderholm *et al.,* 2015). Soderholm *et al*. (2015) focused on subtropical southeast Queensland when creating their thunderstorm climatology, along with exploring the effect of the sea breeze circulation on thunderstorm development using a radar climatology and a field campaign. The focus of this thesis is to explore the role of the sea breeze in the ocean-modified coastal environment using a radiosonde analysis.

3.1 Detecting past occurrences of the sea breeze

Past occurrence of sea breeze days will be established first using an algorithm created by Azorin-Molina *et al*. (2011) which applies a set of criteria to meteorological data such as surface temperature measurements. This algorithm was formulated for use on the Iberian Peninsula and has since been modified by Soderholm *et al*. (2015), with the new criteria better reflecting the characteristics of the southeast Queensland sea breeze (Figure 10). Soderholm *et al*. were able to establish a strong connection between sea breezes and hail-producing convective storms in the Brisbane region using data from weather stations inland from the coast. This thesis will adapt this algorithm to the meteorological observations from Brisbane Airport and will also derive a novel algorithm.

3.1.1 Limitations of existing detection method

The algorithm of Soderholm *et al*. included criteria that discriminated between sea breeze events and non-sea breeze events by changes in relative humidity, maximum wind speed and temperature. An initial analysis of the data showed that these discriminators do not seem as valid for the coastal setting selected for this analysis (compared to the relatively far inland station of Soderholm *et al*.).

For example, the probative analysis suggested that changes of relative humidity, maximum wind speed and temperature exhibit a high variability throughout the sea breeze time period of 1100 to 1700. This variability was as high in many cases as the threshold changes for these variables that were determined as necessary by the algorithm of Soderholm *et al*. to positively identify a sea breeze. In other words, this means that the threshold criteria of Soderholm *et al*. (which require a certain change in maximum wind speed, temperature and relative humidity before and after the sea breeze event) appear less efficacious for the Brisbane Airport locality. In other words, the magnitude of change required for these threshold changes commonly occurred throughout the sea breeze time period itself, making them meaningless. Additionally, this algorithm required that the wind direction not deviate from between 10 and 110 degrees true for at least two hours. At Brisbane Airport the probative analysis suggested that, although any given day may meet the wind direction criterion for the vast majority of the relevant time period, there were common deviations from this required wind direction (usually only a few minutes in length) that led to under-identification of sea breeze days.

For the Archerfield weather station considered by Soderholm *et al*., they acknowledged that the well recognised temperature decrease typically associated with a sea breeze front passage was not observed in their manually determined sea breeze events, possibly due to warm air entrainment as the sea breeze propagated across Brisbane. Such entrainment is unlikely for the Brisbane Airport station considered in this analysis given the proximity of the weather station to the ocean. However, given this proximity it is highly likely that the nearby maritime air mass and the air at the airport are relatively well mixed, meaning that propagation of the maritime air mass inland during the sea breeze would nevertheless be unlikely to produce the pronounced drop in temperature and rise in relative humidity generally associated with the sea breeze front at more inland locations.

3.1.2 Adaptation of existing algorithm

This analysis adopts a modified version of the Soderholm *et al*. algorithm, relaxing the temperature, duration and relative humidity criteria such that the high variability discovered in these variables can be taken into account. This requires the continued use of the criterion that the wind direction must lie within 10 and 110 degrees for at least two hours between 1100 and 1700 and that wind speed not exceed 40 km/h, but not the use of the stricter criteria. To verify the efficacy of this approach this analysis will compare the determined sea breeze days with the manually verified days of Soderholm *et al*. If the vast majority of the manually verified sea breeze days coincide with days on which the analysis determined that a sea breeze occurred, then this will suggest that this approach is valid, provided not too many false positives occur. If coincidence between these two sets of dates is small, this will suggest that this revised algorithm is not applicable to the ocean-modified coastal environment.

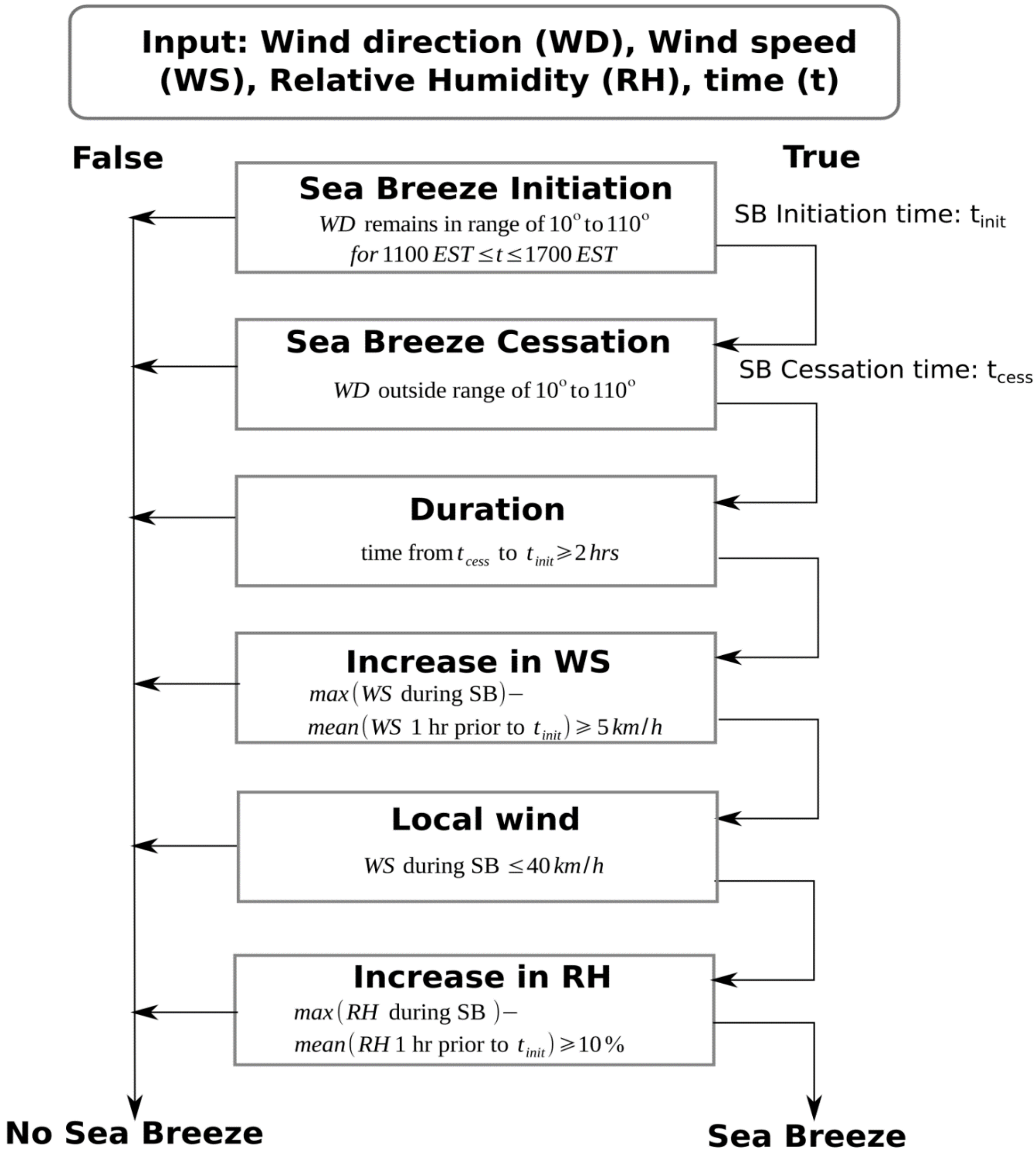

Figure 10: *Flow diagram showing filters applied to identify sea breeze (SB) days based on a single surface weather station dataset at Archerfield by Soderholm et al. (2015). This approach was formulated by Azorin-Molina et al. (2011).*

3.1.3 A new algorithm

Despite the adaptions made to the algorithm, it may nevertheless have limited applicability to Brisbane Airport weather station due to its position within the ocean-modified coastal environment. Therefore, another method for determining sea breeze occurrence is also required. An algorithm using increasing onshore flow, another indicator of sea breeze occurrence, will also be implemented. Ultimately, the final list of sea breeze dates derived using this novel method will include all dates that exhibited increasing onshore flow with direction between 10 and 110 degrees true between either 0900 to 1200, 1200 to 1500 or 0900 to 1500, provided that any particular day not also exhibit a decrease in wind speed between 1200 and 1500. As was the case for the adapted algorithm, this algorithm will use weather station data with one-minute resolution from March 2000 until the end of 2015. Any false positives produced using this method will still have relevance, because increasing onshore flow produces similar changes in boundary layer conditions to those caused by the sea breeze. For more details on the specifics of this algorithm, see Chapter 4.

Both the modified algorithm and the new algorithm will be implemented in Python and applied to data from the Brisbane Airport weather station (number 040842, see Figure 3). The Brisbane Airport weather station data have a temporal resolution of one-minute extending from March 2000 until the end of 2015, and will be used for this entire time period. The data contain numerous meteorological variables, but the primary one that will be considered is wind direction (along with wind speed, temperature and relative humidity, which were used in the probative analysis).

3.2 Detecting past occurrences of severe weather and correlating these to the sea breeze

Having achieved a record of sea breezes at Brisbane Airport, the second objective of the investigation will be to produce a record of severe thunderstorms in the region using volumetric radar data, specifically Maximum Estimated Size of Hail (MESH), an estimate of the maximum hail size that can be expected from a storm. MESH is based on the Severe Hail Index and has a spatial resolution of 0.01 degree for both longitude and latitude and a temporal resolution of 2 minutes. Both MESH and the Severe Hail Index are based on a reflectivity-to-hail relationship (Witt *et al*., 1998). The minimum value for MESH that will be used is 21mm, based on the assumptions described by Soderholm *et al*. (2015). The region considered in this analysis is shown in Figure 11.

These data are sourced from the results of Soderholm *et al*. (2015), so a brief description of their methodology is provided here. For their climatological analysis, Soderholm *et al*. (2015) used a continuous 18-year (July 1997 to June 2014) volumetric reflectivity radar dataset located at Marburg, 50km west of Brisbane. The Marburg dataset was chosen due to its length and central location, which allows for good coverage of Brisbane. Soderholm *et al*. (2015) performed a cell-based analysis of the Marburg archive using the Weather Decision Support System (Lakshmanan and Smith, 2010). This allowed for the detection of storm cells, which were then analysed using Maximum Expected Size of Hail (MESH) grids, which acts as a proxy for the actual hail severity (Cintineo *et al*., 2012). Although Wilson *et al*. (2009) suggested that MESH has an over-forecasting bias, Cintineo *et al.* (2012) demonstrated that MESH can nevertheless provide a useful discriminator between non-severe and severe hail size. Using MESH, Soderholm *et al*. (2015) established a spatial climatology of hailstorm frequency for southeastern Queensland, summarized in Figure 9.

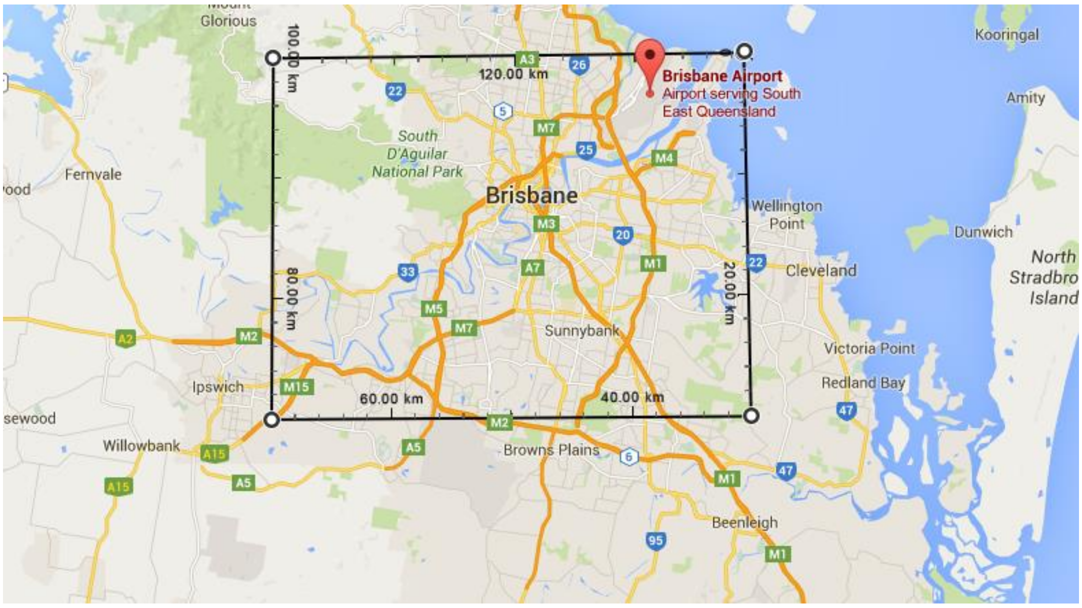

Figure 11: *The region considered for storm identification is shown. The region comprises a 40km by 30km grid with a total area of 1 188 km*^{2}*. The region was selected so as to include Brisbane Airport but to exclude as much of Moreton Bay as possible, given that storms weaken significantly over water. The region is contained within the latitudes -27.362114° and -27.634977° and between the longitudes 153.202320° and 152.806812° (Google Maps, 2016).*

3.3 Comparing indicators of atmospheric stability between sea breeze storm days, non-sea breeze storm days and non-storm days

The analysis will then focus on what atmospheric conditions can lead to, in conjunction with the sea breeze, the initiation of deep convection in the region. Conversely, this will also include an analysis of occurrences of deep convection in the absence of a sea breeze. This will allow for a comparison of the levels of atmospheric instability that were required for the initiation of deep convection in each case. The key indicators for atmospheric stability that will be used are convective available potential energy (CAPE), convective inhibition (CIN) and effective storm relative helicity (ESRH). CAPE is a measure of the positive buoyancy of an air parcel, derived using the environmental temperature lapse rate and the moist adiabatic lapse rate of a particular atmospheric sounding. CAPE within the inflow layer may be especially affected by the moisture brought by the sea breeze and which can lead to the initiation of severe storms, while the continued survival and better organization of a thunderstorm is affected by the increase in shear that accompanies the sea breeze. The effective inflow layer is defined as the first contiguous layer of pressure levels in which a lifted parcel has CAPE greater than 100 joules/kilogram and convective inhibition (CIN) greater than -250 joules/kilogram (Thompson *et al*, 2004). ESRH describes the potential for tornadic storm development within this effective inflow layer. Finally, CIN is a measure of the amount of energy preventing a parcel of air rising to a pressure level at which it can freely convect.

These atmospheric indicators will be compared for sea breeze and non-sea breeze storm days, followed by a consideration of non-storm days. They will be analysed using the Python module SHARPpy (Halbert, 2015), which allows for the calculation of atmospheric variables. The dataset that will be used is Brisbane Aero (number 040842) Upper Air Soundings, which will be analysed for the years 2000 to 2015.

3.4 Assessing the relative importance of various synoptic patterns

After concluding the analysis of the key localized indicators of atmospheric stability, the storm days will be considered in terms of regional synoptic conditions and features of the vertical atmospheric profile that accompanied these storms. The results of this section of the analysis will be qualitative and will focus on assessing the relative importance of these different factors rather than attempting to define specific ‘ideal severe storm conditions’.

The plot types that will be considered are: skew-t plots (generated using SHARPpy during the analysis); morning and afternoon surface synoptic meteorological conditions charts (generated using the Bureau of Meteorology maps portal); and NCEP NCAR reanalysis maps generated by the NOAA/ESRL Physical Sciences Division (drawn from their site http://www.esrl.noaa.gov/psd/).

The basis for the reanalysis data was created by Kalnay *et al*. (1996). These charts will comprise 850 mb*-200 mb wind shear, 850 mb geopotential height, 850 mb geopotential height monthly mean, 500 mb geopotential height and 200 mb vector wind*. A justification for this selection of varaiables is provided in Chapter 5.

Having described the algorithms that will be used to perform the sea breeze analysis and the forecasting tools that will be used to perform the storm analysis, the subsequent chapters of this thesis describe and discuss the results of the analysis. Chapter 4 provides the results of the sea breeze analysis, while Chapter 5 provides the results of the atmospheric vertical profile analysis along with a discussion of the relative usefulness of various synoptic charts for determining the likelihood of severe storms.

Note: although hectopascals (hPa) is generally favoured over millibars and is the SI unit, millibars has been used to maintain consistency with the NCEP NCAR reanalysis charts used in this chapter.

Chapter 4: Sea breeze analysis

This chapter discusses complications that arose in implementing the sea breeze algorithm of Soderholm et al. (2015) and presents the results of the most successful iteration of the sea breeze algorithm. This list of sea breeze days is compared to a list of storm events.

4.1 Initial results – complications in applying the algorithm of Soderholm et al. (2015)

The algorithm adapted from Soderholm *et al*. (2015), as described in the methodology, identified 1899 sea breeze days at Brisbane Airport during the analysis period, with a mean value of 128 sea breeze days per year. This figure is higher than the value derived by Soderholm *et al*. (2016) of 108 sea breeze days per year, and could indicate that some sea breezes occurred at Brisbane Airport weather station but did not propagate inland to the Archerfield station (25 km inland from the coast) analysed by Soderholm *et al.* (Figure 7). However, further analysis showed that there are inherent issues in applying the algorithm of Soderholm *et al.* to the Brisbane Airport site.

A comparison of the sea breeze days derived for Brisbane Airport to manually verified sea breeze days produced by Soderholm *et al*. (2016) at Archerfield showed that the algorithm identified only 32% of those days. Additionally, a comparison of these derived sea breeze days to a list of days on which no sea breeze occurred (according to manual identification) showed that 30% of non-sea breeze days were misidentified as sea breeze days. This suggested that this algorithm, in addition to failing to identify the majority of actual sea breeze days at Brisbane Airport, also produced a large proportion of false positives. Excluding the criterion that the sea breeze must be at least two hours in duration showed that the failure of the algorithm could be partly attributed to the algorithm being too restrictive. This amendment improved the percentage of manually verified sea breeze days detected to 57%. However, it also increased the percentage of false positives to 50%. Although the modified algorithm had some success in determining sea breeze days, it was not sufficiently accurate to allow for the use of these days as a record for comparison with thunderstorm occurrence.

The failure of the modified algorithm was unexpected, given that it was similar to the one used by Soderholm *et al*. (2016). A putative reason for this failure is the coastal location of Brisbane Airport. This type of algorithm detects a change in conditions with the passage of a boundary (i.e. the sea breeze front). Often the coast of Brisbane will have light synoptic northerly to northeasterly winds while surface friction and local wind circulations prevent these onshore winds from reaching further inland (i.e. Archerfield). Under these conditions the sea breeze front would first appear slightly inland rather than on the coast, and not be identifiable at Brisbane Airport. The sea breeze boundary will also likely strengthen as it moves inland from the ocean-modified coastal environment, making it easier to detect at Archerfield.

Although it did not produce a useable list of sea breeze dates, this stage of the analysis did demonstrate that this type of sea breeze algorithm must be implemented at a sufficiently inland locality where the sea breeze front will be better established. The selection of a further inland locality would increase the identification of sea breeze days and reduce the occurrence of false positives. In summary, the ocean-modified coastal environment not only limits what criteria can be used to identify the sea breeze (such as threshold changes in relative humidity or temperature) but also limits the applicability of this type of algorithm in a coastal location.

4.2 Identifying sea breeze days through strengthening onshore wind

Another approach to determining which days exhibited a strong sea breeze is by determining which days had increasing onshore easterly to northerly flow, a fingerprint that will be visible at the Brisbane Airport station. An advantage of this approach is that even if it only identifies a fraction of sea breeze days and includes some false positives, it nevertheless represents a physical process analogous to the sea breeze in terms of storm formation. One of the key reasons that the sea breeze is particularly important for storm genesis is that it brings moist air inland and produces wind shear. Including days with non-sea breeze increasing onshore flow in the analysis is just as valuable as a record that focusses more precisely on the passage of a sea breeze front. Additionally, a strong relationship exists between the sea breeze and increasing onshore flow (Figure 12).

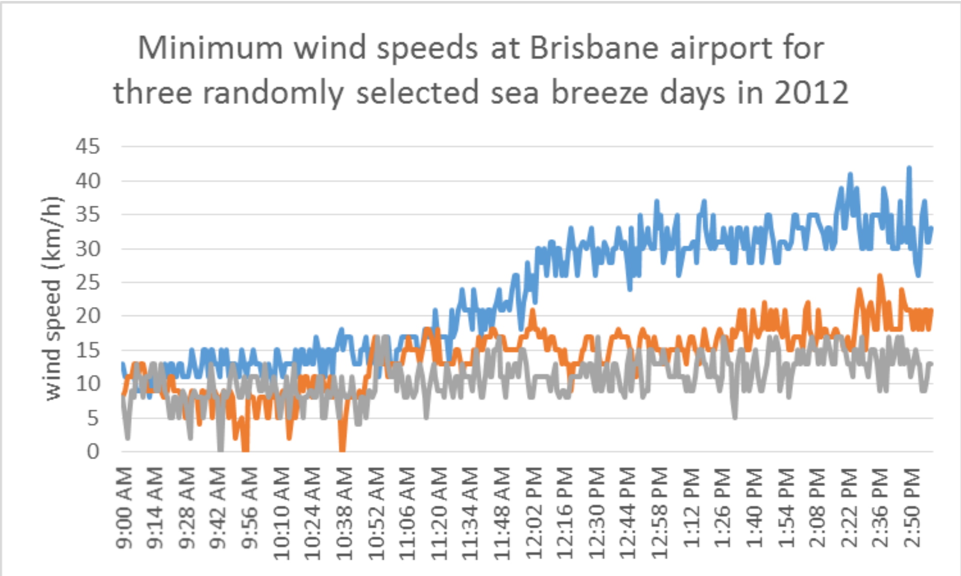

Figure 12: *Three randomly selected manually verified sea breeze days are shown above. Each of the three days exhibits an increase in wind speed from 0900 to 1500.*

Analysing the weather record in this way determined that, from March 2000 to the end of 2015, there were 1925 days that exhibited increasing onshore flow (within 10 to 110 degrees true) between 0900 and 1200. This list included 40% of all manually verified sea breeze days, with a misidentification rate of 23%. By limiting the algorithm to days on which the increasing onshore flow was particularly pronounced, 1231 days were identified. This limited the identification of manually verified sea breeze days to 31%, and also reduced misidentification to 10%.

Considering days in which onshore flow increased over the course of 0900 to 1500 (instead of 0900 to 1200) improved the accuracy of the results, producing a list of 2398 days. This list included 63% of manually verified sea breeze days and only 29% of manually verified non-sea breeze days. The amount of false positives could be reduced by considering only days in which the increase in onshore flow was particularly pronounced, producing a list of 1793 sea breeze days, which included 56% of manually verified sea breeze days and 18% of manually verified non sea breeze days. Restricting the list even further to only the most pronounced events produced a list of 1315 days, which included 44% of manually verified sea breeze days and only 11% of manually verified non-sea breeze days.

A final class of days considered in the analysis was days in which onshore wind increased between 1200 and 1500. This yielded a list of 2335 days, which included 67% of manually verified sea breeze days and 25% of manually verified non-sea breeze days. A more restricted list of 1801 days included 56% of manually verified sea breeze days, and only 17% of manually verified non-sea breeze days.

Given that both the 0900-1500 and 1200-1500 sets of dates produce results with similar accuracy, the choice of which set to use for further analysis had to be determined by other factors. The two lists shared only 70% of the same dates, suggesting that there would be a significant difference between using one compared to the other. It was ultimately decided that the two datasets could be combined, creating a new set that included all days in which onshore flow significantly strengthened from 0900 to 1500 and all unique dates from the 0900 to 1200 results, thereby including all dates in which the wind speed increased overall or in the morning. This combined list included 2108 days and included 61% of manually verified sea breeze days and only 21% of manually verified non-sea breeze days.

A final modification to this list was the removal of all days in the list that exhibited a decreasing wind speed in the afternoon. This created a list of 1965 days, but only marginally changed the accuracy of the list with respect to sea breeze identification. The identification of manually verified sea breeze days was reduced to 60% but this step also reduced the identification of false positives to 20%. Although it had marginal effect on the identification of sea breezes, this final step also removed days in which onshore flow was decreasing in the afternoon. This is useful because increasing onshore flow in the afternoon is analogous to the sea breeze in terms of its contribution to instability, so days in which this flow weakened in the afternoon were not relevant to the analysis. The temporal distribution of days across the analysis period is shown in Figure 13 and Figure 14.

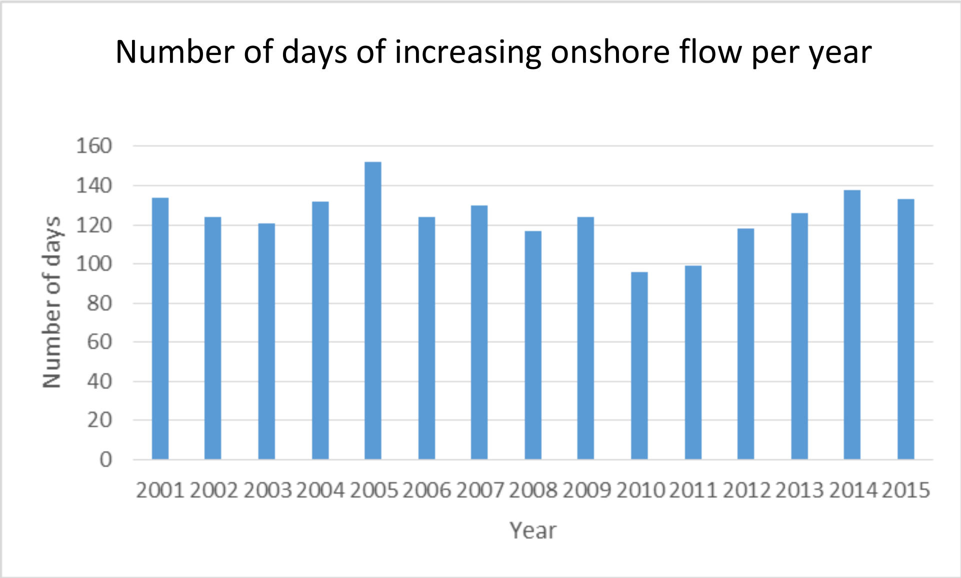

Figure 13: *Number of days of increasing onshore flow per year.*

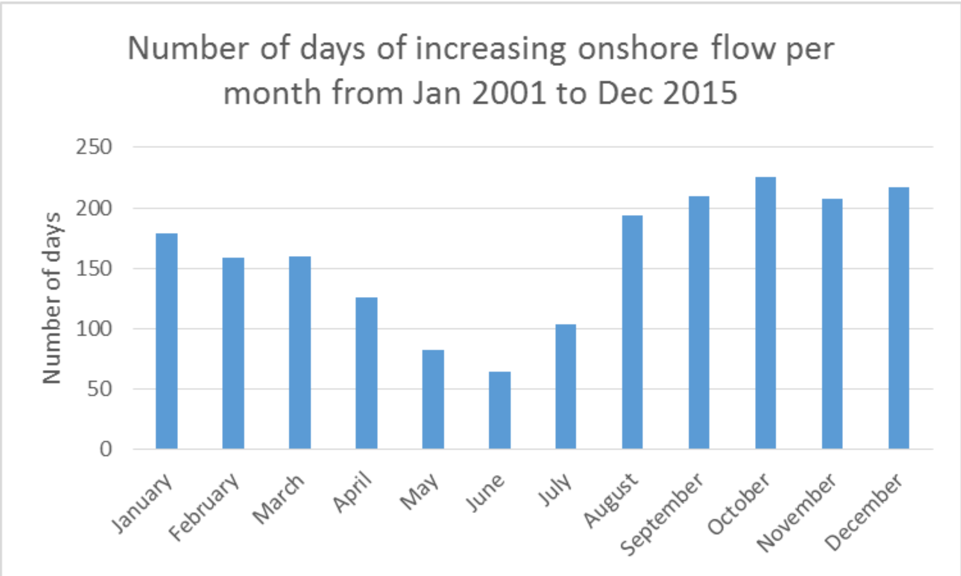

Figure 14: *Number of days of increasing flow per month from Jan 2001 to Dec 2015.*

4.3 Comparing sea breeze events with storm events

Using a latitude and longitude box centred on Brisbane as defined in the methodology, a list of storm days that satisfied a minimum MESH criterion of 21 mm was derived from the volumetric radar data created by Soderholm *et al*. (2015) (Table 2). These data suggest a significant correlation between storm occurrence and increasing onshore flow (sea breeze or otherwise). Of the storms that occurred in eastern Brisbane throughout the analysis period, 54% occurred in the list of 1965 days. The list of 1965 days represents 34% of the total number of days considered in the analysis, suggesting that the figure of 54% indicates a significant correlation between storms in eastern Brisbane and increasing onshore flow and/or the sea breeze. In other words, it is unlikely for as many as 54% of storm days to occur on a list that comprises only 34% of total days without there being a significant link between the two subsets. The nature of this dataset and its small size means that this conditional probability is the only significance test that can be applied until more data are gathered.

The sample size of the data is too small for drawing a meaningful conclusion regarding the variation of the ratio of sea breeze storms to non-sea breeze storms between different months and whether this ratio is dependent on the time of year. However, one interesting result was noted. The ratio of the sea breeze storms to non-sea breeze storms was the lowest in October. Given that the highest number of increasing onshore flow days occurred in October (Figure 14) this cannot be attributed to lower sea breeze prevalence, but may indicate a weakened relationship between the sea breeze and storm formation in October. This may be due to increased synoptic-scale activity becoming the dominant driver of storm occurrence in October, as discussed in section 5.3.

The relationship between the rate of increasing onshore flow and storm severity (described using MESH) is not linear (Figure 15). This relationship can be attributed to the fact that increasing onshore flow does not guarantee storm occurrence. 54% of severe storms (MESH equal to or greater than 21mm) occurred on days with increasing onshore flow (with a gradient of at least 0.5 km/h^2) yet most storm events clustered around gradients of 1.5-2.5 km/h^2, a trend that is pronounced for events greater than 21mm (above the red line). Higher gradient values did not appear to cause greater probability of storms, severe or otherwise, and may have even reduced the probability of storm formation.

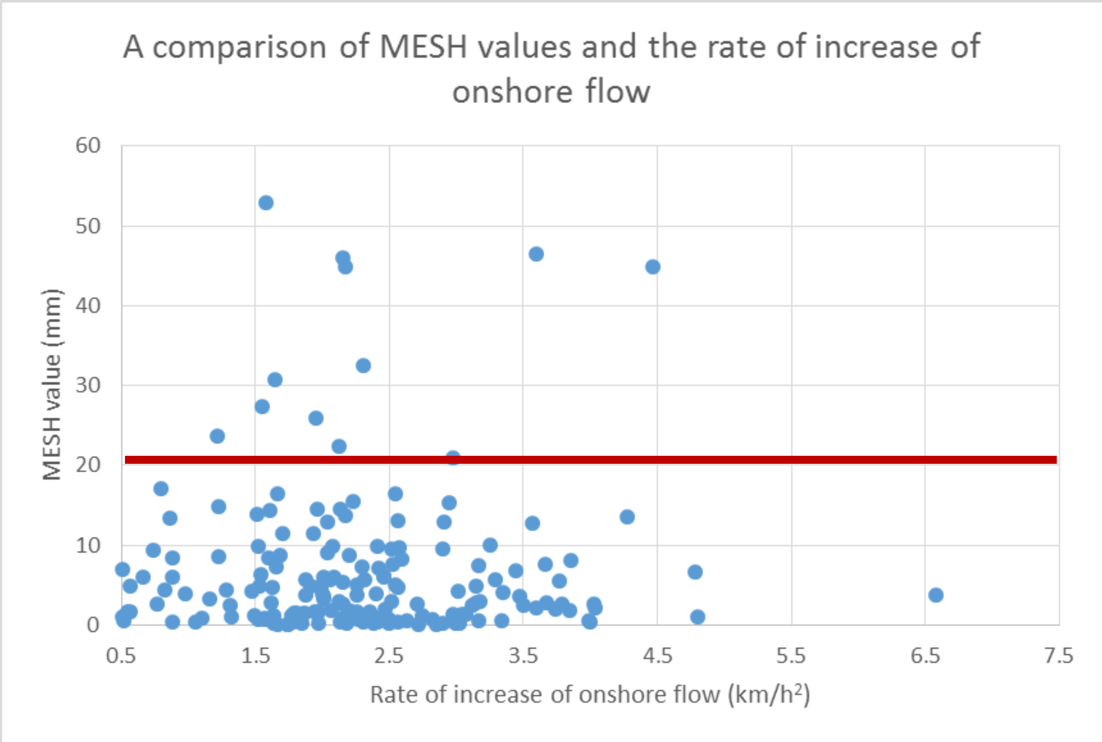

Figure 15: *A comparison of MESH values with the rate of increasing onshore flow shows that there is not a proportional relationship between this rate and the severity of the storm. The red line is the threshold MESH value for severe storms for this analysis (21mm).*

Table 2: *A list of known storm days for eastern Brisbane in the period 2000-2015. 54% of the events occurred on days in which a sea breeze or increasing onshore flow occurred. 'Number of storm cell instances' describes the number of 10 minute instances of a storm cell remaining within the lat-lon box described in the methodology.*

	Number of storm tracks on this day	Number of storm cell instances on this day	Sea breeze or increasing onshore flow day
17/01/2001	1	1	Y
19/02/2003	1	1	Y
26/10/2003	1	1	N
24/01/2004	1	1	Y
25/01/2004	1	1	Y
19/10/2004	1	1	N
9/11/2004	2	4	N
13/12/2004	1	2	N
26/03/2005	1	2	N
19/05/2005	1	1	Y
29/11/2005	2	4	Y
6/01/2006	2	5	Y
4/04/2006	1	1	Y
15/11/2006	2	5	Y
6/01/2008	1	1	N
21/09/2008	1	1	Y
21/10/2008	1	1	Y
16/11/2008	2	4	Y
20/11/2008	3	5	Y
12/08/2009	1	1	Y
17/11/2009	4	5	N
29/11/2009	1	1	N
22/12/2009	1	4	N
15/12/2010	2	5	Y
16/12/2010	3	4	N
3/01/2011	1	1	N
18/01/2011	2	2	N
21/02/2011	1	2	N
13/10/2011	1	2	N
15/10/2011	1	2	N
17/11/2012	1	1	N
18/11/2012	1	3	Y
18/11/2013	3	5	Y
24/11/2013	2	5	N
29/12/2013	1	1	Y
27/10/2014	1	4	Y
27/11/2014	1	4	Y
9/12/2014	2	5	Y
31/01/2015	1	5	Y

Having described the new algorithm for identifying the sea breeze and shown the clear link between the sea breeze and severe storm occurrence, the subsequent chapter presents the results of the radiosonde analysis and a discussion of synoptic conditions and other atmospheric data associated with storms for the analysis period. This is presented on a month-by-month basis.

Chapter 5: Vertical profile of the atmosphere and synoptic conditions analysis

This chapter describes the conditions that are conducive to storm conditions in eastern Brisbane. This includes whether a sea breeze is present, synoptic conditions, and the key descriptors of atmospheric stability produced by this analysis. First, the results of the vertical profile of the atmosphere analysis will be presented, comparing stability indicators between non-sea breeze storm days, sea breeze storm days and non-storm days for the main storm months of January, February, October, November and December. A summary of synoptic and mesoscale meteorological conditions is then presented for each storm day, with the storms again grouped into the main storm months. Framing this analysis around each month allows for a better characterisation of storm conducive conditions for each month and an assessment of the various forecasting tools for each month. Further discussion of these results and their implications will be provided in Chapter 6.

The analysis has already established that the sea breeze is conducive to storms, but this relationship also needs to be considered in the context of the broader meteorological drivers that produce storms for Brisbane. This chapter analyses descriptors of vertical changes in atmospheric conditions and the regional atmospheric circulation patterns using primarily surface synoptic charts, 850 mb geopotential height charts (both on the day of the storm and the average conditions for the month in which the storm occurred), 500 mb geopotential height charts, 850 mb-200 mb wind shear charts and 200 mb vector wind charts. The synoptic charts and reanalysis data that are referenced in this chapter are presented in the appendices along with the skew-t plots generated in this analysis. Given that most severe storms occur in the months of October to February, these are the only months considered in this analysis. The analysis throughout this chapter was completed through graphical interpretation of charts. For this reason, rather than trying to quantify precise 'ideal storm conditions', this chapter instead considers the charts in terms of their relative usefulness for predicting severe storm occurrence.

In order to capture the mesoscale processes affecting storm occurrence, skew-t plots were used to analyse the vertical profile of the atmosphere. CAPE, CIN, ESRH and other descriptors of the vertical profile of the atmosphere are most meaningful when describing a proximity sounding, but are nevertheless useful in this analysis. For the purposes of this analysis, a 'non-storm day' is a day in which a severe storm did not take place (i.e. the MESH value was lower than 21 mm). The results of this radiosonde analysis are presented in Figure 16 and 17. In general, the sea breeze allowed severe storms to take place despite marginal CAPE values and also allowed large CIN values to be overcome. The relationship between the sea breeze and ESRH is less clear, but the results indicate that the sea breeze may increase ESRH. In any case, more data is needed to clarify this particular relationship. The relationship between the sea breeze and these indicators varied for each storm month, and thus is discussed in more detail in each of the subsequent sections.

Before presenting the results, a justification for the choice of synoptic plots and reanalysis data used to characterise each storm day must be provided. A key assumption made in this analysis is that storms are generally more favoured on days in which there exists either low-level convergence or upper-level divergence. Storms are most likely to occur if both of these conditions exist. The surface synoptic charts allow for the identification of surface features that may affect the stability of the atmosphere such as low-pressure systems, low-pressure troughs, monsoon troughs and frontal systems.

Like surface pressure, low geopotential height may indicate a trough and can facilitate near-surface convergence and severe storm formation, while high geopotential height (a ridge) is associated with divergence and generally indicates more stable conditions. Low geopotential height typically occurs due to falling surface pressure (which is directly linked to lower-level convergence and instability) or due to cold air advection taking place below the pressure level considered. Cold air advection can result in storm occurrence through two key mechanisms (at the scale considered in this analysis). This can either be through the creation of positive buoyancy and isentropic lifting ahead of a cold front or surface trough, or through advection in the middle levels of the atmosphere (e.g. at the 850 mb to 700 mb pressure level), creating a less stable atmospheric profile (Sturman and Tapper, 2006). Therefore, 850 mb geopotential height charts allow for determining whether surface pressure features extend into the lower portion of the troposphere. Likewise, the 500 mb geopotential height chart will indicate whether lower atmosphere conditions extend into the middle atmosphere, or whether middle atmospheric instabilty has arisen independently of the lower atmosphere conditions.

By considering surface pressure and geopotential height, it can be determined whether low-level convergence is favoured and conditions are conducive to storms. Upper-level divergence, on the other hand, is identified using the 200 mb vector wind. Although it is not a specific descriptor of divergence, the 200 mb vector wind allows for the identification of which portions of the upper atmosphere are undergoing acceleration or deceleration. The primary feature visible in the vector wind graphs is the subtropical jet stream. Regions in which there are particularly high speeds (jet streaks) may indicate regions of upper-level divergence or convergence. The most important region is termed the Delta region, which is found on the bottom-right hand side of the jet streak (for the southern hemisphere), and which favours upper-level divergence. Additionally, the exit regions of the jet streaks in general tend to support lower-level convergence and lifting, as well as increased cyclonic vorticity at mid-level altitudes (Sturman and Tapper, 2006).

As discussed in Chapter 2, another key factor for the formation of well-organised and sustained storms is wind shear. As can be seen in Figure 18, wind shear between the 850 mb pressure level and 200 mb pressure level shares broad similarities with wind speed at 200 mb (as seen in the vector wind charts). This is primarily due to the fact that the strong 200 mb winds seen in the vector wind charts is perhaps the most significant source of the 850 mb-200 mb wind shear. Despite this similarity, there are enough differences between the charts in Figure 18 that it is not rigorous to use the 200 mb vector wind as a proxy for wind shear. Unfortunately, 850 mb-200 mb wind shear maps were not available for 2015.

Having justified their use in this analysis, these various charts and analysis tools are referenced throughout the following sections in order to characterise the conditions that led to the severe storms throughout the 16 year analysis period.

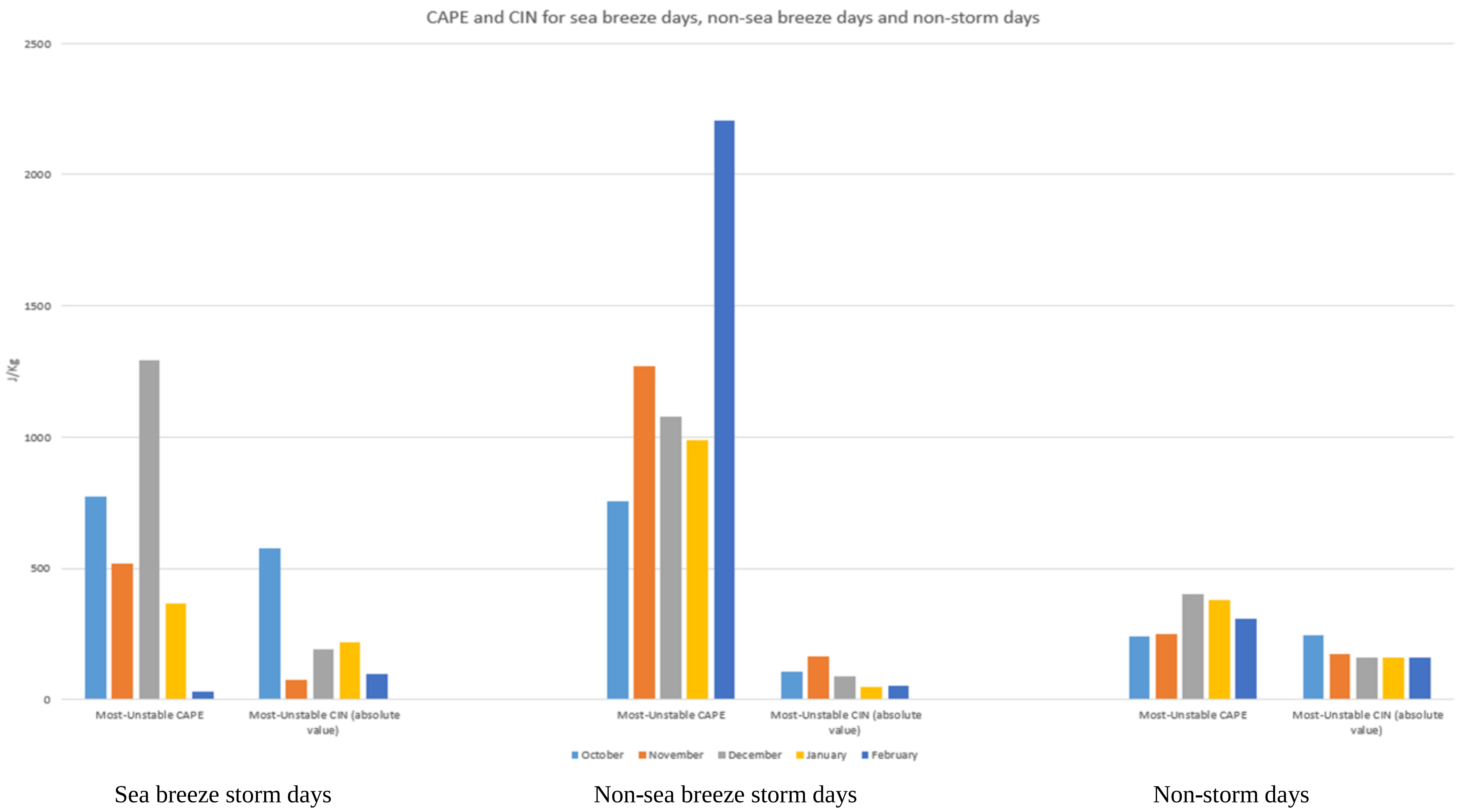

Figure 16: *Monthly (October-February) CAPE and CIN for sea breeze storm days, non-sea breeze storm days and non-storm days. This figure demonstrates that CAPE values tend to be the highest on non-sea breeze storm days and the lowest on non-storm days. The figure also suggests that the sea breeze allowed severe storms to develop despite the occurrence of high levels of CIN.*

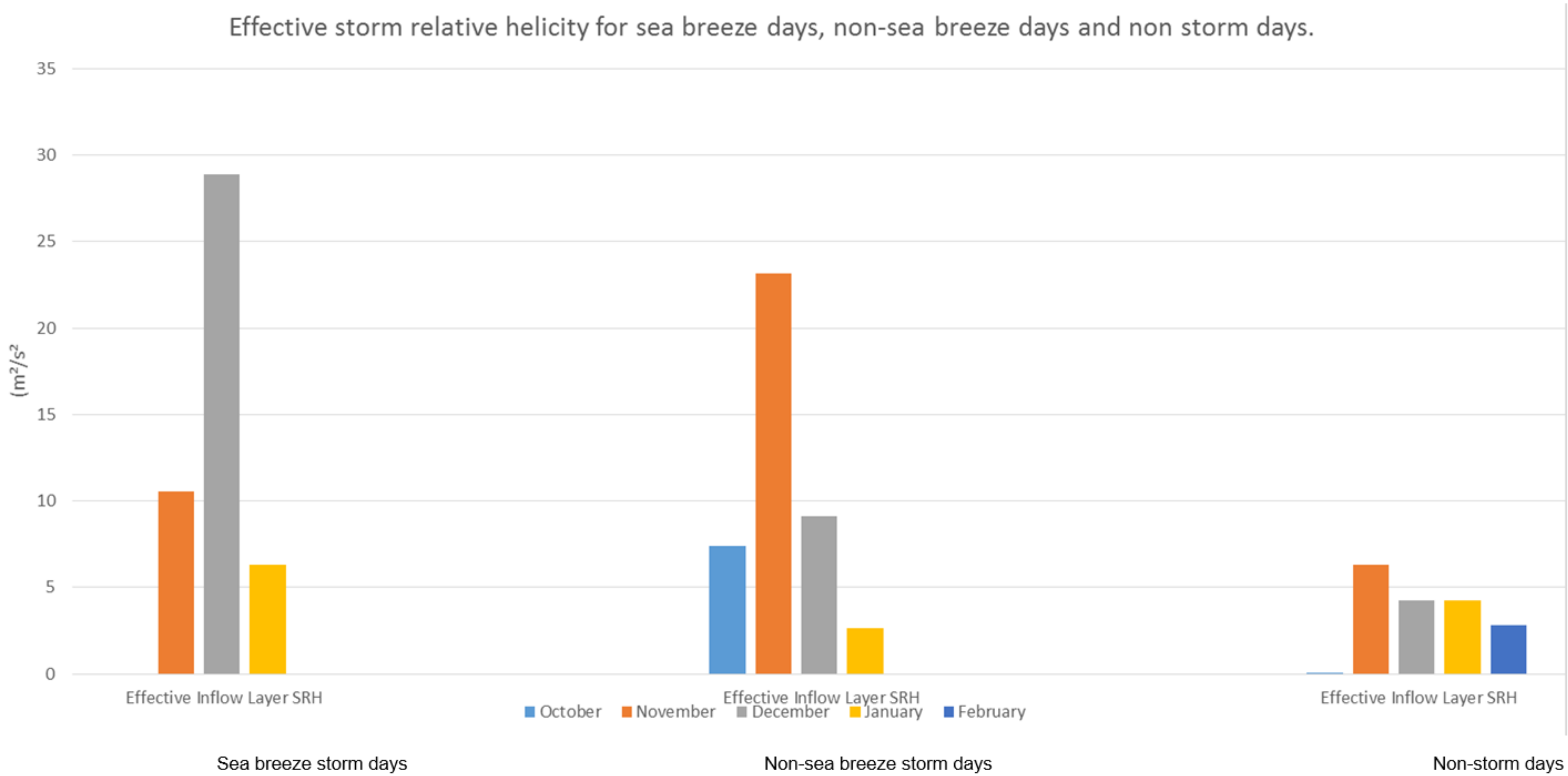

Figure 17: *Monthly (October-February) effective storm relative helicity for sea breeze storm days, non-sea breeze storm days and non-storm days. Although ESRH appears to be the highest on sea breeze days, more data must be used to allow for this conclusion to drawn more rigorously.*

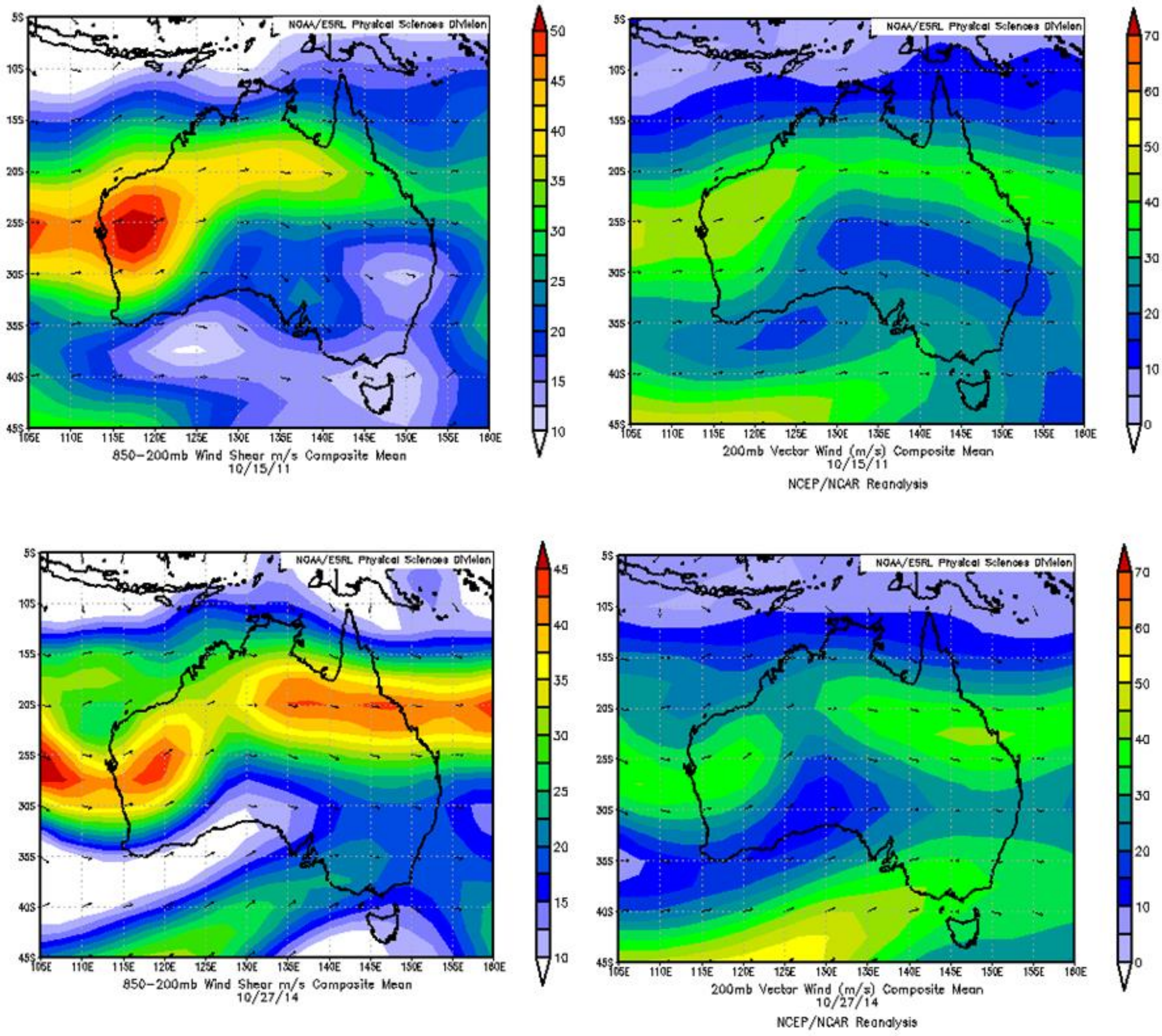

Figure 18: *The 850 mb-200 mb wind shear charts (left) and the 200 mb vector wind chart (right) for two storm days showing that the 200 mb vector wind is similar to, but cannot be used as a proxy for, 850 mb-200 mb wind shear.*

The following sections provide descriptions of the conditions that characterised storm days for each major storm month, with reference to the indicators of atmospheric stability presented in Figure 16 and 17 and to the synoptic charts, reanalysis charts and skew-t plots presented in the appendices. Given this analysis' goal of improving the predictive capacity of storm forecasters, these sections present the results in a tabulated and consistent manner in order to increase their accessibility for later reference.

5.1 January

CAPE

CAPE was significantly higher on non-sea breeze storm days than on sea breeze storm days for January (Figure 16, Table 8 and Table 9). However, non-storm days exhibited even lower CAPE. This suggests that some CAPE was required for either mode of storm for January, but that an increasing onshore wind lowered the threshold value of CAPE required for severe storm formation.

CIN

Similarly, for January storms, CIN was lower on non-sea breeze storm days than sea-breeze storm days, but the highest on non-storm days. This suggests that CIN did inhibit storm formation, but that an onshore wind could help overcome this inhibition for January storms.

ESRH

ESRH was higher on sea-breeze storm days than on non-sea breeze storm days for January, suggesting that an onshore wind had a significant effect on determining ESRH. Non-storm days displayed a slightly higher CAPE than sea-breeze storm days (Figure 17).

Vector wind

The conducive positioning of the jet streak, i.e. with its eastern segment located above Brisbane (which can facilitate lower-level convergence), occurred during some of the storm days for January and may have increased the likelihood of severe storms (Table 3). On other days, however, the positioning of the jet stream was less conducive to upper air divergence and lower-level divergence, suggesting that severe weather could develop regardless of the positioning of jet streaks during January. The conducive positioning of the jet streak, therefore, was not a strictly necessary component for severe storm formation.

Geopotential height and surface synoptics

Similarly, the use of surface synoptic charts, 850 mb geopotential height charts and 500 mb geopotential height charts shows that the positioning of surface and lower-middle atmospheric troughs above Brisbane is a component for some storm events, indicating that these conditions are of course conducive to storm formation but not a strictly necessary requirement. According to the results summarised in Table 3, the presence of a temperature inversion was also a key factor for storm formation for some events.

Mesoscale processes

All of the days that exhibited increasing onshore flow also exhibited a near-surface temperature inversion.

Wind shear

850 mb-200 mb wind shear for January storm days ranged between 15 m/s and 27.5 m/s. Although these values would have favoured more organised and stable storms, they are low compared to the late spring/early summer wind shear values discussed later.

Table 3 : *(continued next page) – Description of synoptic conditions, geopotential height and vector wind conditions for storm events in January.*

Event	Increasing onshore flow	Event Description
31/1/2015	Yes	Refer to Appendix 1: January: 31/1/2015. The skew-t plot shows a minor near-surface temperature inversion. The 200 mb vector wind charts shows that Brisbane was located between two jet streaks, meaning that the upper atmosphere was probably neutral in terms of convergence/divergence. A surface low-pressure trough was located just to the east of Brisbane. 850 mb geopotential height was below that month's average, indicating a lower atmosphere trough. This trend can also be seen in the 500 mb geopotential height graph, with a trough axis extending through Brisbane. Tropical cyclone Ola was present to the south of Papua New Guinea. No 850 mb-200 mb wind shear graph was available for this day.
6/1/2006	Yes	Refer to Appendix 1: January: 6/1/2006. The skew-t plot shows a minor near-surface temperature inversion. The 200 mb vector wind charts show that Brisbane was situated to the north-west of the closest jet-streak, indicating that upper-level divergence was unlikely to be taking place. While a low-pressure system was centred to the west of Brisbane, the 850 mb geopotential height chart does not indicate a low-level trough. A minor trough axis extended to the west of Brisbane for the 500 mb geopotential height. 850 mb-200 mb wind shear was 15 m/s, low compared to the southern surrounding regions.
25/1/2004	Yes	Refer to Appendix 1: January: 25/1/2004. The skew-t plot shows a minor temperature inversion. The 200 mb vector wind shows Brisbane to the eastern side of the jet streak but not in the Delta zone. This suggests that lower-level convergence was favoured but not necessarily upper-level divergence. The synoptic chart indicates that Brisbane was within a relatively low-pressure region, but quite distant from the low-pressure trough. Compared to both the surrounding region and that month's average, the 850 mb geopotential height exhibited a slightly above average geopotential height for that day, but was also centred under a minor trough axis. The 500 mb geopotential height showed no clear trends were present above Brisbane. Likely due to the presence of the jet stream, 850 mb-200 mb wind shear was high on this day, with a value of 27.5 m/s.
24/1/2004	Yes	Refer to Appendix 1: January: 24/1/2004. The skew-t plot shows a minor temperature inversion. The 200 mb vector wind shows that Brisbane is directly under the eastern part of the maximum of the jet streak, suggesting that lower-level convergence may be favoured, but not necessarily upper-level divergence. The synoptic chart indicates that Brisbane was within a relatively low-pressure region, but quite distant from the low-pressure trough. Compared to both the surrounding region and that month's average, the 850 mb mid/low-level atmosphere exhibited a trough above Brisbane. The 500 mb geopotential height shows no clear trends were present above Brisbane. Likely due to the presence of the jet stream, 850 mb-200 mb wind shear was high on this day with a value of 32.5 m/s.
18/1/2011	No	Refer to Appendix 1: January: 18/1/2011. The 200 mb vector wind shows that Brisbane is to the northeast of a jet streak, which may have resulted in a more favourable environment for low-level convergence. A surface trough was present to the west of Brisbane, also favouring low-level convergence. A trough is also present in the 850 mb geopotential height, compared to the surroundings and that month's average. The 500 mb geopotential height chart shows a minor ridge was to the west of Brisbane. 850 mb-200 mb wind shear was 17.5 m/s, low compared to the southern surrounding regions.

Event	Increasing onshore flow	Event Description
3/1/2011	No	Refer to Appendix 1: January: 3/1/2011. Brisbane was sufficiently far from the jet streak that the jet streak was unlikely to have influenced the presence of either divergence or convergence in the upper atmosphere. Two surface troughs were located to either side of Brisbane, suggesting that, although pressure was generally low, surface air would have been diverging at Brisbane towards these two troughs. At 850 mb, however, a significant trough was centred to the right of and encompassing Brisbane, which would have promoted low-level convergence. This system was not present on the monthly average chart. The 500 mb geopotential chart shows a very significant trough was above Brisbane. 850 mb-200 mb wind shear was 17.5 m/s, low compared to the southern surrounding regions.
6/1/2008	No	Refer to Appendix 1: January: 6/1/2008. The 200 mb vector wind shows that Brisbane was located in the eastern segment of a jet streak, meaning that the upper-air was not favourable to lower-level convergence. A surface trough was present to the west of Brisbane, favouring low-level convergence. A trough is also present in the 850 mb geopotential height, compared to the surroundings and that month’s average. A very strong trough in the 500 mb geopotential height chart can also be seen above Brisbane. 850 mb-200 mb wind shear was 22.5 m/s, low compared to the southern surrounding regions.

5.2 February

CAPE

CAPE was significantly higher on non-sea breeze storm days than on sea breeze storm days for February. Non-storm days exhibited slightly higher CAPE than sea breeze storm days (Figure 16, Table 11 and Table 12). This suggests that an increasing onshore wind lowered the threshold value of CAPE required for storm formation throughout this month.

CIN

Similarly, for February storms, CIN was lower on non-sea breeze storm days than sea-breeze storm days, but the highest on non-storm days. This suggests that CIN did inhibit storm formation, but that an onshore wind could help overcome this inhibition for February storms.

ESRH

Not enough meaningful measurements of ESRH were present in the results to draw any conclusions about trends in ESRH throughout February (Figure 17).

Vector wind

Due to a limited sample size (two storm days), the effect of the positioning of the jet stream was unable to be determined (Table 4). However, given the occurrence of storms in the absence of its conducive effect on upper air divergence and lower air convergence, it can be stated that the conducive positioning of the jet stream is not strictly necessary for the formation of severe storms during February.

Geopotential height and surface synoptics

Similarly, the use of surface synoptic charts, 850 mb geopotential height charts and 500 mb geopotential height charts shows that the positioning of surface and lower to middle atmospheric troughs above Brisbane has been a component for some storm events, indicating that these conditions are of course conducive to storm formation but not a strictly necessary component for February storms.

Wind shear

850 mb-200 mb wind shear for February storm days ranged between 17.5 m/s and 27.5 m/s. Although these values would have favoured more organised and prolonged storms, they are low compared to the late spring/early summer wind shear values discussed later.

Table 4: *Description of synoptic conditions, geopotential height and vector wind conditions for storm events in February.*

Event	Increasing onshore flow	Event Description
19/2/2003	Yes	Refer to Appendix 2: February: 19/2/2003. An amorphous and complex jet streak was present over southeast Australia, with Brisbane located to the north of the maximum. The effect of this complex jet streak is too difficult to assess. The synoptic chart shows that no low-pressure system was present at Brisbane. The 850 mb chart shows that the low-middle level of the atmosphere was exhibiting a ridge above Brisbane, indicating stable conditions. The 500 mb geopotential height chart shows a ridge was centred over eastern Australia and a trough centred offshore, suggesting no clear trend for Brisbane. 850 mb-200 mb wind shear was 27.5 m/s, low compared to the southern surrounding regions.
21/2/2011	No	Refer to Appendix 2: February: 21/2/2011. The 200 mb vector wind shows that a jet streak was located to the southwest of Brisbane and another to the southeast, implying no discernible impact on upper air divergence. A surface low-pressure trough was located very close to Brisbane, accompanied by a slightly lower than average (for the month) geopotential height at 850 mb. Surface conditions, therefore, were very conducive to lower-level convergence. The troughs and ridges of the 500 mb geopotential height chart roughly mirror those of the 850 mb chart, but are not indicative of either middle level stability or instability for that day. 850 mb-200 mb wind shear was 17.5 m/s, low compared to the southern surrounding regions.

5.3 October

CAPE

CAPE was very similar for sea-breeze storm days and non-sea breeze storm days, and significantly lower for non-storm days throughout October (Figure 16, Table 14, and Table 15). This suggests that an increasing onshore wind had less impact on lowering the threshold value of CAPE required for storm formation throughout this month compared to the other months considered.

CIN

However, for October storms, CIN was lower on non-sea breeze storm days than non-storm storm days, but the highest on sea-breeze storm days. This suggests that CIN did inhibit storm formation, but that an onshore wind can help overcome this inhibition for October storms.

ESRH

Not enough meaningful measurements of ESRH were present in the results to draw any conclusions about trends in ESRH throughout October (Figure 17).

Vector wind, geopotential height and surface synoptics

As for the other months considered, the conducive positioning of the jet streak, the presence of surface troughs or lower-middle level geopotential height troughs and a temperature inversion are all conducive to severe storm formation, but not strictly necessary (Table 5). Most of the storm days considered in this analysis for October exhibited 850 mb and 500 mb geopotential height troughs. The lower CAPE values occurring during this month suggest that these synoptic-scale contributors to instability are of more importance during October than for the summer months and even November (in which CAPE values are generally higher than October). This is especially evident for the positioning of the jet streak, with some of the storm days exhibiting optimal 200 mb vector wind conditions (i.e. with the delta region of a jet streak positioned above Brisbane).

Wind shear

850 mb-200 mb wind shear for October storm days ranged between 17.5 m/s and 47.5 m/s. Although these values are higher than for January and February and would have significantly favoured more organised and sustained storms, they are nevertheless low compared to the late spring/early summer wind shear values discussed later.

Table 5: *Description of synoptic conditions, geopotential height and vector wind conditions for storm events in October.*

Event	Increasing onshore flow	Event Description
27/10/2014	Yes	Refer to Appendix 3: October: 27/10/2014. The skew-t plots for this day show significant levels of CAPE, and are of particular significance because they show a clear temperature inversion in the lower atmosphere, a feature which postpones convection until the late afternoon and allows for production of greater CAPE and eventually explosive convection. The 200 mb vector wind shows that Brisbane was located in the delta region of a jet streak of the subtropical jet-stream, favouring upper air divergence and lower-level convergence. A low-pressure surface trough was also present to the west of Brisbane, further favouring lower-level convergence. The 850 mb chart however indicates a very shallow trough axis over Brisbane in the low-middle atmosphere, which can be seen to be more shallow and to shift westward in the 500 mb geopotential height chart. 850 mb-200 mb wind shear was 22.5 m/s, low compared to the northern surrounding regions.
15/10/2011	No	Refer to Appendix 3: October: 15/10/2011. The 200 mb vector wind indicates that Brisbane was to the south of a small jet streak, indicating no clear effect on upper lever divergence. Brisbane was located between low and high-pressure systems, with no clear signal of lower-level convergence. The 850 mb chart shows a significant low-middle air trough extending north to Brisbane, favouring lower-level convergence. This trough can also be seen in the 500 mb geopotential height chart. 850 mb-200 mb wind shear was 17.5 m/s, low compared to the northern surrounding regions.
19/10/2004	No	Refer to Appendix 3: October: 19/10/2004. The 200 mb vector wind indicates that Brisbane was to the west of the maximum of a jet streak, which is not indicative of favourable conditions for upper air divergence. A low-pressure trough was present significantly inland of Brisbane, and a trough is present in the geopotential height at 850 mb, suggesting conditions were favourable for lower-level convergence. Interestingly, this trough strengthened and became more coherent in the 500 mb geopotential height. Likely due to the presence of a nearby jet streak, the 850 mb-200 mb wind shear was 47.5 m/s, quite high compared to the other storm events in October.
26/10/2003	No	Refer to Appendix 3: October: 26/10/2003. The skew-t plot shows a small but significant temperature inversion in the low atmosphere. The 200 mb vector wind indicates that Brisbane is in the delta region of the nearest jet streak, obfuscated slightly by another jet streak to the east. This nevertheless indicates favourable conditions for upper air divergence. A surface pressure trough is present far to the west of Brisbane, but may have nevertheless favoured lower-level convergence. This is supported by an 850 mb geopotential height trough extending from the Tasman sea to Brisbane. This trough can be seen in the 500 mb geopotential height chart but was shallower, with a less clear effect on Brisbane. 850 mb-200 mb wind shear was 22.5 m/s, low compared to the northern surrounding regions.

5.4 November

CAPE

CAPE was significantly higher on non-sea breeze storm days than on sea breeze storm days for November. Non-storm days exhibited lower CAPE than sea-breeze storm days (Figure 16, Table 17 and Table 18). This suggests that an increasing onshore wind lowered the threshold value of CAPE required for storm formation throughout this month.

CIN

CIN was very low for all days throughout November. It was the lowest on sea-breeze storm days and the highest on non-storm-days. These results were inconsistent with the other months.

ESRH

ESRH was the highest for non-sea breeze storm days. This is contrary to the results for January and December, which suggested that an onshore wind led to an increased ESRH. The lowest values, however, were on non-storm days (Figure 17).

Vector wind, geopotential height and surface synoptics

As for the other months considered, the conducive positioning of the jet streak, the presence of surface troughs or lower to middle level geopotential height troughs and a temperature inversion are all conducive to severe storm formation, but not strictly necessary (Table 6). However, the majority of the events did occur when a surface trough was close to Brisbane, indicating that this is the most important factor for severe storm formation in November, along with vertical atmospheric instability (as indicated by CAPE, CIN, etc.).

Wind shear

850 mb-200 mb wind shear for November storm days ranged between 7.5 m/s and 52.5 m/s. Most of these values are significantly higher than for the other months considered (with the exception of December). These consistently high wind shear values in November would have significantly favoured the better organisation and longevity of storms during this month, and may account for the more frequent occurrence of storms in November compared to the other months considered in this analysis.

Table 6: *(continued next page) - Description of synoptic conditions, geopotential height and vector wind conditions for storm events in November.*

Event	Increasing onshore flow	Event Description
27/11/2014	Yes	Refer to Appendix 4: November: 27/11/2014. Note: this event is the major storm event of November 2014, and produced in excess of a billion AUD in damages. The 200 mb vector wind shows that Brisbane was present in the delta region of a jet streak, promoting upper air divergence. A low-pressure trough was directly adjacent to Brisbane in the afternoon, suggesting an optimal combination of lower-level convergence and upper-level divergence. No significant trend was present in the 850 mb or 500 mb geopotential height charts. Likely due to the presence of a nearby jet streak, 850 mb-200 mb wind shear was 32.5 m/s, high compared to the lower shear conditions typical of the other months considered in the analysis.
18/11/2012	Yes	Refer to Appendix 4: November: 18/11/2012. The skew-t plot shows a minor temperature inversion preceding this event. Brisbane was located within the southern section a jet streak, with no clear effect on upper air divergence. A surface pressure trough was present directly over Brisbane on the afternoon of the storm suggesting conditions very favourable for lower-level convergence. The 850 mb geopotential height exhibited a weak trough above far east Australia, which was mirrored in the 500 mb geopotential height chart. Likely due to the presence of a nearby jet streak, 850 mb-200 mb wind shear was 45 m/s, high compared to the lower shear conditions typical of the other months considered in the analysis.
15/11/2006	Yes	Refer to Appendix 4: November: 15/11/2006. The skew-t plot shows a minor temperature inversion preceding this event. Brisbane was present in the western segment of a jet streak, suggesting no clear favourability for upper-level divergence. A surface trough was present close to Brisbane, and supported by anomalously low 850 mb geopotential height (a very strong trough), suggesting high favourability for lower-level convergence. This trough extended into the 500 mb geopotential height chart (becoming shallower). Possibly due to the presence of a nearby jet streak, 850 mb-200 mb wind shear was 35 m/s, high compared to the lower shear conditions typical of the other months considered in the analysis.
29/11/2005	Yes	Refer to Appendix 4: November: 29/11/2005. Brisbane was located between low and high-pressure systems, with no clear signal of lower-level convergence. The 850 mb geopotential height chart shows a significant deviation from that month’s average conditions for that variable, indicating moderate favourability for lower-level convergence, supported by a strong trough above southeastern Australia in the 500 mb geopotential height chart. 850 mb-200 mb wind shear was low compared to the northern surrounding regions, at 27.5 m/s.
24/11/2013	No	Refer to Appendix 4: November: 24/11/2013. The 200 mb vector wind shows that Brisbane was located under the centre of a jet streak maximum, with no clear effect on upper-level divergence. A surface trough was adjacent to Brisbane, supported by anomalously low 850 mb and 500 mb geopotential height (with clear troughs present at both pressure levels), suggesting a clear mechanism for lower-level convergence. Likely due to the presence of a nearby jet streak, 850 mb-200 mb wind shear was 52.5 m/s, especially high even compared to the generally high wind shear conditions of November.

Event	Increasing onshore flow	Event Description
17/11/2013	No	Refer to Appendix 4: November: 17/11/2013. The 200 mb vector wind shows that Brisbane was located in the western segment of the maximum of a jet streak, with no clear mechanism for upper-level divergence. A surface trough was present directly over Brisbane, along with a relatively low 850 mb geopotential height compared to that month's average (a minor trough), providing a mechanism for lower-level convergence. No clear trends are present in the 500 mb geopotential height chart for that day. Likely due to the presence of a nearby jet streak, 850 mb-200 mb wind shear was 37.5 m/s, high compared to the lower shear conditions typical of some of the other months considered in the analysis.
29/11/2009	No	Refer to Appendix 4: November: 29/11/2013. The 200 mb vector wind shows that Brisbane was located in the western segment of the maximum of a jet streak, with no clear mechanism for upper-level divergence. A surface trough is located to the west of Brisbane, along with a relatively low 850 mb geopotential height above Brisbane compared to that month's average, providing a clear mechanism for lower-level convergence. The trough in the 850 mb geopotential height was supported by a trough in the 500 mb geopotential height. Likely due to the presence of a nearby jet streak, 850 mb-200 mb wind shear was 45 m/s, high compared to the lower shear conditions typical of some of the other months considered in the analysis.
17/11/2009	No	Refer to Appendix 4: November: 17/11/2009. The skew-t plot shows a clear near-surface temperature inversion above Brisbane. The 200 mb vector wind shows that Brisbane was located in the southwestern segment of a jet streak, providing no clear mechanism for upper-level divergence. A surface trough was located significantly south of Brisbane, migrating over Brisbane during the day, supported by the 850 mb geopotential above Brisbane being slightly lower than that month's average. No clear trends are visible in the 500 mb geopotential chart for that day. 850 mb-200 mb wind shear was 7.5 m/s, low compared to the high shear regions over Northern Queensland.
9/11/2004	No	Refer to Appendix 4: November: 9/11/2004. Brisbane was located to the southeast of a major jet streak (the delta region) but this is obfuscated by another jet streak located further east. Upper air divergence is therefore hard to discern. A surface trough was present over Brisbane during the day, however a relatively high 850 mb geopotential height compared to that month's average was present above Brisbane. A shallow 500 mb geopotential height trough was present over eastern Brisbane. Likely due to the presence of a nearby jet streak, 850 mb-200 mb wind shear was 52.5 m/s, high compared to the lower shear conditions typical of some of the other months considered in the analysis.

5.5 December

CAPE

CAPE was slightly higher on sea breeze storm days than on non-sea breeze storm days for December. However, non-storm storm days exhibited the lowest CAPE (Figure 16, Table 20 and Table 21). This means that, unlike the other months considered, in December, the sea breeze may have increased the threshold CAPE required for a severe storm.

CIN

For December storms, CIN was the lowest on non-sea breeze storm days and the highest on sea-breeze storm days. This suggests that onshore wind can help overcome convective inhibition for January storms.

ESRH

ESRH was higher on sea-breeze storm days than on non-sea breeze storm days for December, suggesting that onshore wind had a significant effect on determining ESRH for this month (Figure 17).

Vector wind, geopotential height and surface synoptics

As for the other months considered, the conducive positioning of the jet streak, the presence of surface troughs, lower and middle level geopotential height troughs and a temperature inversion are all conducive to severe storm formation, but not strictly necessary (Table 7). Most events did occur when a surface trough was close to Brisbane, indicating that this is the most important factor for severe storm formation in December, along with vertical atmospheric instability (as indicated by CAPE, CIN, etc.). Interestingly, most storm days did also exhibit 200 mb vector wind conditions conducive to upper air divergence, suggesting that upper air divergence may a play a more important role in storm formation for December (at least compared to the other summer months).

Wind shear

850 mb-200 mb wind shear for December storm days ranged between 22.5 m/s and 57.5 m/s. Most of these values are significantly higher than for the other months considered (with the exception of November). These consistently high wind shear values in December would have significantly favoured the better organisation and longevity of storms during this month.

Table 7: *(continued next page) - Description of synoptic conditions, geopotential height and vector wind conditions for storm events in December.*

Event	Increasing onshore flow	Event Description
9/12/2004	Yes	Refer to Appendix 5: December: 9/12/2004. Brisbane was located under the eastern segment of a jet streak, providing a mechanism for enhanced lower-level convergence. A surface pressure trough was present over Brisbane, further contributing to lower-level convergence. The 850 mb geopotential height shows a relatively low value height above Brisbane compared to that month's average. A significant 500 mb geopotential height trough was present above South Australia, and its presence may have influenced the middle level air above Brisbane. Likely due to the presence of a nearby jet streak, 850 mb-200 mb wind shear was 57.5 m/s, high compared to the lower shear conditions typical of some of the other months considered in the analysis.
29/12/2013	Yes	Refer to Appendix 5: December: 29/12/2013. The skew-t plot shows a significant temperature inversion on this day. Brisbane was located in the eastern segment of a jet streak, nearby to a surface trough and with a relatively low 850 mb geopotential height (compared to that month's average), providing a clear mechanism for lower-level convergence. This trough is also present in the 500 mb geopotential height chart, but was positioned more to the east. 850 mb-200 mb shear was low compared to the southern surrounding regions at 22.5 m/s.
16/12/2010	Yes	Refer to Appendix 5: December: 16/12/2010. A minor temperature inversion was present on this day. Brisbane was located in the eastern segment of a jet streak, which supports lower-level convergence. Brisbane showed no clear trend in surface conditions, but exhibited lower than average 850 mb geopotential height, with a shallow trough extending through Brisbane. The 500 mb geopotential height chart shows a very shallow trough extending along the east coast of Australia for that day. Likely due to the presence of a nearby jet streak, 850 mb-200 mb wind shear was 37.5 m/s, high compared to the shear conditions typical of some of the other months considered in the analysis.
22/12/2009	No	Refer to Appendix 5: December: 22/12/2009. A small near-surface temperature inversion was present on this day. Brisbane was located in the delta region of a jet streak, providing a mechanism for upper air divergence. Surface conditions and 850 mb geopotential height, however, showed no clear mechanism for lower-level convergence. The 500 mb geopotential height chart, on the other hand, shows a distinct but broad trough above eastern Australia for that day. 850 mb-200 mb shear was low compared to the western surrounding regions at 22.5 m/s.

13/12/2004	No	Refer to Appendix 5: December: 13/12/2004. A significant near-surface temperature inversion was present on this day. Brisbane was located in the northern segment of a jet streak, providing no clear mechanism for upper air divergence. Over the course of the day a low-pressure system moved close to Brisbane, providing a mechanism for lower-level divergence, which was supported by an anomalously low 850 mb geopotential height above Brisbane compared to that month's average. The 850 mb geopotential height trough was supported by a broad but significant 500 mb geopotential height trough centred over Tasmania but which extended across much of eastern Australia. Likely due to the presence of a nearby jet streak, 850 mb-200 mb wind shear was 35 m/s, high compared to the lower shear conditions typical of some of the other months considered in the analysis.

Having provided a tabulated and graphical description of conditions that are conducive to storms for the major storm months and demonstrating the relationship between the sea breeze and indicators of atmospheric instability, the subsequent chapter, Discussion and conclusions, describes the key outcomes of this thesis. A flow chart is presented which synthesises the results presented in Chapter 4, Chapter 5 and the appendices.

Chapter 6: Discussion and Conclusions

This chapter describes the key outcomes of this analysis, as presented in the previous two chapters of this thesis. This includes a discussion of the development of the novel sea breeze algorithm, the analysis of the vertical profile of the atmosphere, and the analysis of the synoptic and reanalysis meteorological conditions. Along with presenting future options for extending this analysis, the contextual relevance and significance of this analysis are considered.

6.1 Sea breeze analysis

6.1.1 Inapplicability of the algorithm of Soderholm *et al*. (2015) to the ocean-modified coastal environment

As discussed in section 4.1, the sea breeze algorithm created by Soderholm *et al*. (2015) was adapted to Brisbane Airport weather station data, with limited success. In section 4.2, the ocean-modified coastal environment obfuscated the signal in the weather data that the algorithm of Soderholm *et al*. (2015) was designed to identify. Although the results presented in section 4.1 were therefore unusable for further analysis, they were evidence of the inapplicability of algorithms that detect the passage of the sea breeze front to the ocean-modified coastal environment. Although these results are intuitive, it was nevertheless an important step to demonstrate the non-applicability of this type of algorithm to an ocean-modified coastal environment.

6.1.2 Applicability of detecting the sea breeze through increasing onshore flow

In contrast to an algorithm that detects the passage of the sea breeze front, the algorithm developed in this thesis that detects sea breeze events via increasing onshore flow has applicability in the ocean-modified coastal environment. Additionally, for analyses that are specifically considering the role of the onshore flow component of the sea breeze in determining atmospheric stability and the initiation of storms, the expansion of the analysis from strictly defined sea breeze days to a more inclusive set of days that exhibited increasing onshore flow was valid because it nevertheless allows for a consideration of this component of the sea breeze, that is, increasing onshore flow.

However, when considering these results for potential future studies of the sea breeze, the demonstrated superiority of the algorithm of Soderholm *et al*. (2015) at accurately identifying sea breeze events must be considered. If the weather station in question is proximal to the coast but outside of the ocean-modified coastal environment, the demonstrated efficacy of an algorithm that detects the passage of the sea breeze front within that particular setting suggests that it should be used in lieu of the method developed in this thesis. Additionally, if the key focus of any future research is not specifically storm analysis, but rather the creation of an accurate list of sea breeze events, the significant number of false positives produced from the method developed in this thesis indicates that it should not be used for that purpose. If only weather station data from within the ocean-modified coastal environment are available, however, then the demonstrated superiority of the increasing onshore flow algorithm for that purpose suggests it should be used in lieu of the original algorithm. In other words, the strength of the new algorithm is its applicability to coastal weather stations that are very close to the ocean, and for which a further inland station is not available.

6.2 Storm analysis

6.2.1 Comparing the occurrence of onshore flow events to severe storm events

As discussed in section 4.3, the conditional probability of a severe storm event occurring during the analysis period given that the day had exhibited increasing onshore flow was 54%. The level of coincidence between these two sets was significant, especially because of the size of the universal set (i.e. all dates considered in the analysis, comprising nearly 16 years). This result accords with the literature discussed in section 2.2.2, especially the results of Soderholm *et al*. (2015) and Peter *et al.* (2015). This analysis' results and the precedent analyses discussed in section 2.2.2 show that when forecasters assess the likelihood of severe storm development over Brisbane (and for any region with a significant sea breeze), the presence or absence of the sea breeze (and relevant onshore airflow more generally) must be considered.

6.2.2 Key indicators of atmospheric stability

As discussed in section 5.1 to 5.6, comparing sea breeze storm days, non-sea breeze storm days and non-storm days from October-February in the period 2000-2015 reveals some interesting differences in atmospheric characteristics. However, the limited number of storm days for some months indicated that this analysis must be repeated for a longer time period once these data become available in order to produce more rigorous results.

Nevertheless, some initial conclusions regarding the role of the sea breeze in severe storm development can be drawn. In general, the results suggested that the presence of increasing onshore flow lowered the threshold value of CAPE required for severe storm formation, as well as allowing storms to take place despite relatively high CIN values. The ESRH data were sparser, but onshore flow also seemed to increase ESRH for most of the months considered. These results suggest that a radiosonde climatology supports the results of radar climatologies conducted for the region such as that by Soderholm *et al*. (2015) and case studies such as that by Peter *et al*. (2015). Although further work is required, these results indicate that forecasters should consider the effect of the sea breeze, especially bearing in mind that low CAPE and high CIN values may not necessarily indicate actual atmospheric stability, as the presence of the sea breeze may allow storm initiation despite these marginal CAPE and CIN values.

6.2.3 Regional synoptic conditions analysis

This section of the analysis, as discussed in Chapter 5, was the section most limited by the short time period of available data, and by the imprecision of graphically interpreting and attributing synoptic conditions to the various storm days. Surface pressure troughs, 850 mb geopotential height troughs, 500 mb geopotential height troughs, upper-level divergence as indicated by the 200 mb vector wind, and high 850 mb-200 mb wind shear were all demonstrated to be conducive to severe storms, especially in spring (October and November) when CAPE values were generally lower and storm formation was more dependent on regional environmental conditions. However, many storm events lacked either some or all of these environmental conditions, indicating that although these conditions are conducive to storms, they are not strictly necessary for severe storm formation, and that other factors such as mesoscale instability may allow storm formation to take place in their absence.

The objective of Chapter 5 was not a quantitative description of an idealised ‘perfect storm day’ but rather to assess some of the tools available to a forecaster. This allowed for determining their relative usefulness in determining the probability of severe storm formation. In other words, some conditions (such as the presence of a low-pressure system or high CAPE) were more consistently present on severe storm days than others (such as a trough at 500 mb or the conducive positioning of the jet stream). The relative importance of the various conducive factors as determined in Chapter 5 is illustrated in Figure 19. For the months of January and February, the role of CAPE and CIN became more significant as diurnal heating was greater. For spring and December, synoptic-scale processes played a larger role.

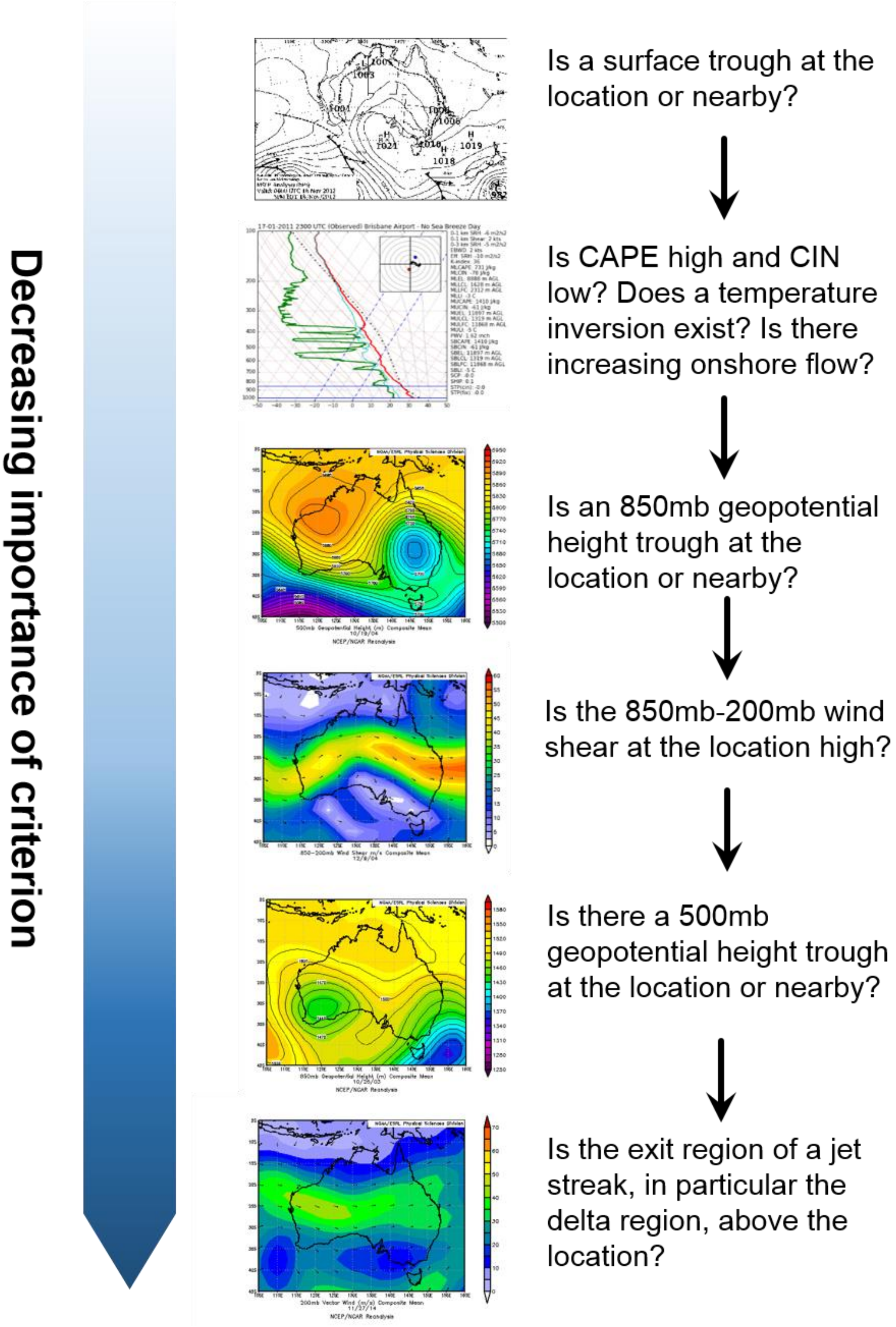

Figure 19: *Ranking of 'storm conducive criteria' according to their usefulness in severe storm prediction. Although all of the criteria shown in this figure were conducive to severe storm formation, they are shown here in order of decreasing importance, as determined using the results presented in Chapter 4 and Chapter 5. Examples of each of the conducive criteria (with regards to Brisbane) are shown, drawn from the appendices of this thesis.*

6.3 Synthesis: project outcomes, limitations and recommendations

6.3.1 Outcomes

This analysis makes a clear contribution to the understanding of severe storms in Brisbane, especially the role of the sea breeze on atmospheric stability. The specific outcomes of the analysis are listed below.

1. The results clearly demonstrated the inapplicability of a sea-breeze front detection algorithm to a weather station within the ocean-modified coastal environment.
2. An applicable algorithm was developed and applied to Brisbane Airport weather station data, providing the basis for future studies that wish to reconstruct sea breeze history but which only have access to weather station data within the ocean-modified coastal environment.
3. The results reinforced the link between sea breeze occurrence and severe storms as described in the literature in section 2.2.2, allowing for the calculation of a conditional probability for whether increasing onshore flow was present given that a severe storm had occurred. The results also demonstrated that there was not a linear relationship between the rate of increase in onshore flow and the severity of the storm.
4. The results showed that, in general, sea breeze storm days exhibited lower CAPE and higher CIN, suggesting that the threshold levels of atmospheric instability required for storm formation were lower for sea breeze days.
5. The analysis showed that known predictors of severe storms such as surface pressure troughs and strong wind shear were indeed applicable to Brisbane. More significantly, this analysis allowed for the ranking of these various indicators according to the apparent importance of their link to severe storms and, in turn, their usefulness to forecasters.

6.3.2 Limitations

Although significant outcomes were achieved, some aspects of the analysis were limited by the amount of available data. The key limitations are presented below.

1. Although this analysis produced an applicable algorithm for stations within the ocean-modified coastal environment, the lower accuracy of this algorithm means that the algorithm developed by Soderholm *et al.* (2015) should be favoured if weather station data are available outside of the ocean-modified coastal environment.

2. This analysis assessed the occurrence and relative importance of the various indicators of synoptic and mesoscale atmospheric instability (e.g. inversions and surface pressure troughs) graphically, meaning that these results were qualitative rather than quantitative. Although the graphical method allowed for the easy comparison of conditions between Brisbane and other locations, it introduced subjectivity into these results.

6.3.3 Recommendations for future analysis

Given the outcomes and limitations of this analysis discussed above, some key recommendations for future analysis can be made. These recommendations, given below, describe how more rigorous and statistically significant findings could be achieved, along with general recommendations for similar sea breeze analyses.

1. Future studies of the link between the sea breeze and severe storms must choose their sea breeze detection algorithm according to the respective strengths and weaknesses of the algorithms as described in section 6.1. If the locality is within the ocean-modified coastal environment, it is better to use the algorithm derived in this thesis. If not, it is better to use an algorithm that detects the passage of the sea breeze front, such as that derived by Soderholm *et al*. (2015).
2. By either expanding the latitude-longitude box considered, extending the analysis time period or replicating the analysis in similar localities around southeast Queensland, the number of storm events could be increased to more rigorously determine the link between sea breeze occurrence and severe storms. This would also allow for a more rigorous consideration of the link between the sea breeze and atmospheric stability indicators, specifically CAPE, CIN and ESRH. Thirty years of data would likely allow for a sufficiently large sample size to draw conclusions with greater confidence.
3. Although a graphical assessment of synoptic conditions will remain the easiest and most available method for forecasters, future studies must strive to quantify further the effect of synoptic or mesoscale conditions on Brisbane. This will allow for more rigorous results and eventually allow for not only the ranking of the various synoptic and mesoscale analysis tools but also ultimately the assignation of a ‘weighted’ value to each type. This will allow forecasters to not only favour a particular chart when different charts contradict, but to also sum the weighted values assigned to each chart type, allowing for calculating an actual probability of severe storm formation.

6.4 Implications

The high cost of severe storms in Australia, estimated at $284 million per year (BTE, 2001), necessitates an improved understanding of severe storm formation for the region. This is especially critical for coastal Queensland, where rainfall is becoming less frequent and more concentrated in extreme rainfall events. As mean global surface temperature increases and precipitation patterns change, it is likely that coastal Queensland will become even more vulnerable to extreme precipitation events, whilst simultaneously becoming more reliant on these events to break long dry spells.

This holds true especially for thunderstorm hotspot regions such as Brisbane, where an understanding of both local meteorological processes such as the sea breeze and broader regional processes such as surface pressure troughs allows for an improved predictive capacity for severe storms. This thesis has extended this understanding for Brisbane, a key growth area on the Australian east coast, but the results also have implications for many analogous regions, such as *Cfa* climate regions that also have significant inland topography. The results of this thesis demonstrate, therefore, that it is highly likely that the sea breeze has a significant impact on storm formation for many regions in eastern Asia, southeast South America, southeast United States and transitional regions around the Mediterranean. For these regions as well, this improvement in the understanding of severe storm formation, along with future improvements, will assist in mitigating the impact of severe weather. As precipitation patterns change due to climate change and result in greater severe storm impacts for many regions worldwide, this improved understanding is a necessity.

References

Adlerman, E., and K. Drogemeier. (2005). "The dependence of numerically simulated cyclic mesocyclogenesis upon environmental vertical wind shear." Mon. Wea. Rev., 133.

Allen, J., and D. Karoly. (2013). "A climatology of Australian severe thunderstorm environments 1979-2011: inter-annual variability and ENSO influence." Int. J. Climatol., 34.

Allen, J., D. Karoly, and G. Mills. (2011). "A severe thunderstorm climatology for Australia and associated thunderstorm environments." Australian Meteorological and Oceanographic Journal, 61.

American Meteorological Society. (2015). "Glossary of Meteorology." http://glossary.ametsoc.org/?id=hodograph1 (accessed 13 May 2016).

Atkins, N., R. Wakimoto, and T. Weckwerth. (1995). "Observations of the sea-breeze front during CaPE. Part II: Dual-Doppler and aircraft analysis." Mon. Wea. Rev., 123.

Australian Broadcasting Corporation. (2014). "Brisbane storm: Supercell damage bill could reach $150 million, Campbell Newman says." http://www.abc.net.au/news/2014-11-28/brisbane-storms-68000-residents-still-without-power/5924112 (accessed 22 February 2016).

Australian Emergency Institute. "Disaster Information 435." https://www.emknowledge.gov.au/disaster-information/ (accessed 8 April 2016).

Azorin-Molina, C., S. Tijm, and D. Chen. (2011). "Development of selection algorithms and databases for sea breeze studies." Theor. Appl. Climatol., 106.

Bellon, A., and I. Zawadzki. (2003). "A 9-year summary of radar characteristics of mesocyclonic storms and of deep convection in southern Quebec." Atmosphere-Ocean, 41.

Brisbane Airport Corporation. (2016). "Brisbane Airport's New Parallel Runway." http://www.bne.com.au/corporate/bne-major-projects/brisbane-airports-new-parallel-runway (accessed 22 February 2016).

Bunkers, M., B. Klimowski, J. Zeitler, R. Thompson, and M. Weisman. (2000). "Predicting Supercell Motion Using a New Hodograph Technique." Weather and Forecasting: Vol. 15, No.1.

Bureau of Transport Economics. (2001). "Economic Costs of Natural Disasters in Australia." Bureau of Transport Economics Report 103, Canberra.

Bureau of Meteorology. (2016). "Climate Data Online." http://www.bom.gov.au/climate/averages/tables/cw_040214.shtml (accessed 22 February 2016).

Bureau of Meteorology. (2016). "About Severe Storms Archive." http://www.bom.gov.au/australia/stormarchive/about.shtml (accessed 1 April 2016).

Bureau of Meteorology. (2016). "Wind speed and direction rose." http://www.bom.gov.au/cgi-bin/climate/cgi_bin_scripts/windrose_selector.cgi?period=Annual&type=9&location=40223&Submit=Get+Rose (accessed 4 April 2016).

Cai, W., P. Whetton, and A. Pittock. (2001). "Fluctuations of the relationship between ENSO and northeast Australian rainfall." Clim. Dynam., 17.

Callaghan, J. (1996). "Review of Severe Thunderstorm Forecasting and the Severe Thunderstorm Warning Service in The Southeast Coast District of Queensland." 5th Australian Severe Thunderstorm Conference, Avoca Beach, New South Wales, Australia.

Chen, X., Z. Kun, and M. Xue. (2014). "Spatial and temporal characteristics of warm season convection over Pearl River Delta region, China, based on 3 years of operational radar data." Journal of Geophysical Research: Atmospheres, 119.

Cintineo, J., *et al*. (2012). "An Objective High-Resolution Hail Climatology of the Contiguous United States." Weather and Forecasting 27.

Colby, J., and P. Frank. (1984). "Convective Inhibition as a Predictor of Convection during AVE-SESAME II". Mon. Wea. Rev 112.

Coniglio, M., S. Corfidi, and J. Kain. (2011). "Environment and early evolution of the 8 May 2009 derecho-producing convective system." Mon.Wea. Rev., 139.

Davies-Jones, R., D. Burgess, and M. Foster. (1990). "Test of helicity as a tornado forecast parameter." Preprints, 16th Conf. on Severe Local Storms.

Dixon, M., and G. Wiener. (1993). "TITAN: Thunderstorm Identification, Tracking, Analysis, and Nowcasting—A Radar-based Methodology." J. Atmos. Ocean. Technol., 10.

Doswell, C. (2001). "Severe Convective Storms - An Overview." Amer. Meteor. Soc. 1–26.

Doswell, C., B. Maddox. (1996). "Flash flood forecast-ing: an ingredients-based methodology." Weather and Forecasting 11.

Dowdy, A., and Y. Kuleshov (2014). "Climatology of lightning activity in Australia: Spatial and seasonal variability." Aust. Meteorol. Oceanogr. J., 64.

Droegemeier, K., S. Lazarus, and R. Davies Jones. (1993). "The influence of helicity on numerically simulated convective storms." Mon. Wea. Rev., 121.

Flay, S., and J. Nott. (2007). "Effect of ENSO on Queensland seasonal landfalling cyclone activity." Int. J. Climatol., 27.

Fovell, R. (2005). "Convective initiation ahead of the sea-breeze front." Mon. Wea. Rev., 133.

Garcia, S., and M. Kayano. (2007). "Climatological aspects of Hadley, Walker and monsoon circulations in two phases of the Pacific Decadal Oscillation." Theor. Appl. Climatol., 91.

George, J. (1960). "Weather Forecasting for Aeronautics." Academic Press, New York, USA.

Geerts, B. (2001). "Estimating Downburst-Related Maximum Surface Wind Speeds by Means of Proximity Soundings in New South Wales, Australia." Weather and Forecasting, 16.

Geoscience Australia. (2007) "Where does severe weather occur?" Commonwealth of Australia, https://web.archive.org/web/20090621231613/http://www.ga.gov.au/hazards/severeweather/where.jsp (accessed 5 May 2016).

Google Maps (2016) www.google.com.au/maps

Goudenhoofdt, E., and L. Delobbe. (2013). "Statistical characteristics of convective storms in Belgium derived from volumetric weather radar observations." J. Appl. Meteor. Climatol., 52.

Grant, A., and K. Walsh. (2001). "Interdecadal variability in north-east Australia tropical cyclone formation." Atmos. Sci. Lett., 2.

Griffiths, D., K. Batt and T. Casinader. (1993). "Severe thunder-storms in New South Wales: climatology and means of assessing theimpact of climate change." Climatic Change 25.

Haberlie, A., W. Ashley, and T. Pingel. (2015). "The effect of urbanisation on the climatology of thunderstorm initiation." Q. J. R. Meteorol. Soc. 141.

Halbert, K. (2015). "SHARPpy: Fuelling the Python Cult. Preprinst, 5th Symposium on Advances in Modelling and Analysis Using Python, Phoenix, USA.

Hand, W., and G. Cappelluti. (2011). "A global hail climatology using the UK Met Office convection diagnosis procedure (CDP) and model analyses." Meteorological Applications, 18.

Harper, B., and J. Callaghan. (1998). "Modelling of Severe Thunderstorms in South East Queensland." 6th Australian Severe Storms Conference, Bardon, Queensland, Australia.

Haylock, M., and N. Nicholls. (2000). "Trends in extreme rainfall indices for an updated high quality data set for Australia, 1910–1998." Int. J. Climatol., 20.

Holcombe, G. and G. Moynihan. (1978). "An Investigation of the Brisbane Tornado of 4 November 1973." Meteorological Note 97. Department of Science, Australian Bureau of Meteorology.

Hopkins, L., and G. Holland. (1997). "Australian heavy-rain days and associated east coast cyclones: 1958–92." J. Climate, 10.

Hutchinson, M., H. Nix, and J. McMahon. (1992) “Climate constraints on cropping system”. in Pearson, C. “Field Crop Ecosystems of the World.” Elsevier.

Insurance Council of Australia. (2015). "10 Years of Catastrophe." http://www.tiki-toki.com/timeline/entry/568110/Ten-Years-of-Catastrophe (accessed 5 April 20126).

Iribarne, J., and W. Godson. (1981). “Atmospheric Thermodynamics, 2nd Edition.” Reidel Publishing Company, Dordrecht, the Netherlands.

Jimenez, A. (2015). " One year anniversary of destructive Brisbane hailstorm." ABC, http://www.abc.net.au/news/2015-11-27/brisbane-hail-storm-one-year-anniversary-reminds-to-prepare/6978196 (accessed 8 April 2016).

Johnson, F., M. Hutchinson, C. The, C. Beesley, J. Green. (2015). “Topographic relationships for design rainfalls over Australia.” Journal of Hydrology, 533.

Kalnay, E. *et al*. (1996). “The NCEP/NCAR Reanalysis 40-year Project”. Bull. Amer. Meteor. Soc., 77.

Kamburova, P., and F. Ludlam. (1966). "Rainfall evaporation in thunderstorm downdrafts." Quart. J. Roy. Meteor. Soc., 92.

Karan, H., and K. Knupp. (2009). "Radar and Profiler Analysis of Colliding Boundaries: A Case Study." Mon. Wea. Rev., 128.

Kerr, B. and G. Darkow. (1996). "Storm-relative winds and helicity in the tornadic thunderstorm environment." Wea. Forecasting, 11,.

Kirkpatrick, C., and E. McCaul. (2008). "Storm-Relative Flow and its Relationship to Low-Level Vorticity in Simulated Storms." 24th Conference on Severe Local Storms.

Klingaman, N. P. (2012). "A literature survey of key rainfall drivers in Queensland, Australia: Rainfall variability and change. Rainfall in Queensland, Part 1." Office of Climate Change, QCCCE Research Rep.

Kottek, M., J. Grieser, C. Beck, B. Rudolf, and F. Rubel. (2006). "World Map of the Köppen-Geiger climate classification updated." Meteorologische Zeitschrift, Vol. 15, No. 3,.

Lakshmanan, V., and T. Smith. (2010). "An Objective Method of Evaluating and Devising Storm-476 Tracking Algorithms." Wea. Forecasting., 25.

Lee, J. (2002). "Tornado proximity soundings from the NCEP/NCAR reanalysis data." Unpublished MS Thesis, University of Oklahoma.

Linacre, E., and B. Geerts. (1997). "*Climates & Weather Explained*." Routledge, London.

Lough, J. (1991). "Rainfall variations in Queensland, Australia." Int. J. Climatol., 11.

Lough, J. M. (1993). "Variations of some season rainfall characteristics in Queensland, Australia: 1921– 1987." Int. J. Climatol., 13.

Lyons, W. F. and M. Bonnel. (1992). "Daily meso-scale rainfall in the tropical wet/dry climate of the Townsville area, North-east Queensland during the 1988–1989 wet season: synoptic-scale airflow considerations." Int. J. Climatol., 12.

May, P. (1999). "Thermodynamic and Vertical Velocity Structure of Two Gust Fronts Observed with a wind Profiler/RASS during MCTEX." Mon. Wea. Rev., 127.

McCaul, E., and M. Weisman. (2001). “The sensitivity of simulated supercell structure and intensity to variations in the shapes of environmental buoyancy and shear profiles.” Mon. Wea. Rev., 129.

Miller, S., B. Keim, R. Talbot, and H. Mao. (2003). "Sea breeze; Structure, Forecasing and Impacts." Reviews of Geophysics, 41.

Moncrieff, M. and M. Miller. (1976). “The dynamics and simulation of tropical cumulonimbus and squall lines”. Q. J. R. Meteorol. Soc., 120.

National Weather Service. (2013) “June 13th 2012 Severe Storms.” National Weather Service Weather Forecast Office, http://www.srh.noaa.gov/fwd/?n=june132012 (accessed 5 May 2016).

Oke, T. (1978). "Boundary Layer Climates." Methuen, London.

Oort, A., Yienger, J. (1996). " Observed interannual variability in the Hadley circulation and its connection to ENSO." J. Climate. 9.

OzCoasts. (2016). "South-East Queensland region." Geoscience Australia.

Parackal, K., M. Mason, D. Henderson, D. Smith, J. Ginger. (2015). "Investigation of Damage : Brisbane 27 November 2014 Severe Storm Event." Technical Report No. 60. 47pp. Cyclone Testing Station. James Cook University, Townsville, Queensland, Australia.

Passmore, D. (2013). "Brisbane Airport bosses will ask the ACCC to approve an increase in passenger landing charges to fund a new runway." The Courier Mail http://www.couriermail.com.au/news/queensland/brisbane-airport-bosses-will-ask-the-accc-to-approve-an-increase-in-passenger-landing-charges-to-fund-a-new-runway/story-e6freoof-1226616249970 (accessed 22 Februart 2016).

Peter, J. R., M. J. Manton, R. J. Potts, P. T. May, S. M. Collis and L. Wilson. (2015). "Radar-derived statistics of convective storms in Southeast Queensland." Int. J. Climatol., 54.

Potts, R., T. Keenan, and P. May. (2000). "Radar characteristics of storms in the Sydney area." Mon. Wea. Rev., 128.

Prasad, R. (2012). "Climate change adaptation at Brisbane Airport." Colonial First State Global Asset Management http://igcc.org.au/Resources/Documents/Infrasrtucture_Brisbane_Airport_Dec12.pdf (accessed 22 February 2016).

Proctor, J. (1989). "Numerical simulations of an isolated microburst. Part II: Sensitivity experiments." J. Atmos. Sci., 46.

Puygrenier, V., F. Lohou, B. Campistron, F. Saïd, G. Pigeon, B. Bénech, and D. Serça. (2005). "Investigation on the fine structure of sea-breeze during ESCOMPTE experiment." Atmos. Res., 74.

Rasmussen, E., and D. Blanchard. (1998). "A baseline climatology of sounding-derived supercell and tornado forecast parameters." Weather and Forecasting 13.

Rasmussen, E., and J. Straka. (1998). "Variations in supercell morphology. Part 1: Observations of the role of upper-level storm-relative flow." Mon. Wea. Rev., 126.

Richter, H., P. Justin, and S. Collis. (2014). "Analysis of a Destructive Wind Storm on 16 November 2008 in Brisbane." Australia. Mon. Wea. Rev. 142.

Risbey, J., M. Pook, P. McIntosh, C. Ummenhofer, and G. Meyers. (2009). "Characteristics and variability of synoptic features associated with cool season rainfall in south-eastern Australia." Int. J. Climatol., 29.

Risbey, J., M. Pook, P. McIntosh, M. Wheeler, and H. Hendon. (2009). "On the remote drivers of rainfall variability in Australia." Mon. Wea. Rev., 137.

Rotunno, R., J. Klemp, and M. Weisman. (1988). "A theory for strong, long-lived squall lines." J. Atmos. Sci., 45.

Rotunno, R., and M. Weisman. (2003). "Comments on Linear and nonlinear propagation of supercell storms." J. Atmos. Sci., 60.

Rudlosky, S., and H. Fuelberg. (2013). "Documenting Storm Severity in the Mid-Atlantic Region Using Lightning and Radar Information." Mon. Wea. Rev., 141.

Ryan, C. (1992). "Dynamical Classification of Australian Thunderstorms." Meteorology Study, No. 40, Monash University.

Schuster, S., R. Blong, and M. Speer. (2005). "A hail climatology of the greater Sydney area and New South Wales, Australia." International Journal of Climatolology 25.

Simpson, J., D. Mansfield, and J. Milford. (1977). "Inland penetration of sea-breeze fronts." Q. J. R. Meteorol. Soc., 103.

Skywarn Deutschland. (2013). "South and East – Thunderstorm with hail." http://forum.skywarn.de/viewtopic.php?f=64&t=10555&sid=3ca2e9cadd626e87454032247831efaa#p68549 (accessed 5 May 2016).

Soderholm, J., *et al*. (2015). "The Coastal Convective Interactions Experiment (CCIE): Understanding the role of sea breezes for hailstorm hotspots in Eastern Australia." Bulletin of the American Meteorological Society.

Soderholm, J., *et al*. (2016). "Long-term trends and drivers of hailstorm variability in Southeast Queensland, Australia." University of Queensland, Climate Research Group, St Lucia, QLD, Australia.

Srivastava, R. (1985). " A simple model of evaporatively driven downdraft: Application to microburst downdraft." Atmos. Sci., 42.

Storm Prediction Center. (2016). "Significant Hail Parameter." https://www.google.com.au/webhp?sourceid=chrome-instant&ion=1&espv=2&ie=UTF-8#q=significant%20hail%20parameter (accessed 13 May 2016).

Sturman, S., and N. Tapper. (2006). "The weather and climate of Australia and New Zealand – 2nd Edition" Oxford University Press, Melbourne.

Suppiah, R., and K Hennessey. (1998). "Trends in total rainfall, heavy rain events and number of dry days in Australia, 1910–1990." Int. J. Climatol., 10.

Tebaldi, C., K. Hayhoe, J. Arblaster, and G. Meehl. (2006). "Going to the extremes: An inter-comparison of model-simulated historical and future changes in extreme events." Climatic Change, 79.

Tessendorf, S., *et al*. (2012). "The Queensland Cloud Seeding Research Program." Bull. Amer. Meteor. Soc., 93.

The University Corporation for Atmospheric Research. (2016). "The Sea Breeze." http://www.meted.ucar.edu/fire/fwx/media/graphics/sbfmapc.gif. (accessed 8 April 2016).

Thompson, R., R. Edwards, J. Hart, K. Elmore, and P. Markowski. (2003). "Close proximity soundings within supercell environments obtained from the Rapid Update Cycle." Wea. Forecasting, 18.

Thompson, R. (2004). "An Update to the Supercell Composite and Significant Tornado Parameters". Storm Prediction Center, http://www.spc.noaa.gov/publications/thompson/stp_scp.pdf (accessed 13 May 2016).

Thompson, R., R., Edwards, and C. Mead. (2004). “Effective Storm-Relative Helicity in Supercell Thunderstorm Environments.” 22nd Conference on Severe Local Storms, Hyannis.

Thompson, R. (2016). “Explanation of SPC Severe Weather Parameters.””http://www.spc.noaa.gov/exper/mesoanalysis/help/begin.html (accessed 13 May 2016).

United National Atlas of the Oceans. (2010). "Human Settlements on the Coast." http://www.oceansatlas.org/servlet/CDSServlet?status=ND0xODc3JjY9ZW4mMzM9KiYzNz1rb3M (accessed 11 February 2016).

Vecchi, G., and B. Soden. (2007). "Increased tropical Atlantic wind shear in model projections of global warming." Geophys. Res. Lett., 34.

Wang, G., and H. Hendon. (2007). "Sensitivity of Australian rainfall to inter-El Niño variations." J. Climate, 20.

Weckwerth, T. (2000). "The effect of small-scale moisture variability on thunderstorm initiation." Mon. Wea. Rev., 128.

Weckwerth, T., H. Murphey, C. Flamant, J. Goldstein, and C. Pettet. (2008). "An Observational Study of Convection Initiation on 12 June 2002 during IHOP_2002." Mon. Wea. Rev., 136.

Weckwerth, T., J. Wilson, M. Hagen, T. Emerson, J. Pinto, D. Rife, and a. L. Grebe. (2011). "Radar climatology of the COPS region." Quart. J. Roy. Meteor. Soc., 137.

Weisman, M., and J. Klemp. (1982). "The dependence of numerically simulated convective storms on vertical wind shear and buoyancy." Mon. Wea. Rev., 110.

Weisman, M. L., and R. Rotunno. (2000). "The use of vertical wind shear versus helicity in interpreting supercell dynamics." The use of vertical wind shear versus helicity in interpreting supercell dynamics. J. Atmos. Sci., 57.

Wheeler, M., and J. McBride. (2005). "Australian–Indonesian monsoon. Intraseasonal variability in the atmosphere–ocean climate system." Springer, Berlin, Germany.

Wheeler, M., H. Hendon, S. Cleland, A. Donald, and H. Meinke. (2009). "Impacts of the Madden– Julian Oscillation on Australian rainfall and circulation." J. Climate, 22.

Wilson, C., K. Ortega, and V. Lakshmanan. (2009). "Evaluating multi-radar, multi-sensor hail diagnosis with high resolution hail reports." 25th Conf. on IIPS, Phoenix, AZ, Amer. Meteor. Soc.

Wilson, J., and D. Megenhardt. (1997). "Thunderstorm initiation, organization, and lifetime associated with Florida boundary layer convergence lines." Mon. Wea. Rev., 125.

Witt, A., M. Eilts, G. Stumpf, J Johnson, E. Mitchell, and K. Thomas. (1998). “An enhanced hail detection algorithm for the WSR-88D.” Wea. Forecasting, 13.

Yeo, C. (2005). "Severe thunderstorms in the Brisbane region and a relationship to the El Niño Southern Oscillation." Aust. Met. Mag. 54.

Pleases note: All synoptic charts in the following appendices were provided by the Australian Bureau of Meteorology. NCEP NCAR reanalysis charts were generated by the NOAA/ESRL Physcial Sciences Division and were drawn from their site http://www.esrl.noaa.gov/psd/. The basis for the reanalysis data was created by Kalnay *et al*. (1996). These appendices present the key atmospheric conditions for each of the storm events considered in this analysis, ordered in terms of when they appeared in Chapter 5. These 'snaphots' of the atmosphere are used in Chapter 5 to characterise severe storm conditions for each of the major storm months (January, February, October, November and December).

The Skew-T plots were generated using SHARPpy and Brisbane Upper Air Soundings. The acronyms and variables included on each skew-t plot are defined in the glossary. In lieu of providing an identical legend and axes for every single skew-t plot, a guide for interpreting each skew-t plot is presented below. This approach was favoured because it allowed the appendices to be more accessible without superfluous information for each chart.

Blank values for each table in this section indicate that the variable was not applicable for that sounding, that the data were corrupted, or that the weather module SHARPpy used to plot the skew-t graphs was unable to calculate the variable for that sounding. All calculated averages ignore soundings that did not take place at 2300 UTC or 0000 UTC. In order to increase the usefulness of this analysis for storm prediction, the appendixes are divided into the main storm months, October, November and December, January and February.

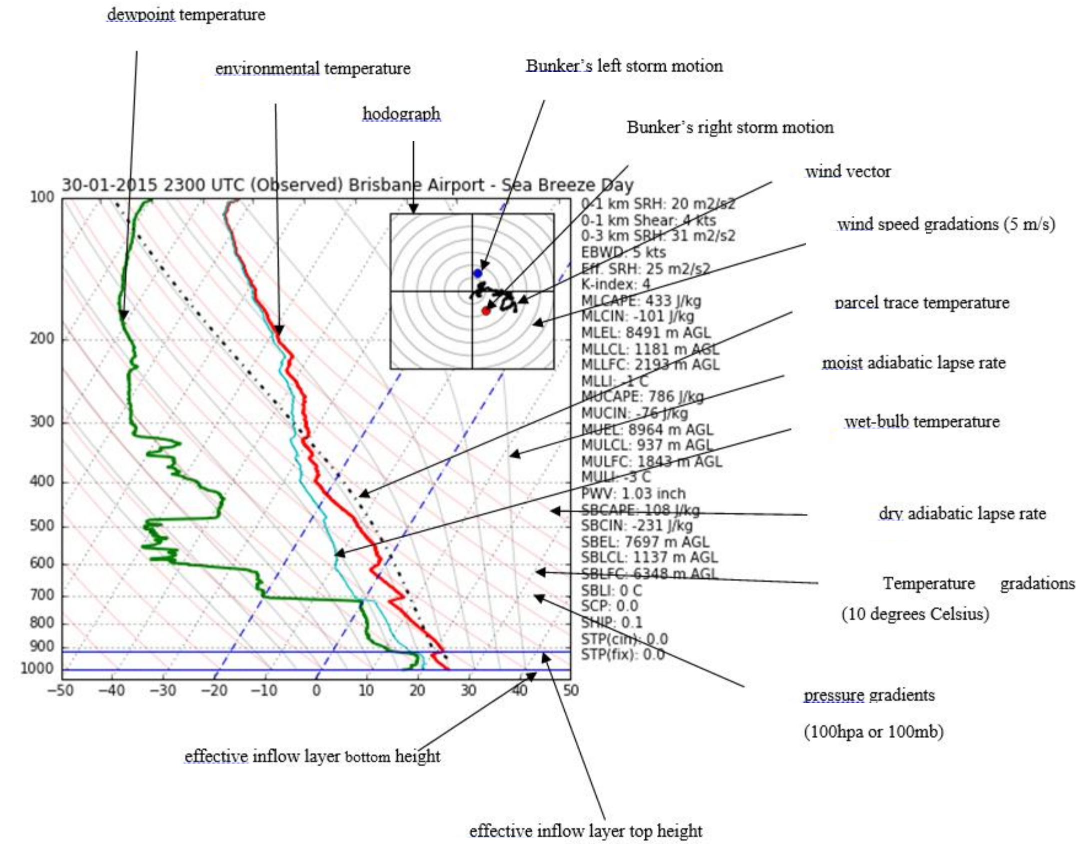

Figure 20: *A guide for interpreting the skew-t plots provided in the appendices. The horizontal axis (as demonstrated using the temperature gradations) is temperature (in degrees Celsius) and the vertical axis (as demonstrated using the pressure gradients) is pressure (in hectopascals or millibars).*

Appendix 1: January

Sea breeze storms

Table 8: Atmospheric conditions for severe storms on sea breeze days for January

Date	Time (UTC)	Most-Unstable CAPE	Most-Unstable CIN	Most-Unstable LCL	Most-Unstable LFC	Most-Unstable EL	Most-Unstable LI	0-3 km Pressure-Weighted Mean Wind (kt)	0-6 km Shear (kt)	0-3 km Storm Relative Helicity [m2/s2]	Effective Inflow Layer Bottom Height (m AGL)	Effective Inflow Layer Top Height (m AGL)	Effective Inflow Layer SRH (m2/s2)	Effective Bulk Wind Difference
16/01/2001	2300	14.89	-394.68	1894.41	7206.51	7471.00	-0.28	1.27	11.68	49.26	-100.00	-100.00		
23/01/2004	2300	859.40	-75.00	892.82	2413.00	11520.69	-4.01	2.20	13.56	12.69		1195.00	5.11	1.55
24/01/2004	2300	253.52	-298.75	770.82	7914.00	11197.00	-1.56	0.36	9.36		-115.00	-115.00		
5/01/2006	2300	335.46	-99.49	849.18	6507.00	10877.00	-1.02	7.31	21.08	17.68		155.00	7.47	1.42
	average	365.82	-216.98	1101.81	6010.13	10266.42	-1.72	2.78	13.92	26.54	-107.50	283.75	6.29	1.49

Non-sea breeze storms

Table 9: Atmospheric conditions for severe storms on non-sea breeze days for January

Date	Time (UTC)	Most-Unstable CAPE	Most-Unstable CIN	Most-Unstable LCL	Most-Unstable LFC	Most-Unstable EL	Most-Unstable LI	0-3 km Pressure-Weighted Mean Wind (kt)	0-6 km Shear (kt)	0-3 km Storm Relative Helicity [m2/s2]	Effective Inflow Layer Bottom Height (m AGL)	Effective Inflow Layer Top Height (m AGL)	Effective Inflow Layer SRH (m2/s2)	Effective Bulk Wind Difference
5/01/2008	2300	1000.15	-48.33	438.09	1379.80	10104.00	-4.45	7.04	20.96	29.43		709.00	15.13	3.82
2/01/2011	2300	976.68		1044.75	1044.75	11004.00	-3.96	5.54	3.01	-11.49	10.00	1205.00	-20.48	8.09
	average	988.41	-48.33	741.42	1212.28	10554.00	-4.20	6.29	11.99	8.97	10.00	957.00	-2.67	5.95

Non-storm days

Table 10: Atmospheric conditions for non-storm days for January

Date	Time (UTC)	Most-Unstable CAPE	Most-Unstable CIN	Most-Unstable LCL	Most-Unstable LFC	Most-Unstable EL	Most-Unstable LI	0-3 km Pressure-Weighted Mean Wind (kt)	0-6 km Shear (kt)	0-3 km Storm Relative Helicity [m2/s2]	Effective Inflow Layer Bottom Height (m AGL)	Effective Inflow Layer Top Height (m AGL)	Effective Inflow Layer SRH (m2/s2)	Effective Bulk Wind Difference
	average	377.0281	-161.663	1104.145	4360.879	6671.277	0.518324	6.033208	10.02692	13.72537	1.041009	308.3982	4.262726	4.797887

31/1/2015

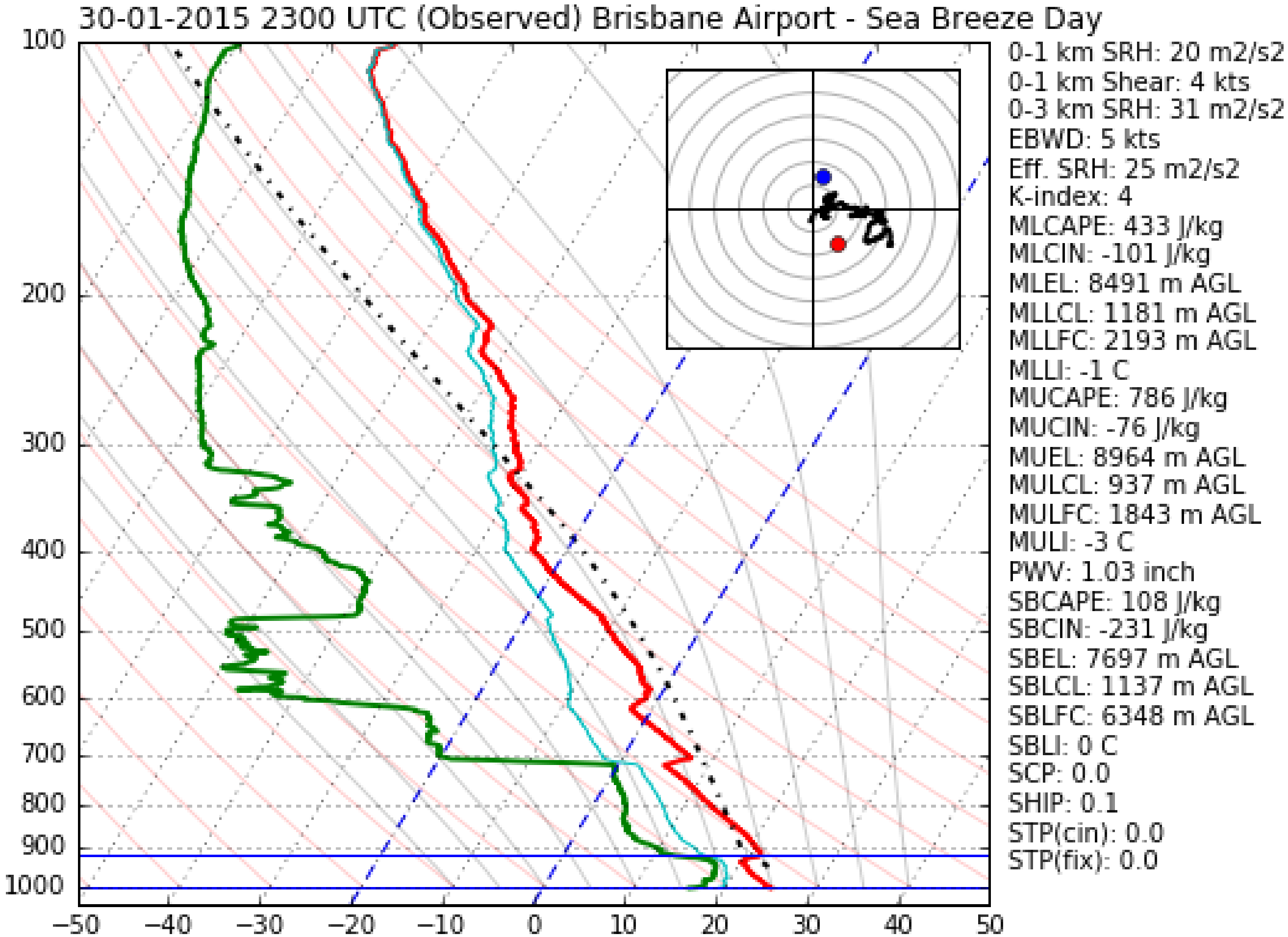

30-01-2015 2300 UTC (Observed) Brisbane Airport - Sea Breeze Day
100
200
300
400
500
600
700
800
900
1000
−50 −40 −30 −20 −10 0 10 20 30 40 50
0-1 km SRH: 20 m2/s2
0-1 km Shear: 4 kts
0-3 km SRH: 31 m2/s2
EBWD: 5 kts
Eff. SRH: 25 m2/s2
K-index: 4
MLCAPE: 433 J/kg
MLCIN: -101 J/kg
MLEL: 8491 m AGL
MLLCL: 1181 m AGL
MLLFC: 2193 m AGL
MLLI: -1 C
MUCAPE: 786 J/kg
MUCIN: -76 J/kg
MUEL: 8964 m AGL
MULCL: 937 m AGL
MULFC: 1843 m AGL
MULI: -3 C
PWV: 1.03 inch
SBCAPE: 108 J/kg
SBCIN: -231 J/kg
SBEL: 7697 m AGL
SBLCL: 1137 m AGL
SBLFC: 6348 m AGL
SBLI: 0 C
SCP: 0.0
SHIP: 0.1
STP(cin): 0.0
STP(fix): 0.0

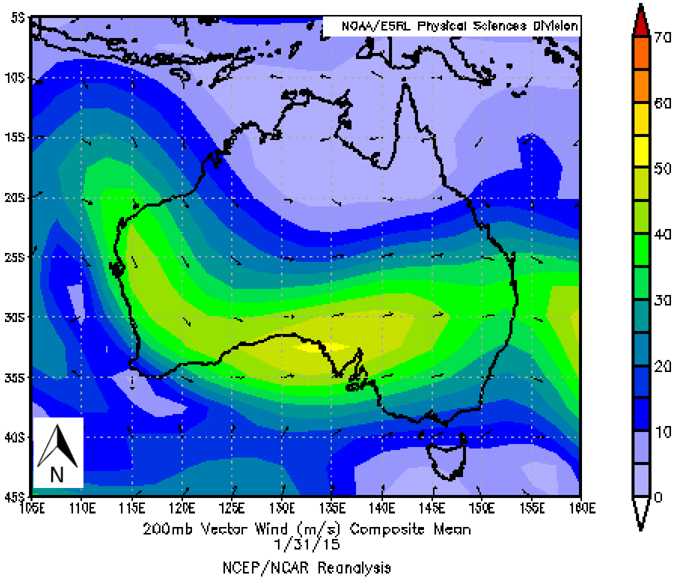
NOAA/ESRL Physical Sciences Division
200mb Vector Wind (m/s) Composite Mean
1/31/15
NCEP/NCAR Reanalysis
70 60 50 40 30 20 10 0

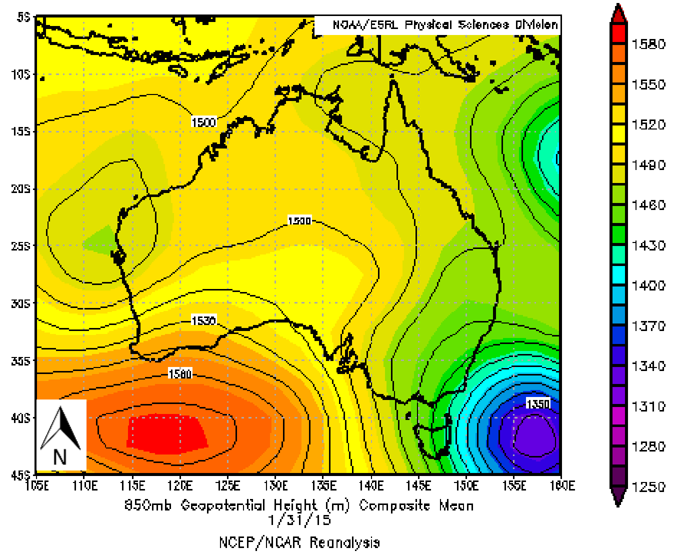
NOAA/ESRL Physical Sciences Division
850mb Geopotential Height (m) Composite Mean
1/31/15
NCEP/NCAR Reanalysis
1580 1550 1520 1490 1460 1430 1400 1370 1340 1310 1280 1250

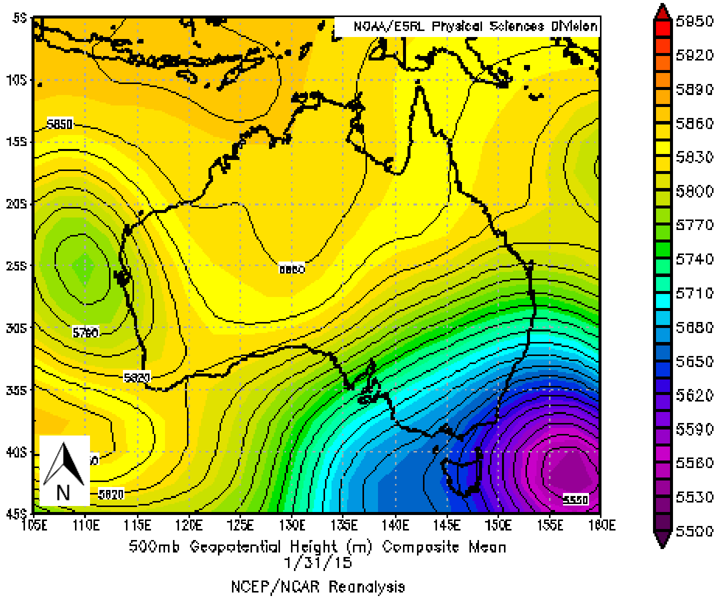
NOAA/ESRL Physical Sciences Division
500mb Geopotential Height (m) Composite Mean
1/31/15
NCEP/NCAR Reanalysis
5950 5920 5890 5860 5830 5800 5770 5740 5710 5680 5650 5620 5590 5560 5530 5500

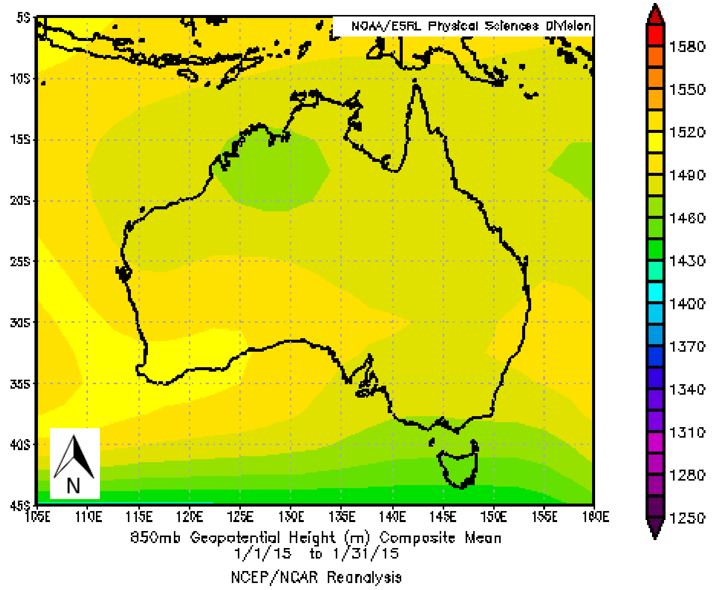
NOAA/ESRL Physical Sciences Division
850mb Geopotential Height (m) Composite Mean
1/1/15 to 1/31/15
NCEP/NCAR Reanalysis
1580 1550 1520 1490 1460 1430 1400 1370 1340 1310 1280 1250

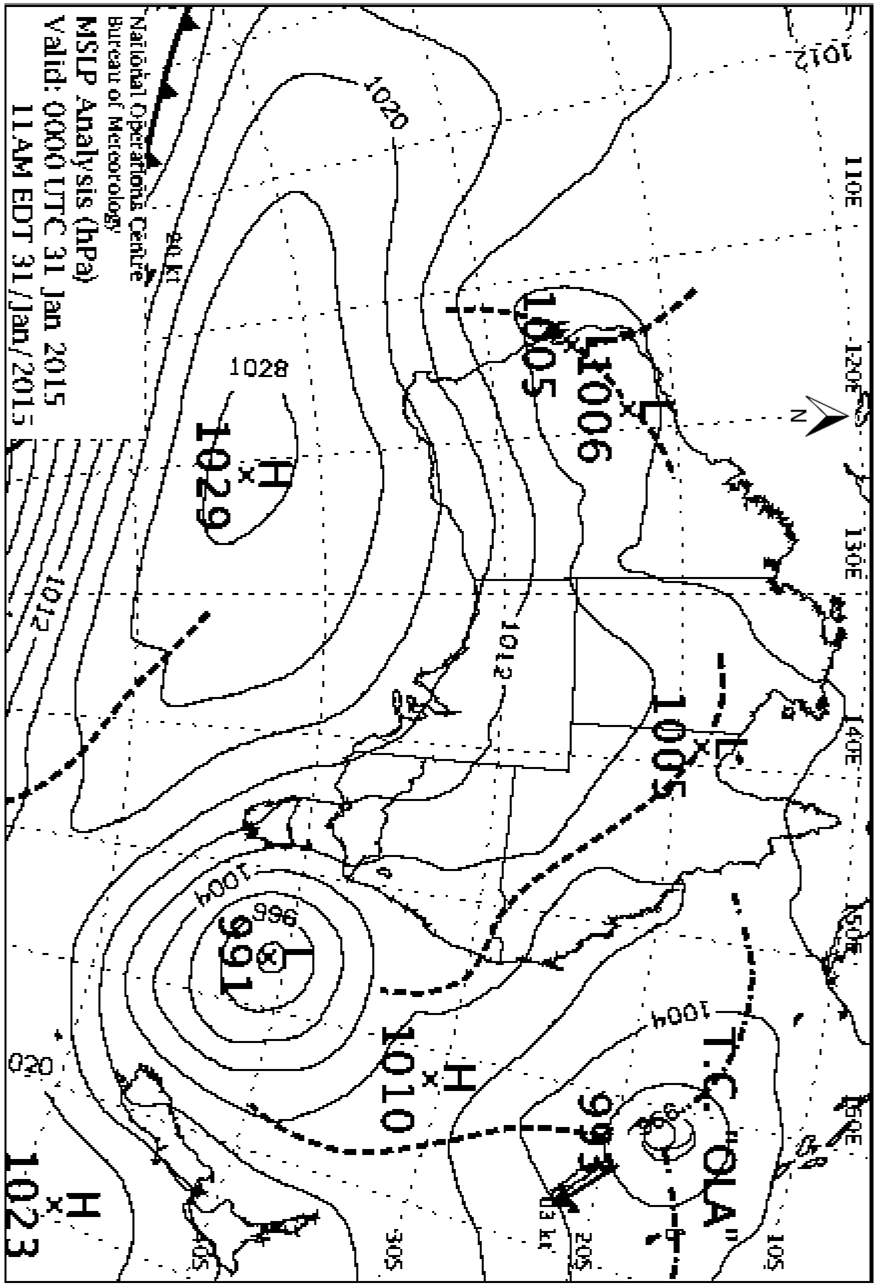
National Operations Centre
Bureau of Meteorology
MSLP Analysis (hPa)
Valid: 0000 UTC 31 Jan 2015
11AM EDT 31/Jan/2015
T.C. "OLA"
1029
1006
1005
991
1010
1023
993

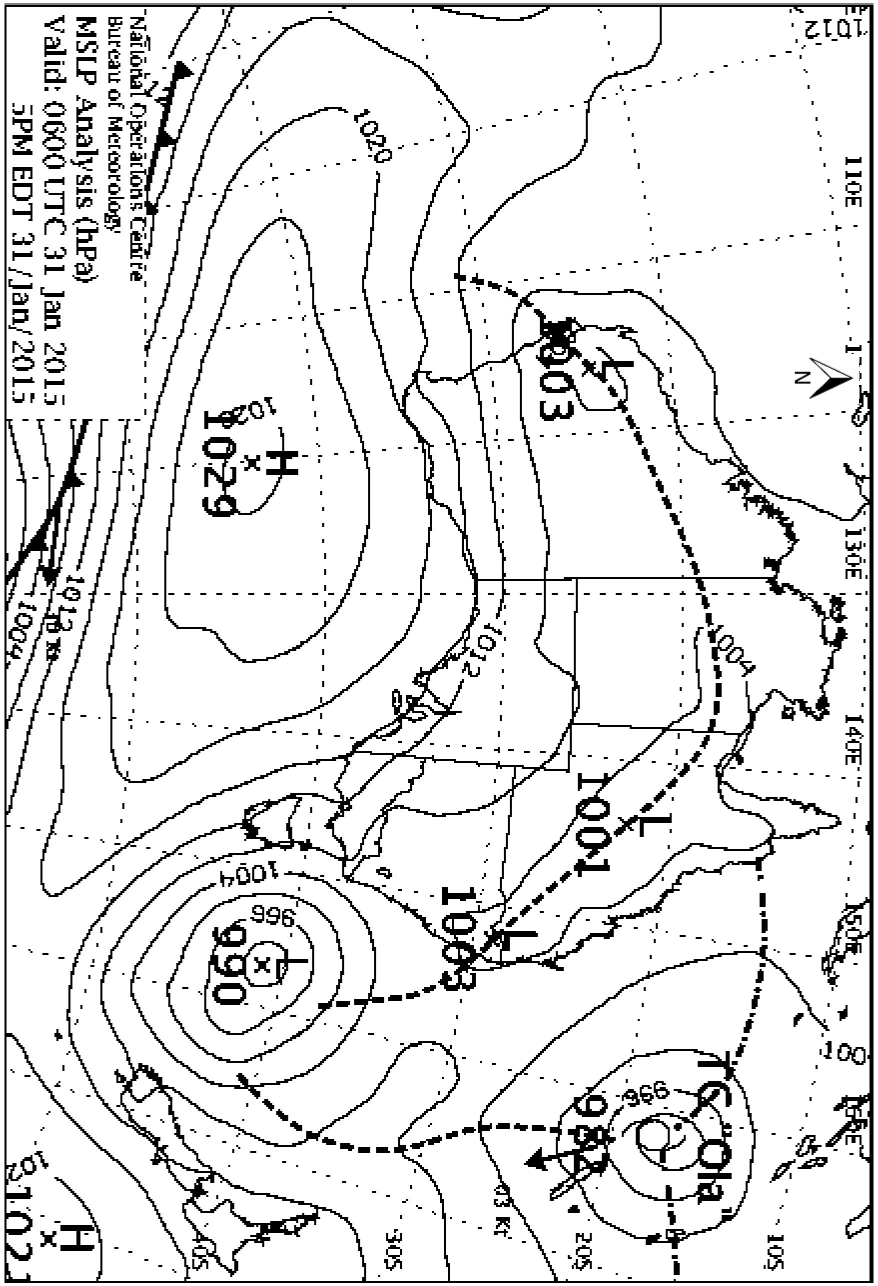
National Operations Centre
Bureau of Meteorology
MSLP Analysis (hPa)
Valid: 0600 UTC 31 Jan 2015
5PM EDT 31/Jan/2015
TC "Ola"
1029
1003
1001
990

6/1/2006

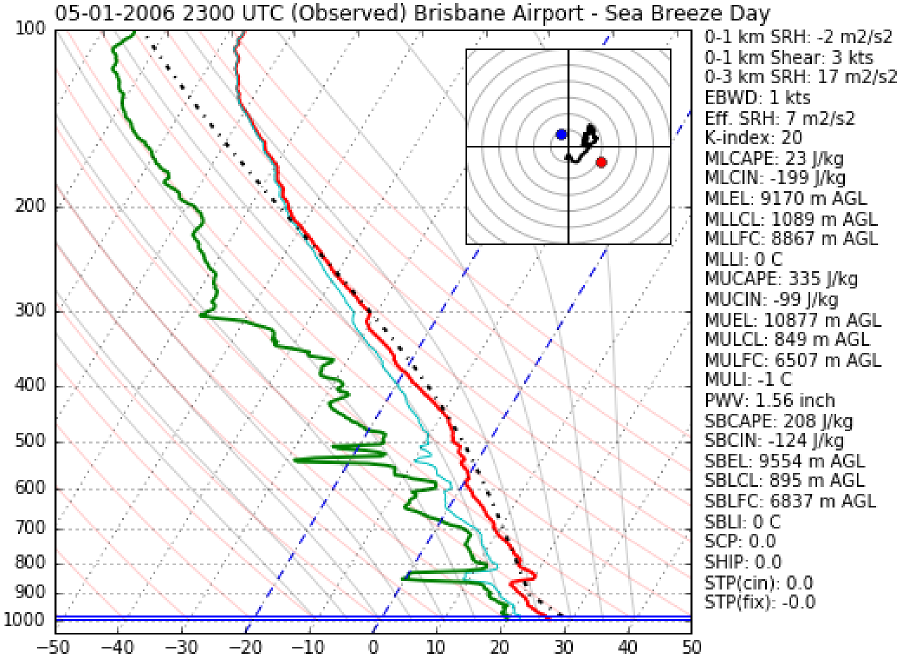
05-01-2006 2300 UTC (Observed) Brisbane Airport - Sea Breeze Day
0-1 km SRH: -2 m2/s2
0-1 km Shear: 3 kts
0-3 km SRH: 17 m2/s2
EBWD: 1 kts
Eff. SRH: 7 m2/s2
K-index: 20
MLCAPE: 23 J/kg
MLCIN: -199 J/kg
MLEL: 9170 m AGL
MLLCL: 1089 m AGL
MLLFC: 8867 m AGL
MLLI: 0 C
MUCAPE: 335 J/kg
MUCIN: -99 J/kg
MUEL: 10877 m AGL
MULCL: 849 m AGL
MULFC: 6507 m AGL
MULI: -1 C
PWV: 1.56 inch
SBCAPE: 208 J/kg
SBCIN: -124 J/kg
SBEL: 9554 m AGL
SBLCL: 895 m AGL
SBLFC: 6837 m AGL
SBLI: 0 C
SCP: 0.0
SHIP: 0.0
STP(cin): 0.0
STP(fix): -0.0

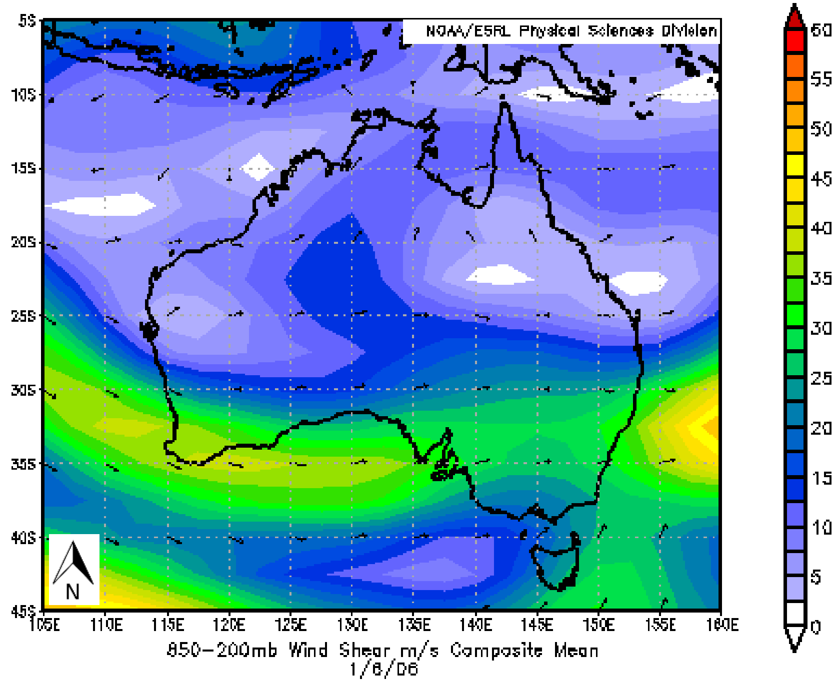
NOAA/ESRL Physical Sciences Division
850–200mb Wind Shear m/s Composite Mean
1/6/06

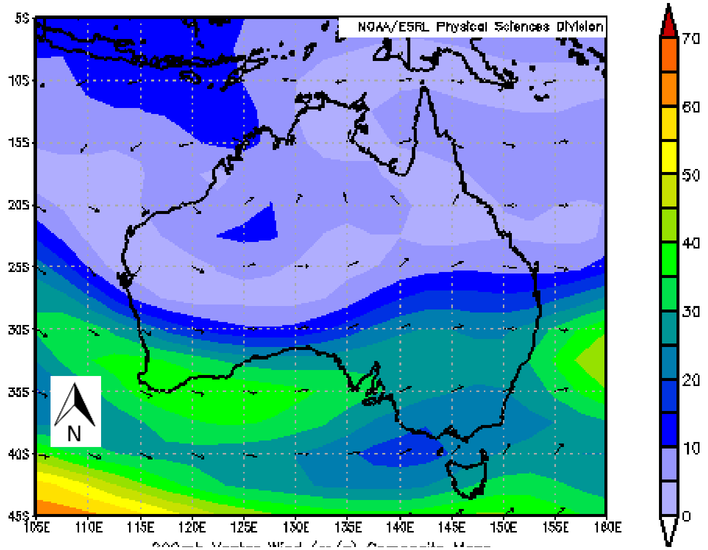
NOAA/ESRL Physical Sciences Division
0
10
20
30
40
50
60
70

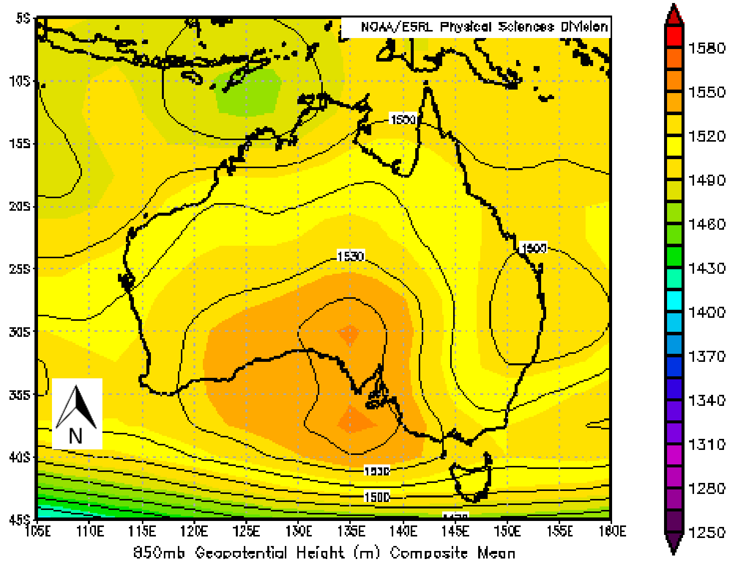
NOAA/ESRL Physical Sciences Division
850mb Geopotential Height (m) Composite Mean
1250
1280
1310
1340
1370
1400
1430
1460
1490
1520
1550
1580

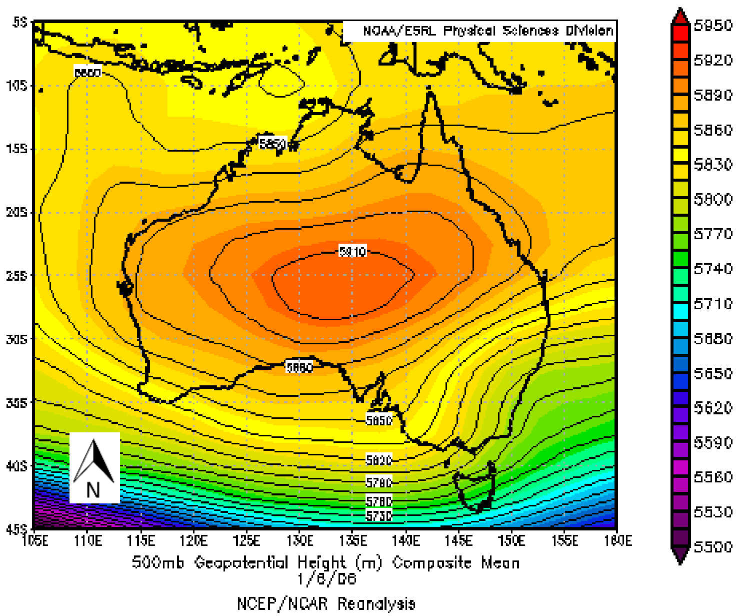
NOAA/ESRL Physical Sciences Division
500mb Geopotential Height (m) Composite Mean
1/6/06
NCEP/NCAR Reanalysis
5500
5530
5560
5590
5620
5650
5680
5710
5740
5770
5800
5830
5860
5890
5920
5950

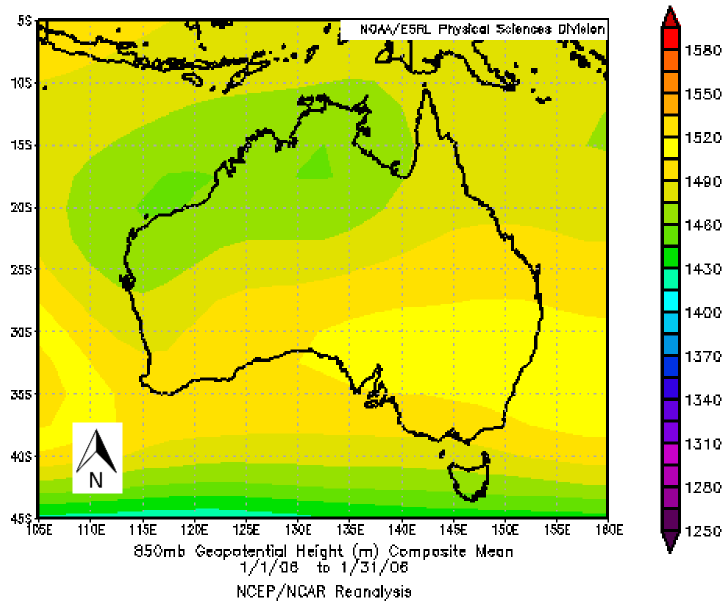
NOAA/ESRL Physical Sciences Division
850mb Geopotential Height (m) Composite Mean
1/1/06 to 1/31/06
NCEP/NCAR Reanalysis
1250
1280
1310
1340
1370
1400
1430
1460
1490
1520
1550
1580

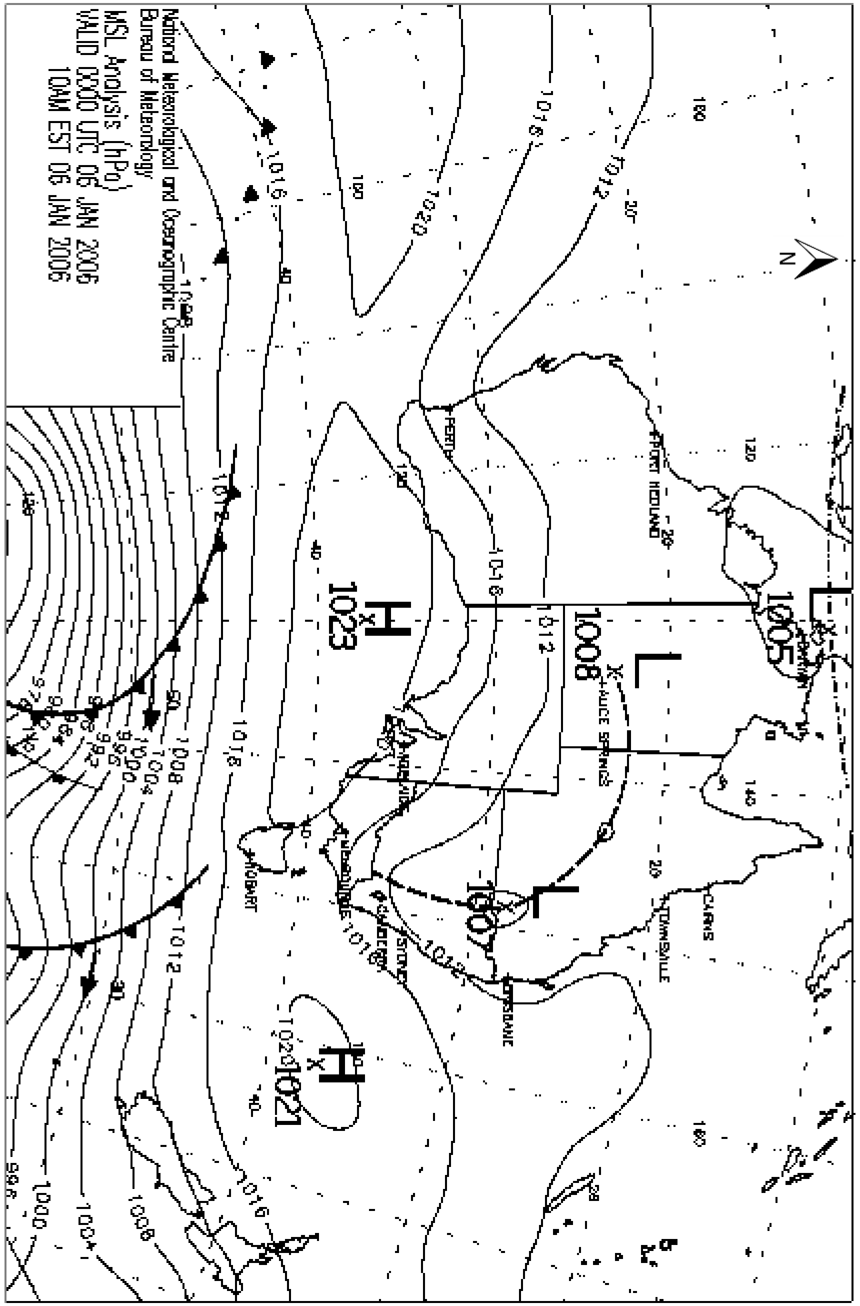
National Meteorological and Oceanographic Centre
Bureau of Meteorology
MSL Analysis (hPa)
VALID 0000 UTC 06 JAN 2006
10AM EST 06 JAN 2006
H
1023
H
1021
L
1008
L
1005
L
1007
PERTH
PORT HEDLAND
ALICE SPRINGS
ADELAIDE
MELBOURNE
HOBART
SYDNEY
BRISBANE
CAIRNS
TOWNSVILLE

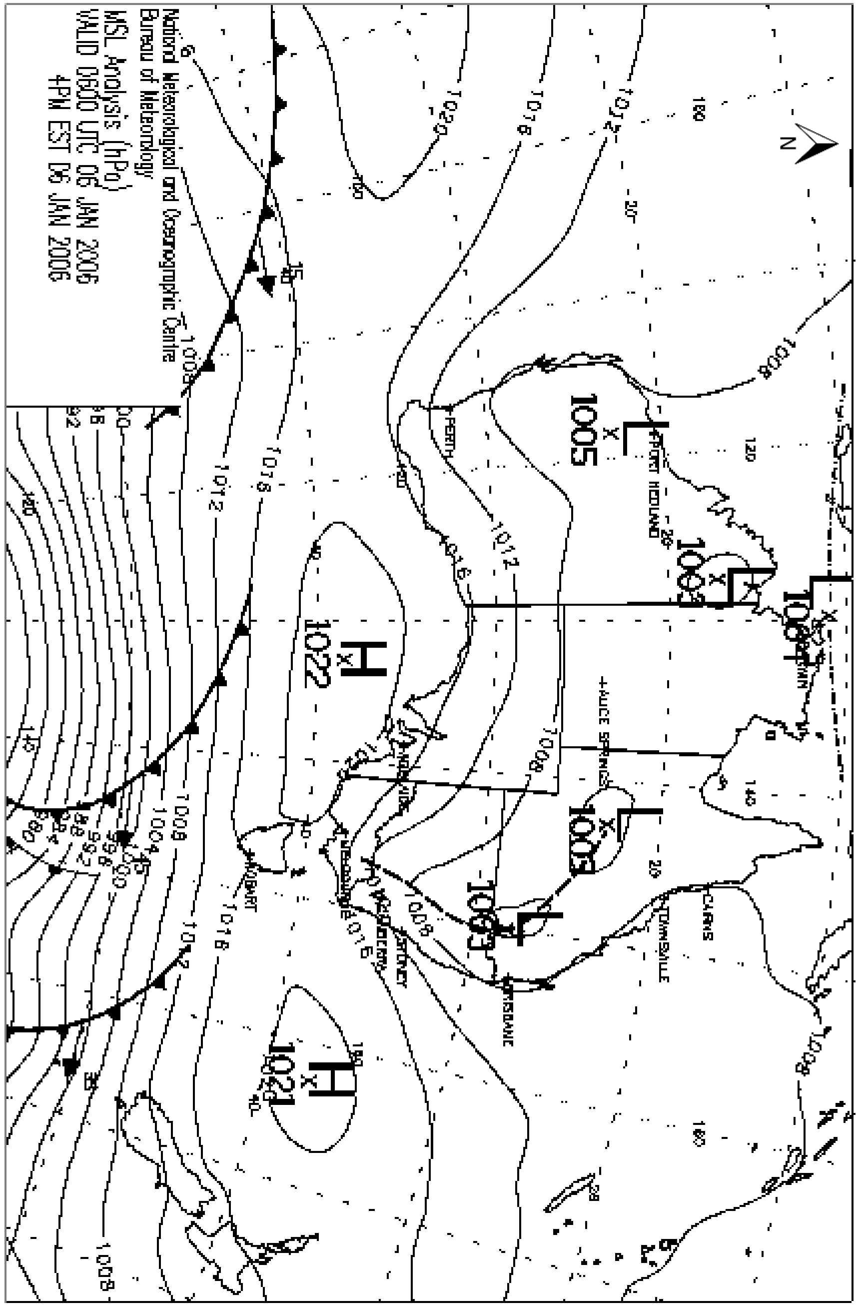
National Meteorological and Oceanographic Centre
Bureau of Meteorology
MSL Analysis (hPa)
VALID 0600 UTC 06 JAN 2006
4PM EST 06 JAN 2006
H
1022
H
1021
L
1005
L
1003
PERTH
PORT HEDLAND
ALICE SPRINGS
ADELAIDE
MELBOURNE
HOBART
SYDNEY
BRISBANE
CAIRNS
TOWNSVILLE

25/1/2004

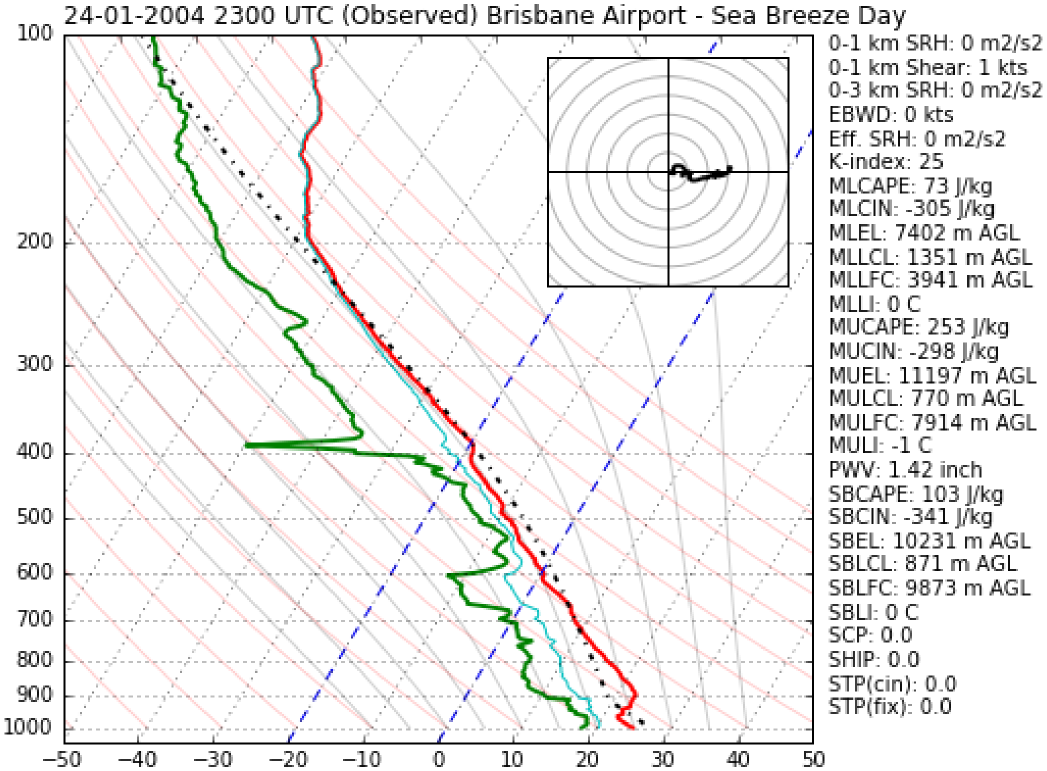
24-01-2004 2300 UTC (Observed) Brisbane Airport - Sea Breeze Day
0-1 km SRH: 0 m2/s2
0-1 km Shear: 1 kts
0-3 km SRH: 0 m2/s2
EBWD: 0 kts
Eff. SRH: 0 m2/s2
K-index: 25
MLCAPE: 73 J/kg
MLCIN: -305 J/kg
MLEL: 7402 m AGL
MLLCL: 1351 m AGL
MLLFC: 3941 m AGL
MLLI: 0 C
MUCAPE: 253 J/kg
MUCIN: -298 J/kg
MUEL: 11197 m AGL
MULCL: 770 m AGL
MULFC: 7914 m AGL
MULI: -1 C
PWV: 1.42 inch
SBCAPE: 103 J/kg
SBCIN: -341 J/kg
SBEL: 10231 m AGL
SBLCL: 871 m AGL
SBLFC: 9873 m AGL
SBLI: 0 C
SCP: 0.0
SHIP: 0.0
STP(cin): 0.0
STP(fix): 0.0

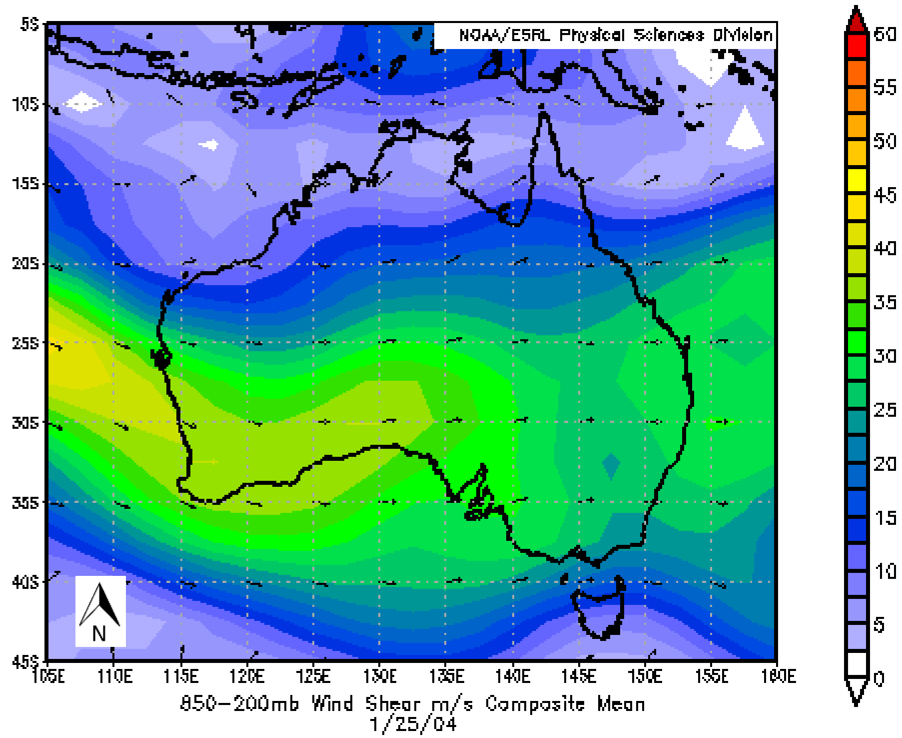
NOAA/ESRL Physical Sciences Division
N
850–200mb Wind Shear m/s Composite Mean
1/25/04

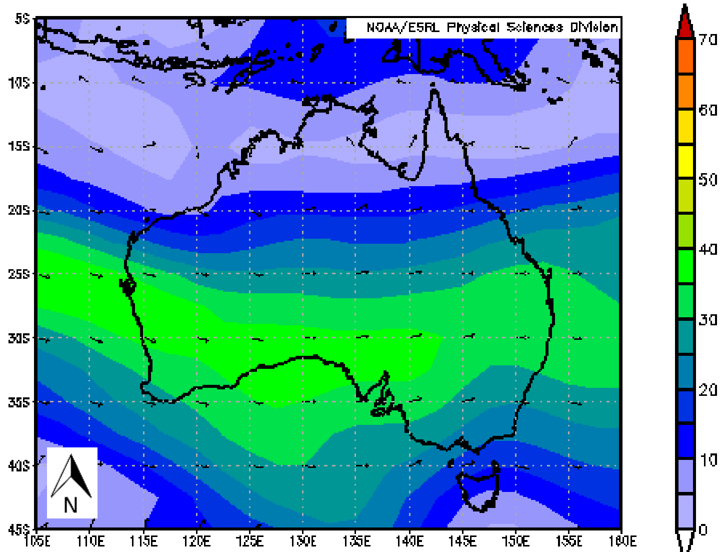

200mb Vector Wind (m/s) Composite Mean
1/25/04
NCEP/NCAR Reanalysis

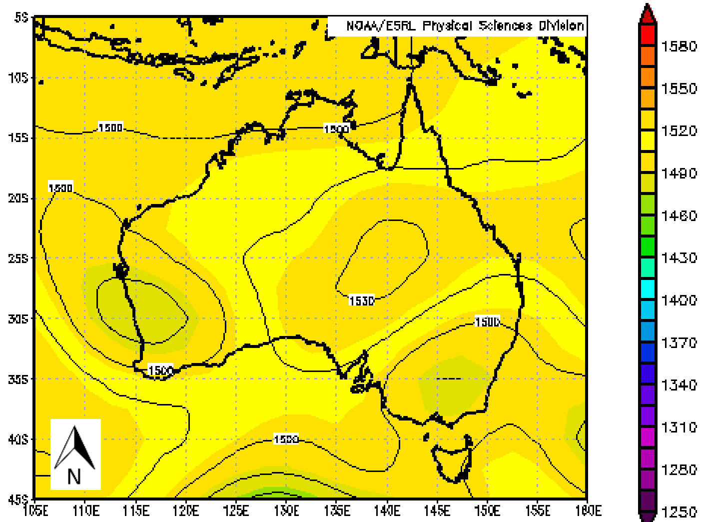

850mb Geopotential Height (m) Composite Mean
1/25/04
NCEP/NCAR Reanalysis

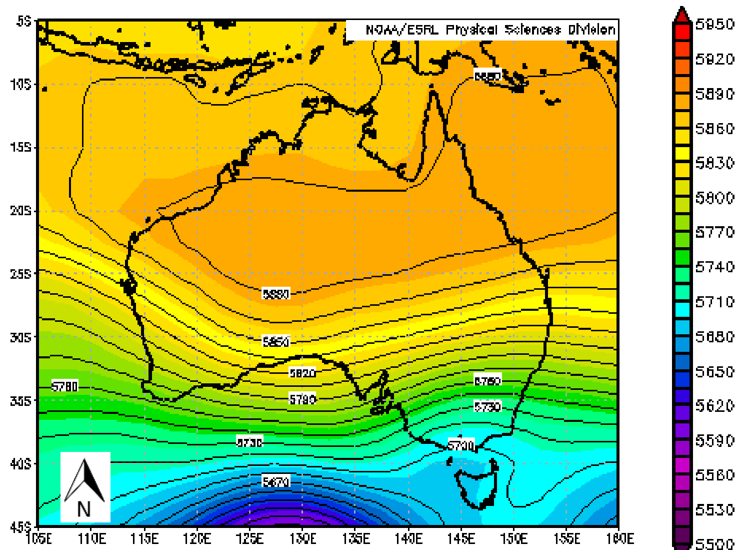

500mb Geopotential Height (m) Composite Mean
1/25/04
NCEP/NCAR Reanalysis

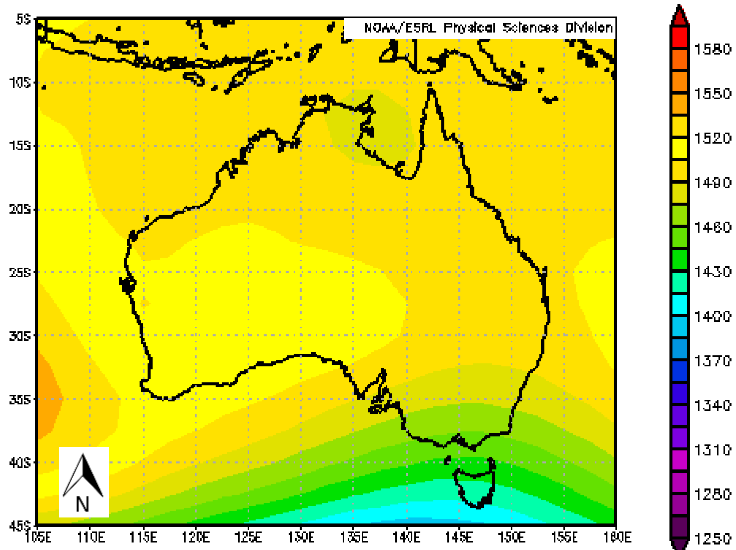

850mb Geopotential Height (m) Composite Mean
1/1/04 to 1/31/04
NCEP/NCAR Reanalysis

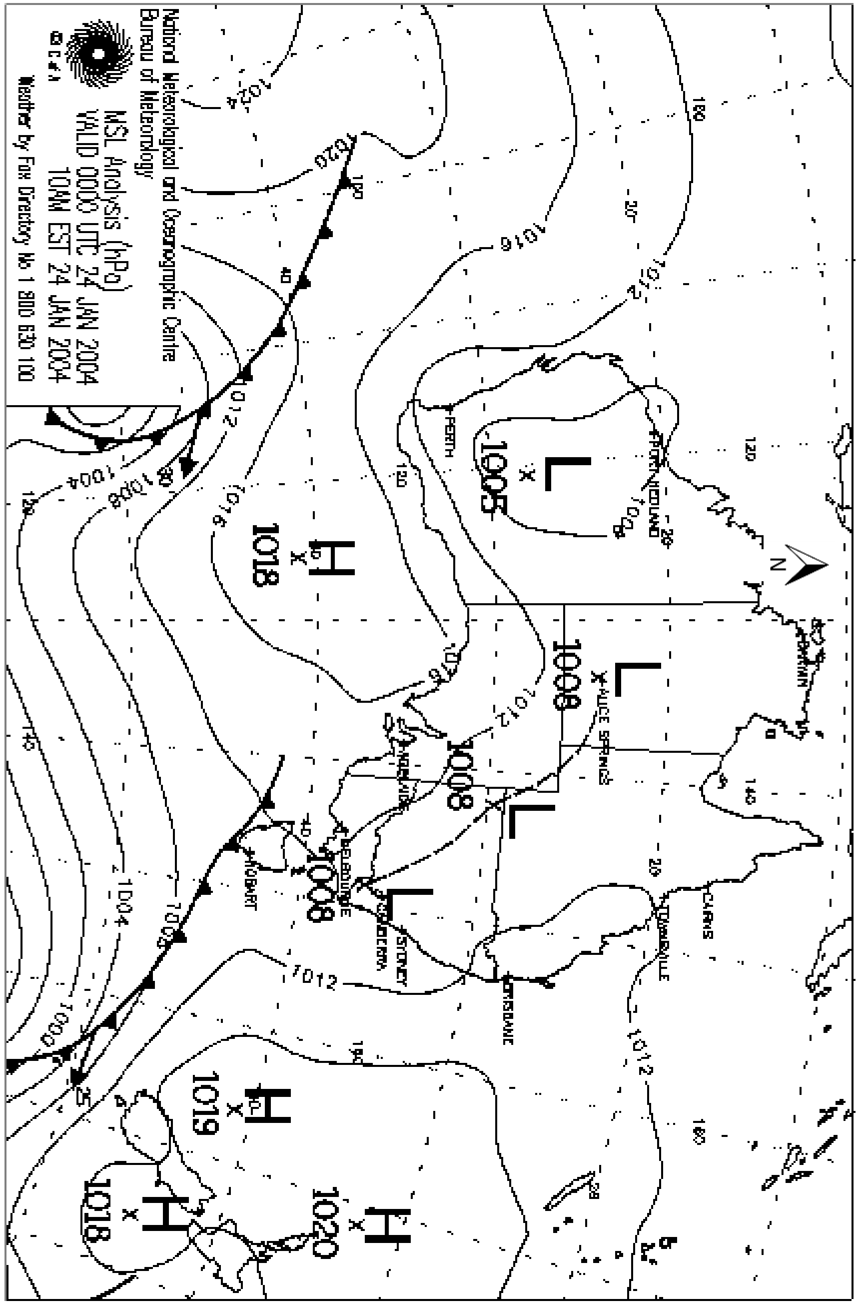
National Meteorological and Oceanographic Centre
Bureau of Meteorology
MSL Analysis (hPa)
VALID 0000 UTC 24 JAN 2004
10AM EST 24 JAN 2004
Weather by Fax Directory No 1 800 630 100

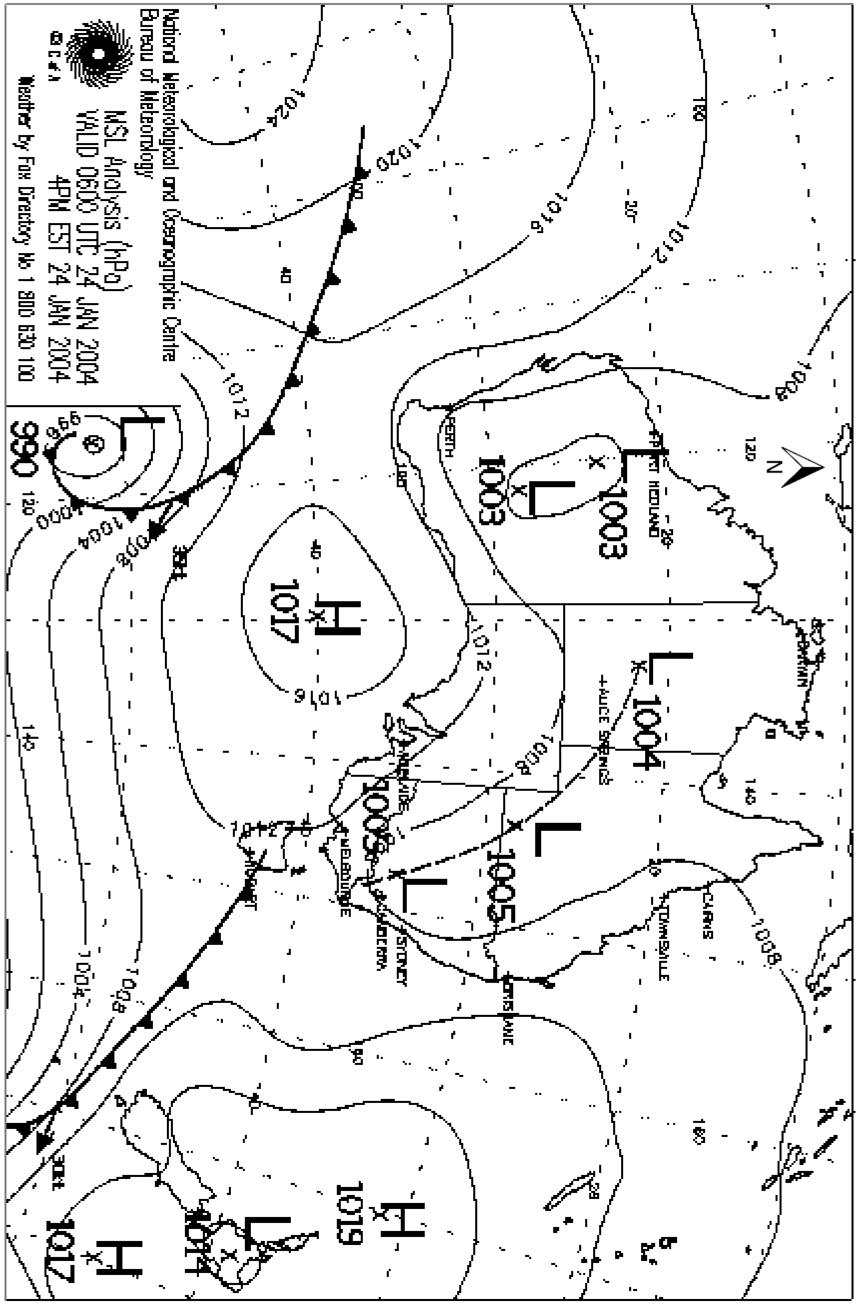
National Meteorological and Oceanographic Centre
Bureau of Meteorology
MSL Analysis (hPa)
VALID 0600 UTC 24 JAN 2004
4PM EST 24 JAN 2004
Weather by Fax Directory No 1 800 630 100

24/1/2004

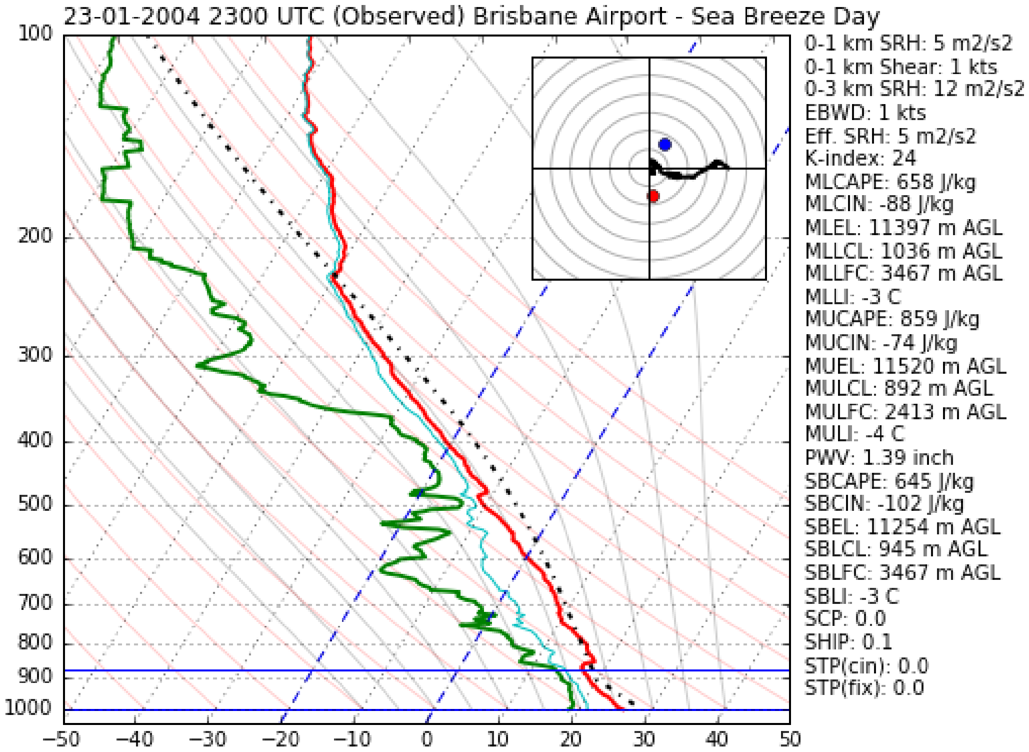
23-01-2004 2300 UTC (Observed) Brisbane Airport - Sea Breeze Day
0-1 km SRH: 5 m2/s2
0-1 km Shear: 1 kts
0-3 km SRH: 12 m2/s2
EBWD: 1 kts
Eff. SRH: 5 m2/s2
K-index: 24
MLCAPE: 658 J/kg
MLCIN: -88 J/kg
MLEL: 11397 m AGL
MLLCL: 1036 m AGL
MLLFC: 3467 m AGL
MLLI: -3 C
MUCAPE: 859 J/kg
MUCIN: -74 J/kg
MUEL: 11520 m AGL
MULCL: 892 m AGL
MULFC: 2413 m AGL
MULI: -4 C
PWV: 1.39 inch
SBCAPE: 645 J/kg
SBCIN: -102 J/kg
SBEL: 11254 m AGL
SBLCL: 945 m AGL
SBLFC: 3467 m AGL
SBLI: -3 C
SCP: 0.0
SHIP: 0.1
STP(cin): 0.0
STP(fix): 0.0

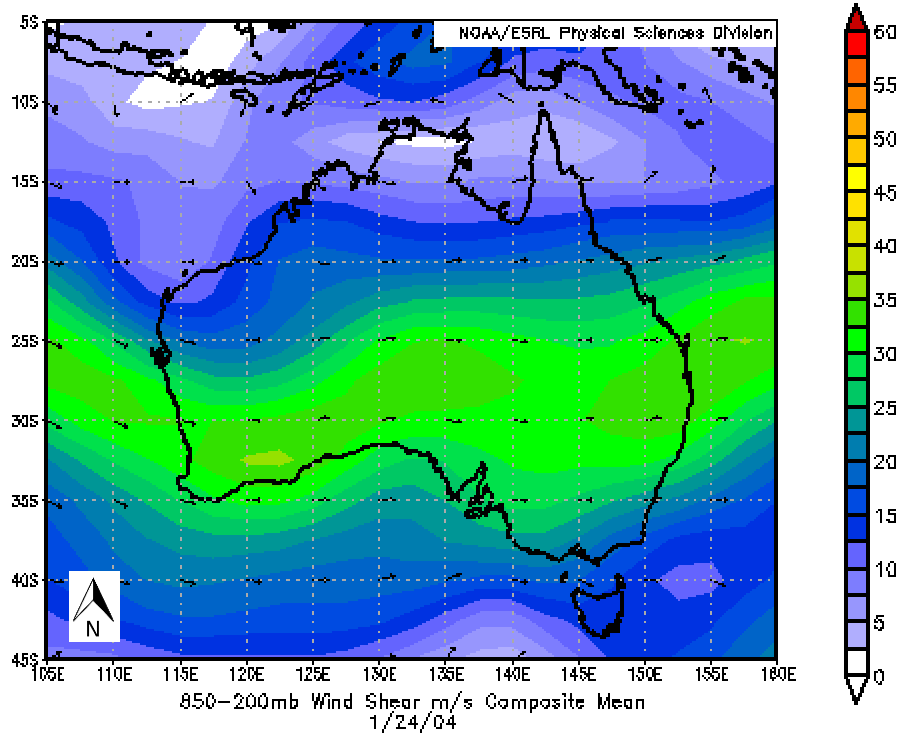
NOAA/ESRL Physical Sciences Division
850–200mb Wind Shear m/s Composite Mean
1/24/04

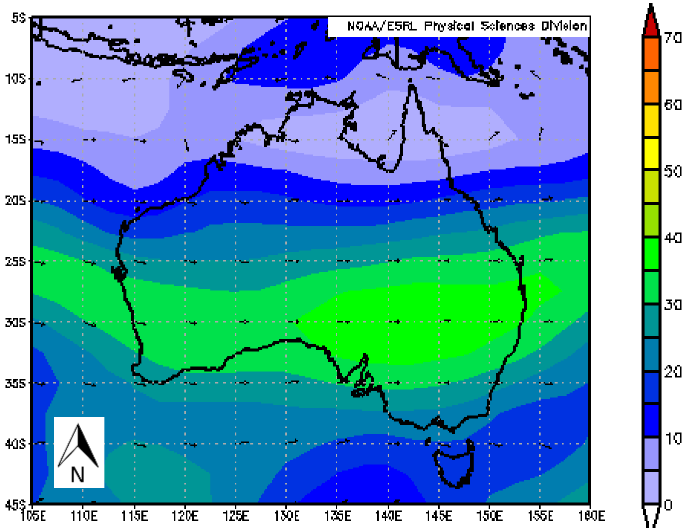

200mb Vector Wind (m/s) Composite Mean
1/24/04
NCEP/NCAR Reanalysis

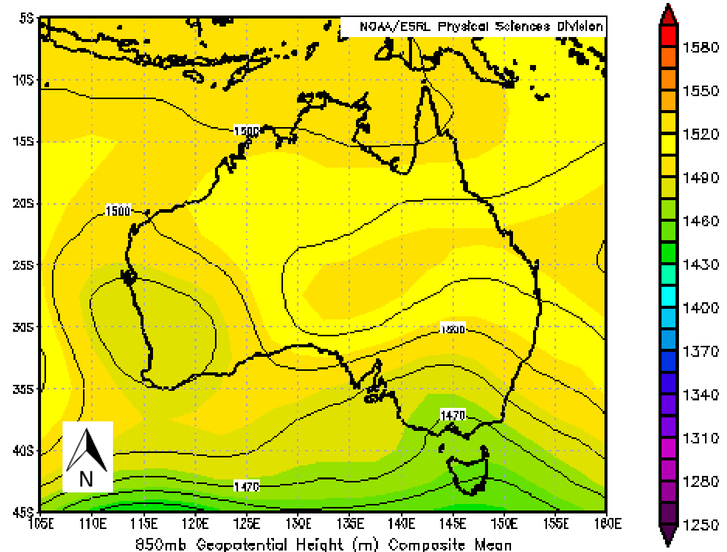

850mb Geopotential Height (m) Composite Mean
1/24/04
NCEP/NCAR Reanalysis

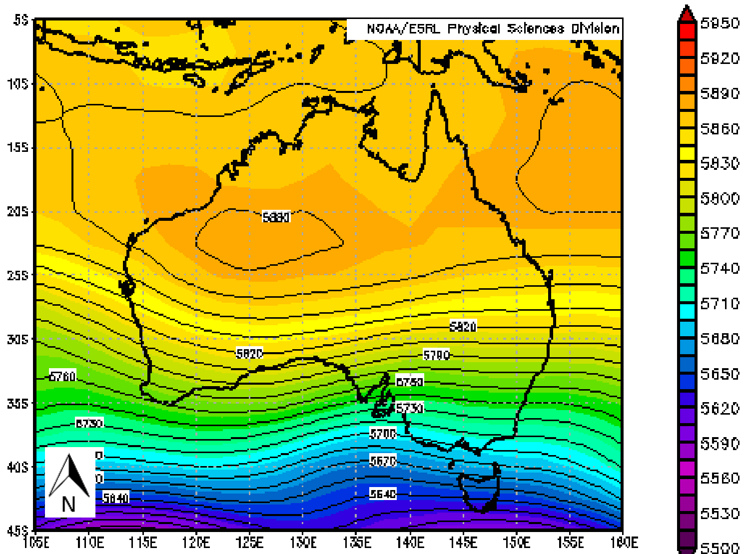

500mb Geopotential Height (m) Composite Mean
1/24/04
NCEP/NCAR Reanalysis

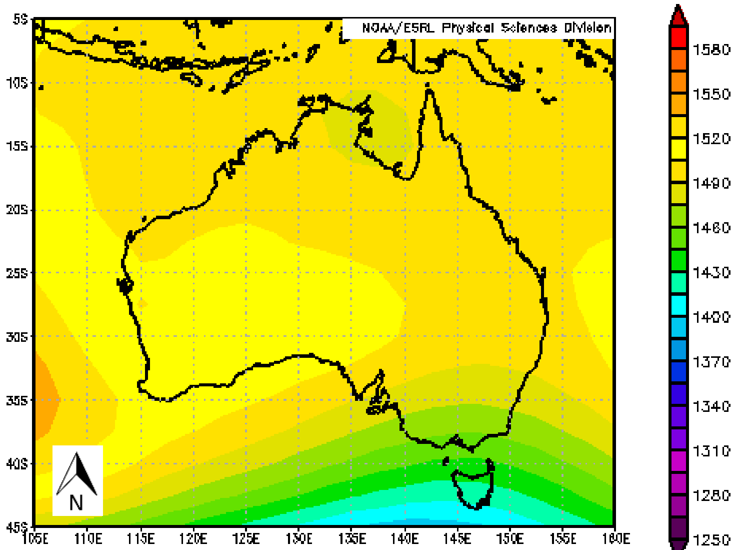

850mb Geopotential Height (m) Composite Mean
1/1/04 to 1/31/04
NCEP/NCAR Reanalysis

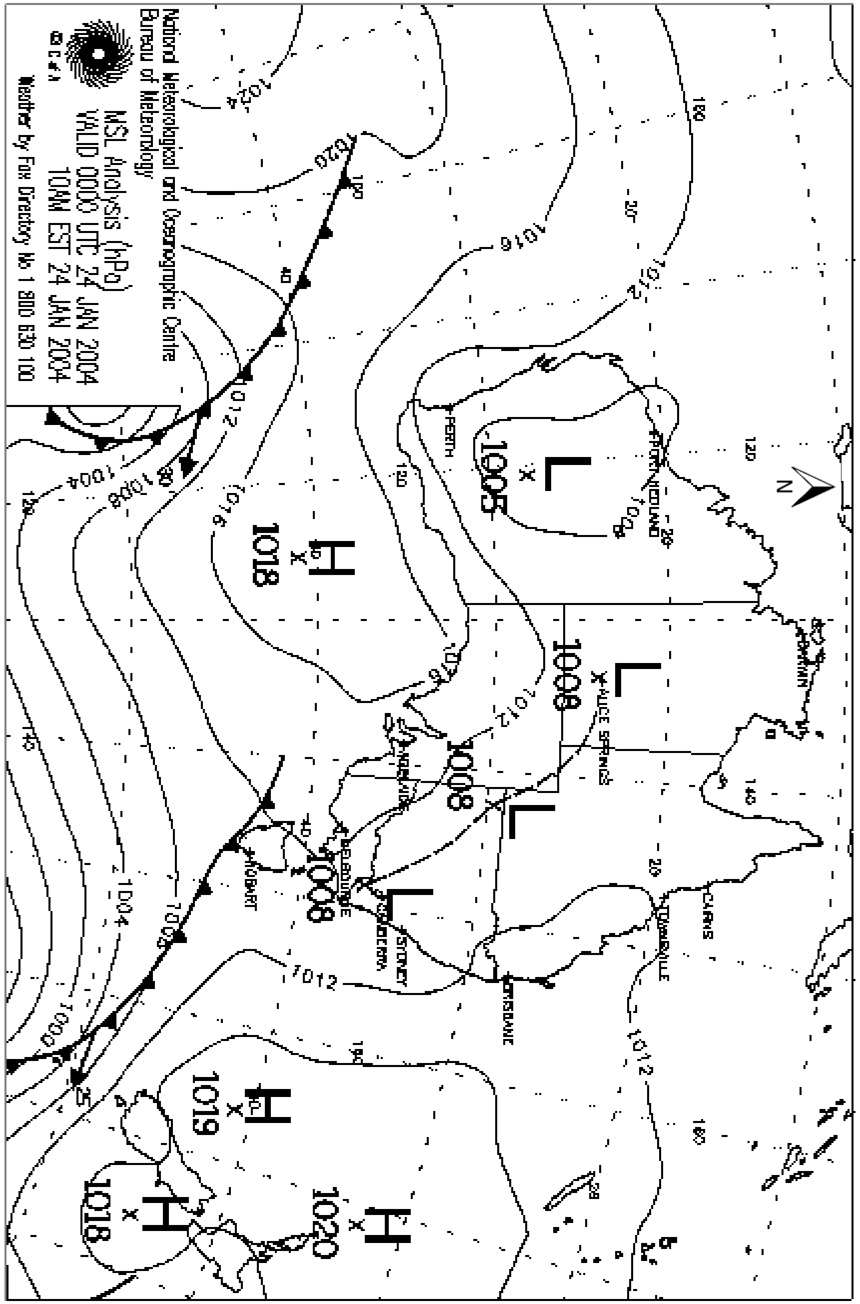
National Meteorological and Oceanographic Centre
Bureau of Meteorology
MSL Analysis (hPa)
VALID 0000 UTC 24 JAN 2004
10AM EST 24 JAN 2004
Weather by Fax Directory No 1 900 630 100
PERTH
PORT HEDLAND
DARWIN
ALICE SPRINGS
ADELAIDE
MELBOURNE
CANBERRA
SYDNEY
HOBART
BRISBANE
TOWNSVILLE
CAIRNS

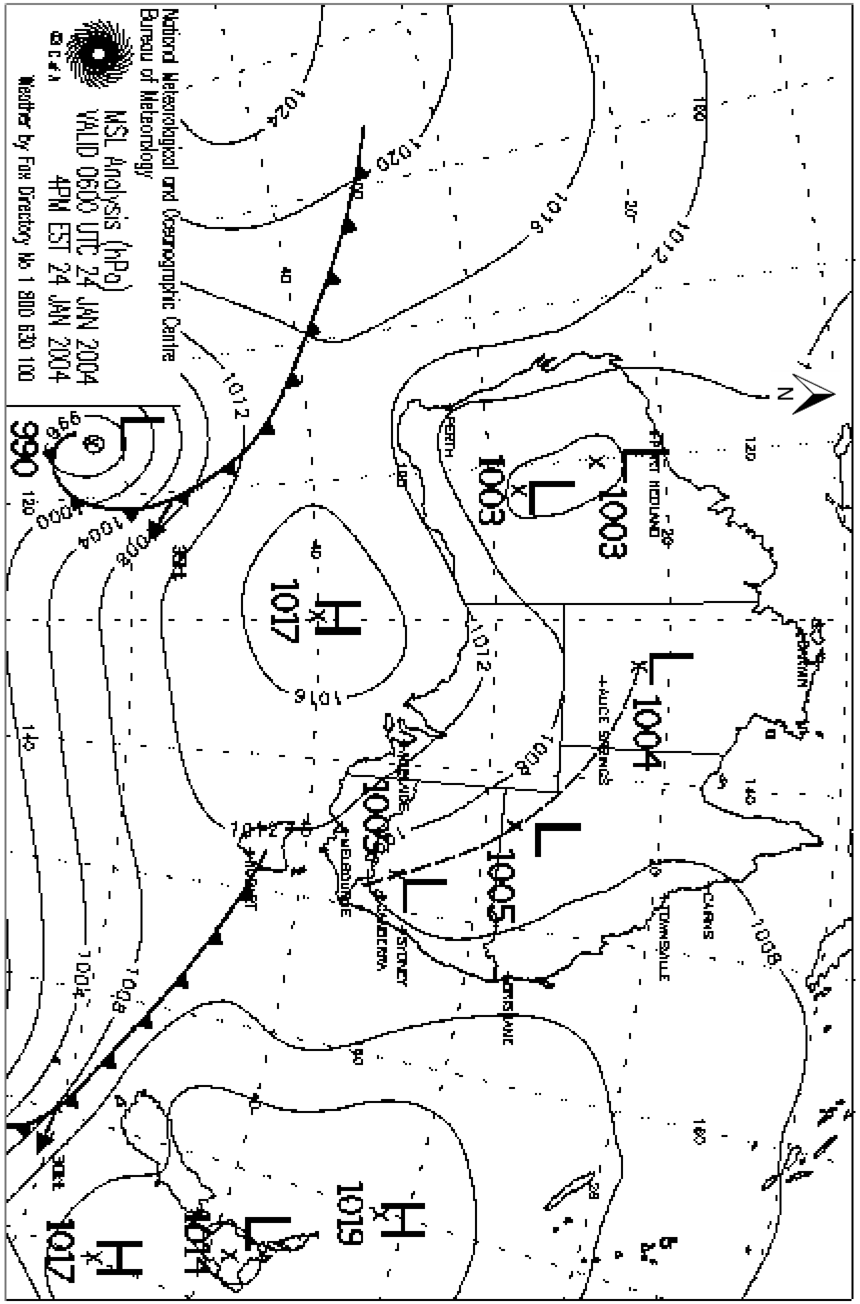
National Meteorological and Oceanographic Centre
Bureau of Meteorology
MSL Analysis (hPa)
VALID 0600 UTC 24 JAN 2004
4PM EST 24 JAN 2004
Weather by Fax Directory No 1 900 630 100
PERTH
PORT HEDLAND
DARWIN
ALICE SPRINGS
ADELAIDE
MELBOURNE
CANBERRA
SYDNEY
HOBART
BRISBANE
TOWNSVILLE
CAIRNS

18/1/2011

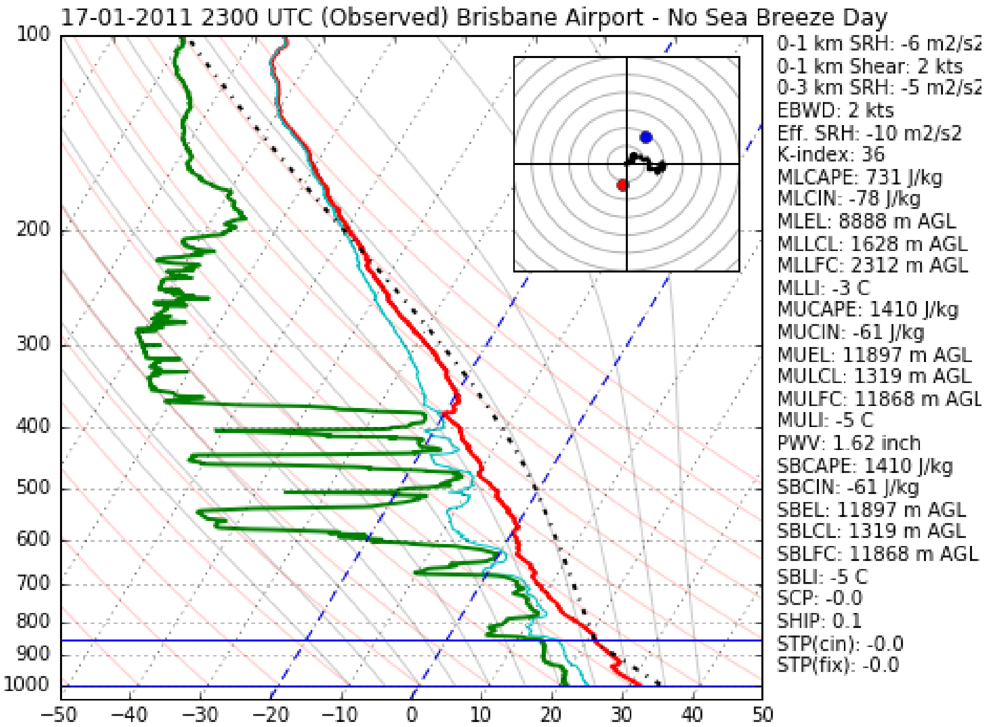
17-01-2011 2300 UTC (Observed) Brisbane Airport - No Sea Breeze Day
0-1 km SRH: -6 m2/s2
0-1 km Shear: 2 kts
0-3 km SRH: -5 m2/s2
EBWD: 2 kts
Eff. SRH: -10 m2/s2
K-index: 36
MLCAPE: 731 J/kg
MLCIN: -78 J/kg
MLEL: 8888 m AGL
MLLCL: 1628 m AGL
MLLFC: 2312 m AGL
MLLI: -3 C
MUCAPE: 1410 J/kg
MUCIN: -61 J/kg
MUEL: 11897 m AGL
MULCL: 1319 m AGL
MULFC: 11868 m AGL
MULI: -5 C
PWV: 1.62 inch
SBCAPE: 1410 J/kg
SBCIN: -61 J/kg
SBEL: 11897 m AGL
SBLCL: 1319 m AGL
SBLFC: 11868 m AGL
SBLI: -5 C
SCP: -0.0
SHIP: 0.1
STP(cin): -0.0
STP(fix): -0.0

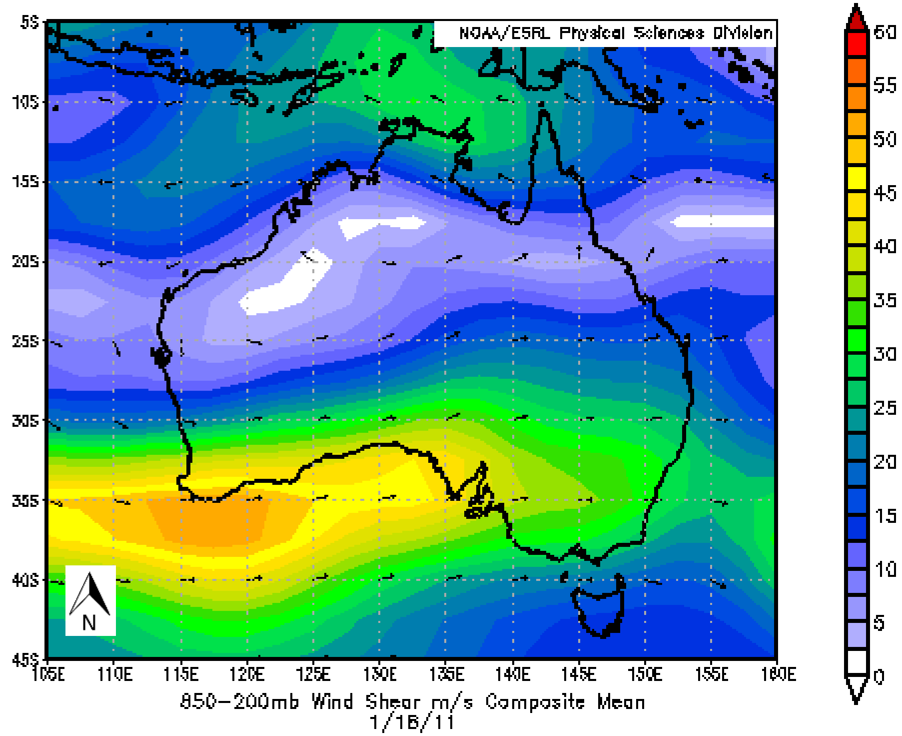
NOAA/ESRL Physical Sciences Division
850−200mb Wind Shear m/s Composite Mean
1/18/11

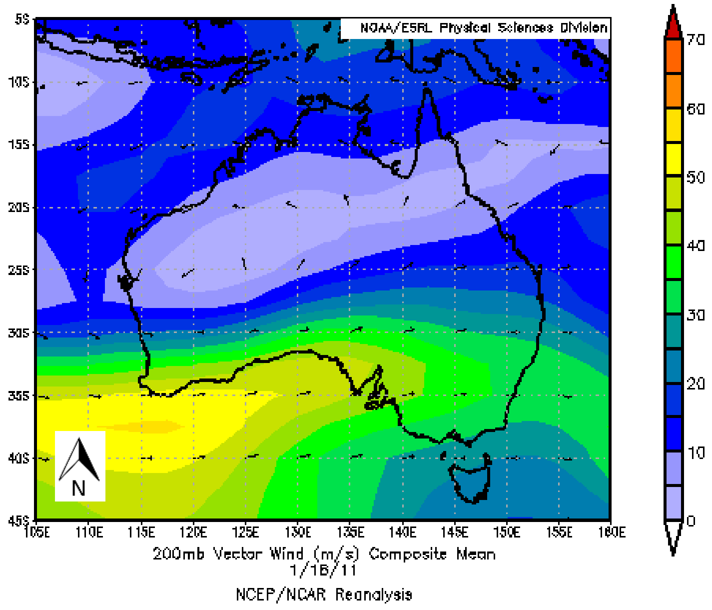
NOAA/ESRL Physical Sciences Division
N
200mb Vector Wind (m/s) Composite Mean
1/16/11
NCEP/NCAR Reanalysis

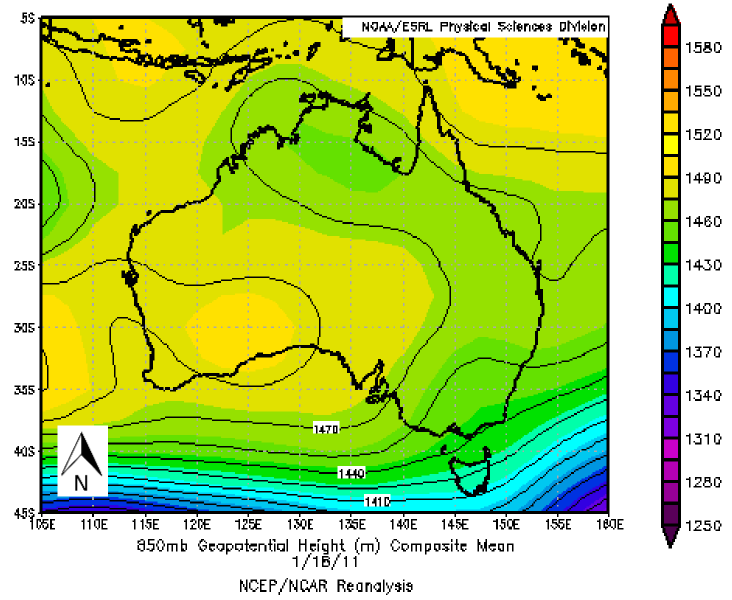
NOAA/ESRL Physical Sciences Division
N
850mb Geopotential Height (m) Composite Mean
1/16/11
NCEP/NCAR Reanalysis

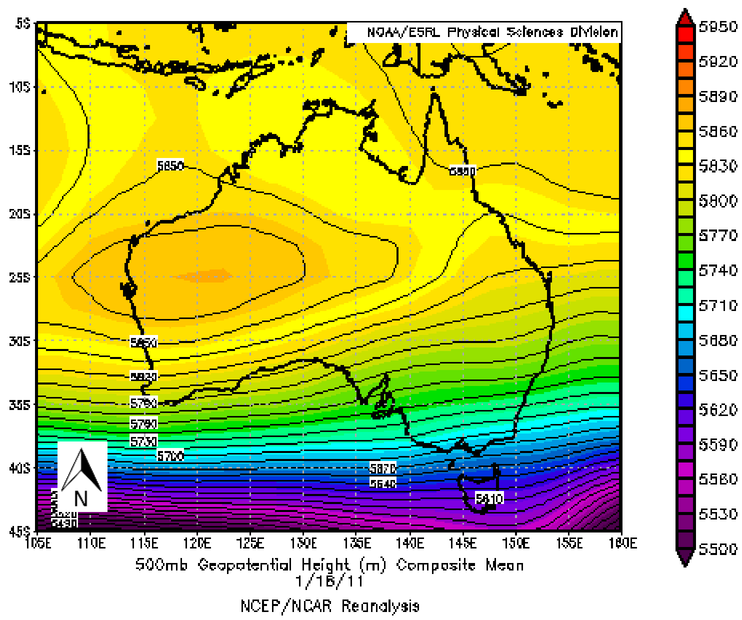
NOAA/ESRL Physical Sciences Division
N
500mb Geopotential Height (m) Composite Mean
1/16/11
NCEP/NCAR Reanalysis

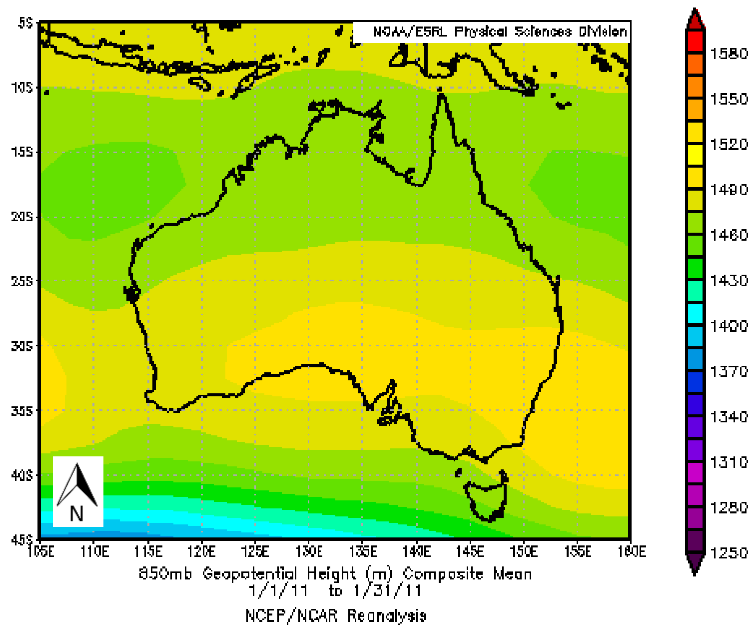
NOAA/ESRL Physical Sciences Division
N
850mb Geopotential Height (m) Composite Mean
1/1/11 to 1/31/11
NCEP/NCAR Reanalysis

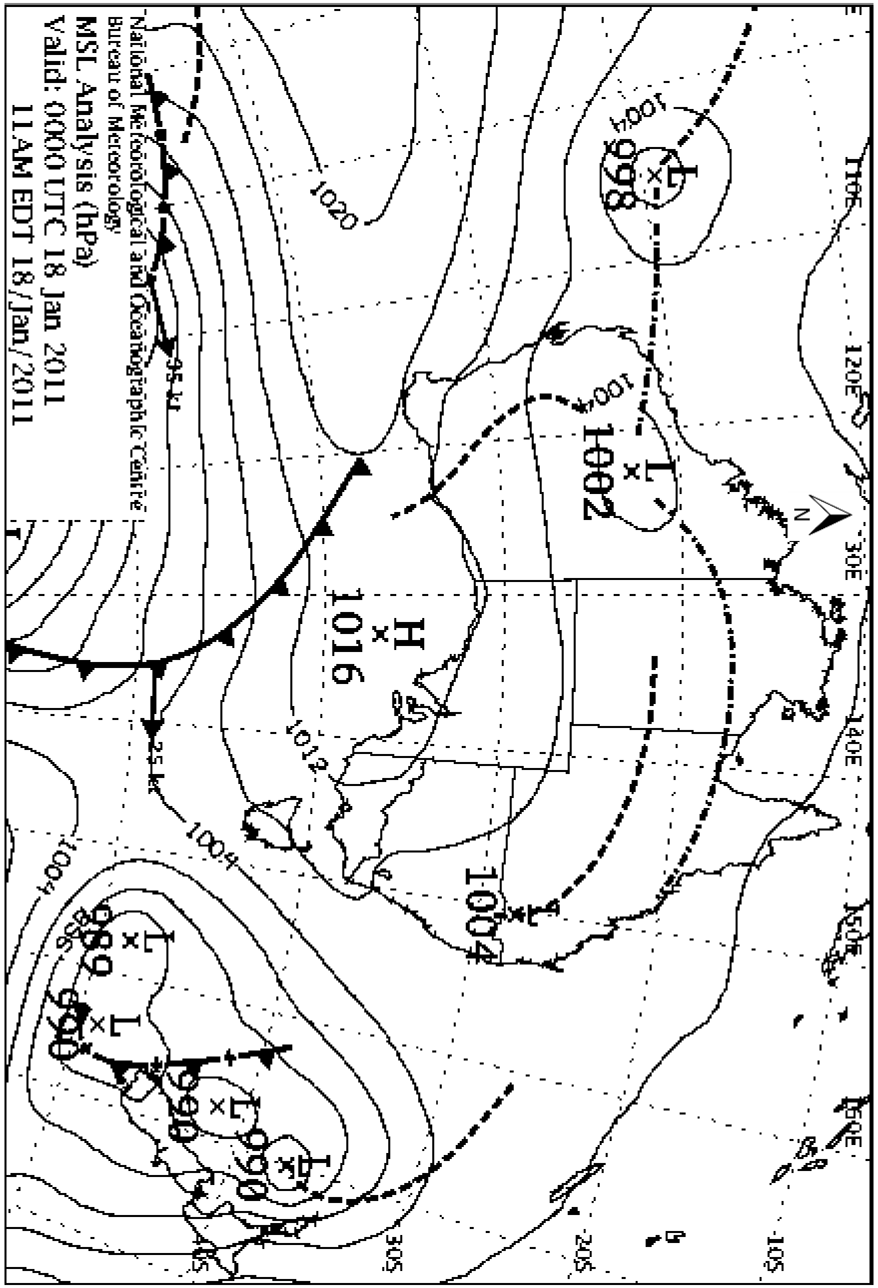
National Meteorological and Oceanographic Centre
Bureau of Meteorology
MSL Analysis (hPa)
Valid: 0000 UTC 18 Jan 2011
11AM EDT 18/Jan/2011

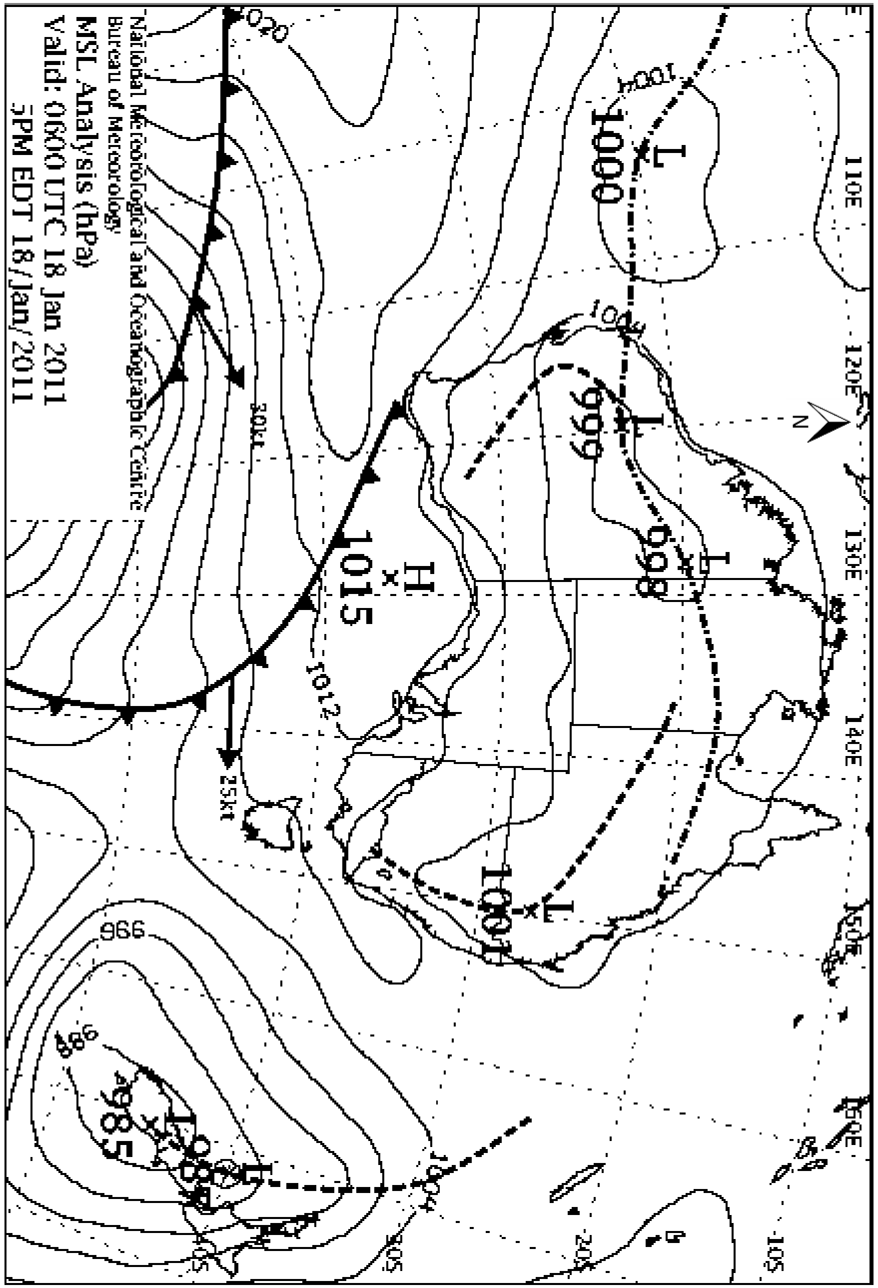
National Meteorological and Oceanographic Centre
Bureau of Meteorology
MSL Analysis (hPa)
Valid: 0600 UTC 18 Jan 2011
5PM EDT 18/Jan/2011

3/1/2011

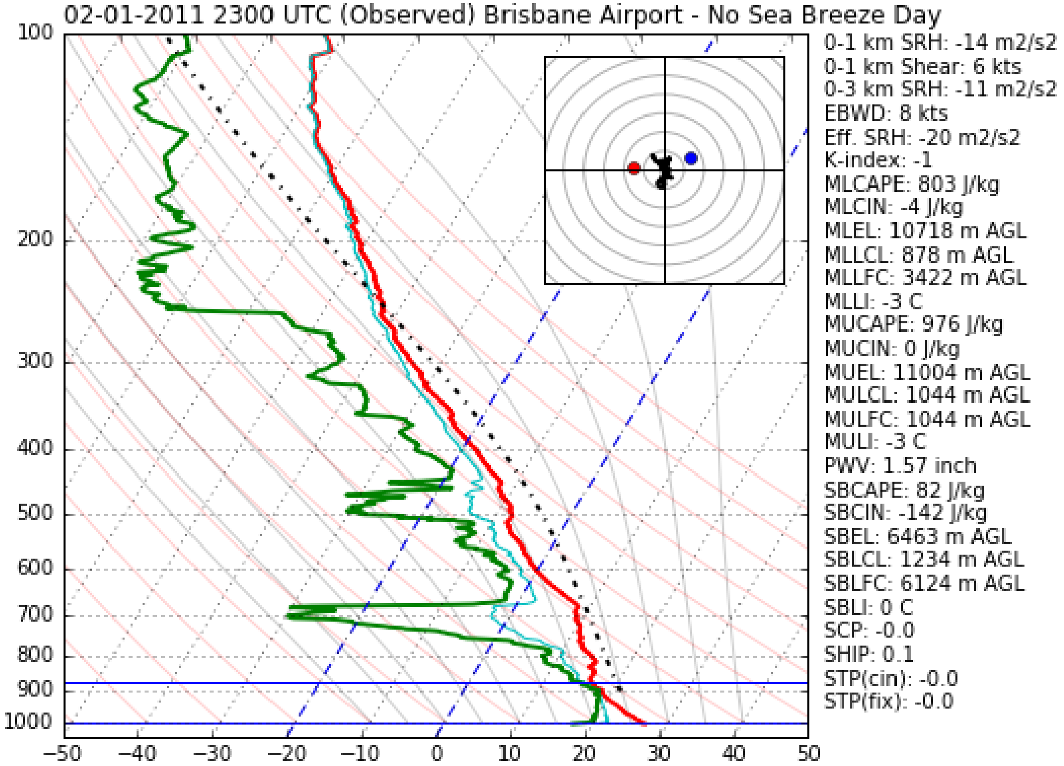
02-01-2011 2300 UTC (Observed) Brisbane Airport - No Sea Breeze Day
0-1 km SRH: -14 m2/s2
0-1 km Shear: 6 kts
0-3 km SRH: -11 m2/s2
EBWD: 8 kts
Eff. SRH: -20 m2/s2
K-index: -1
MLCAPE: 803 J/kg
MLCIN: -4 J/kg
MLEL: 10718 m AGL
MLLCL: 878 m AGL
MLLFC: 3422 m AGL
MLLI: -3 C
MUCAPE: 976 J/kg
MUCIN: 0 J/kg
MUEL: 11004 m AGL
MULCL: 1044 m AGL
MULFC: 1044 m AGL
MULI: -3 C
PWV: 1.57 inch
SBCAPE: 82 J/kg
SBCIN: -142 J/kg
SBEL: 6463 m AGL
SBLCL: 1234 m AGL
SBLFC: 6124 m AGL
SBLI: 0 C
SCP: -0.0
SHIP: 0.1
STP(cin): -0.0
STP(fix): -0.0

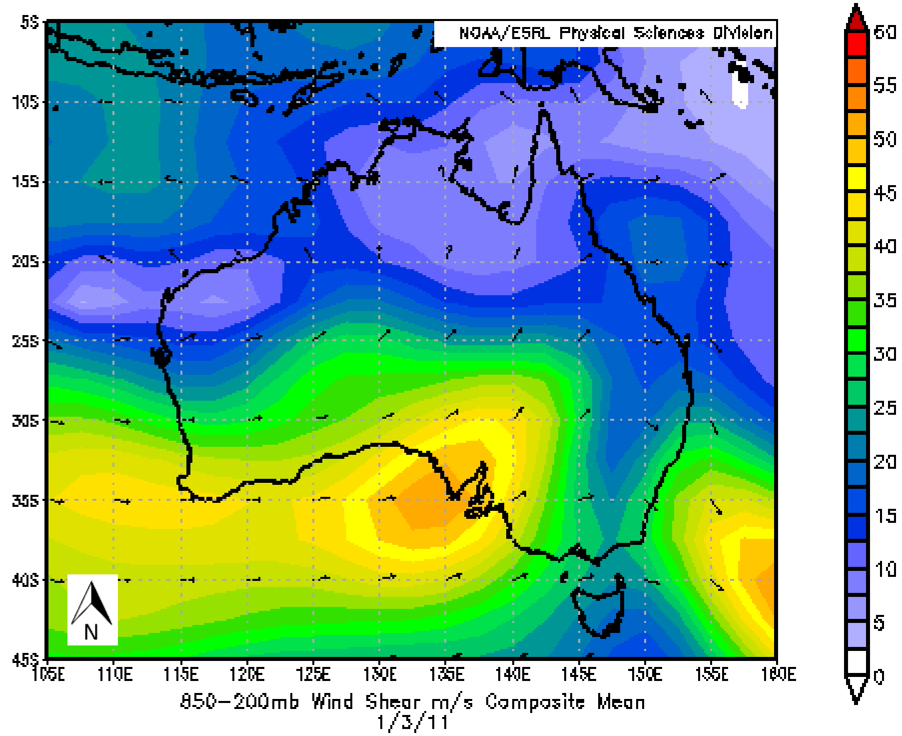
NOAA/ESRL Physical Sciences Division
N
850–200mb Wind Shear m/s Composite Mean
1/3/11

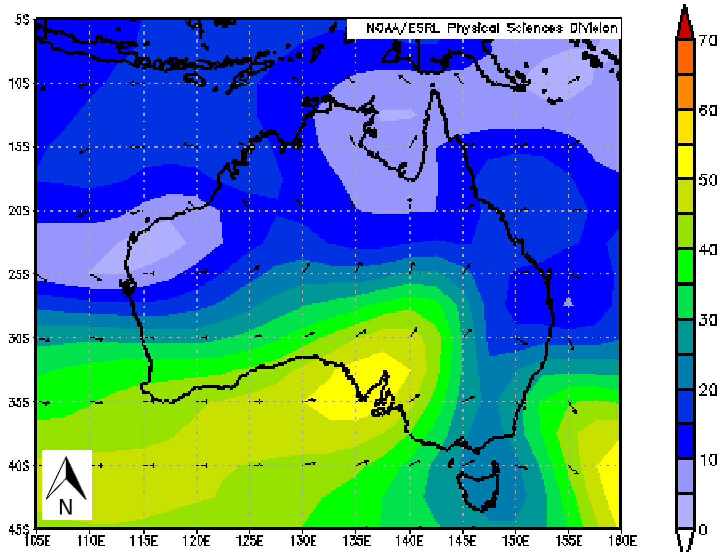

200mb Vector Wind (m/s) Composite Mean
1/3/11
NCEP/NCAR Reanalysis

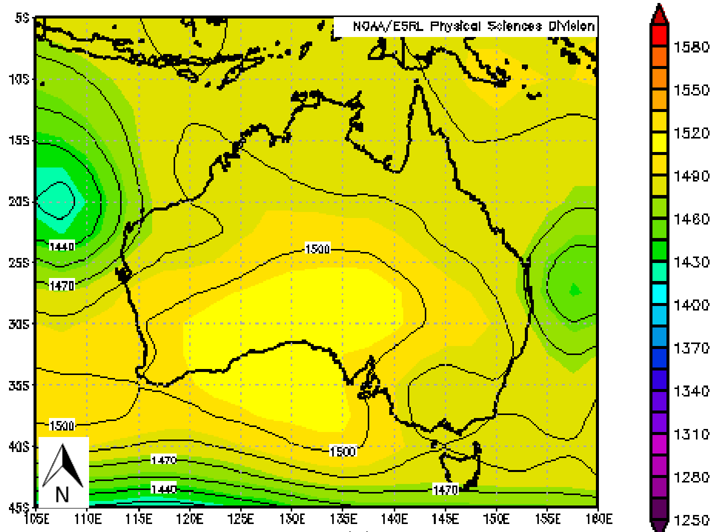

850mb Geopotential Height (m) Composite Mean
1/3/11
NCEP/NCAR Reanalysis

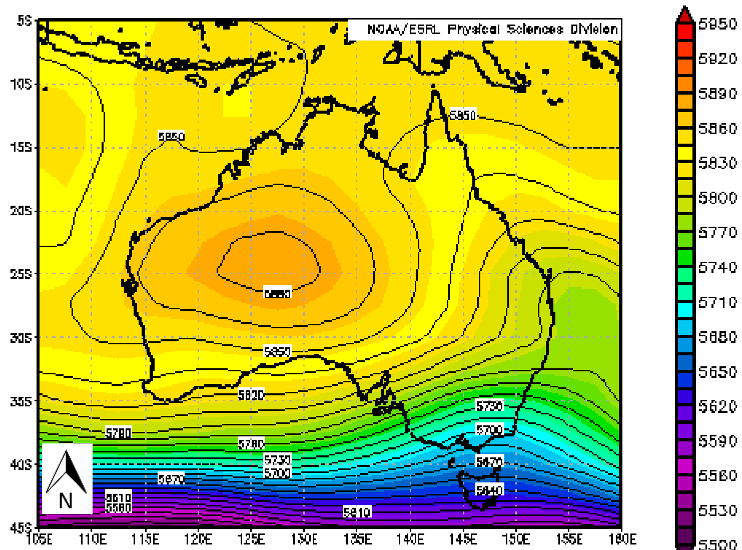

500mb Geopotential Height (m) Composite Mean
1/3/11
NCEP/NCAR Reanalysis

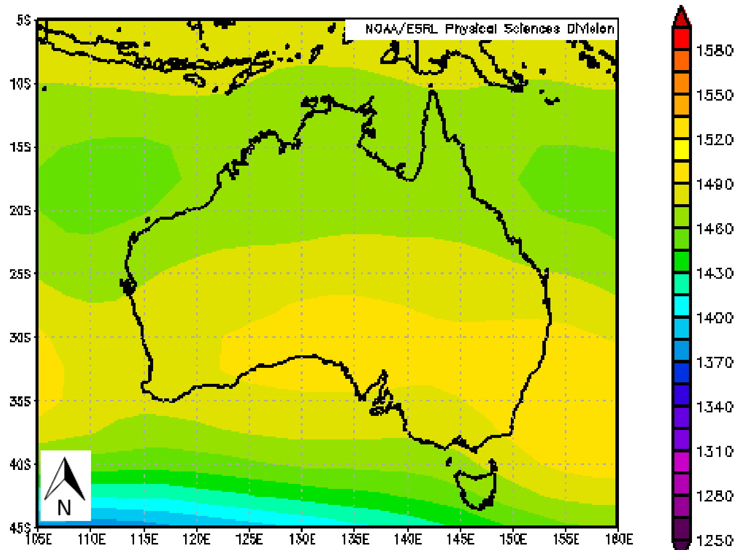

850mb Geopotential Height (m) Composite Mean
1/1/11 to 1/31/11
NCEP/NCAR Reanalysis

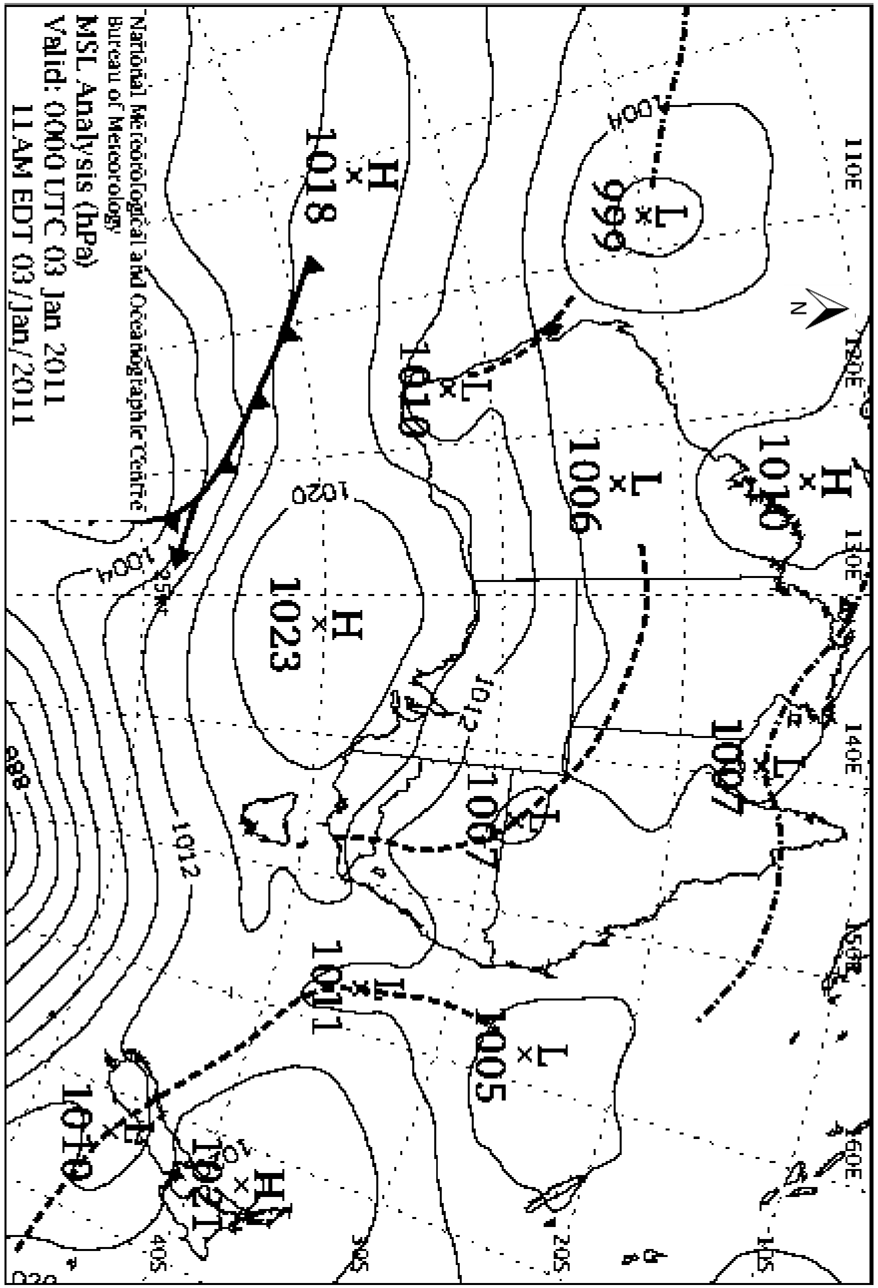
National Meteorological and Oceanographic Centre
Bureau of Meteorology
MSL Analysis (hPa)
Valid: 0000 UTC 03 Jan 2011
11AM EDT 03/Jan/2011

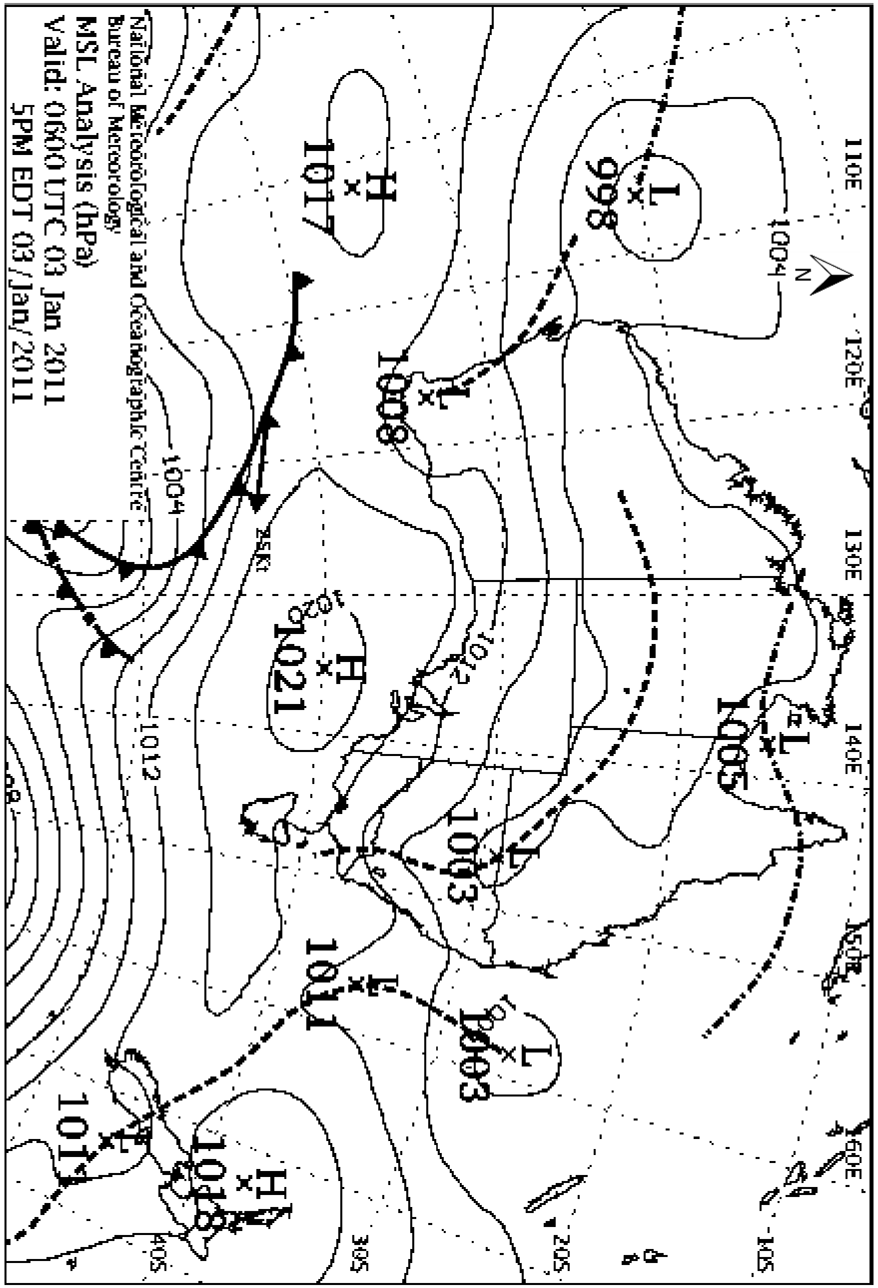
National Meteorological and Oceanographic Centre
Bureau of Meteorology
MSL Analysis (hPa)
Valid: 0600 UTC 03 Jan 2011
5PM EDT 03/Jan/2011

6/1/2008

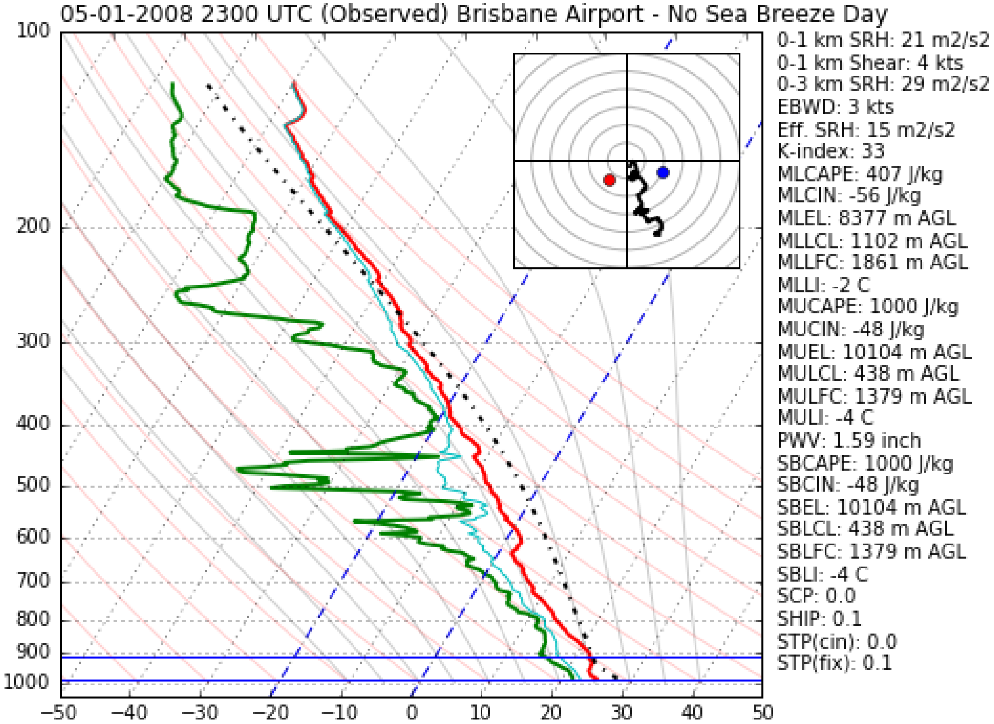
05-01-2008 2300 UTC (Observed) Brisbane Airport - No Sea Breeze Day
0-1 km SRH: 21 m2/s2
0-1 km Shear: 4 kts
0-3 km SRH: 29 m2/s2
EBWD: 3 kts
Eff. SRH: 15 m2/s2
K-index: 33
MLCAPE: 407 J/kg
MLCIN: -56 J/kg
MLEL: 8377 m AGL
MLLCL: 1102 m AGL
MLLFC: 1861 m AGL
MLLI: -2 C
MUCAPE: 1000 J/kg
MUCIN: -48 J/kg
MUEL: 10104 m AGL
MULCL: 438 m AGL
MULFC: 1379 m AGL
MULI: -4 C
PWV: 1.59 inch
SBCAPE: 1000 J/kg
SBCIN: -48 J/kg
SBEL: 10104 m AGL
SBLCL: 438 m AGL
SBLFC: 1379 m AGL
SBLI: -4 C
SCP: 0.0
SHIP: 0.1
STP(cin): 0.0
STP(fix): 0.1
100
200
300
400
500
600
700
800
900
1000
−50 −40 −30 −20 −10 0 10 20 30 40 50

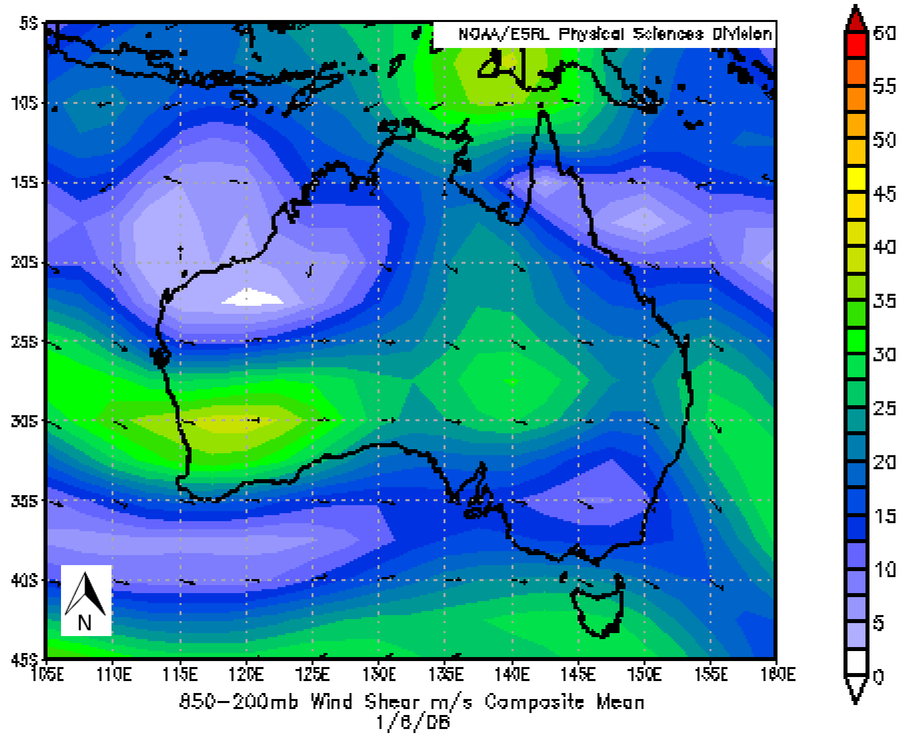
NOAA/ESRL Physical Sciences Division
5S 10S 15S 20S 25S 30S 35S 40S 45S
105E 110E 115E 120E 125E 130E 135E 140E 145E 150E 155E 160E
N
850–200mb Wind Shear m/s Composite Mean
1/6/08
60 55 50 45 40 35 30 25 20 15 10 5 0

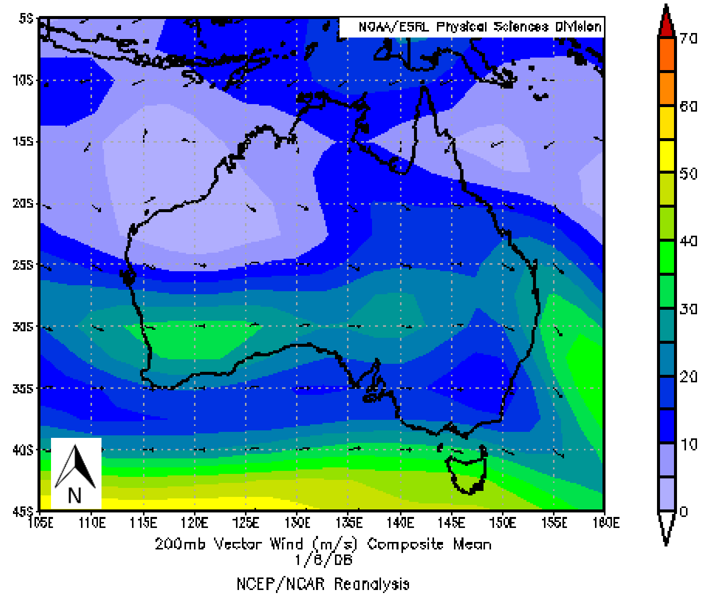
NOAA/ESRL Physical Sciences Division
200mb Vector Wind (m/s) Composite Mean
1/6/08
NCEP/NCAR Reanalysis

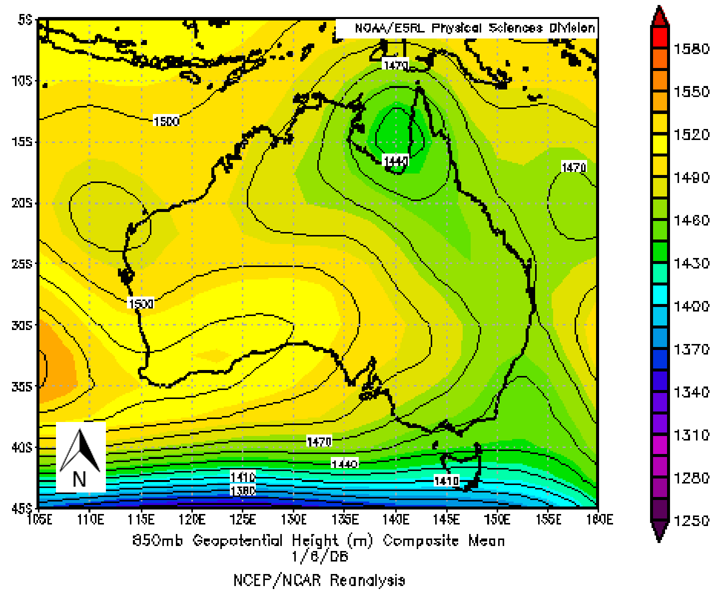
NOAA/ESRL Physical Sciences Division
850mb Geopotential Height (m) Composite Mean
1/6/08
NCEP/NCAR Reanalysis

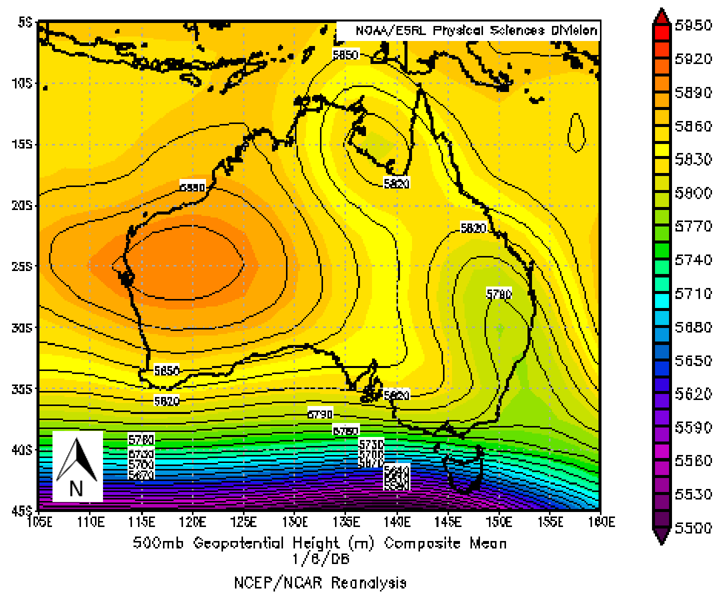
NOAA/ESRL Physical Sciences Division
500mb Geopotential Height (m) Composite Mean
1/6/08
NCEP/NCAR Reanalysis

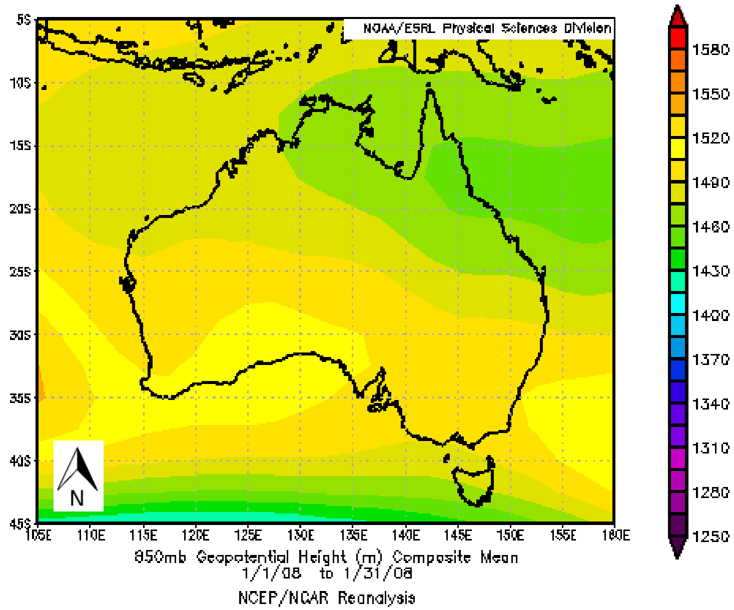
NOAA/ESRL Physical Sciences Division
850mb Geopotential Height (m) Composite Mean
1/1/08 to 1/31/08
NCEP/NCAR Reanalysis

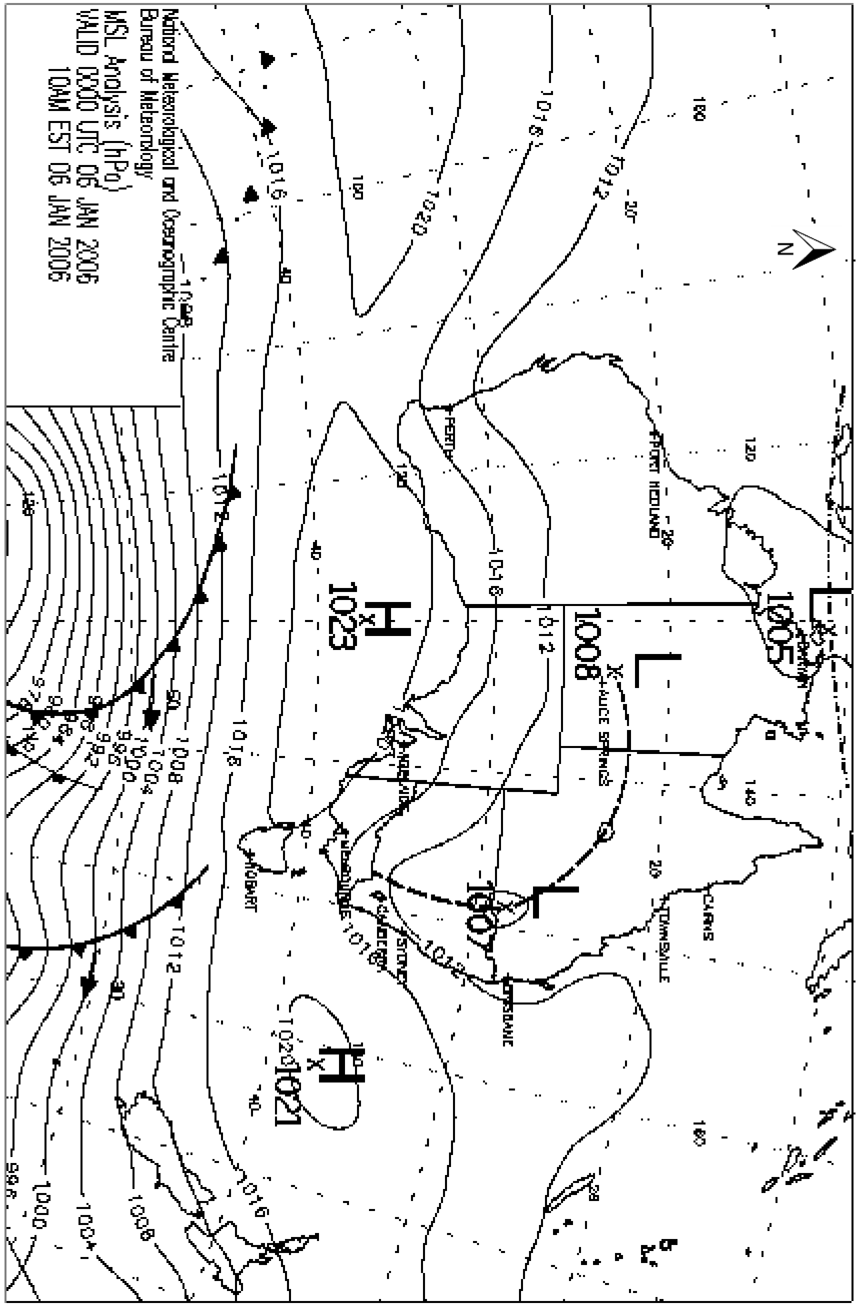
National Meteorological and Oceanographic Centre
Bureau of Meteorology
MSL Analysis (hPa)
VALID 0000 UTC 06 JAN 2006
10AM EST 06 JAN 2006

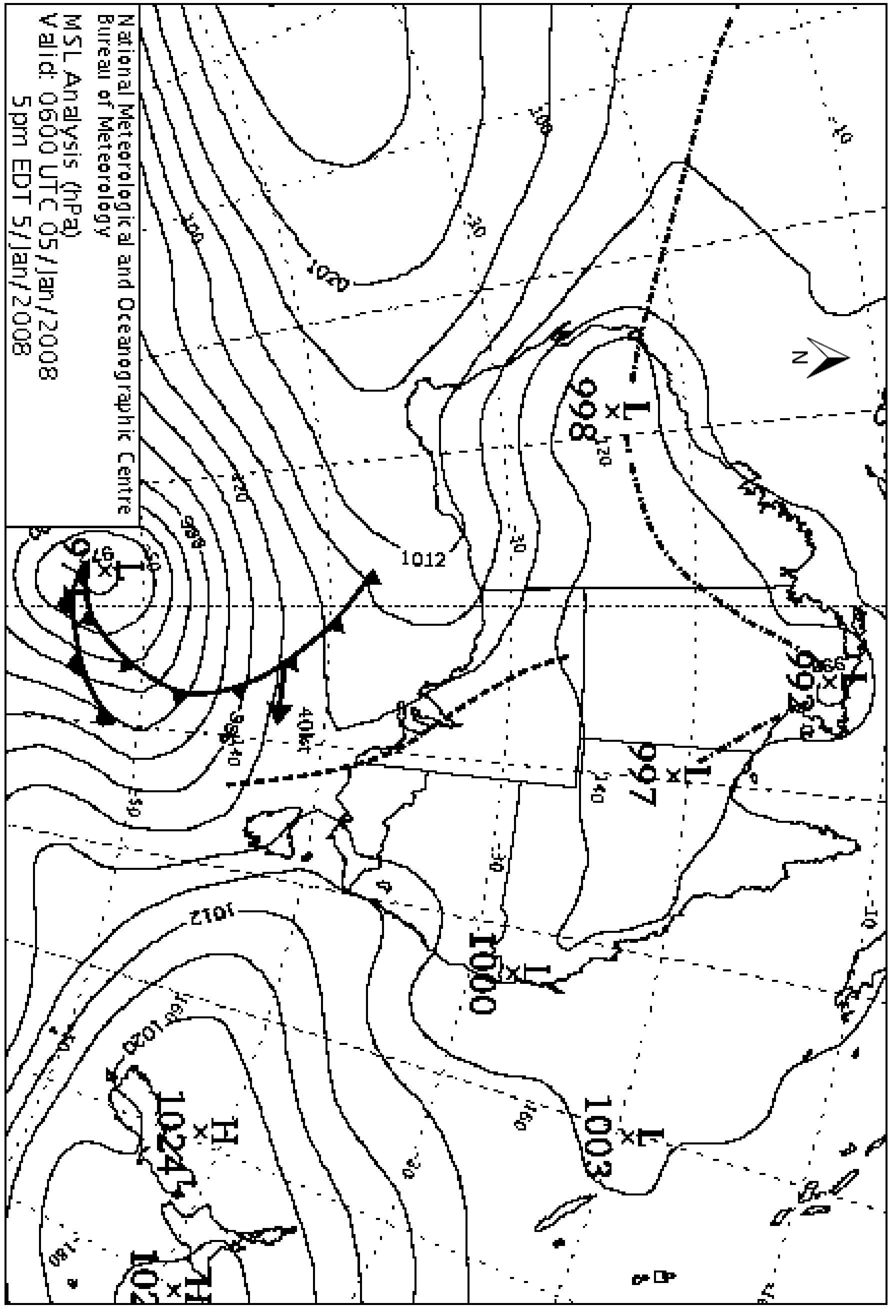
National Meteorological and Oceanographic Centre
Bureau of Meteorology
MSL Analysis (hPa)
Valid: 0600 UTC 05/Jan/2008
5pm EDT 5/Jan/2008

Appendix 2: February

Sea breeze storms

Table 11: Atmospheric conditions for severe storms on sea breeze days for February

Date	Time (UTC)	Most-Unstable CAPE	Most-Unstable CIN	Most-Unstable LCL	Most-Unstable LFC	Most-Unstable EL	Most-Unstable LI	0-3 km Pressure-Weighted Mean Wind (kt)	0-6 km Shear (kt)	0-3 km Storm Relative Helicity [m2/s2]	Effective Inflow Layer Bottom Height (m AGL)	Effective Inflow Layer Top Height (m AGL)	Effective Inflow Layer SRH (m2/s2)	Effective Bulk Wind Difference
18/02/2003	2300	28.59	-96.57	1162.44	4041.00	5702.00	0.71	2.75	9.30	16.31	-84.00	-84.00	0.00	0.00

Non-sea breeze storms

Table 12: Atmospheric conditions for severe storms on non-sea breeze days for February

Date	Time (UTC)	Most-Unstable CAPE	Most-Unstable CIN	Most-Unstable LCL	Most-Unstable LFC	Most-Unstable EL	Most-Unstable LI	0-3 km Pressure-Weighted Mean Wind (kt)	0-6 km Shear (kt)	0-3 km Storm Relative Helicity [m2/s2]	Effective Inflow Layer Bottom Height (m AGL)	Effective Inflow Layer Top Height (m AGL)	Effective Inflow Layer SRH (m2/s2)	Effective Bulk Wind Difference
20/02/2011	2300	2207.73	-53.43	647.13	1728.50	14127.66	-6.40					2169.00		

Non-storm days

Table 13: Atmospheric conditions for non-storm days for February

Date	Time (UTC)	Most-Unstable CAPE	Most-Unstable CIN	Most-Unstable LCL	Most-Unstable LFC	Most-Unstable EL	Most-Unstable LI	0-3 km Pressure-Weighted Mean Wind (kt)	0-6 km Shear (kt)	0-3 km Storm Relative Helicity [m2/s2]	Effective Inflow Layer Bottom Height (m AGL)	Effective Inflow Layer Top Height (m AGL)	Effective Inflow Layer SRH (m2/s2)	Effective Bulk Wind Difference
	average	306.5222	-159.677	1097.683	3865.28	6494.976	0.868187	5.93585	10.77261	12.80453	19.37234	274.8765	2.838405	3.921994

19/2/2003

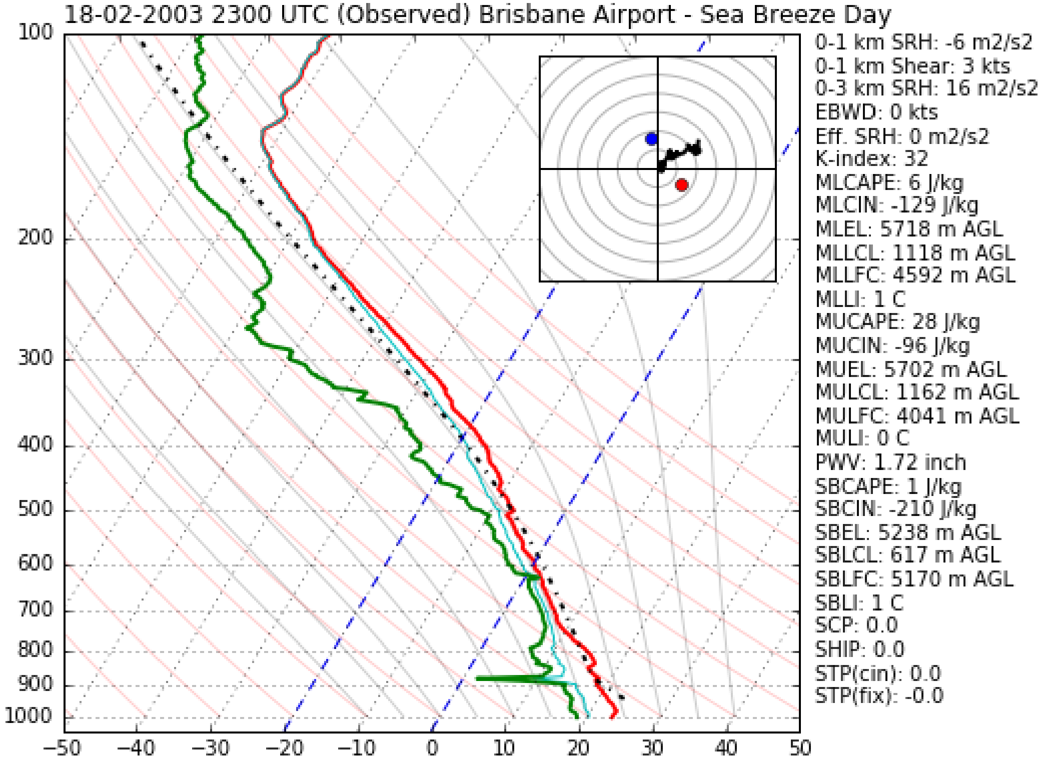
18-02-2003 2300 UTC (Observed) Brisbane Airport - Sea Breeze Day
0-1 km SRH: -6 m2/s2
0-1 km Shear: 3 kts
0-3 km SRH: 16 m2/s2
EBWD: 0 kts
Eff. SRH: 0 m2/s2
K-index: 32
MLCAPE: 6 J/kg
MLCIN: -129 J/kg
MLEL: 5718 m AGL
MLLCL: 1118 m AGL
MLLFC: 4592 m AGL
MLLI: 1 C
MUCAPE: 28 J/kg
MUCIN: -96 J/kg
MUEL: 5702 m AGL
MULCL: 1162 m AGL
MULFC: 4041 m AGL
MULI: 0 C
PWV: 1.72 inch
SBCAPE: 1 J/kg
SBCIN: -210 J/kg
SBEL: 5238 m AGL
SBLCL: 617 m AGL
SBLFC: 5170 m AGL
SBLI: 1 C
SCP: 0.0
SHIP: 0.0
STP(cin): 0.0
STP(fix): -0.0

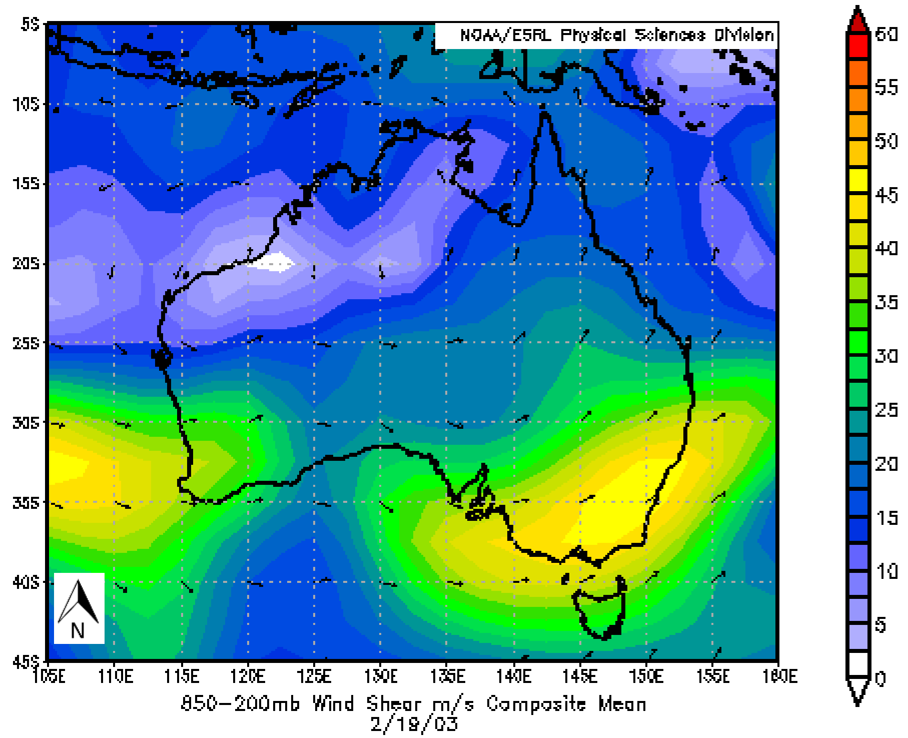
NOAA/ESRL Physical Sciences Division
850–200mb Wind Shear m/s Composite Mean
2/19/03
N

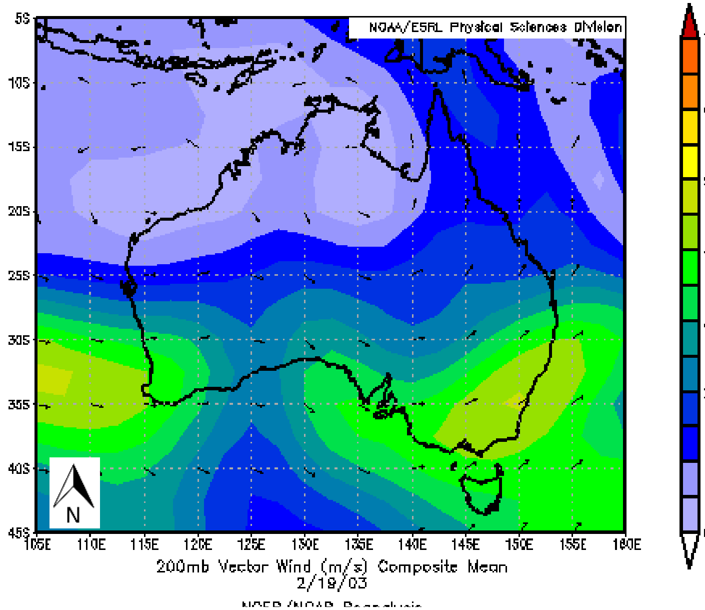
NOAA/ESRL Physical Sciences Division
200mb Vector Wind (m/s) Composite Mean
2/19/03
0
10
20
30
40
50
60
70

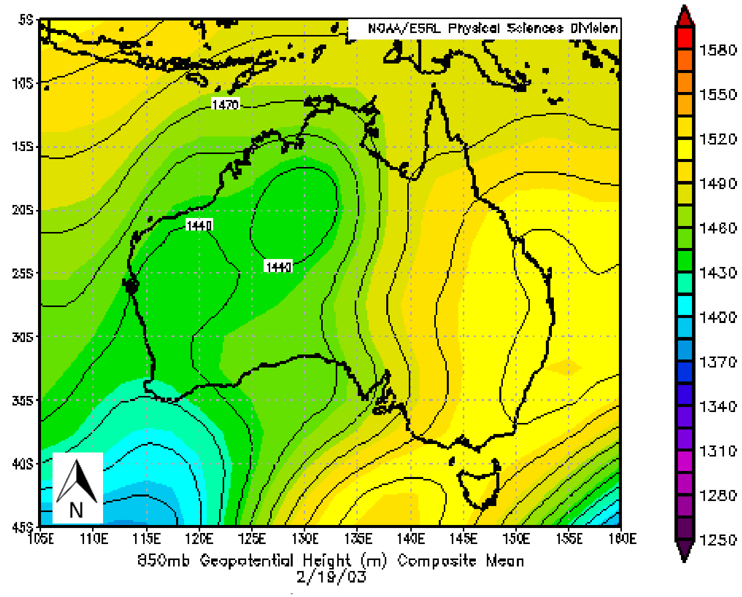
NOAA/ESRL Physical Sciences Division
850mb Geopotential Height (m) Composite Mean
2/19/03
1250
1280
1310
1340
1370
1400
1430
1460
1490
1520
1550
1580

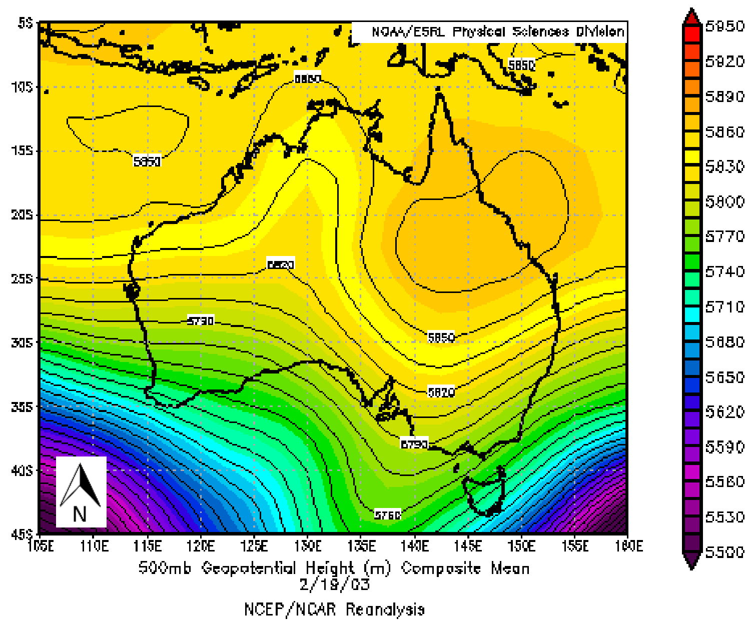
NOAA/ESRL Physical Sciences Division
500mb Geopotential Height (m) Composite Mean
2/19/03
NCEP/NCAR Reanalysis
5500
5530
5560
5590
5620
5650
5680
5710
5740
5770
5800
5830
5860
5890
5920
5950

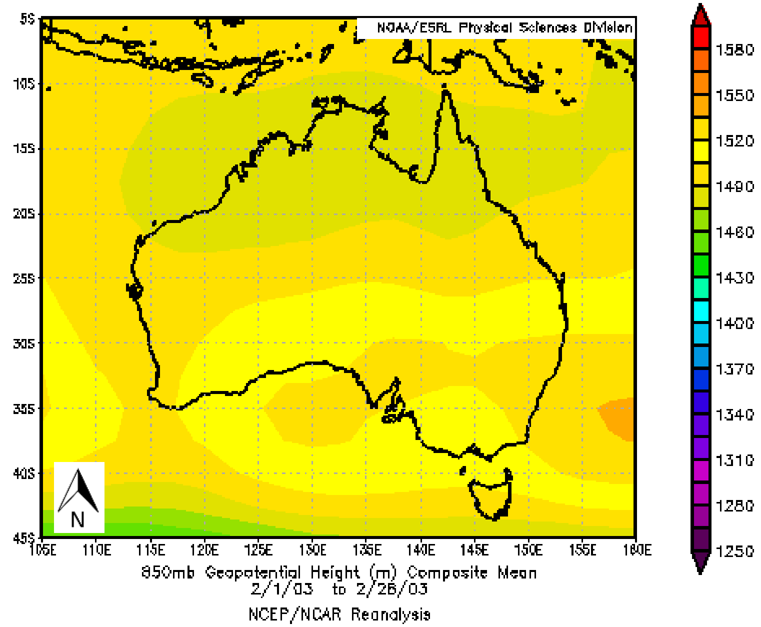
NOAA/ESRL Physical Sciences Division
850mb Geopotential Height (m) Composite Mean
2/1/03 to 2/28/03
NCEP/NCAR Reanalysis
1250
1280
1310
1340
1370
1400
1430
1460
1490
1520
1550
1580

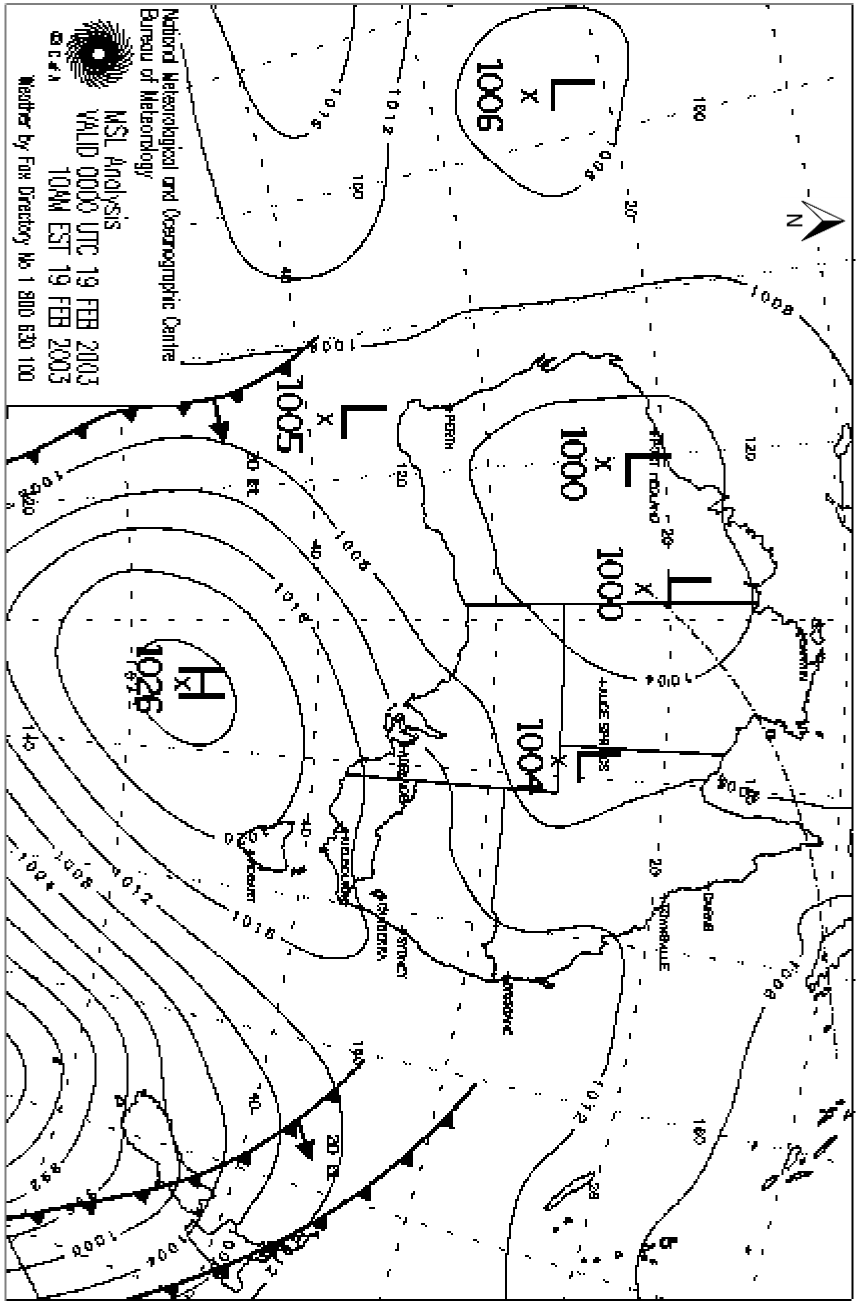

National Meteorological and Oceanographic Centre
Bureau of Meteorology
MSL Analysis
VALID 0000 UTC 19 FEB 2003
10AM EST 19 FEB 2003
Weather by Fax Directory No 1 900 630 100

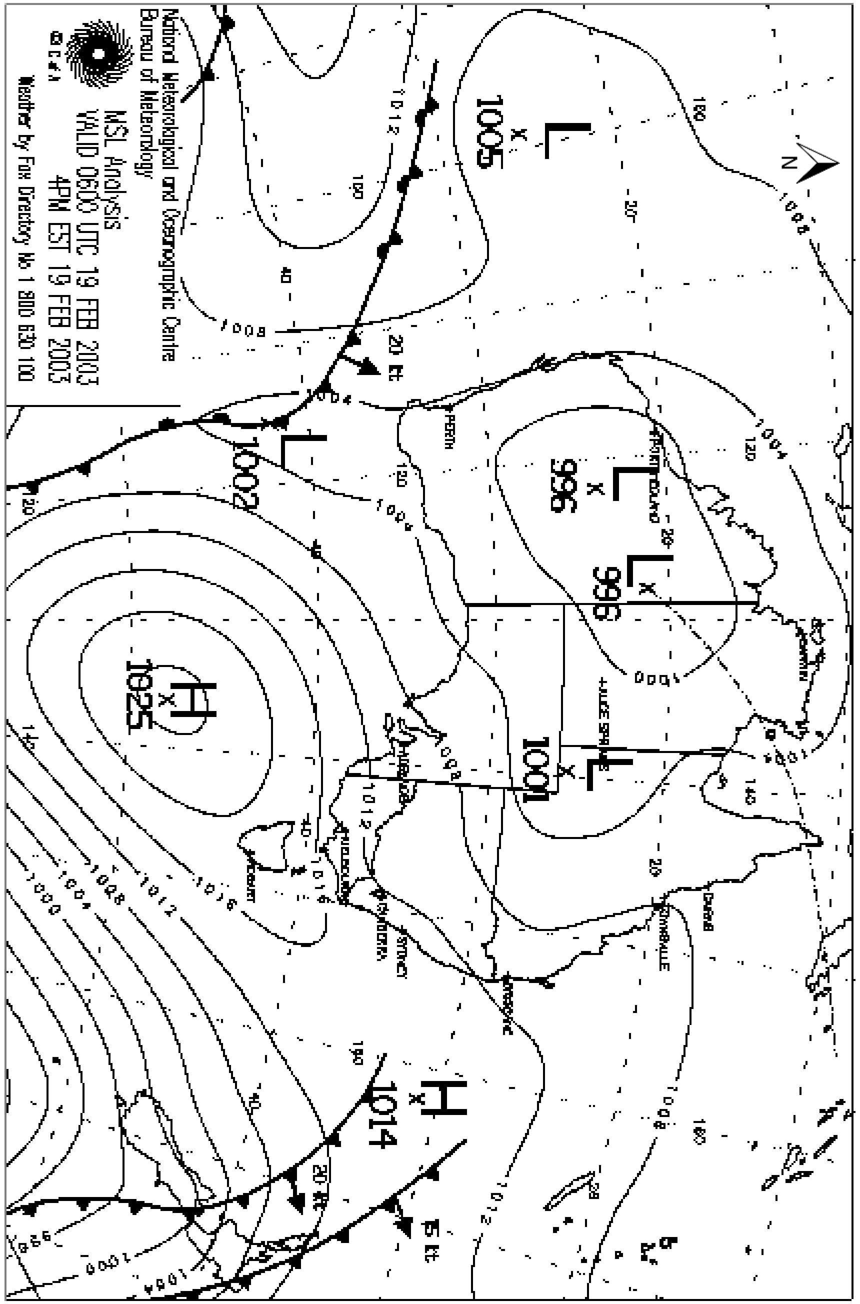

National Meteorological and Oceanographic Centre
Bureau of Meteorology
MSL Analysis
VALID 0600 UTC 19 FEB 2003
4PM EST 19 FEB 2003
Weather by Fax Directory No 1 900 630 100

21/2/2011

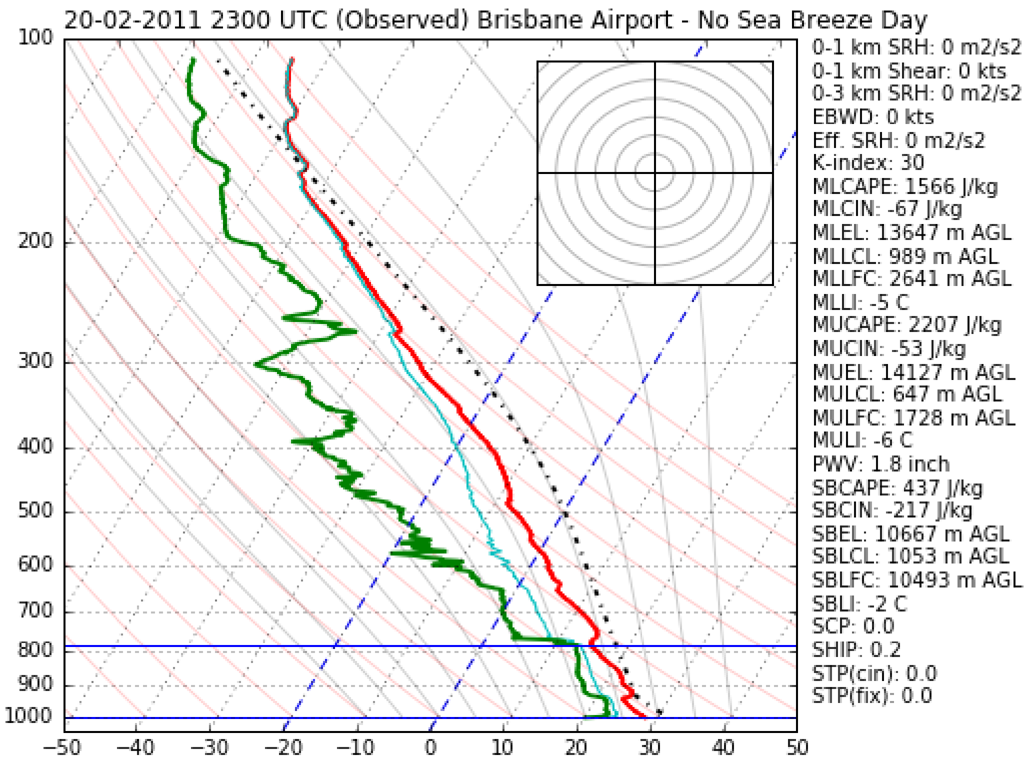
20-02-2011 2300 UTC (Observed) Brisbane Airport - No Sea Breeze Day
0-1 km SRH: 0 m2/s2
0-1 km Shear: 0 kts
0-3 km SRH: 0 m2/s2
EBWD: 0 kts
Eff. SRH: 0 m2/s2
K-index: 30
MLCAPE: 1566 J/kg
MLCIN: -67 J/kg
MLEL: 13647 m AGL
MLLCL: 989 m AGL
MLLFC: 2641 m AGL
MLLI: -5 C
MUCAPE: 2207 J/kg
MUCIN: -53 J/kg
MUEL: 14127 m AGL
MULCL: 647 m AGL
MULFC: 1728 m AGL
MULI: -6 C
PWV: 1.8 inch
SBCAPE: 437 J/kg
SBCIN: -217 J/kg
SBEL: 10667 m AGL
SBLCL: 1053 m AGL
SBLFC: 10493 m AGL
SBLI: -2 C
SCP: 0.0
SHIP: 0.2
STP(cin): 0.0
STP(fix): 0.0

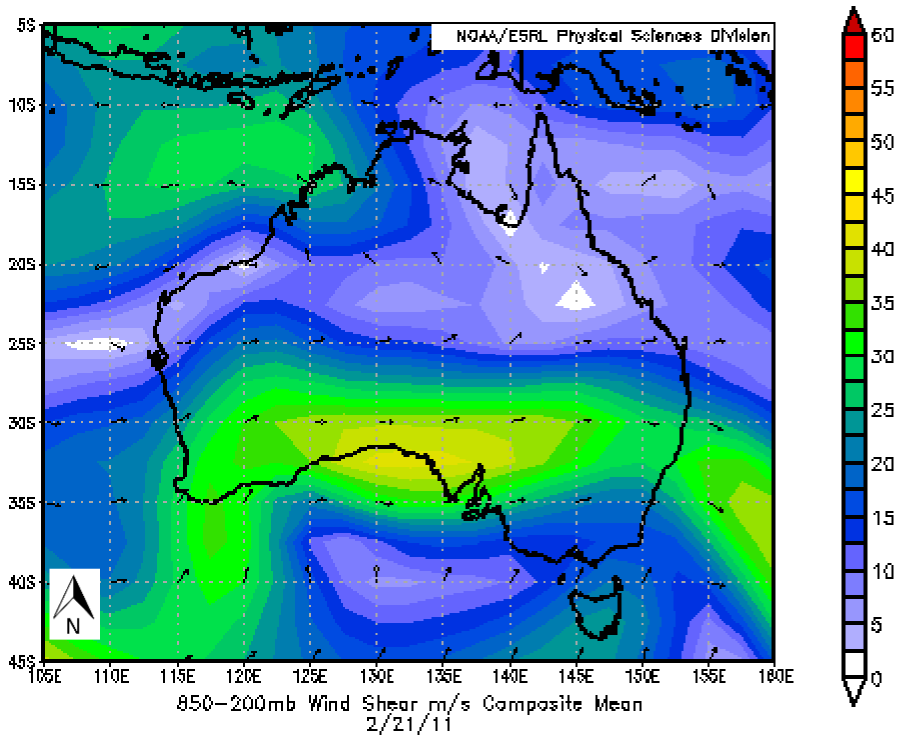
NOAA/ESRL Physical Sciences Division
N
850−200mb Wind Shear m/s Composite Mean
2/21/11

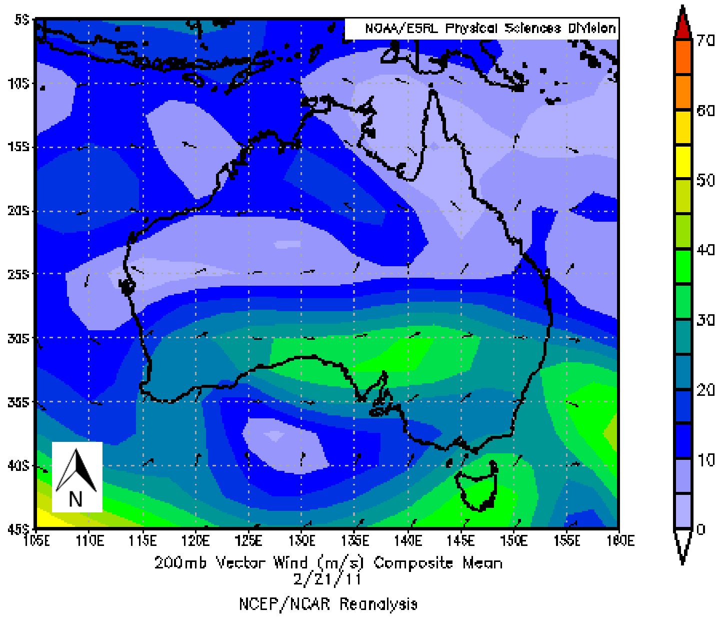
NOAA/ESRL Physical Sciences Division
200mb Vector Wind (m/s) Composite Mean
2/21/11
NCEP/NCAR Reanalysis

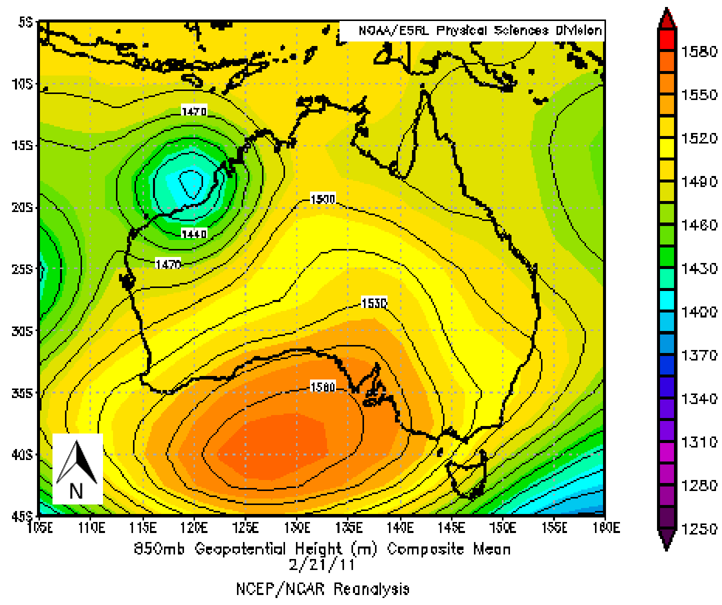
NOAA/ESRL Physical Sciences Division
850mb Geopotential Height (m) Composite Mean
2/21/11
NCEP/NCAR Reanalysis

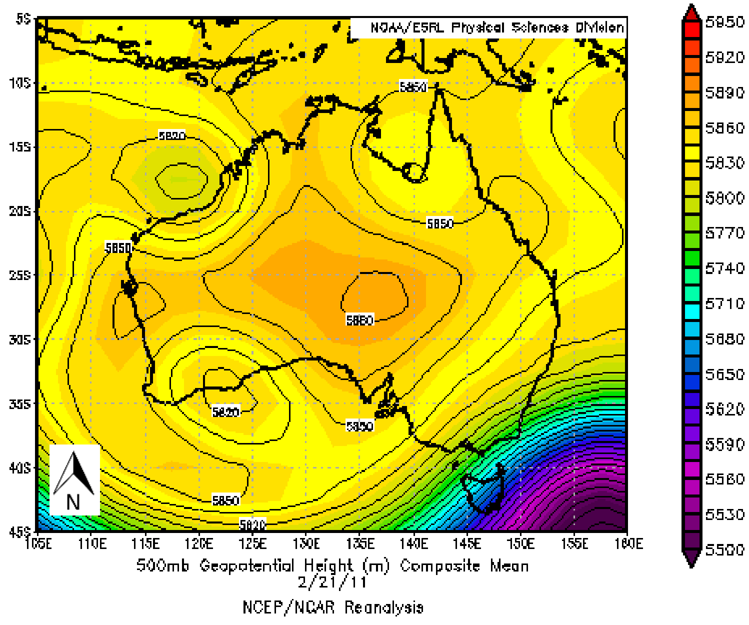
NOAA/ESRL Physical Sciences Division
500mb Geopotential Height (m) Composite Mean
2/21/11
NCEP/NCAR Reanalysis

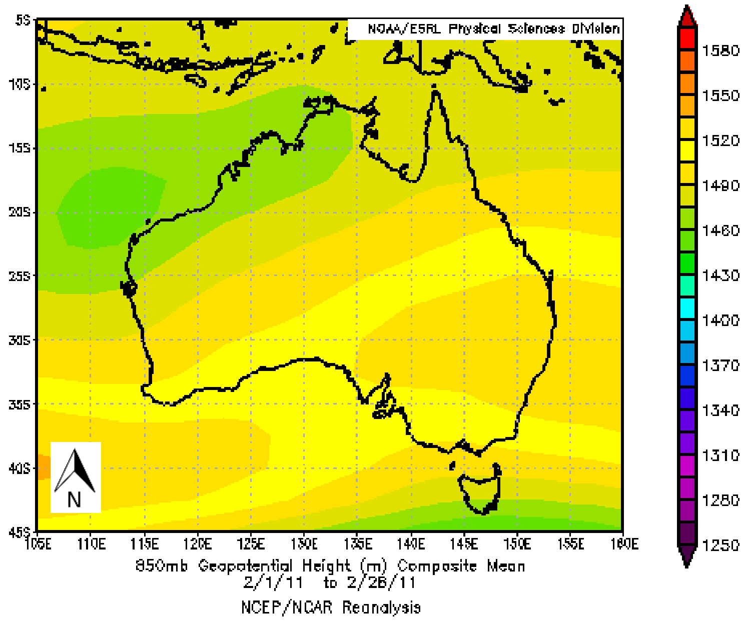
NOAA/ESRL Physical Sciences Division
850mb Geopotential Height (m) Composite Mean
2/1/11 to 2/28/11
NCEP/NCAR Reanalysis

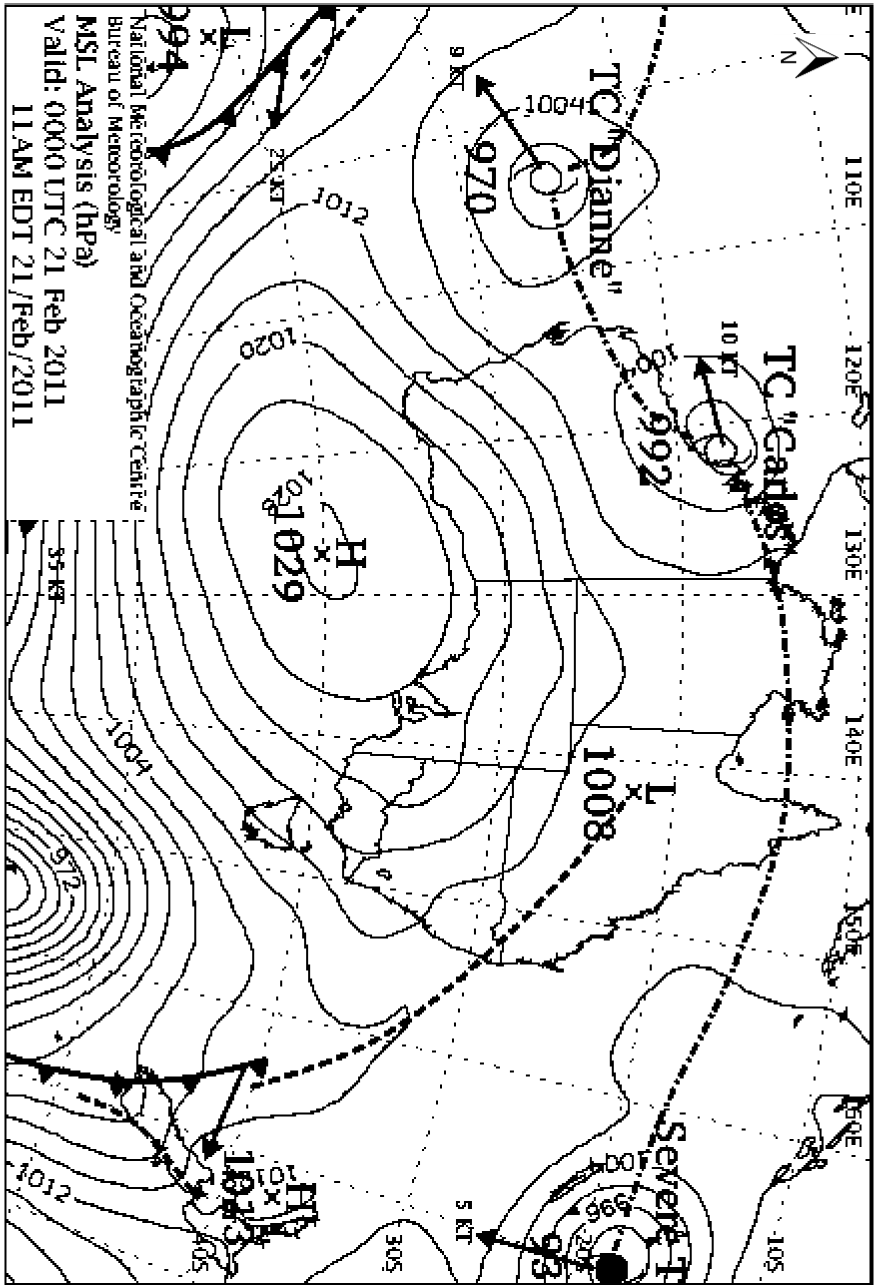
National Meteorological and Oceanographic Centre
Bureau of Meteorology
MSL Analysis (hPa)
Valid: 0000 UTC 21 Feb 2011
11AM EDT 21/Feb/2011
TC "Dianne"
TC "Carlos"
H
1029
L
1008
970
992
1020
1012
1004

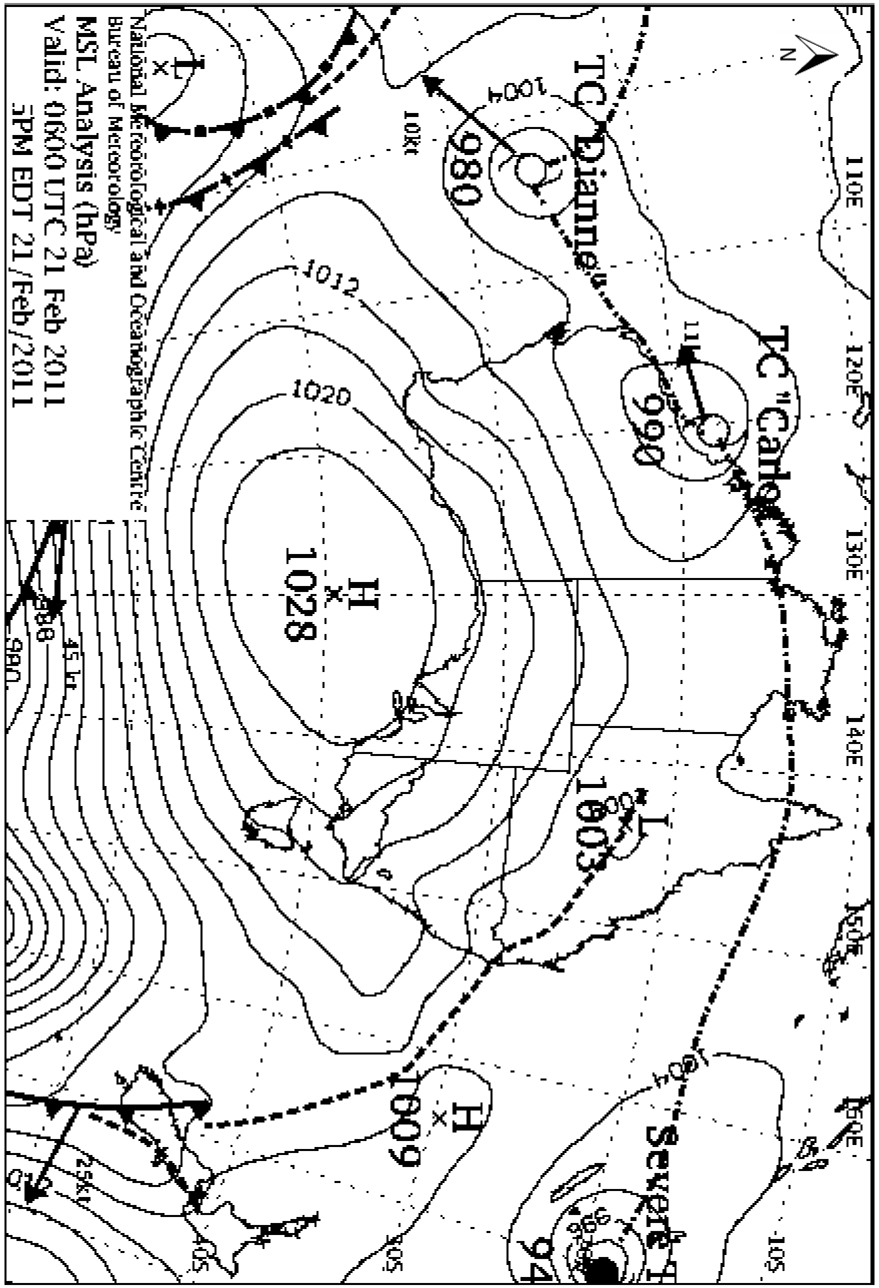
National Meteorological and Oceanographic Centre
Bureau of Meteorology
MSL Analysis (hPa)
Valid: 0600 UTC 21 Feb 2011
TC "Dianne"
TC "Carlos"
H
1028
L
1003
H
1009
980
990
1020
1012

Appendix 3: October

Sea breeze storms

Table 14: Atmospheric conditions for severe storms on sea breeze days for October

Date	Time (UTC)	Most-Unstable CAPE	Most-Unstable CIN	Most-Unstable LCL	Most-Unstable LFC	Most-Unstable EL	Most-Unstable LI	0-3 km Pressure-Weighted Mean Wind (kt)	0-6 km Shear (kt)	0-3 km Storm Relative Helicity [m2/s2]	Effective Inflow Layer Bottom Height (m AGL)	Effective Inflow Layer Top Height (m AGL)	Effective Inflow Layer SRH (m2/s2)	Effective Bulk Wind Difference
20/10/2008	2300			887.74	--	887.74	1.36	1.46	19.41	-7.34	-36.00	-36.00		
26/10/2014	2300	772.91	-577.69	831.09	3750.00	10726.00	-3.87	6.78	13.61		-33.00	-33.00		
27/10/2014	500	2371.17	-383.76	1397.74	2993.00	11918.00	-9.26	6.10	19.61		-32.00	-32.00		
	average	772.91	-577.69	831.09	3750.00	10726.00	-3.87	6.78	13.61		-33.00	-33.00		

Non-sea breeze storms

Table 15: Atmospheric conditions for severe storms on non-sea breeze days for October

Date	Time (UTC)	Most-Unstable CAPE	Most-Unstable CIN	Most-Unstable LCL	Most-Unstable LFC	Most-Unstable EL	Most-Unstable LI	0-3 km Pressure-Weighted Mean Wind (kt)	0-6 km Shear (kt)	0-3 km Storm Relative Helicity [m2/s2]	Effective Inflow Layer Bottom Height (m AGL)	Effective Inflow Layer Top Height (m AGL)	Effective Inflow Layer SRH (m2/s2)	Effective Bulk Wind Difference
25/10/2003	2300	1063.32	-243.62	867.31	3301.48	10813.00	-3.86	14.37	27.44	10.54		53.00		
18/10/2004	2300	166.26	-93.58	955.14	3654.00	8829.00	-0.59	5.15	18.80	34.74	687.00	687.00		
12/10/2011	2300	1215.69	-8.29	468.99	814.50	10177.60	-4.50	4.08	14.45	29.69	32.00	1059.00	-0.41	3.15
14/10/2011	2300	583.94	-87.52	456.43	11201.00	11391.00	-2.30	11.47	15.04	31.06		352.00	15.24	3.50
	average	757.30	-108.25	686.97	4742.74	10302.65	-2.81	8.77	18.93	26.51	359.50	537.75	7.41	3.33

Non-storm days

Table 16: Atmospheric conditions for non-storm days for October

Date	Time (UTC)	Most-Unstable CAPE	Most-Unstable CIN	Most-Unstable LCL	Most-Unstable LFC	Most-Unstable EL	Most-Unstable LI	0-3 km Pressure-Weighted Mean Wind (kt)	0-6 km Shear (kt)	0-3 km Storm Relative Helicity [m2/s2]	Effective Inflow Layer Bottom Height (m AGL)	Effective Inflow Layer Top Height (m AGL)	Effective Inflow Layer SRH (m2/s2)	Effective Bulk Wind Difference
	average	240.5597	-244.836	1654.41	3298.227	4329.697	3.036136	5.427145	16.90897	27.45856	-19.8216	90.51794	0.051586	3.771586

27/10/2014

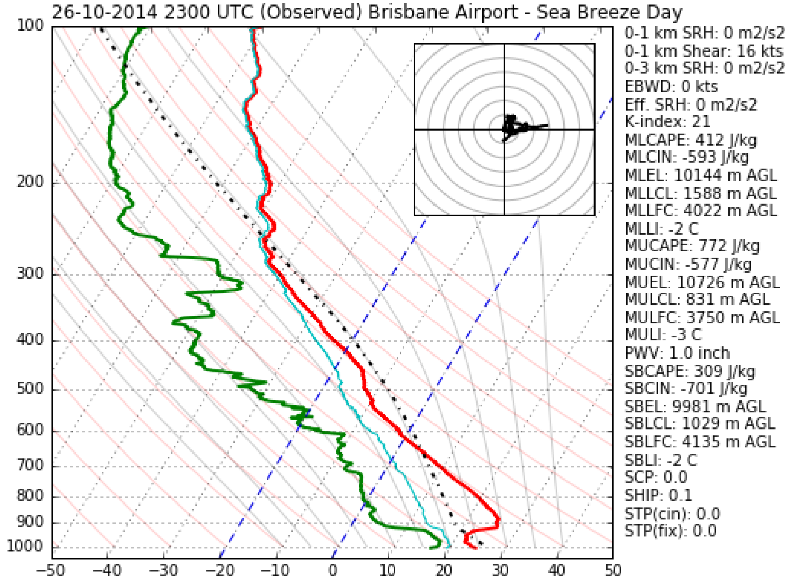
26-10-2014 2300 UTC (Observed) Brisbane Airport - Sea Breeze Day
0-1 km SRH: 0 m2/s2
0-1 km Shear: 16 kts
0-3 km SRH: 0 m2/s2
EBWD: 0 kts
Eff. SRH: 0 m2/s2
K-index: 21
MLCAPE: 412 J/kg
MLCIN: -593 J/kg
MLEL: 10144 m AGL
MLLCL: 1588 m AGL
MLLFC: 4022 m AGL
MLLI: -2 C
MUCAPE: 772 J/kg
MUCIN: -577 J/kg
MUEL: 10726 m AGL
MULCL: 831 m AGL
MULFC: 3750 m AGL
MULI: -3 C
PWV: 1.0 inch
SBCAPE: 309 J/kg
SBCIN: -701 J/kg
SBEL: 9981 m AGL
SBLCL: 1029 m AGL
SBLFC: 4135 m AGL
SBLI: -2 C
SCP: 0.0
SHIP: 0.1
STP(cin): 0.0
STP(fix): 0.0

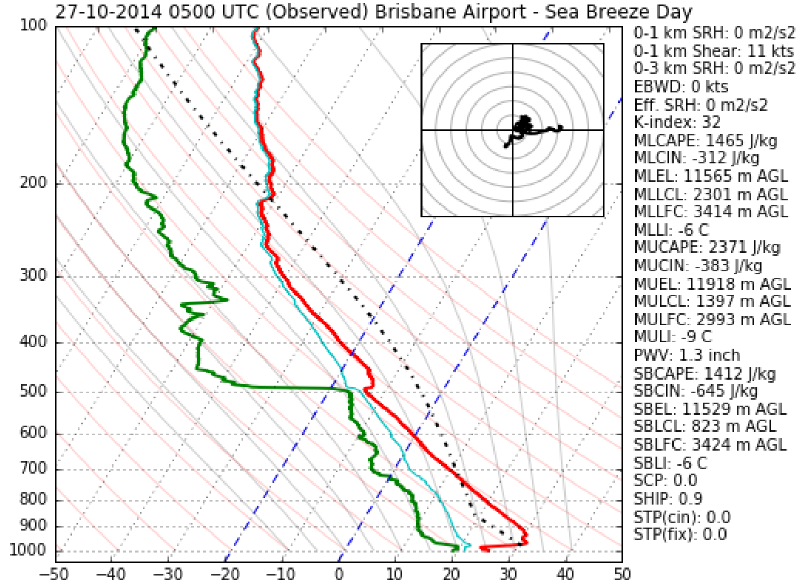
27-10-2014 0500 UTC (Observed) Brisbane Airport - Sea Breeze Day
0-1 km SRH: 0 m2/s2
0-1 km Shear: 11 kts
0-3 km SRH: 0 m2/s2
EBWD: 0 kts
Eff. SRH: 0 m2/s2
K-index: 32
MLCAPE: 1465 J/kg
MLCIN: -312 J/kg
MLEL: 11565 m AGL
MLLCL: 2301 m AGL
MLLFC: 3414 m AGL
MLLI: -6 C
MUCAPE: 2371 J/kg
MUCIN: -383 J/kg
MUEL: 11918 m AGL
MULCL: 1397 m AGL
MULFC: 2993 m AGL
MULI: -9 C
PWV: 1.3 inch
SBCAPE: 1412 J/kg
SBCIN: -645 J/kg
SBEL: 11529 m AGL
SBLCL: 823 m AGL
SBLFC: 3424 m AGL
SBLI: -6 C
SCP: 0.0
SHIP: 0.9
STP(cin): 0.0
STP(fix): 0.0

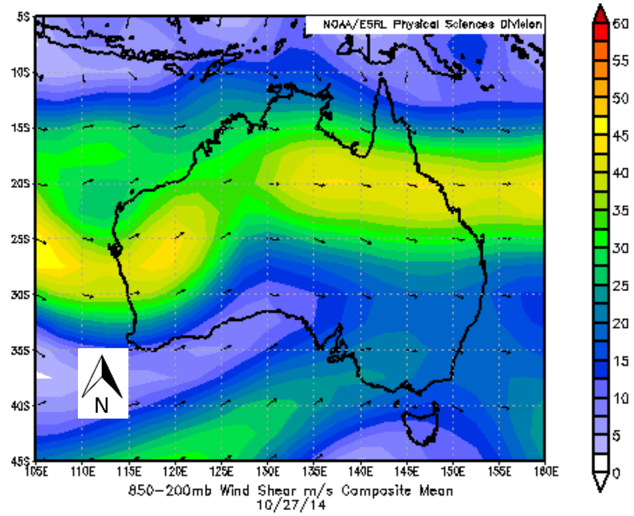
NOAA/ESRL Physical Sciences Division
N
850-200mb Wind Shear m/s Composite Mean
10/27/14

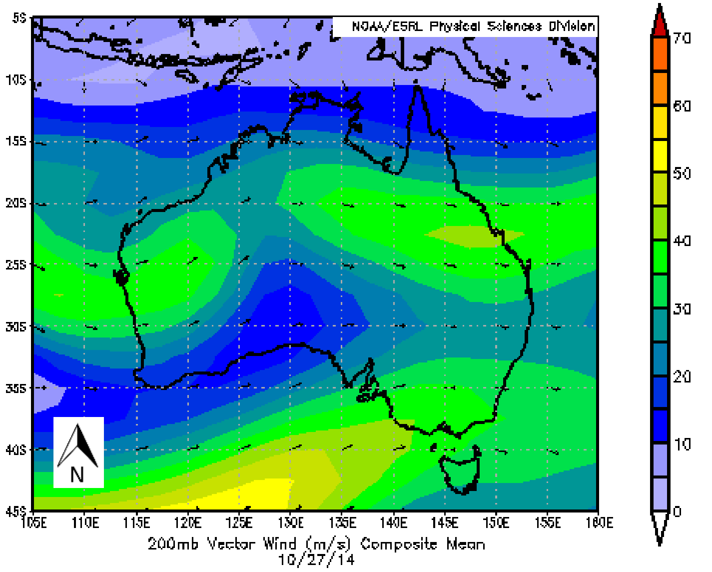
NOAA/ESRL Physical Sciences Division
N
200mb Vector Wind (m/s) Composite Mean
10/27/14

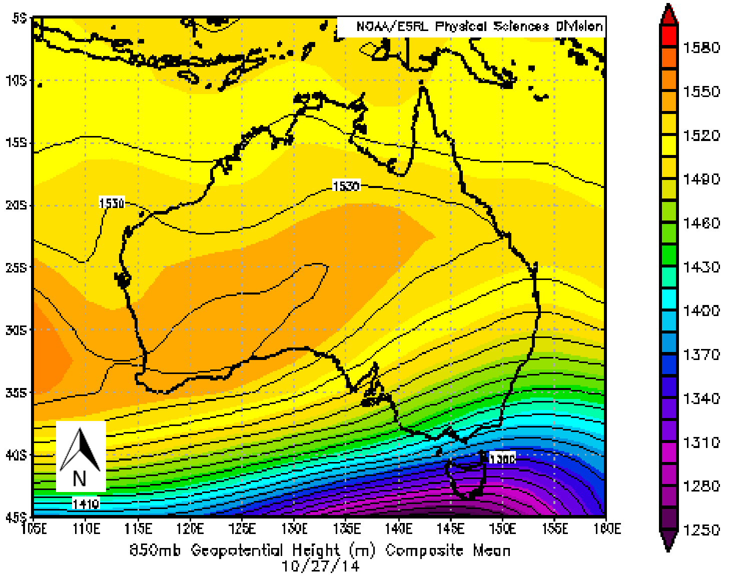
NOAA/ESRL Physical Sciences Division
N
850mb Geopotential Height (m) Composite Mean
10/27/14

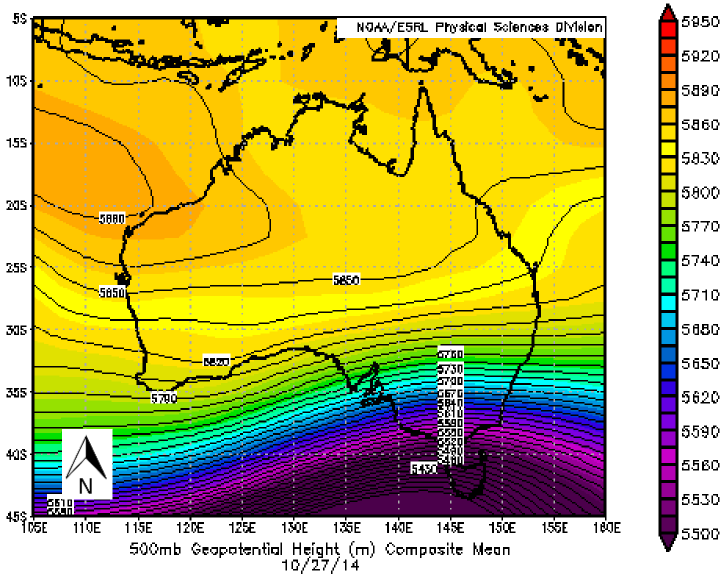
NOAA/ESRL Physical Sciences Division
N
500mb Geopotential Height (m) Composite Mean
10/27/14
NCEP/NCAR Reanalysis

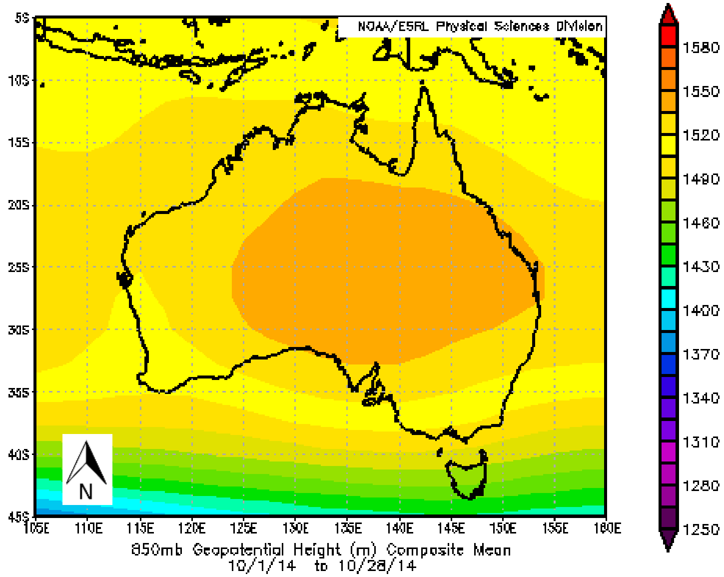
NOAA/ESRL Physical Sciences Division
N
850mb Geopotential Height (m) Composite Mean
10/1/14 to 10/28/14
NCEP/NCAR Reanalysis

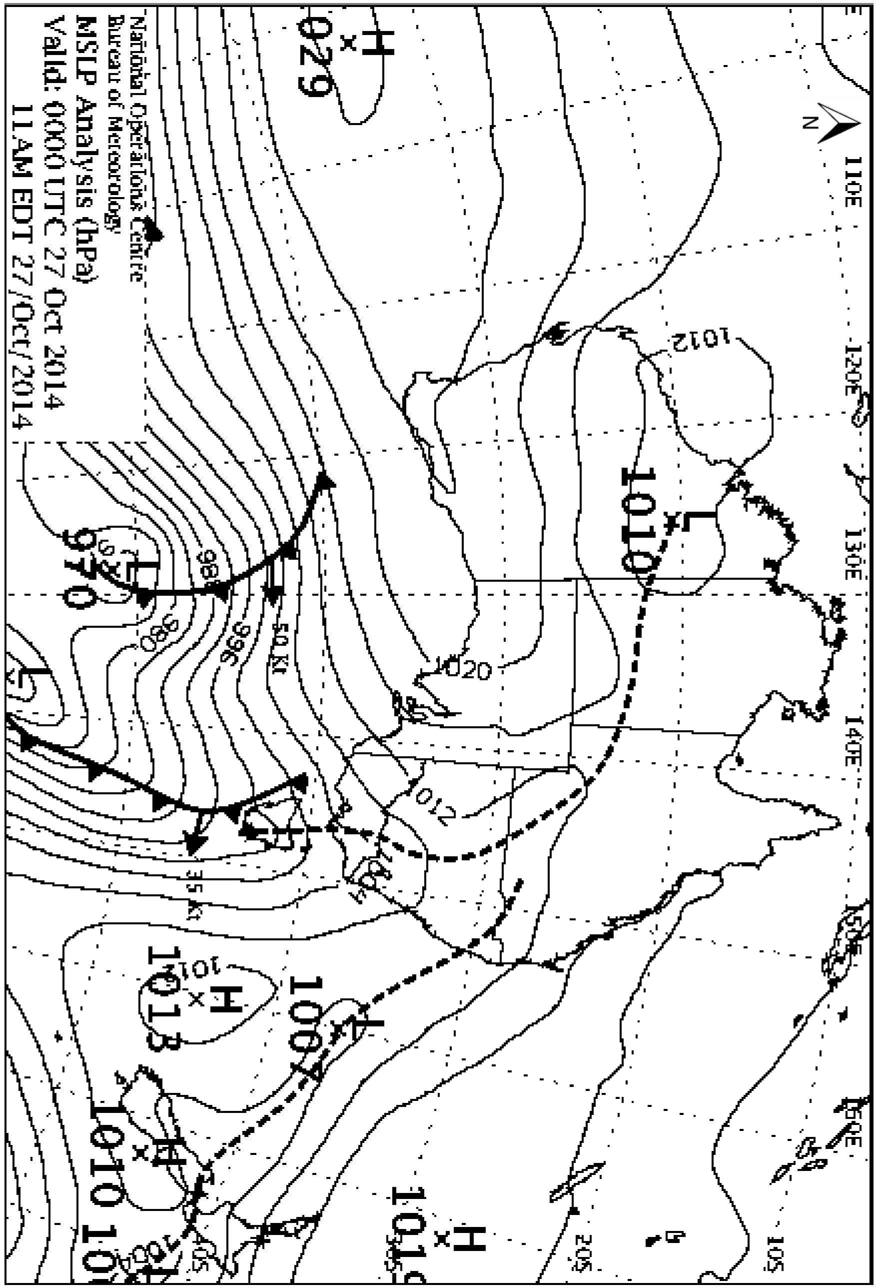
National Operations Centre
Bureau of Meteorology
MSLP Analysis (hPa)
Valid: 0000 UTC 27 Oct 2014
11AM EDT 27/Oct/2014

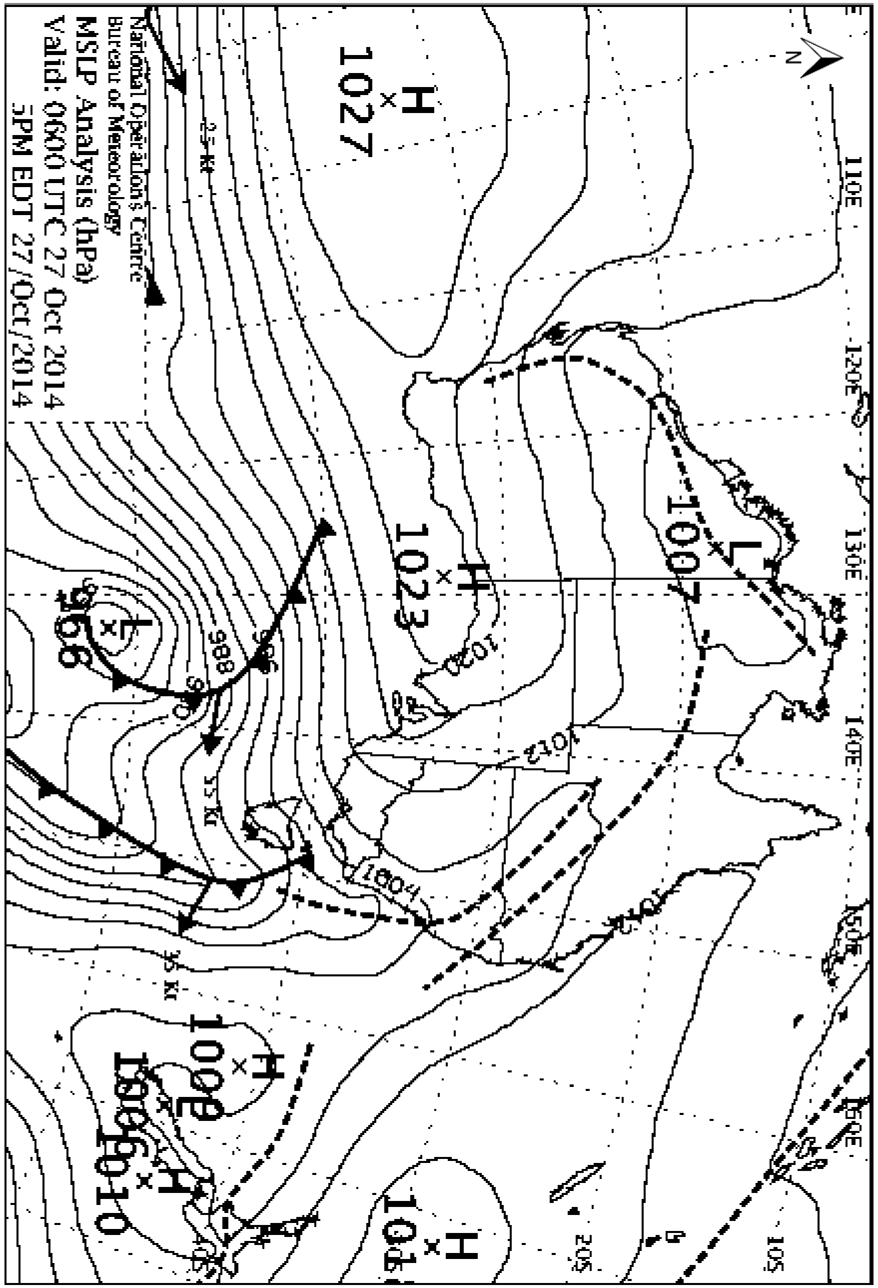
National Operations Centre
Bureau of Meteorology
MSLP Analysis (hPa)
Valid: 0600 UTC 27 Oct 2014
5PM EDT 27/Oct/2014

15/10/2011

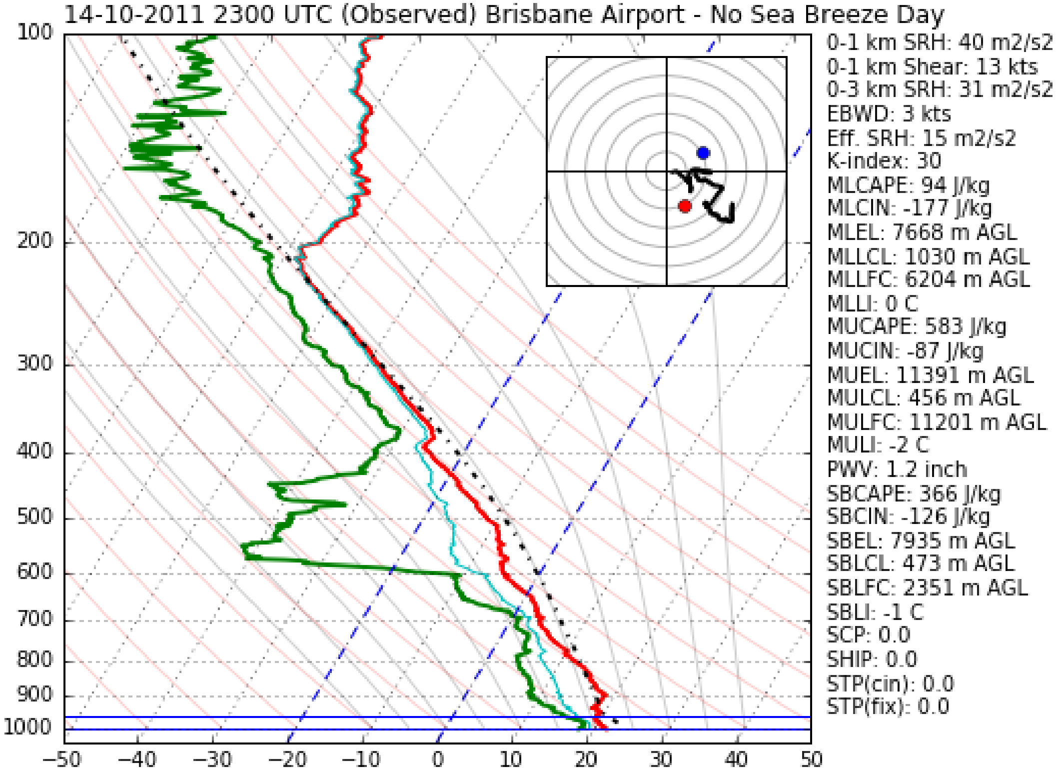
14-10-2011 2300 UTC (Observed) Brisbane Airport - No Sea Breeze Day
0-1 km SRH: 40 m2/s2
0-1 km Shear: 13 kts
0-3 km SRH: 31 m2/s2
EBWD: 3 kts
Eff. SRH: 15 m2/s2
K-index: 30
MLCAPE: 94 J/kg
MLCIN: -177 J/kg
MLEL: 7668 m AGL
MLLCL: 1030 m AGL
MLLFC: 6204 m AGL
MLLI: 0 C
MUCAPE: 583 J/kg
MUCIN: -87 J/kg
MUEL: 11391 m AGL
MULCL: 456 m AGL
MULFC: 11201 m AGL
MULI: -2 C
PWV: 1.2 inch
SBCAPE: 366 J/kg
SBCIN: -126 J/kg
SBEL: 7935 m AGL
SBLCL: 473 m AGL
SBLFC: 2351 m AGL
SBLI: -1 C
SCP: 0.0
SHIP: 0.0
STP(cin): 0.0
STP(fix): 0.0

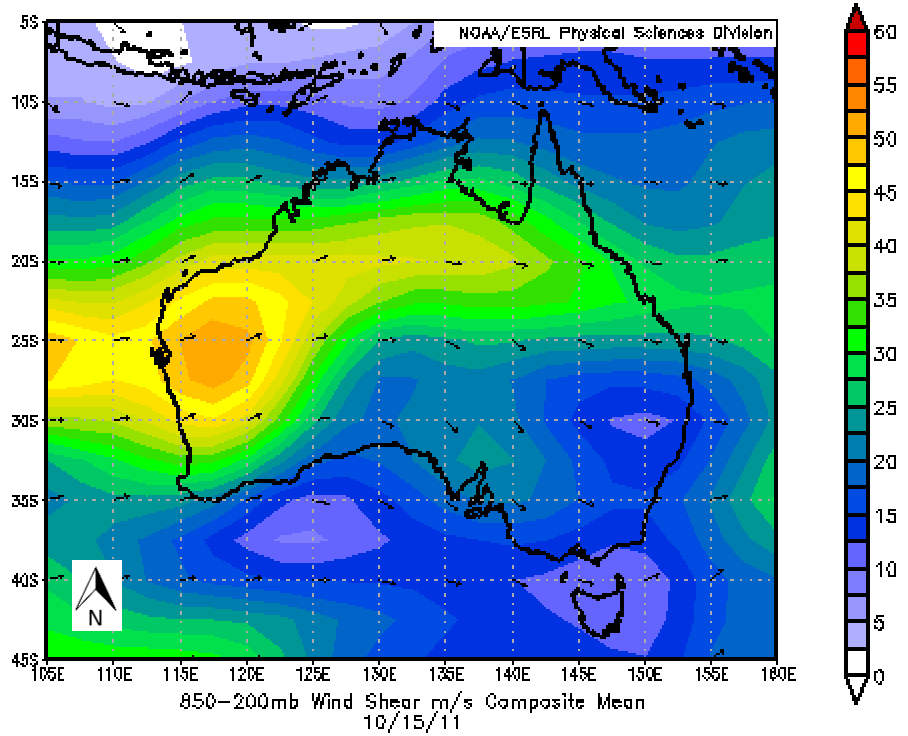
NOAA/ESRL Physical Sciences Division
N
850–200mb Wind Shear m/s Composite Mean
10/15/11

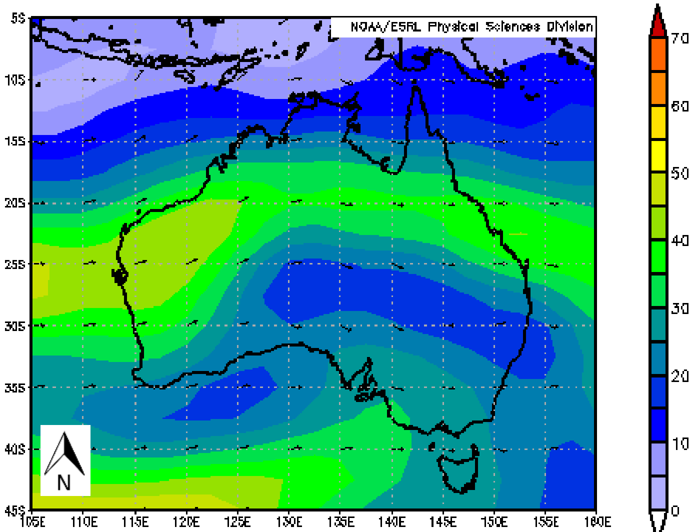

200mb Vector Wind (m/s) Composite Mean
10/15/11
NCEP/NCAR Reanalysis

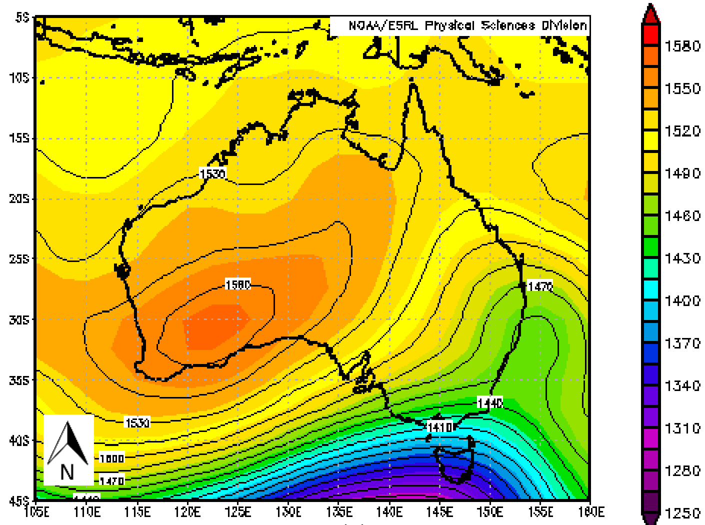

850mb Geopotential Height (m) Composite Mean
10/15/11
NCEP/NCAR Reanalysis

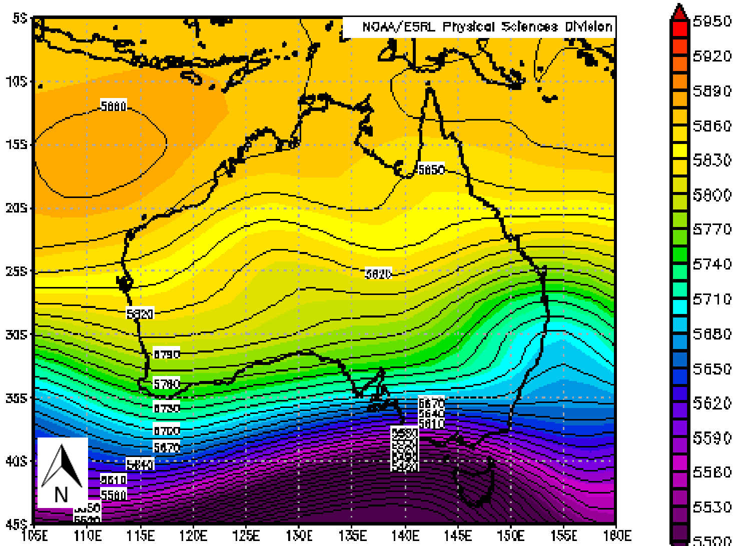

500mb Geopotential Height (m) Composite Mean
10/15/11
NCEP/NCAR Reanalysis

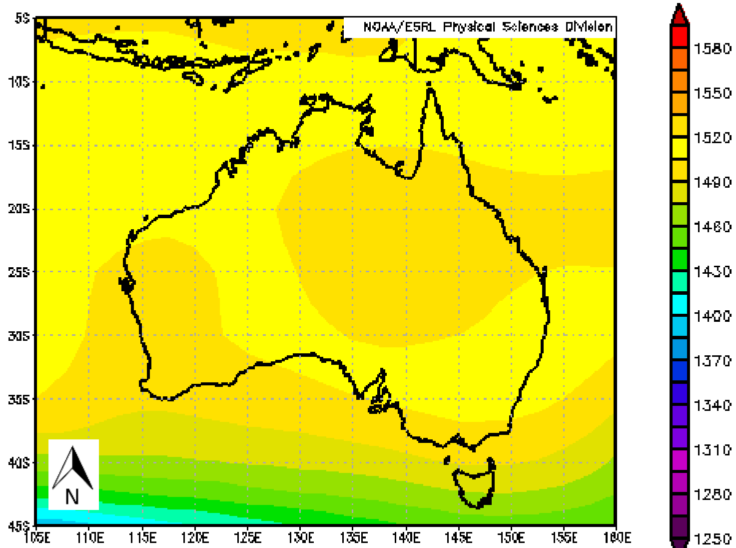

850mb Geopotential Height (m) Composite Mean
10/1/11 to 10/28/11
NCEP/NCAR Reanalysis

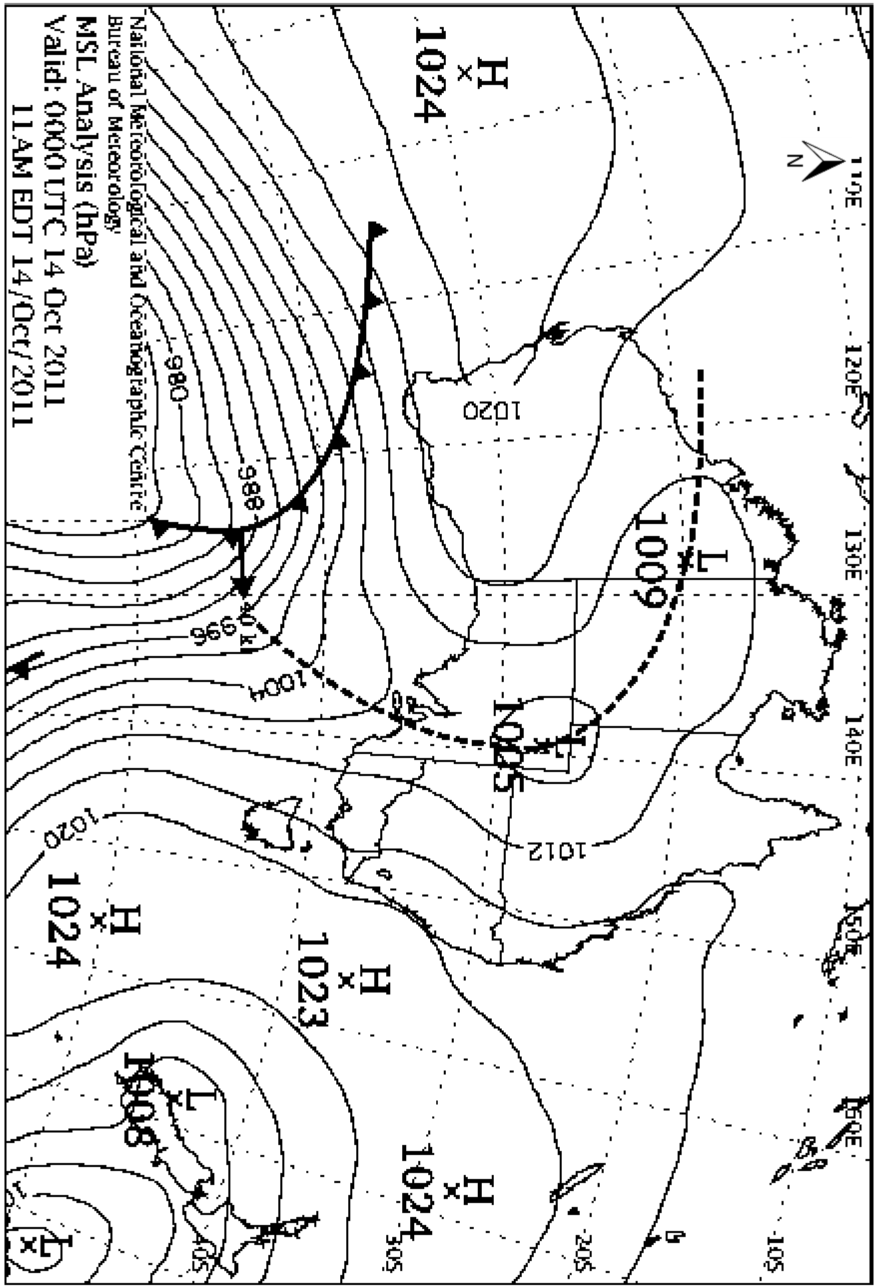
National Meteorological and Oceanographic Centre
Bureau of Meteorology
MSL Analysis (hPa)
Valid: 0000 UTC 14 Oct 2011
11AM EDT 14/Oct/2011

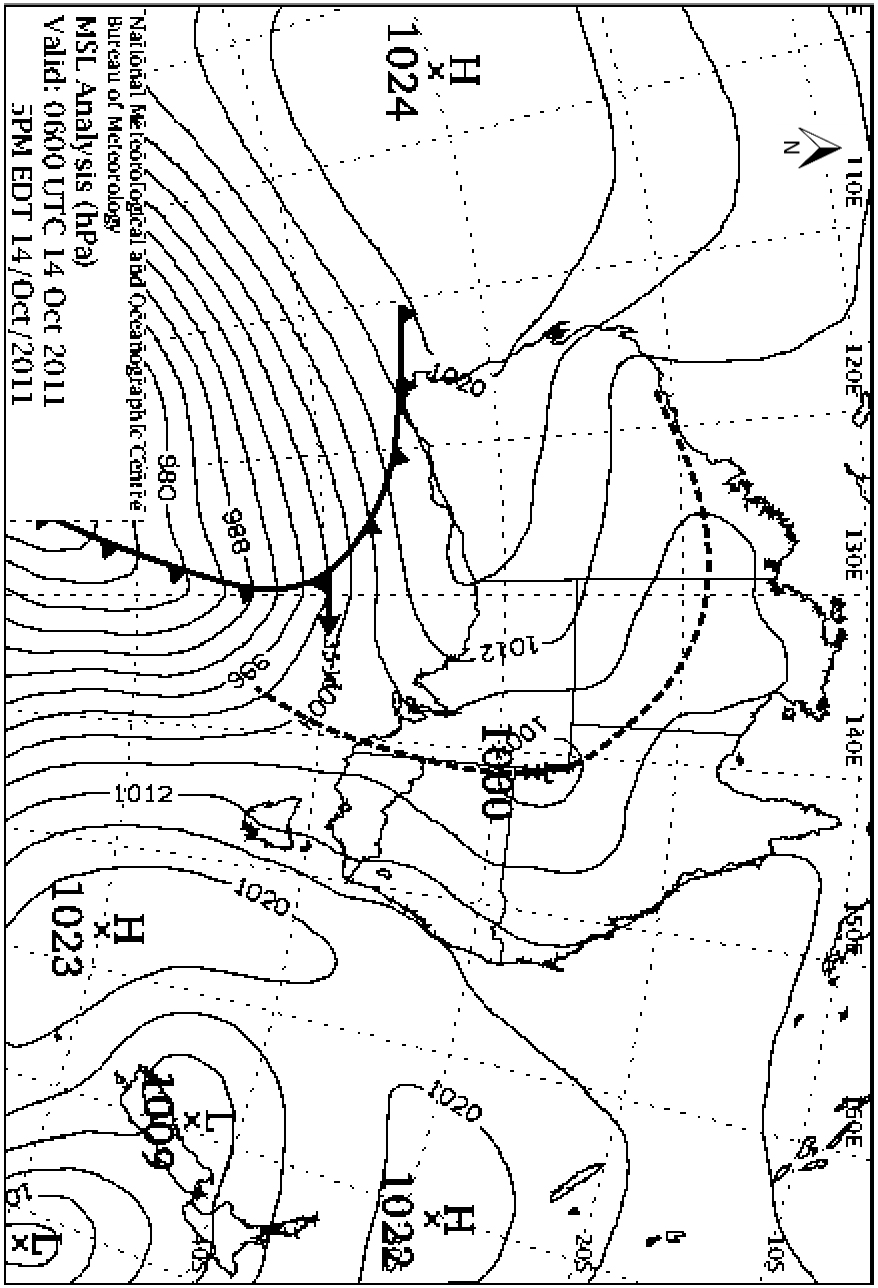
National Meteorological and Oceanographic Centre
Bureau of Meteorology
MSL Analysis (hPa)
Valid: 0600 UTC 14 Oct 2011
5PM EDT 14/Oct/2011

19/10/2004

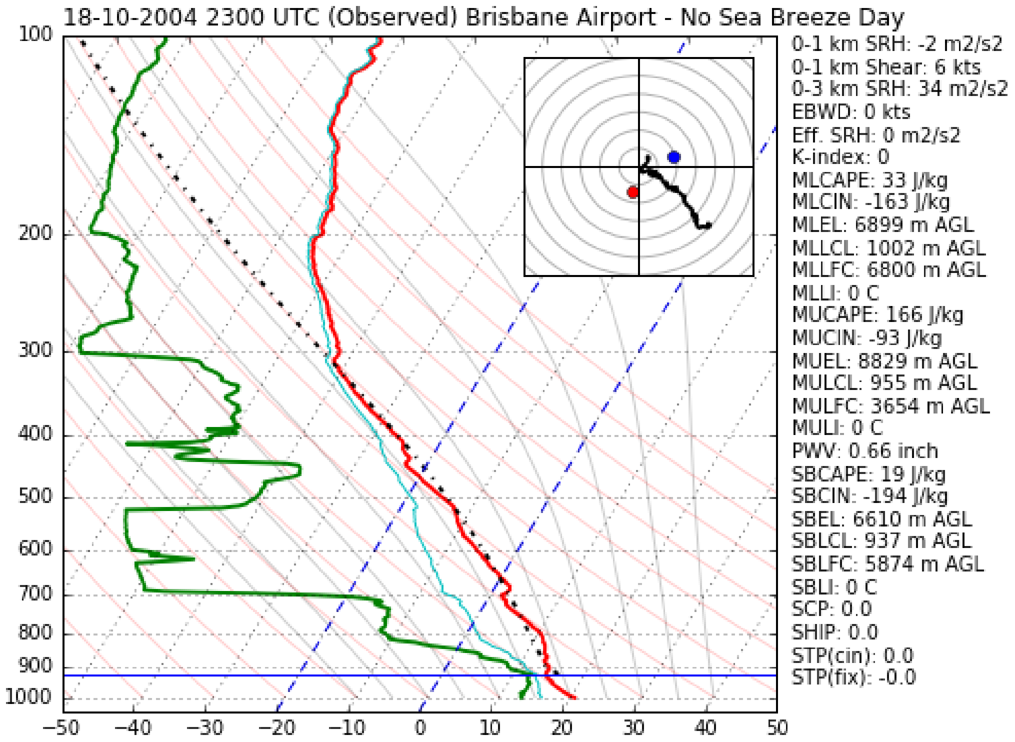
18-10-2004 2300 UTC (Observed) Brisbane Airport - No Sea Breeze Day
0-1 km SRH: -2 m2/s2
0-1 km Shear: 6 kts
0-3 km SRH: 34 m2/s2
EBWD: 0 kts
Eff. SRH: 0 m2/s2
K-index: 0
MLCAPE: 33 J/kg
MLCIN: -163 J/kg
MLEL: 6899 m AGL
MLLCL: 1002 m AGL
MLLFC: 6800 m AGL
MLLI: 0 C
MUCAPE: 166 J/kg
MUCIN: -93 J/kg
MUEL: 8829 m AGL
MULCL: 955 m AGL
MULFC: 3654 m AGL
MULI: 0 C
PWV: 0.66 inch
SBCAPE: 19 J/kg
SBCIN: -194 J/kg
SBEL: 6610 m AGL
SBLCL: 937 m AGL
SBLFC: 5874 m AGL
SBLI: 0 C
SCP: 0.0
SHIP: 0.0
STP(cin): 0.0
STP(fix): -0.0

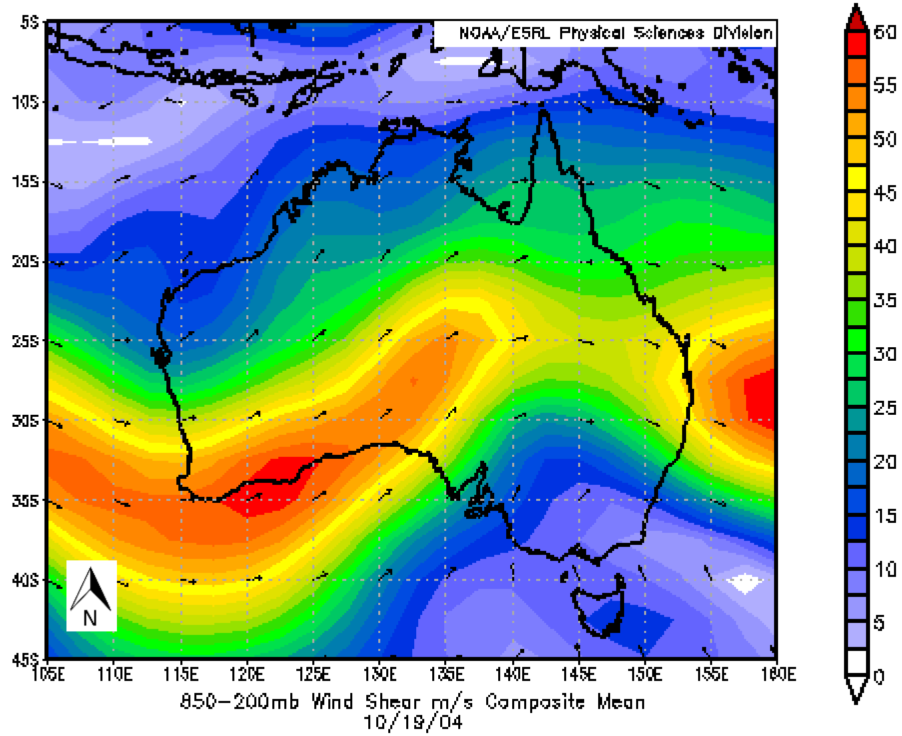
NOAA/ESRL Physical Sciences Division
N
850–200mb Wind Shear m/s Composite Mean
10/19/04

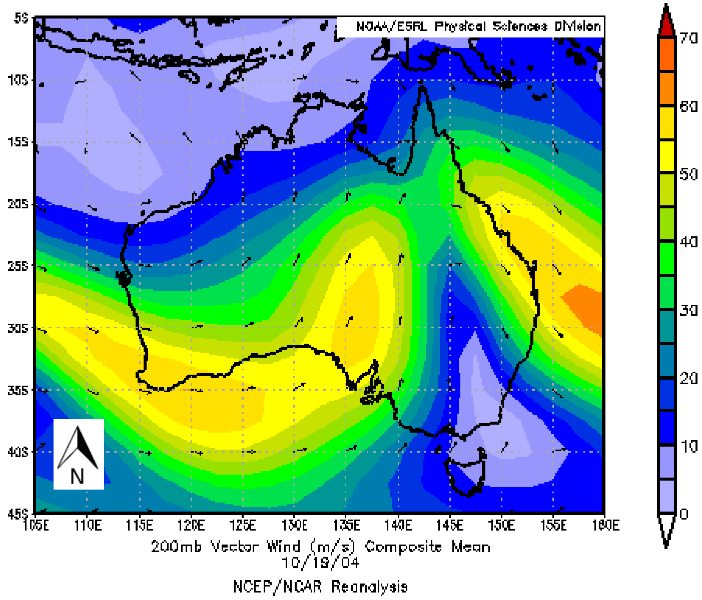
NOAA/ESRL Physical Sciences Division
5S
10S
15S
20S
25S
30S
35S
40S
45S
105E 110E 115E 120E 125E 130E 135E 140E 145E 150E 155E 160E
N
70
60
50
40
30
20
10
0
200mb Vector Wind (m/s) Composite Mean
10/19/04
NCEP/NCAR Reanalysis

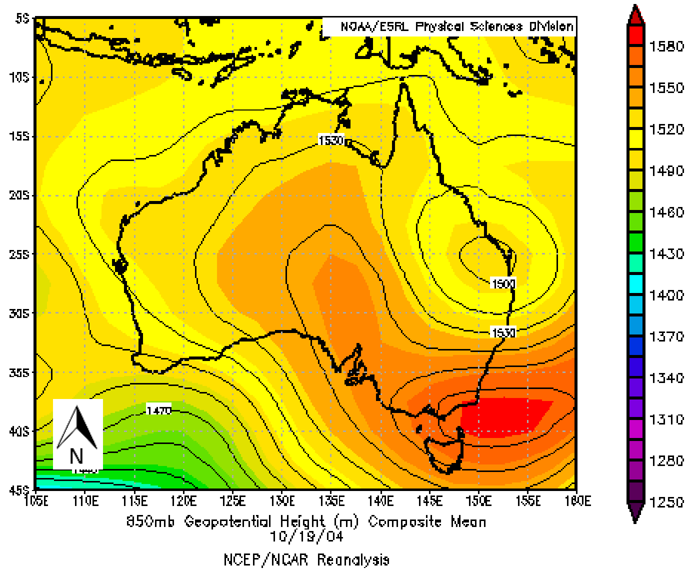
NOAA/ESRL Physical Sciences Division
5S
10S
15S
20S
25S
30S
35S
40S
45S
105E 110E 115E 120E 125E 130E 135E 140E 145E 150E 155E 160E
1530
1500
1530
1470
N
1580
1550
1520
1490
1460
1430
1400
1370
1340
1310
1280
1250
850mb Geopotential Height (m) Composite Mean
10/19/04
NCEP/NCAR Reanalysis

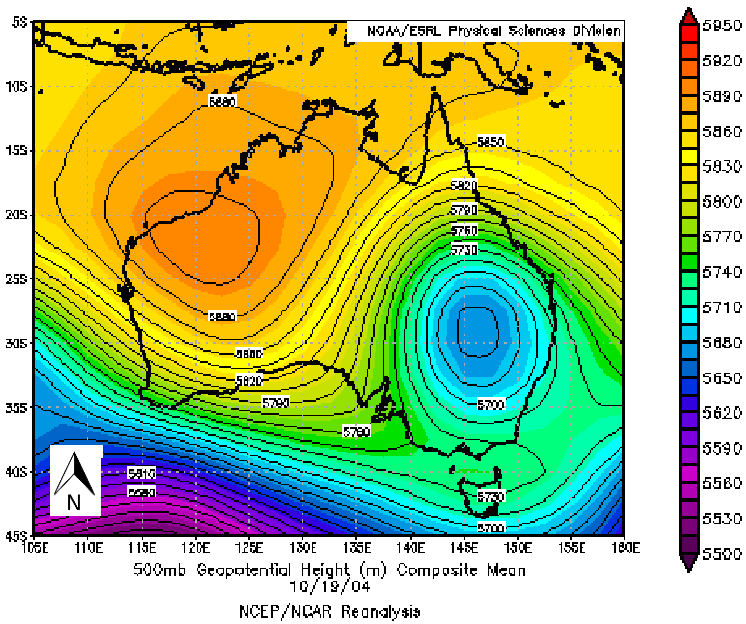
NOAA/ESRL Physical Sciences Division
5S
10S
15S
20S
25S
30S
35S
40S
45S
105E 110E 115E 120E 125E 130E 135E 140E 145E 150E 155E 160E
5880
5850
5820
5790
5760
5730
5880
5850
5820
5790
5760
5700
5730
5700
N
5950
5920
5890
5860
5830
5800
5770
5740
5710
5680
5650
5620
5590
5560
5530
5500
500mb Geopotential Height (m) Composite Mean
10/19/04
NCEP/NCAR Reanalysis

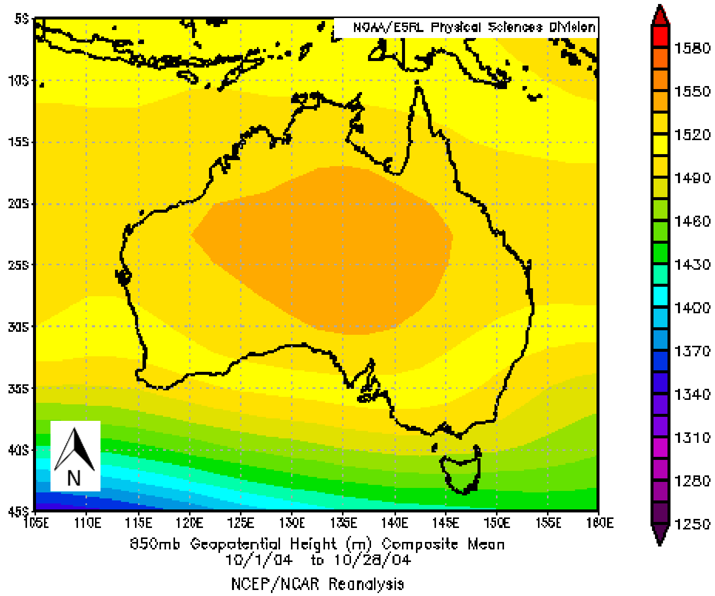
NOAA/ESRL Physical Sciences Division
5S
10S
15S
20S
25S
30S
35S
40S
45S
105E 110E 115E 120E 125E 130E 135E 140E 145E 150E 155E 160E
N
1580
1550
1520
1490
1460
1430
1400
1370
1340
1310
1280
1250
850mb Geopotential Height (m) Composite Mean
10/1/04 to 10/28/04
NCEP/NCAR Reanalysis

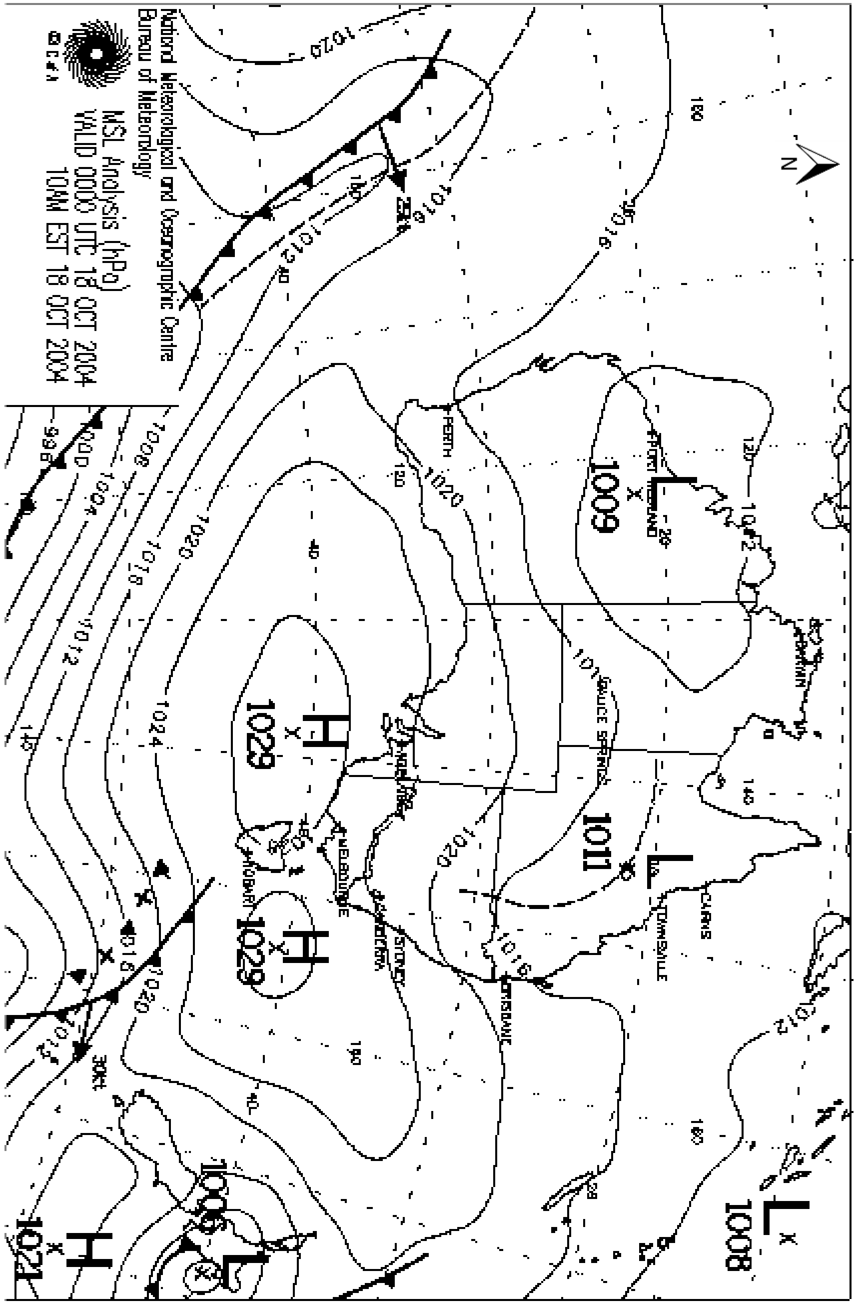
National Meteorological and Oceanographic Centre
Bureau of Meteorology
MSL Analysis (hPa)
VALID 0000 UTC 18 OCT 2004
10AM EST 18 OCT 2004

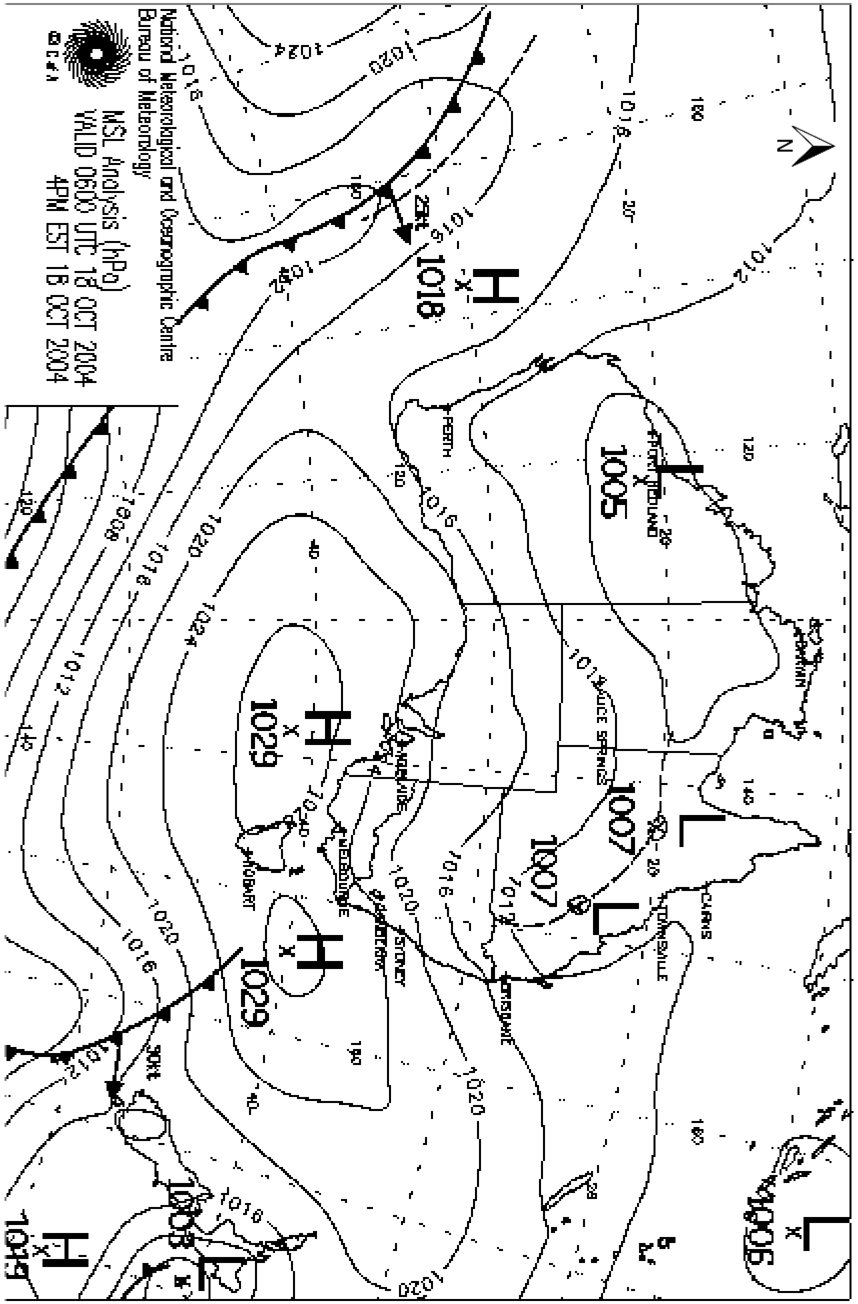
National Meteorological and Oceanographic Centre
Bureau of Meteorology
MSL Analysis (hPa)
VALID 0600 UTC 18 OCT 2004
4PM EST 18 OCT 2004

26/10/2003

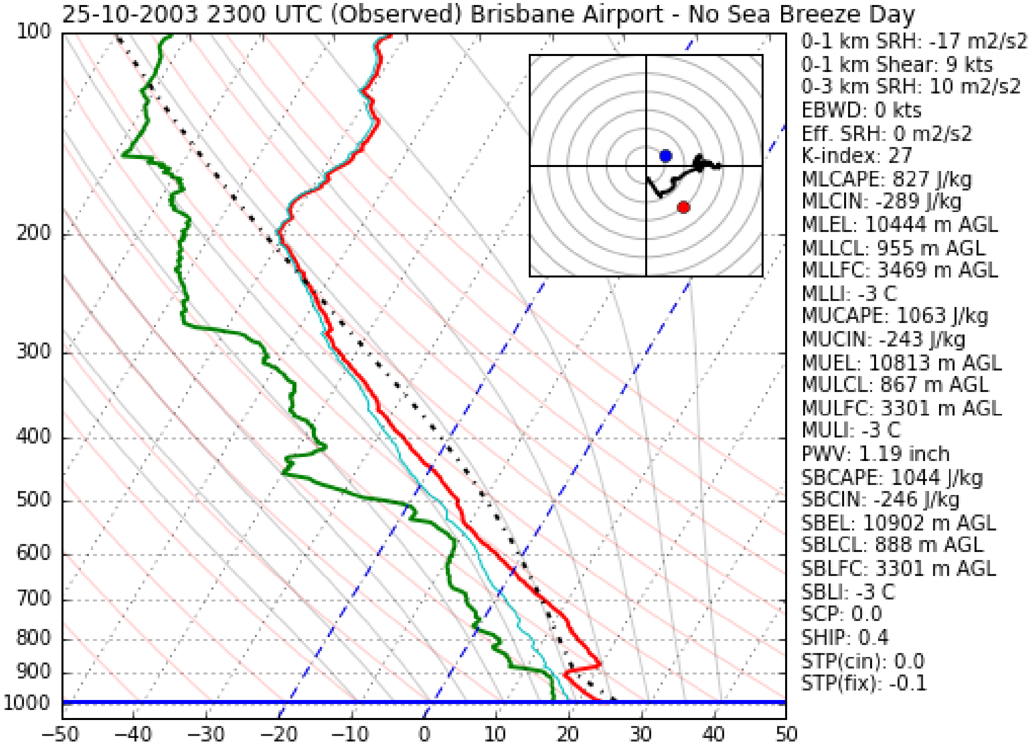
25-10-2003 2300 UTC (Observed) Brisbane Airport - No Sea Breeze Day
0-1 km SRH: -17 m2/s2
0-1 km Shear: 9 kts
0-3 km SRH: 10 m2/s2
EBWD: 0 kts
Eff. SRH: 0 m2/s2
K-index: 27
MLCAPE: 827 J/kg
MLCIN: -289 J/kg
MLEL: 10444 m AGL
MLLCL: 955 m AGL
MLLFC: 3469 m AGL
MLLI: -3 C
MUCAPE: 1063 J/kg
MUCIN: -243 J/kg
MUEL: 10813 m AGL
MULCL: 867 m AGL
MULFC: 3301 m AGL
MULI: -3 C
PWV: 1.19 inch
SBCAPE: 1044 J/kg
SBCIN: -246 J/kg
SBEL: 10902 m AGL
SBLCL: 888 m AGL
SBLFC: 3301 m AGL
SBLI: -3 C
SCP: 0.0
SHIP: 0.4
STP(cin): 0.0
STP(fix): -0.1

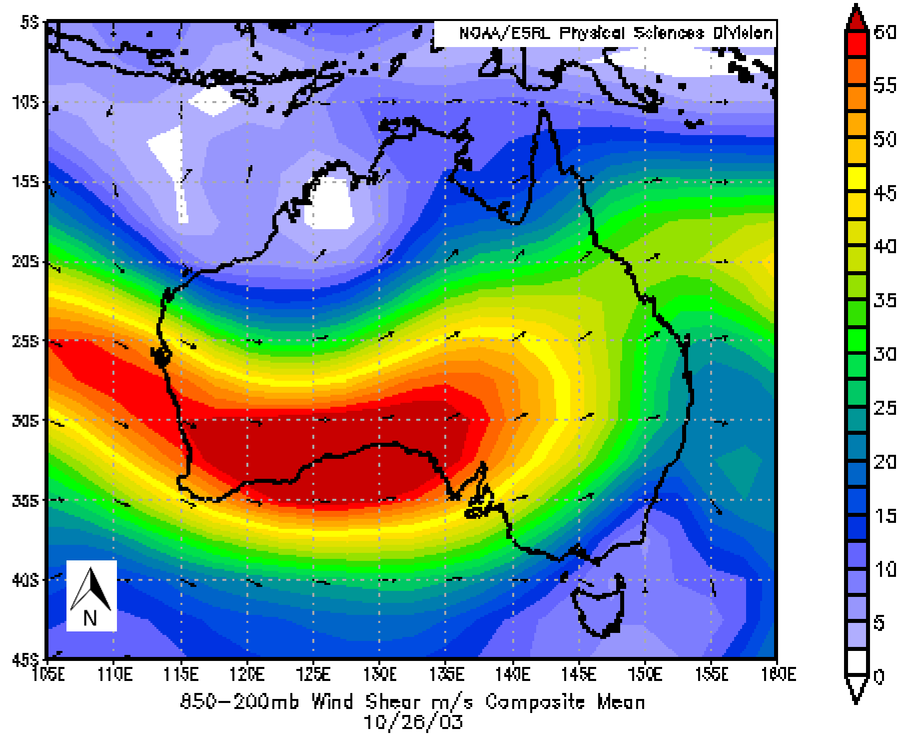
NOAA/ESRL Physical Sciences Division
N
850–200mb Wind Shear m/s Composite Mean
10/26/03

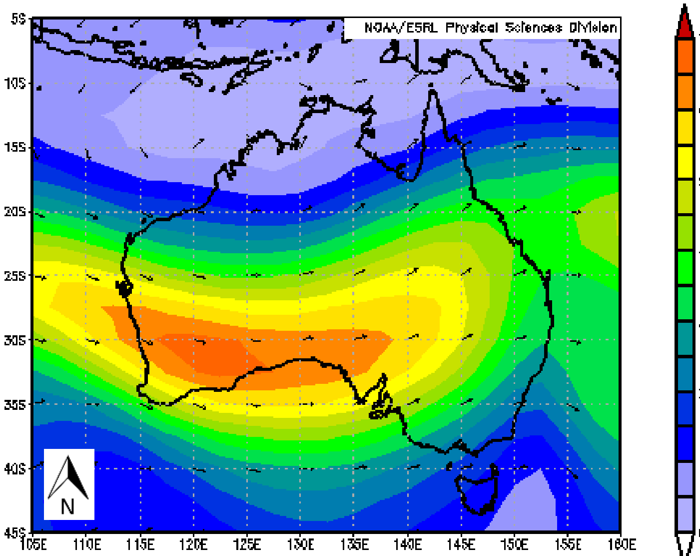

200mb Vector Wind (m/s) Composite Mean
10/26/03
NCEP/NCAR Reanalysis

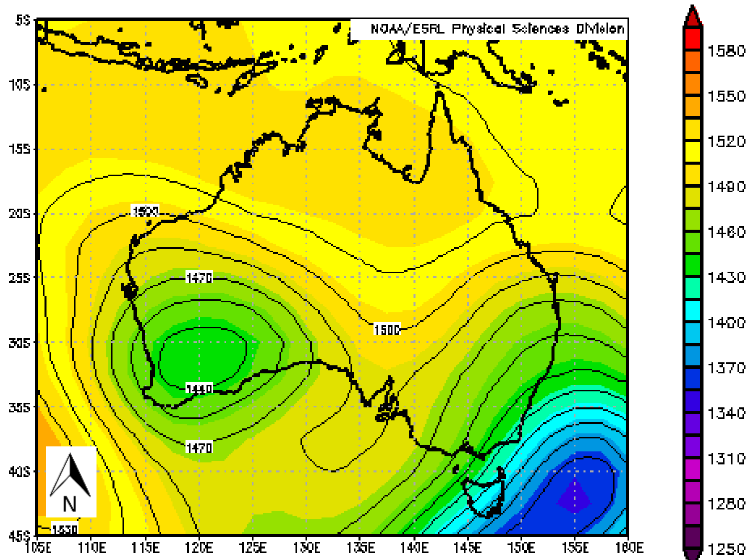

850mb Geopotential Height (m) Composite Mean
10/26/03
NCEP/NCAR Reanalysis

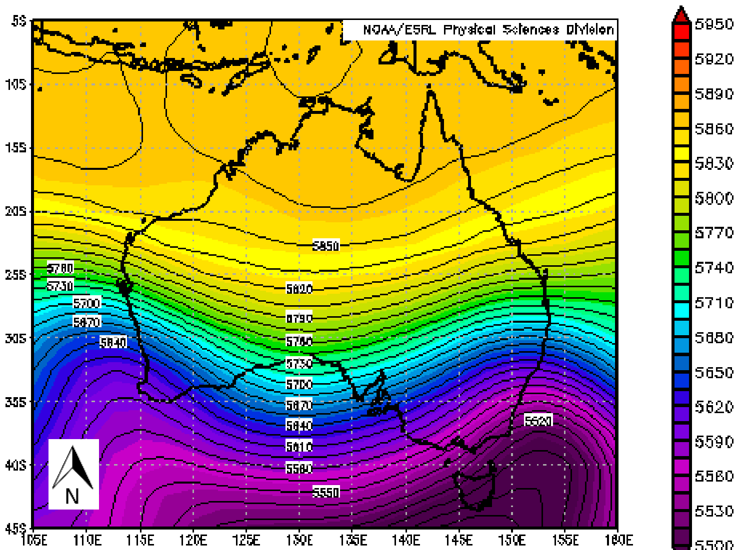

500mb Geopotential Height (m) Composite Mean
10/26/03
NCEP/NCAR Reanalysis

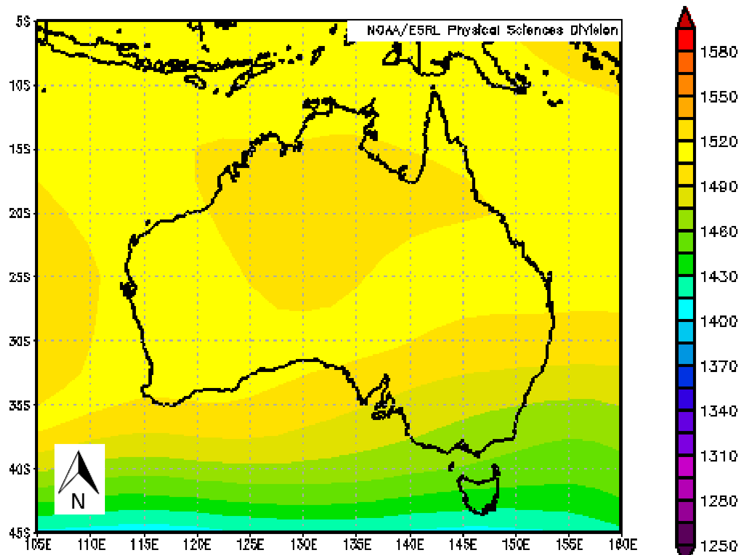

850mb Geopotential Height (m) Composite Mean
10/1/03 to 10/28/03
NCEP/NCAR Reanalysis

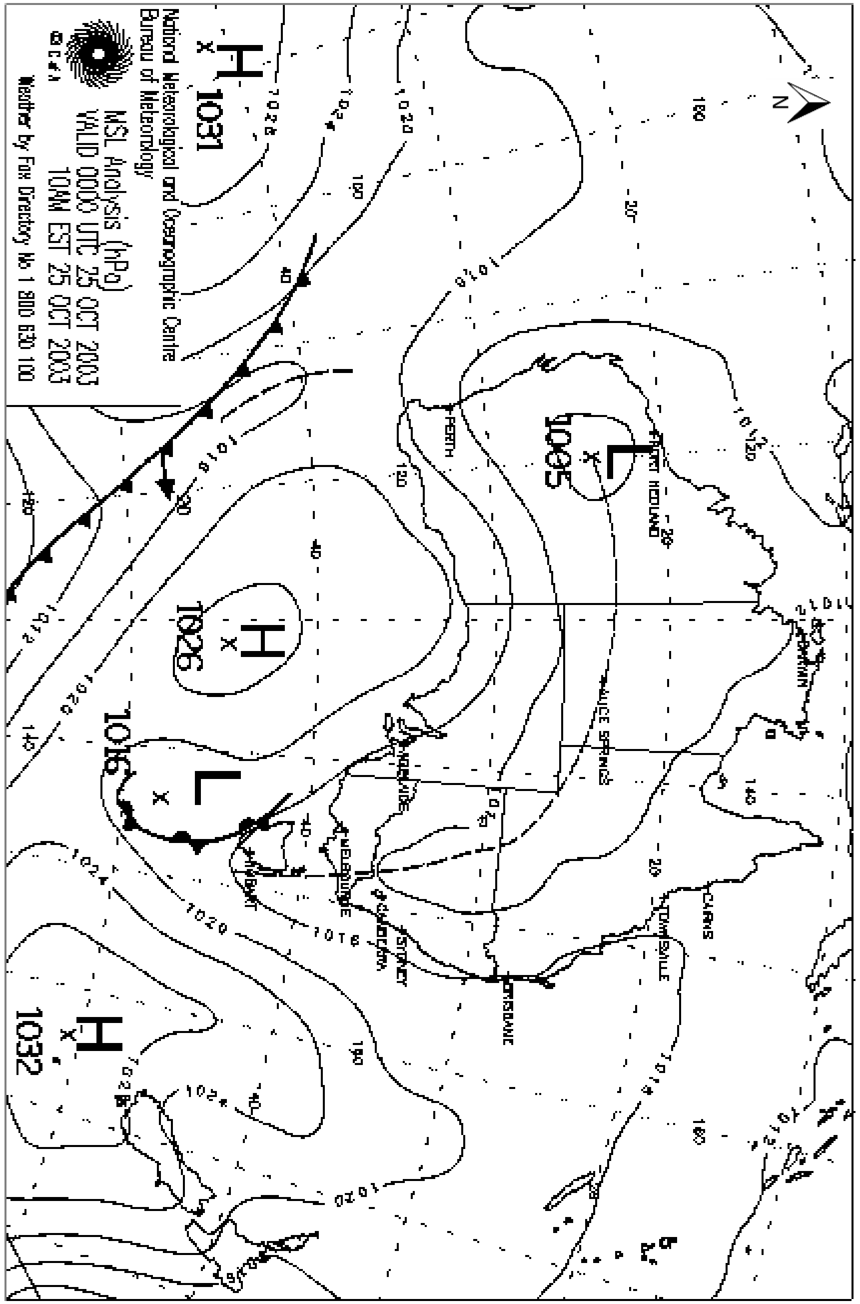
National Meteorological and Oceanographic Centre
Bureau of Meteorology
MSL Analysis (hPa)
VALID 0000 UTC 25 OCT 2003
10AM EST 25 OCT 2003
Weather by Fax Directory No 1 800 630 100
H 1031
L 1005
H 1026
L 1016
H 1032

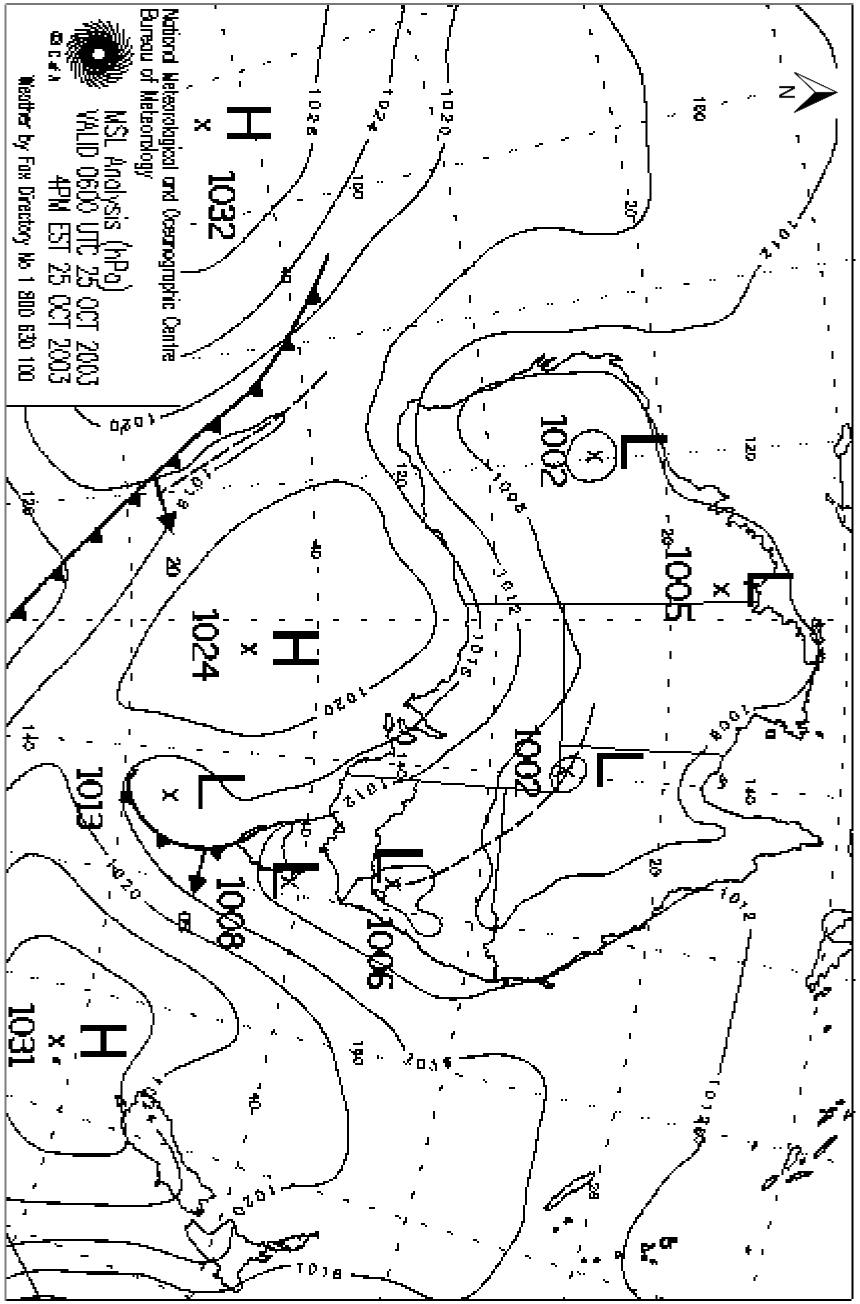
National Meteorological and Oceanographic Centre
Bureau of Meteorology
MSL Analysis (hPa)
VALID 0600 UTC 25 OCT 2003
4PM EST 25 OCT 2003
Weather by Fax Directory No 1 800 630 100
H 1032
L 1002
L 1005
H 1024
L 1002
L 1013
L 1008
L 1006
H 1031

Appendix 4: November

Sea breeze storms

Table 17: Atmospheric conditions for severe storms on sea breeze days for November

Date	Time (UTC)	Most-Unstable CAPE	Most-Unstable CIN	Most-Unstable LCL	Most-Unstable LFC	Most-Unstable EL	Most-Unstable LI	0-3 km Pressure-Weighted Mean Wind (kt)	0-6 km Shear (kt)	0-3 km Storm Relative Helicity [m2/s2]	Effective Inflow Layer Bottom Height (m AGL)	Effective Inflow Layer Top Height (m AGL)	Effective Inflow Layer SRH (m2/s2)	Effective Bulk Wind Difference
28/11/2005	2300	118.93	-44.30	890.79	4960.00	7193.47	-0.79	4.10	23.48	58.82	51.00	51.00		
14/11/2006	2300	1485.85	-29.47	1131.00	2156.00	11350.05	-5.86	12.58	30.49	48.03	0.00	1399.00	27.75	8.54
15/11/2008	2300	433.50	-187.09	843.01	3369.44	11432.25	-1.02	2.95	16.95	38.85	33.00	561.00	15.24	4.83
19/11/2008	2300	191.66	-94.12	1791.58	7831.50	9712.00	-0.14	7.50	19.23	38.43	964.00	1190.00	12.49	3.29
18/11/2012	0	500.91	-18.62	2139.83	2866.00	9490.00	-4.34	11.13	20.29	-2.97				
17/11/2013	2300	158.91	-66.57	947.06	2430.00	6592.00	-1.63	6.74	16.31	57.61	51.00	280.00	-2.85	1.10
26/11/2014	2300	83.74	-67.57	1311.89	7527.00	8607.50	-0.34	0.68	12.11	16.82	-28.00	-28.00		
27/11/2014	400	1172.94	-92.17	1003.58	2168.50	12571.00	-3.69	3.16	14.76	38.92		327.00	0.13	3.56
	average	518.30	-74.99	1257.34	4163.56	9618.53	-2.23	6.10	19.20	36.81	178.50	540.00	10.55	4.26

Non-sea breeze storms

Table 18: Atmospheric conditions for severe storms on non-sea breeze days for November

Date	Time (UTC)	Most-Unstable CAPE	Most-Unstable CIN	Most-Unstable LCL	Most-Unstable LFC	Most-Unstable EL	Most-Unstable LI	0-3 km Pressure-Weighted Mean Wind (kt)	0-6 km Shear (kt)	0-3 km Storm Relative Helicity [m2/s2]	Effective Inflow Layer Bottom Height (m AGL)	Effective Inflow Layer Top Height (m AGL)	Effective Inflow Layer SRH (m2/s2)	Effective Bulk Wind Difference
8/11/2004	2300	533.18	-78.15	914.96	2884.00	9288.00	-3.21	3.88	16.81	19.09		686.00	-2.72	1.43
16/11/2009	2300	898.23	-545.38	1048.36	3789.90	12032.00	-3.76	7.90	11.36		-22.00	-22.00		
28/11/2009	2300	916.99	-158.93	939.15	2667.00	10408.00	-3.48	9.00	17.87	4.52	9.00	2148.00	15.15	7.17
17/11/2012	500	1140.55	-81.26	841.55	3027.44	11112.00	-5.09	3.96	16.67	47.37		1736.00	-5.16	1.95
23/11/2013	2300	1316.13	-73.41	536.43	11231.00	11399.00	-4.42	9.15	18.62	73.50		1974.00	21.17	6.37
24/11/2013	300	2806.00	-41.62	616.62	1316.00	12731.00	-8.04	9.89	24.07	85.81		2273.00	87.26	20.88
	average	1268.51	-163.12	816.18	4152.56	11161.67	-4.67	7.30	17.57	46.06	-6.50	1465.83	23.14	7.56

Non-storm days

Table 19: Atmospheric conditions for non-storm days for November

Date	Time (UTC)	Most-Unstable CAPE	Most-Unstable CIN	Most-Unstable LCL	Most-Unstable LFC	Most-Unstable EL	Most-Unstable LI	0-3 km Pressure-Weighted Mean Wind (kt)	0-6 km Shear (kt)	0-3 km Storm Relative Helicity [m2/s2]	Effective Inflow Layer Bottom Height (m AGL)	Effective Inflow Layer Top Height (m AGL)	Effective Inflow Layer SRH (m2/s2)	Effective Bulk Wind Difference
	average	247.7509	-175.202	1385.027	4079.921	5162.132	1.637501	4.930798	13.97998	22.06289	-14.8297	140.4527	6.322663	4.223999

27/11/2014

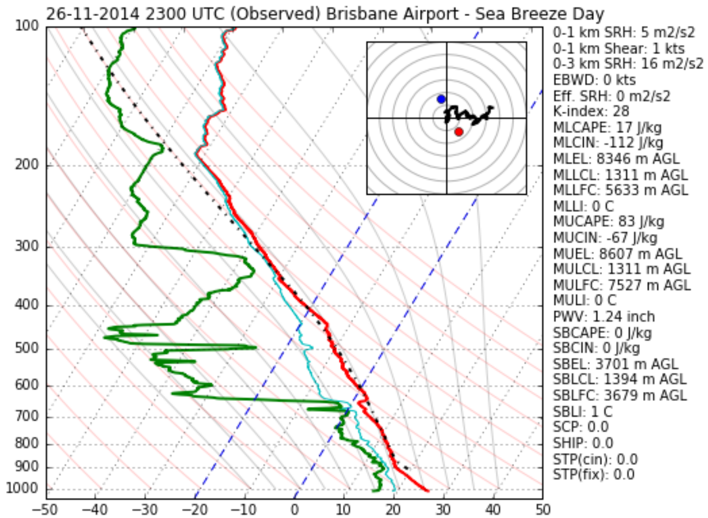
26-11-2014 2300 UTC (Observed) Brisbane Airport - Sea Breeze Day
0-1 km SRH: 5 m2/s2
0-1 km Shear: 1 kts
0-3 km SRH: 16 m2/s2
EBWD: 0 kts
Eff. SRH: 0 m2/s2
K-index: 28
MLCAPE: 17 J/kg
MLCIN: -112 J/kg
MLEL: 8346 m AGL
MLLCL: 1311 m AGL
MLLFC: 5633 m AGL
MLLI: 0 C
MUCAPE: 83 J/kg
MUCIN: -67 J/kg
MUEL: 8607 m AGL
MULCL: 1311 m AGL
MULFC: 7527 m AGL
MULI: 0 C
PWV: 1.24 inch
SBCAPE: 0 J/kg
SBCIN: 0 J/kg
SBEL: 3701 m AGL
SBLCL: 1394 m AGL
SBLFC: 3679 m AGL
SBLI: 1 C
SCP: 0.0
SHIP: 0.0
STP(cin): 0.0
STP(fix): 0.0

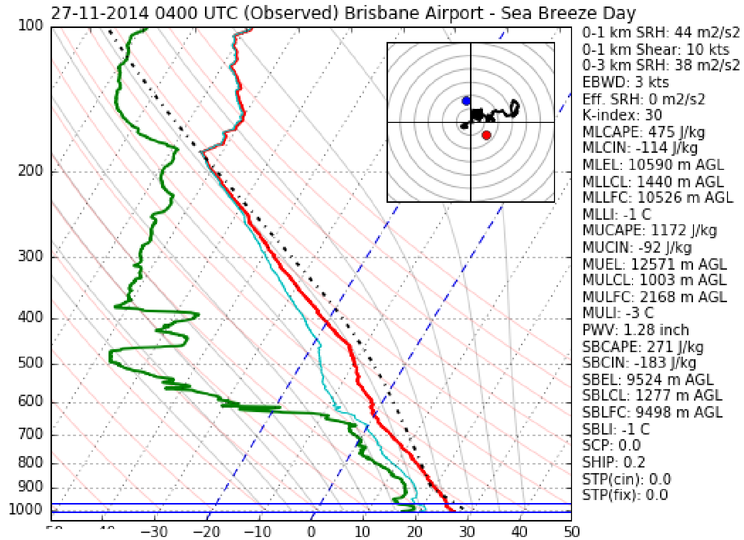
27-11-2014 0400 UTC (Observed) Brisbane Airport - Sea Breeze Day
0-1 km SRH: 44 m2/s2
0-1 km Shear: 10 kts
0-3 km SRH: 38 m2/s2
EBWD: 3 kts
Eff. SRH: 0 m2/s2
K-index: 30
MLCAPE: 475 J/kg
MLCIN: -114 J/kg
MLEL: 10590 m AGL
MLLCL: 1440 m AGL
MLLFC: 10526 m AGL
MLLI: -1 C
MUCAPE: 1172 J/kg
MUCIN: -92 J/kg
MUEL: 12571 m AGL
MULCL: 1003 m AGL
MULFC: 2168 m AGL
MULI: -3 C
PWV: 1.28 inch
SBCAPE: 271 J/kg
SBCIN: -183 J/kg
SBEL: 9524 m AGL
SBLCL: 1277 m AGL
SBLFC: 9498 m AGL
SBLI: -1 C
SCP: 0.0
SHIP: 0.2
STP(cin): 0.0
STP(fix): 0.0

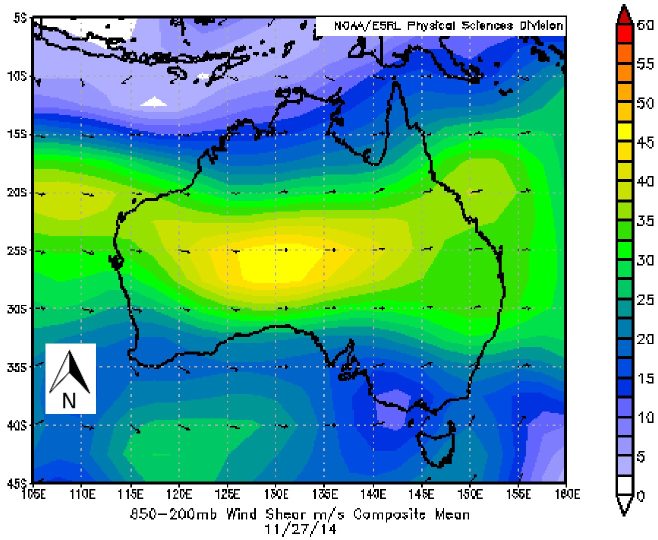
NOAA/ESRL Physical Sciences Division
N
850-200mb Wind Shear m/s Composite Mean
11/27/14

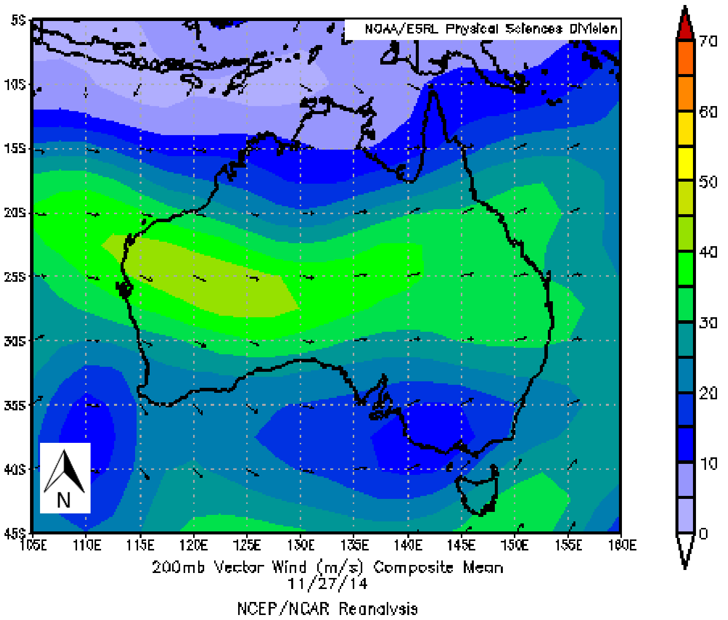
NOAA/ESRL Physical Sciences Division
200mb Vector Wind (m/s) Composite Mean
11/27/14
NCEP/NCAR Reanalysis

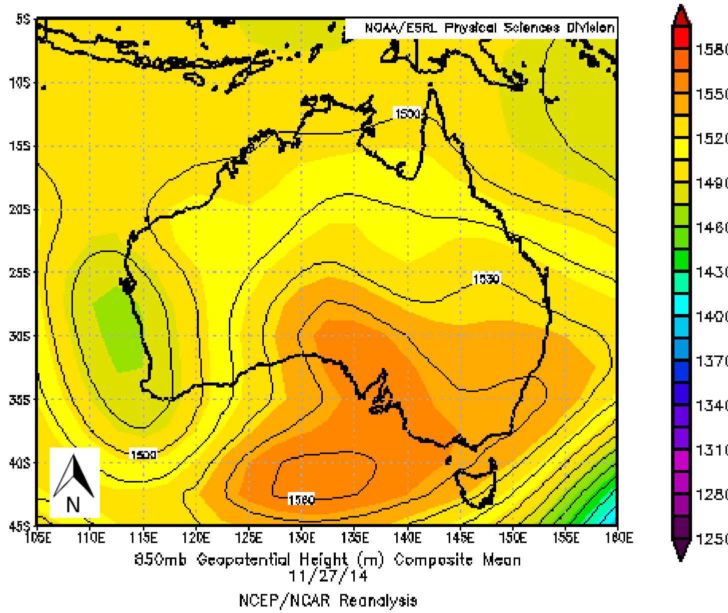
NOAA/ESRL Physical Sciences Division
850mb Geopotential Height (m) Composite Mean
11/27/14
NCEP/NCAR Reanalysis

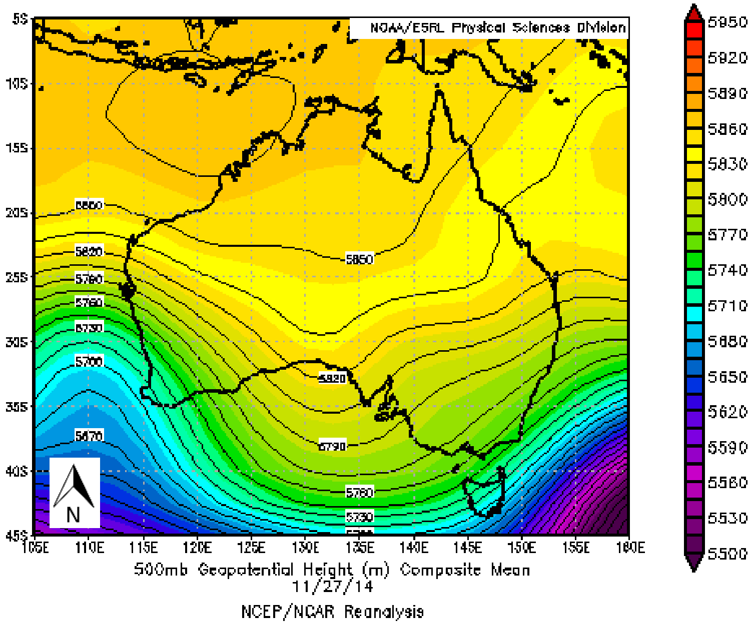
NOAA/ESRL Physical Sciences Division
500mb Geopotential Height (m) Composite Mean
11/27/14
NCEP/NCAR Reanalysis

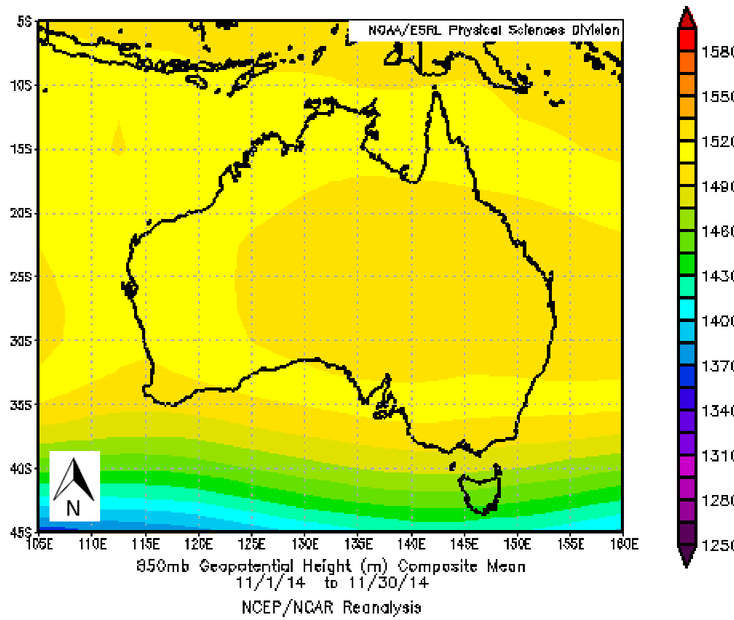
NOAA/ESRL Physical Sciences Division
850mb Geopotential Height (m) Composite Mean
11/1/14 to 11/30/14
NCEP/NCAR Reanalysis

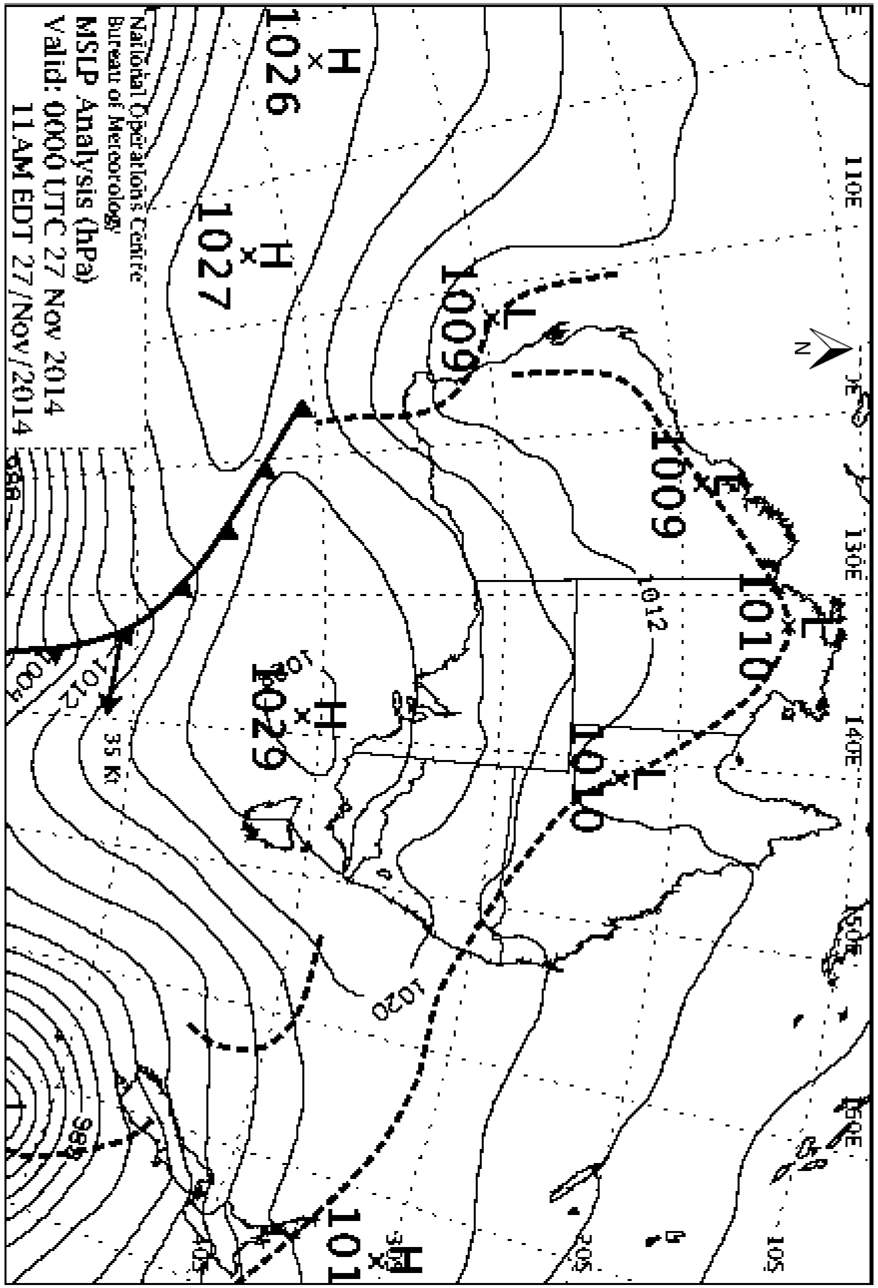
National Operations Centre
Bureau of Meteorology
MSLP Analysis (hPa)
Valid: 0000 UTC 27 Nov 2014
11AM EDT 27/Nov/2014

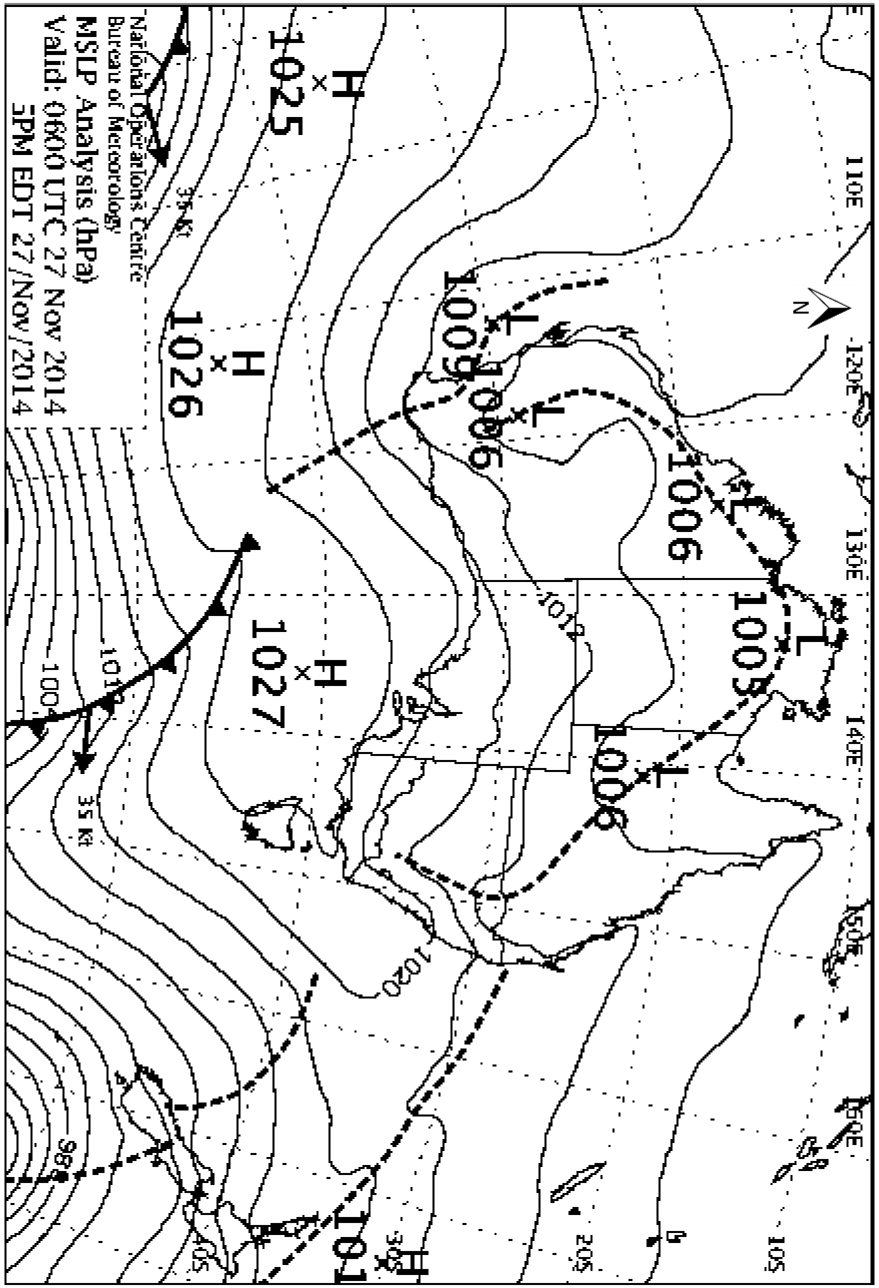
National Operations Centre
Bureau of Meteorology
MSLP Analysis (hPa)
Valid: 0600 UTC 27 Nov 2014
3PM EDT 27/Nov/2014

18/11/2012

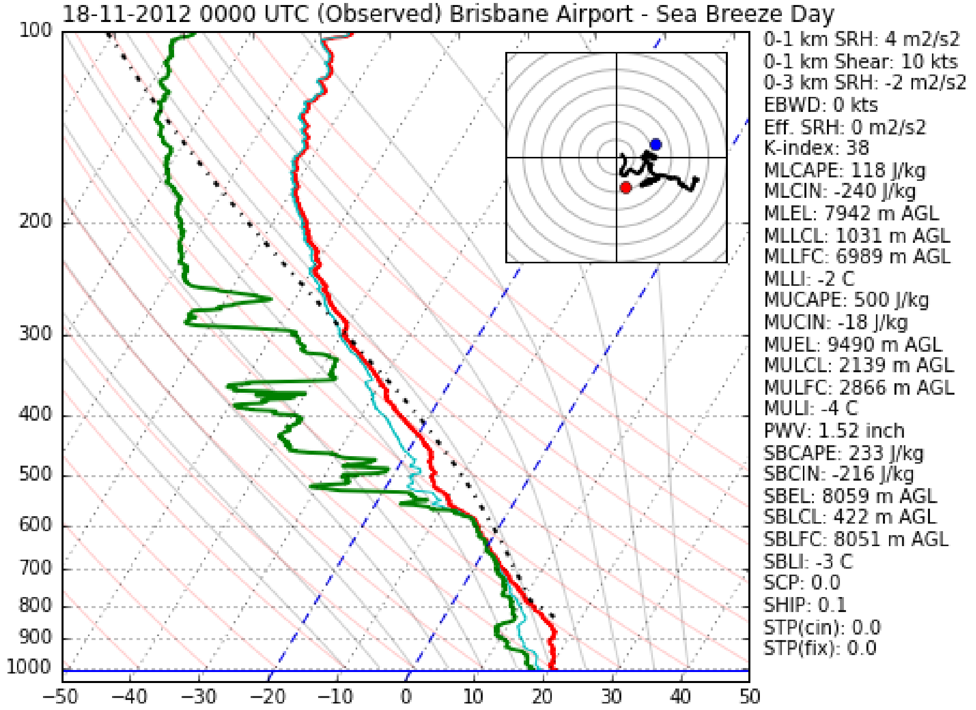
18-11-2012 0000 UTC (Observed) Brisbane Airport - Sea Breeze Day
0-1 km SRH: 4 m2/s2
0-1 km Shear: 10 kts
0-3 km SRH: -2 m2/s2
EBWD: 0 kts
Eff. SRH: 0 m2/s2
K-index: 38
MLCAPE: 118 J/kg
MLCIN: -240 J/kg
MLEL: 7942 m AGL
MLLCL: 1031 m AGL
MLLFC: 6989 m AGL
MLLI: -2 C
MUCAPE: 500 J/kg
MUCIN: -18 J/kg
MUEL: 9490 m AGL
MULCL: 2139 m AGL
MULFC: 2866 m AGL
MULI: -4 C
PWV: 1.52 inch
SBCAPE: 233 J/kg
SBCIN: -216 J/kg
SBEL: 8059 m AGL
SBLCL: 422 m AGL
SBLFC: 8051 m AGL
SBLI: -3 C
SCP: 0.0
SHIP: 0.1
STP(cin): 0.0
STP(fix): 0.0

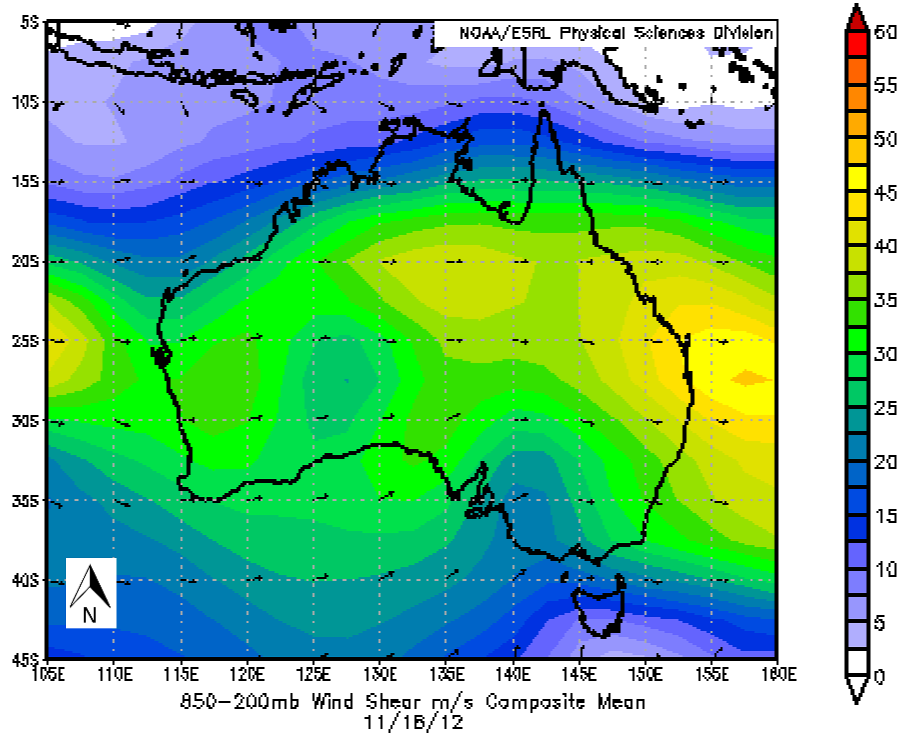
NOAA/ESRL Physical Sciences Division
N
850–200mb Wind Shear m/s Composite Mean
11/18/12

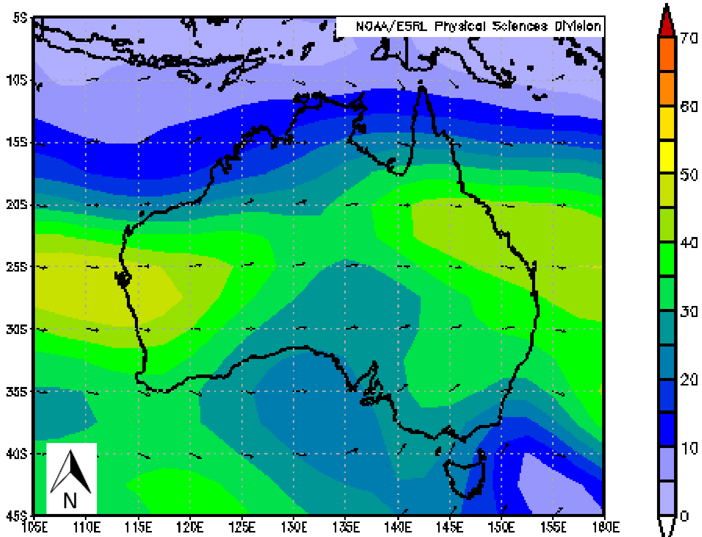

200mb Vector Wind (m/s) Composite Mean
11/16/12
NCEP/NCAR Reanalysis

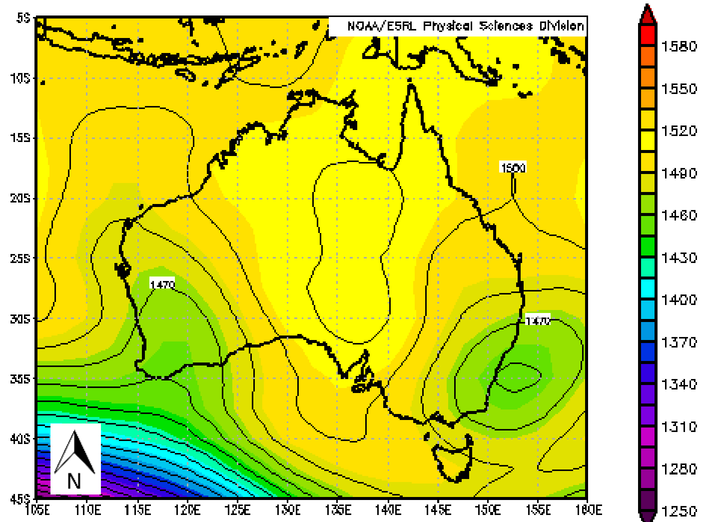

850mb Geopotential Height (m) Composite Mean
11/16/12
NCEP/NCAR Reanalysis

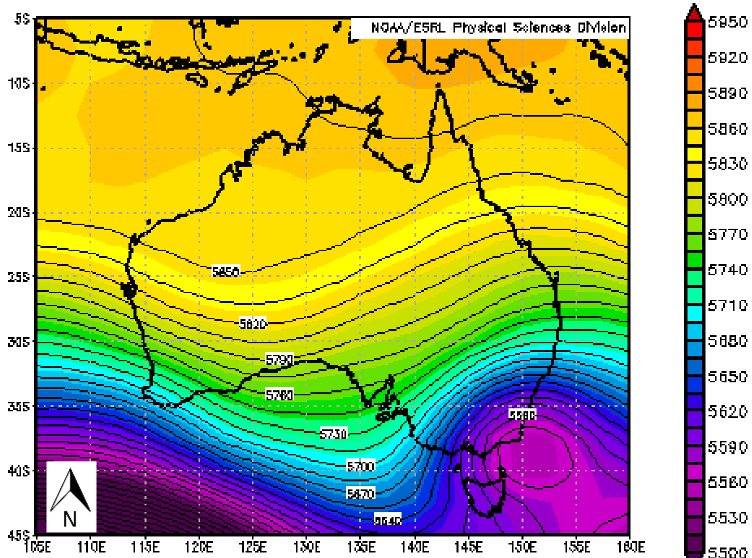

500mb Geopotential Height (m) Composite Mean
11/16/12
NCEP/NCAR Reanalysis

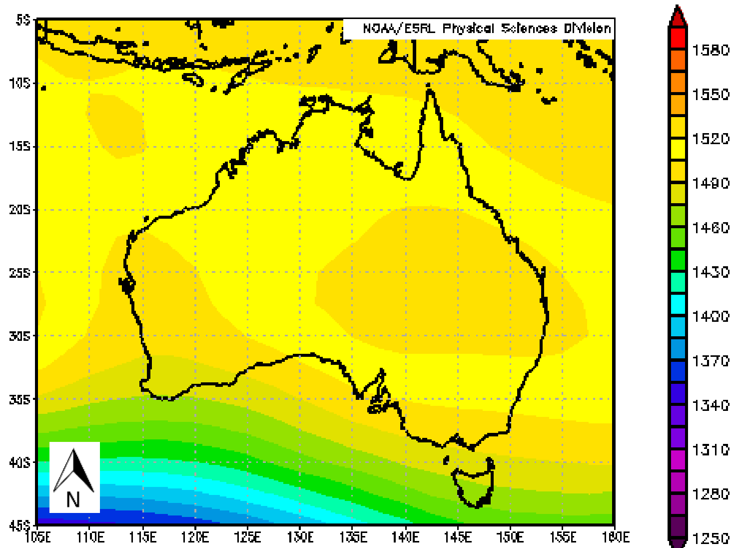

850mb Geopotential Height (m) Composite Mean
11/1/12 to 11/30/12
NCEP/NCAR Reanalysis

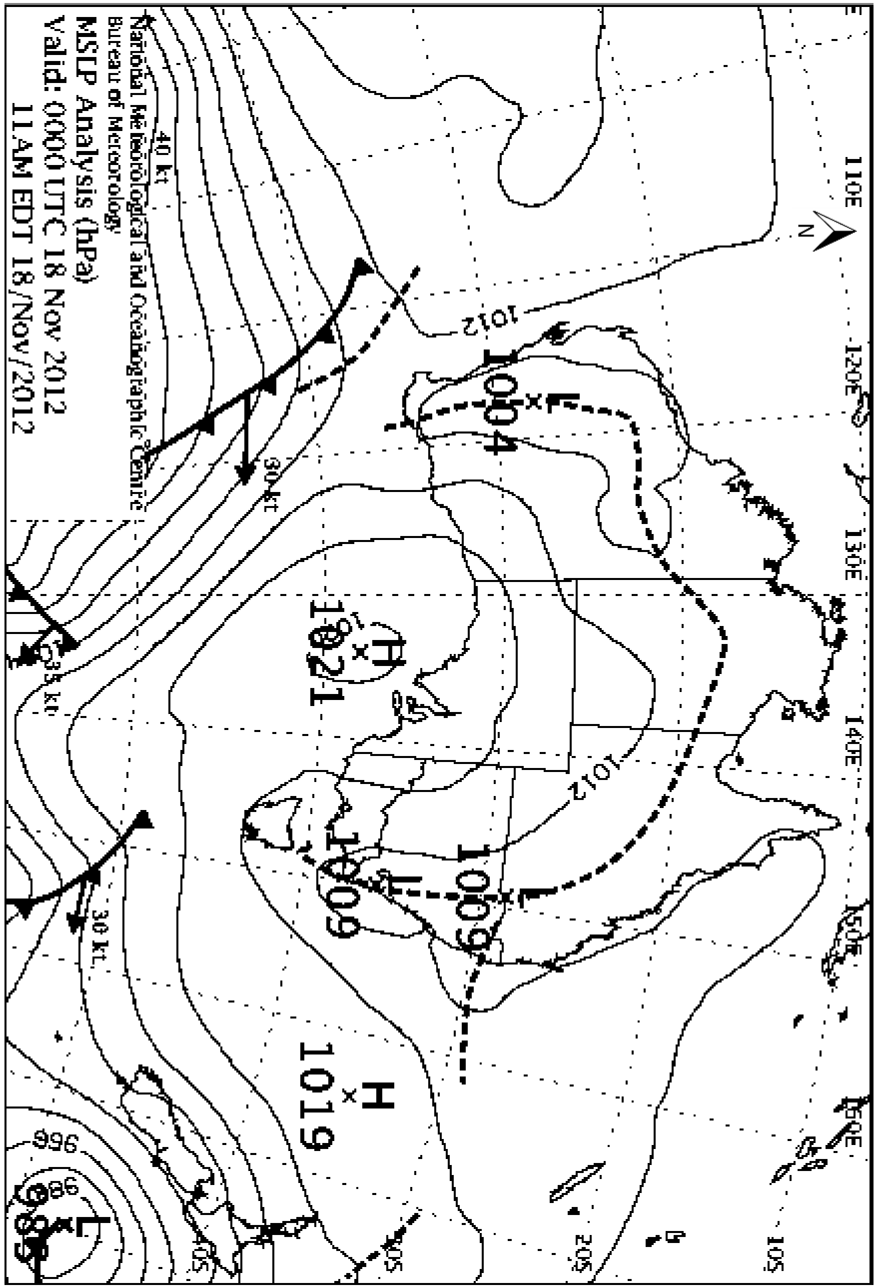
National Meteorological and Oceanographic Centre
Bureau of Meteorology
MSLP Analysis (hPa)
Valid: 0000 UTC 18 Nov 2012
11AM EDT 18/Nov/2012

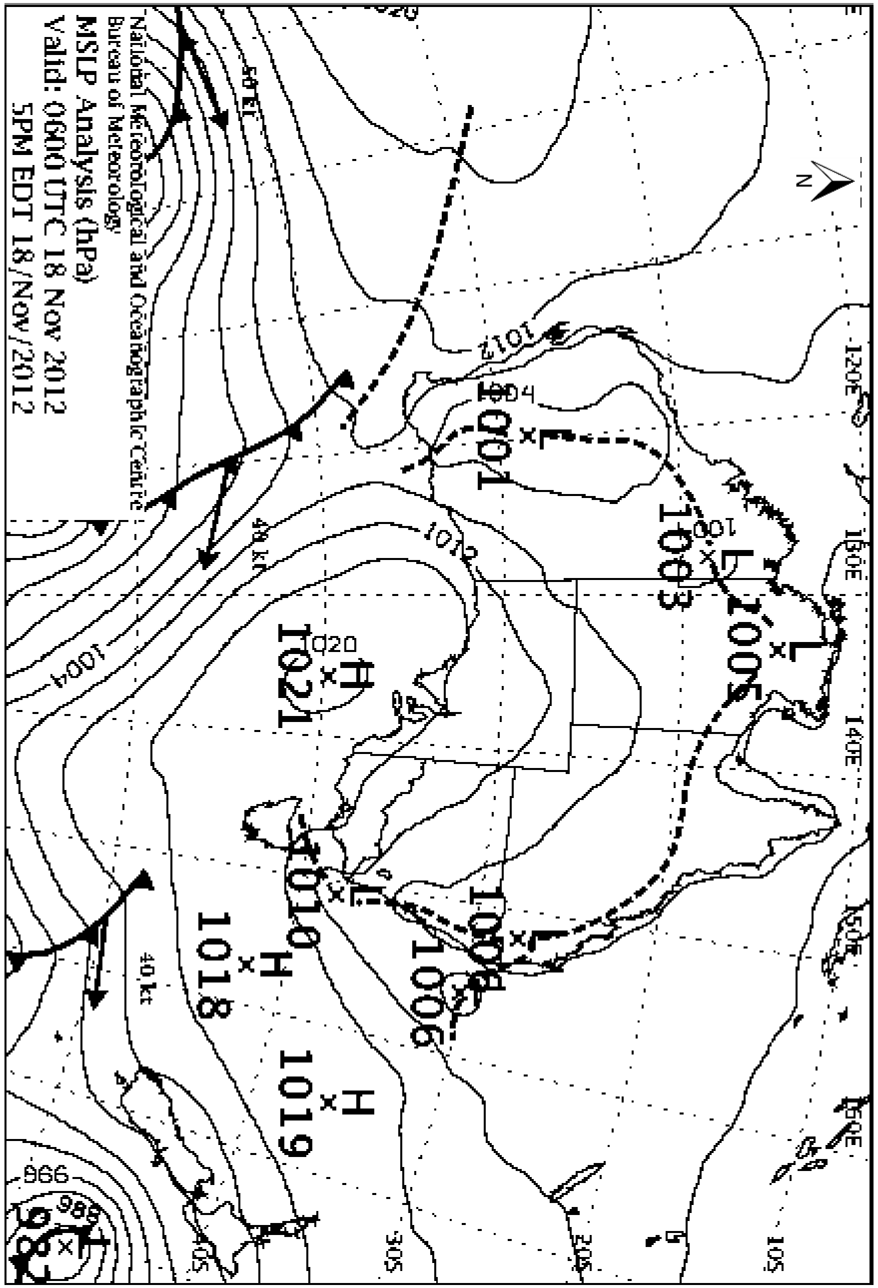
National Meteorological and Oceanographic Centre
Bureau of Meteorology
MSLP Analysis (hPa)
Valid: 0600 UTC 18 Nov 2012
5PM EDT 18/Nov/2012

15/11/2006

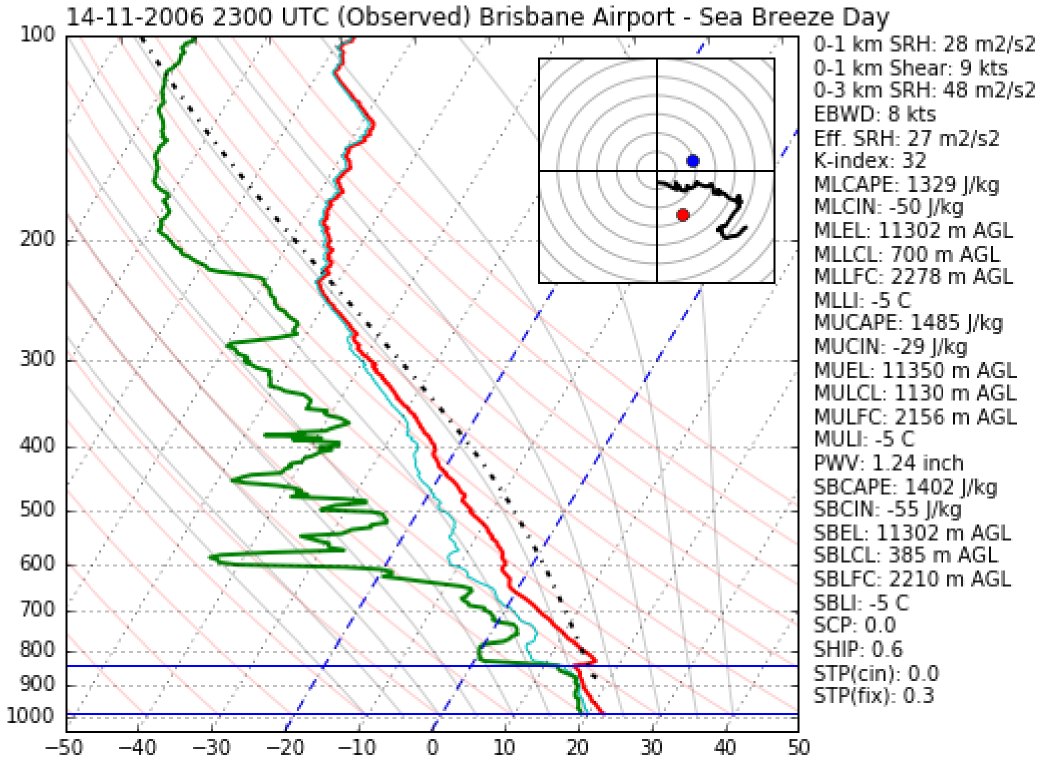
14-11-2006 2300 UTC (Observed) Brisbane Airport - Sea Breeze Day
0-1 km SRH: 28 m2/s2
0-1 km Shear: 9 kts
0-3 km SRH: 48 m2/s2
EBWD: 8 kts
Eff. SRH: 27 m2/s2
K-index: 32
MLCAPE: 1329 J/kg
MLCIN: -50 J/kg
MLEL: 11302 m AGL
MLLCL: 700 m AGL
MLLFC: 2278 m AGL
MLLI: -5 C
MUCAPE: 1485 J/kg
MUCIN: -29 J/kg
MUEL: 11350 m AGL
MULCL: 1130 m AGL
MULFC: 2156 m AGL
MULI: -5 C
PWV: 1.24 inch
SBCAPE: 1402 J/kg
SBCIN: -55 J/kg
SBEL: 11302 m AGL
SBLCL: 385 m AGL
SBLFC: 2210 m AGL
SBLI: -5 C
SCP: 0.0
SHIP: 0.6
STP(cin): 0.0
STP(fix): 0.3

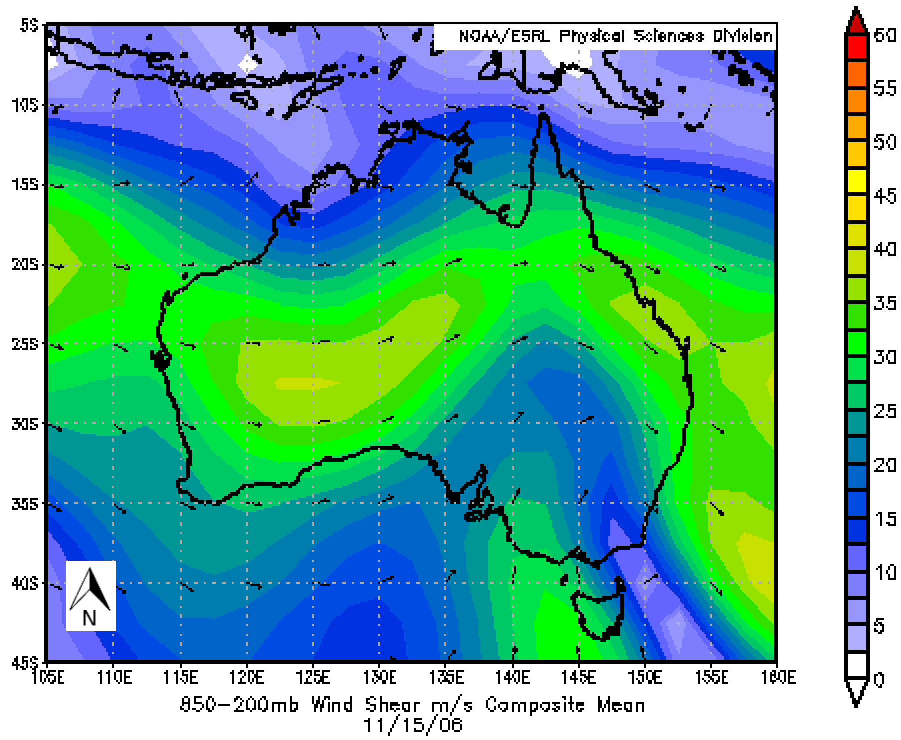
NOAA/ESRL Physical Sciences Division
850–200mb Wind Shear m/s Composite Mean
11/15/06
N

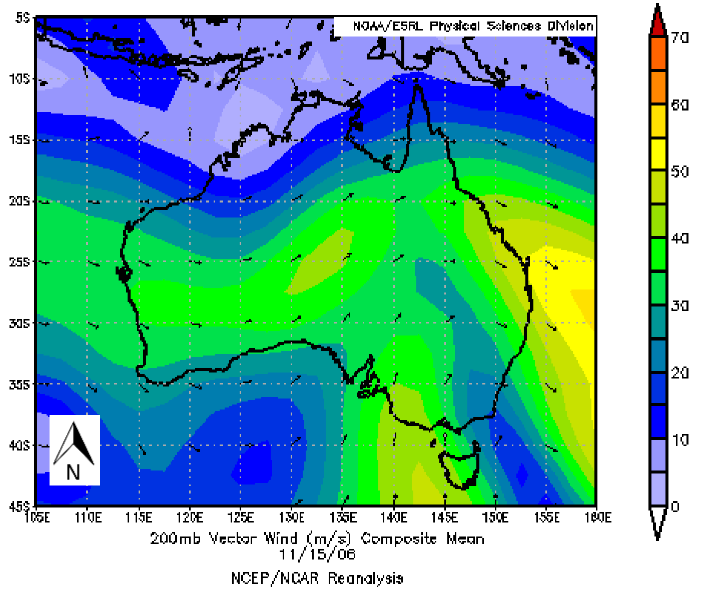
NOAA/ESRL Physical Sciences Division
200mb Vector Wind (m/s) Composite Mean
11/15/06
NCEP/NCAR Reanalysis

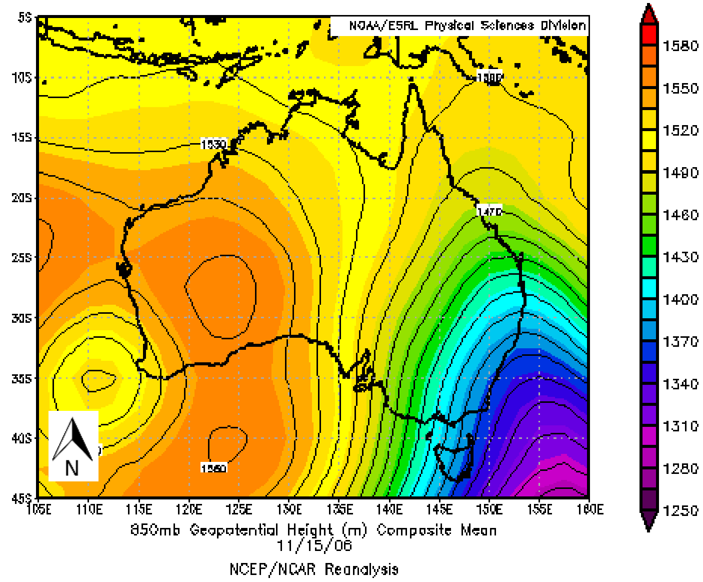
NOAA/ESRL Physical Sciences Division
850mb Geopotential Height (m) Composite Mean
11/15/06
NCEP/NCAR Reanalysis

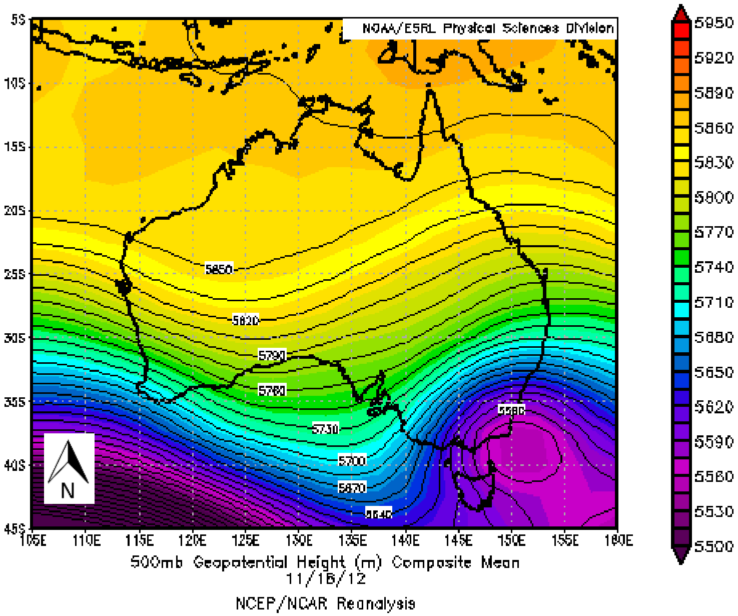
NOAA/ESRL Physical Sciences Division
500mb Geopotential Height (m) Composite Mean
11/16/12
NCEP/NCAR Reanalysis

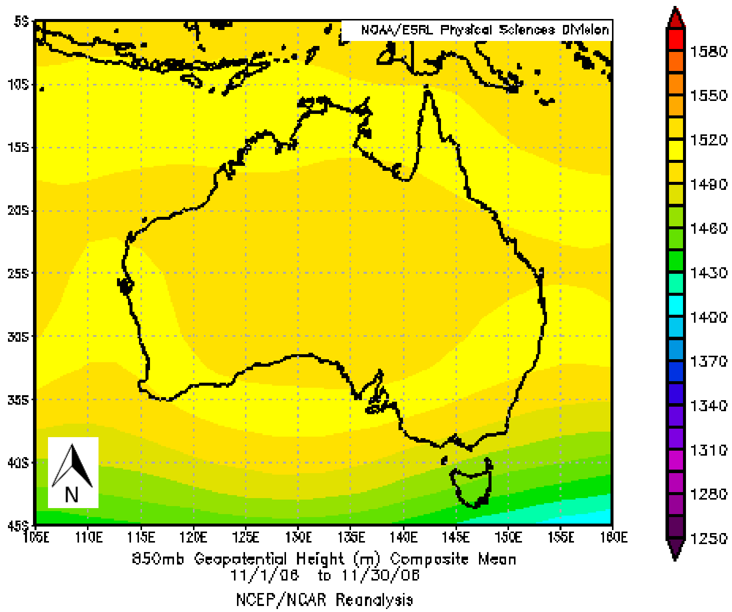
NOAA/ESRL Physical Sciences Division
850mb Geopotential Height (m) Composite Mean
11/1/06 to 11/30/06
NCEP/NCAR Reanalysis

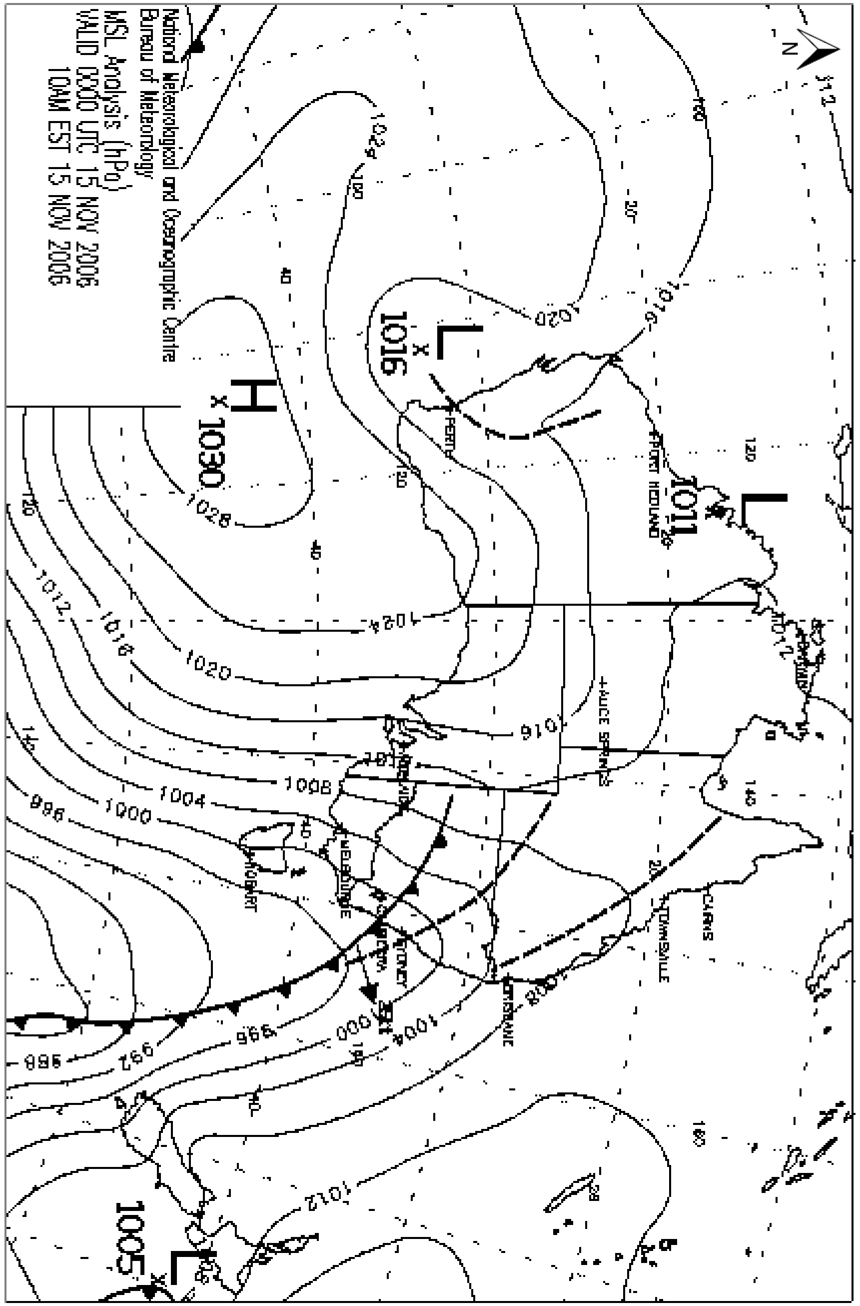
National Meteorological and Oceanographic Centre
Bureau of Meteorology
MSL Analysis (hPa)
VALID 0000 UTC 15 NOV 2006
10AM EST 15 NOV 2006

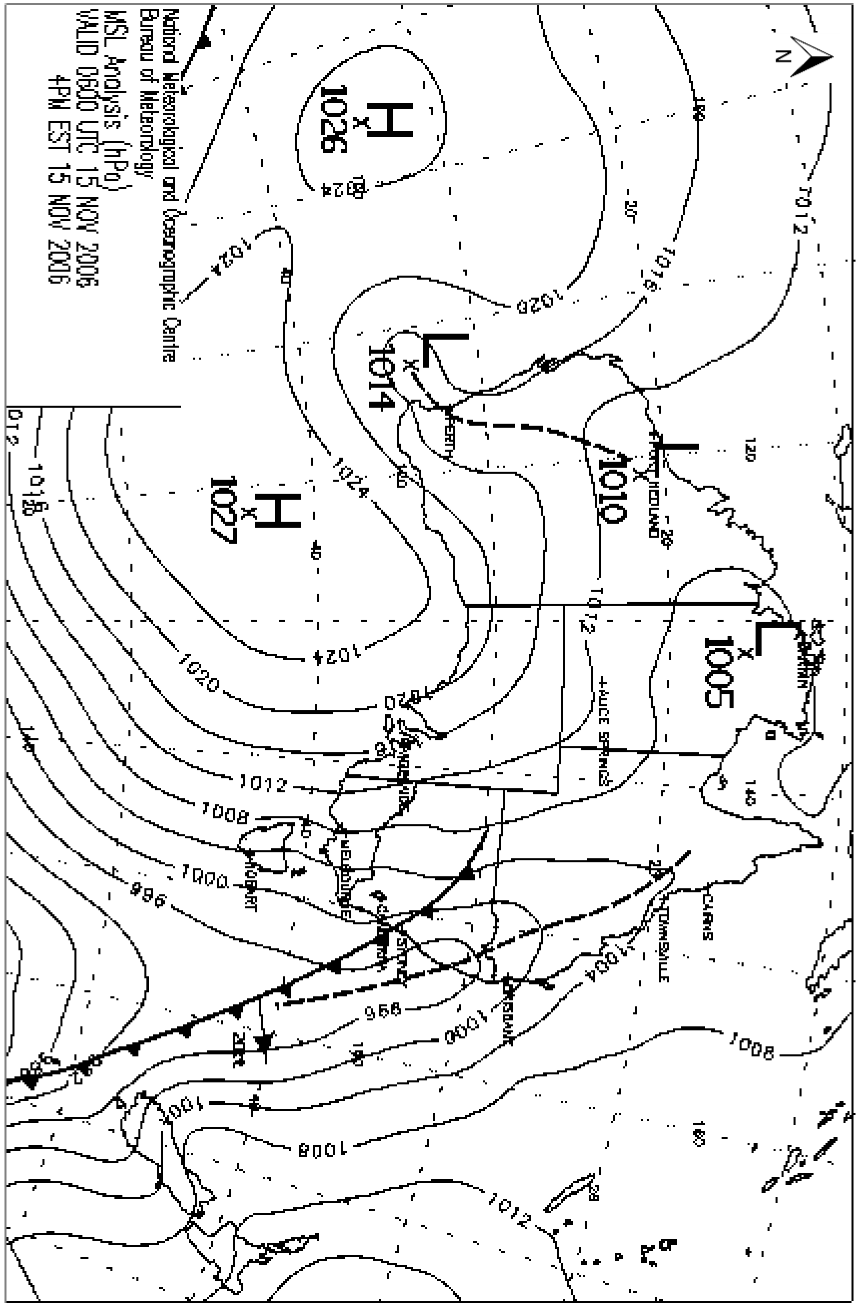
National Meteorological and Oceanographic Centre
Bureau of Meteorology
MSL Analysis (hPa)
VALID 0600 UTC 15 NOV 2006
4PM EST 15 NOV 2006

29/11/2005

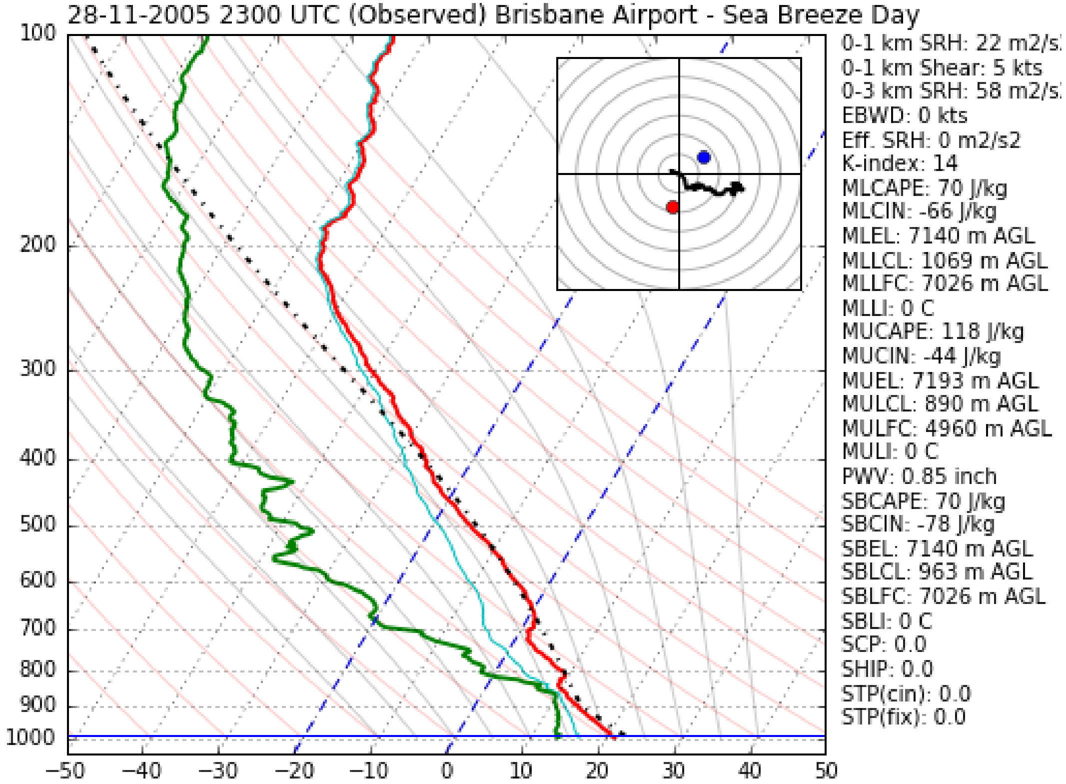
28-11-2005 2300 UTC (Observed) Brisbane Airport - Sea Breeze Day
0-1 km SRH: 22 m2/s2
0-1 km Shear: 5 kts
0-3 km SRH: 58 m2/s2
EBWD: 0 kts
Eff. SRH: 0 m2/s2
K-index: 14
MLCAPE: 70 J/kg
MLCIN: -66 J/kg
MLEL: 7140 m AGL
MLLCL: 1069 m AGL
MLLFC: 7026 m AGL
MLLI: 0 C
MUCAPE: 118 J/kg
MUCIN: -44 J/kg
MUEL: 7193 m AGL
MULCL: 890 m AGL
MULFC: 4960 m AGL
MULI: 0 C
PWV: 0.85 inch
SBCAPE: 70 J/kg
SBCIN: -78 J/kg
SBEL: 7140 m AGL
SBLCL: 963 m AGL
SBLFC: 7026 m AGL
SBLI: 0 C
SCP: 0.0
SHIP: 0.0
STP(cin): 0.0
STP(fix): 0.0

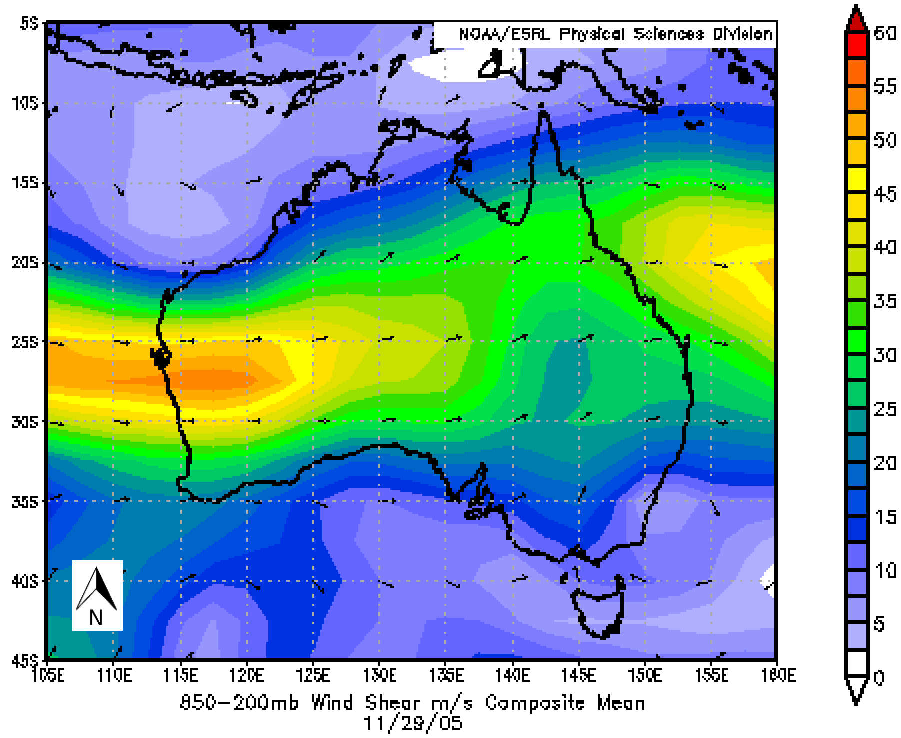
NOAA/ESRL Physical Sciences Division
N
850–200mb Wind Shear m/s Composite Mean
11/29/05

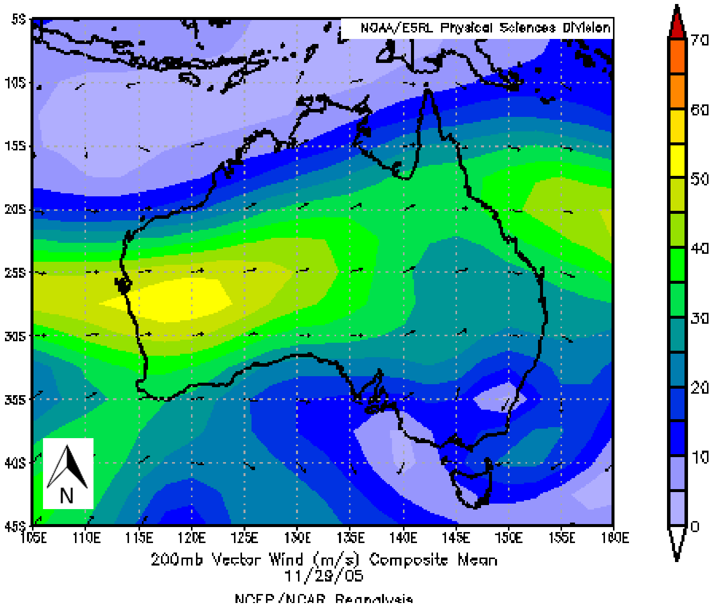
NOAA/ESRL Physical Sciences Division
200mb Vector Wind (m/s) Composite Mean
11/29/05
NCEP/NCAR Reanalysis

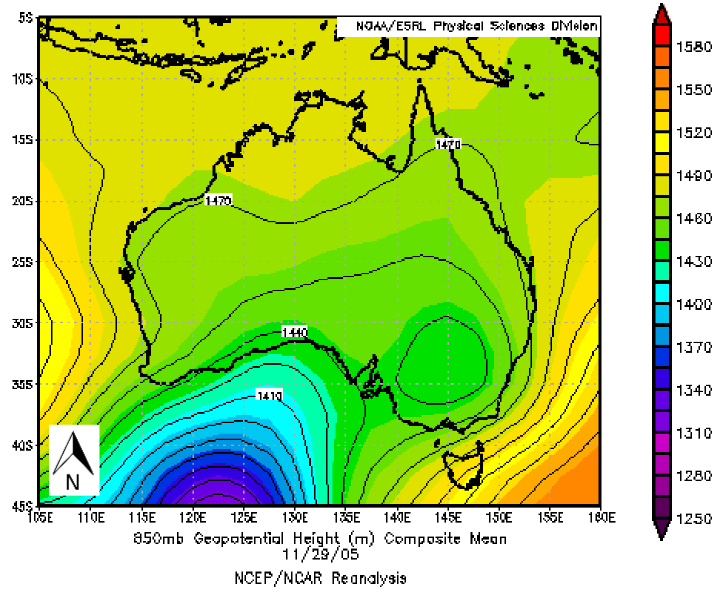
NOAA/ESRL Physical Sciences Division
850mb Geopotential Height (m) Composite Mean
11/29/05
NCEP/NCAR Reanalysis

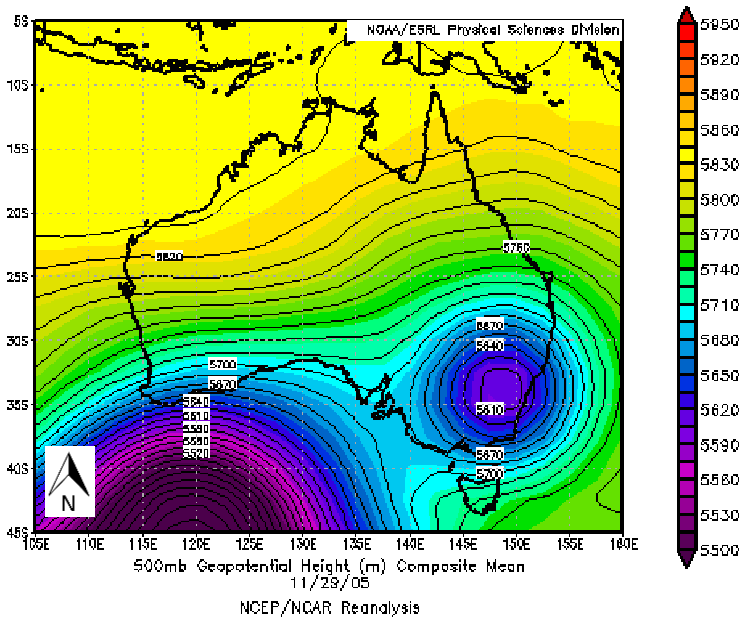
NOAA/ESRL Physical Sciences Division
500mb Geopotential Height (m) Composite Mean
11/29/05
NCEP/NCAR Reanalysis

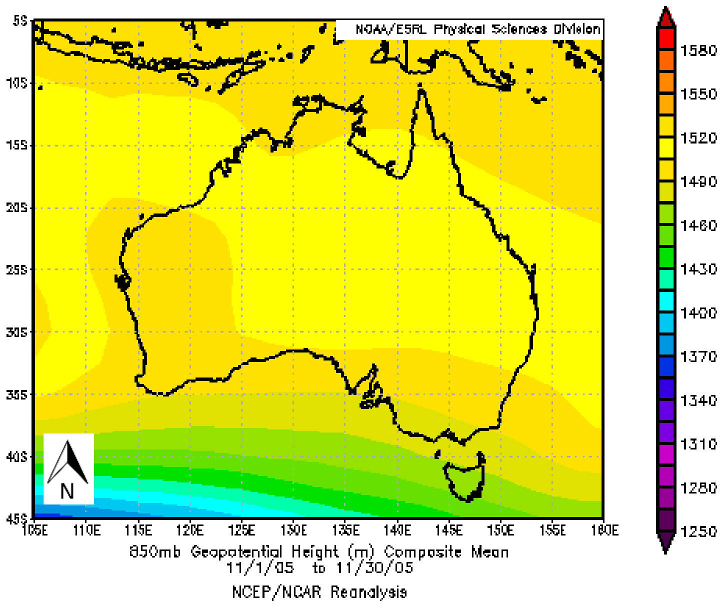
NOAA/ESRL Physical Sciences Division
850mb Geopotential Height (m) Composite Mean
11/1/05 to 11/30/05
NCEP/NCAR Reanalysis

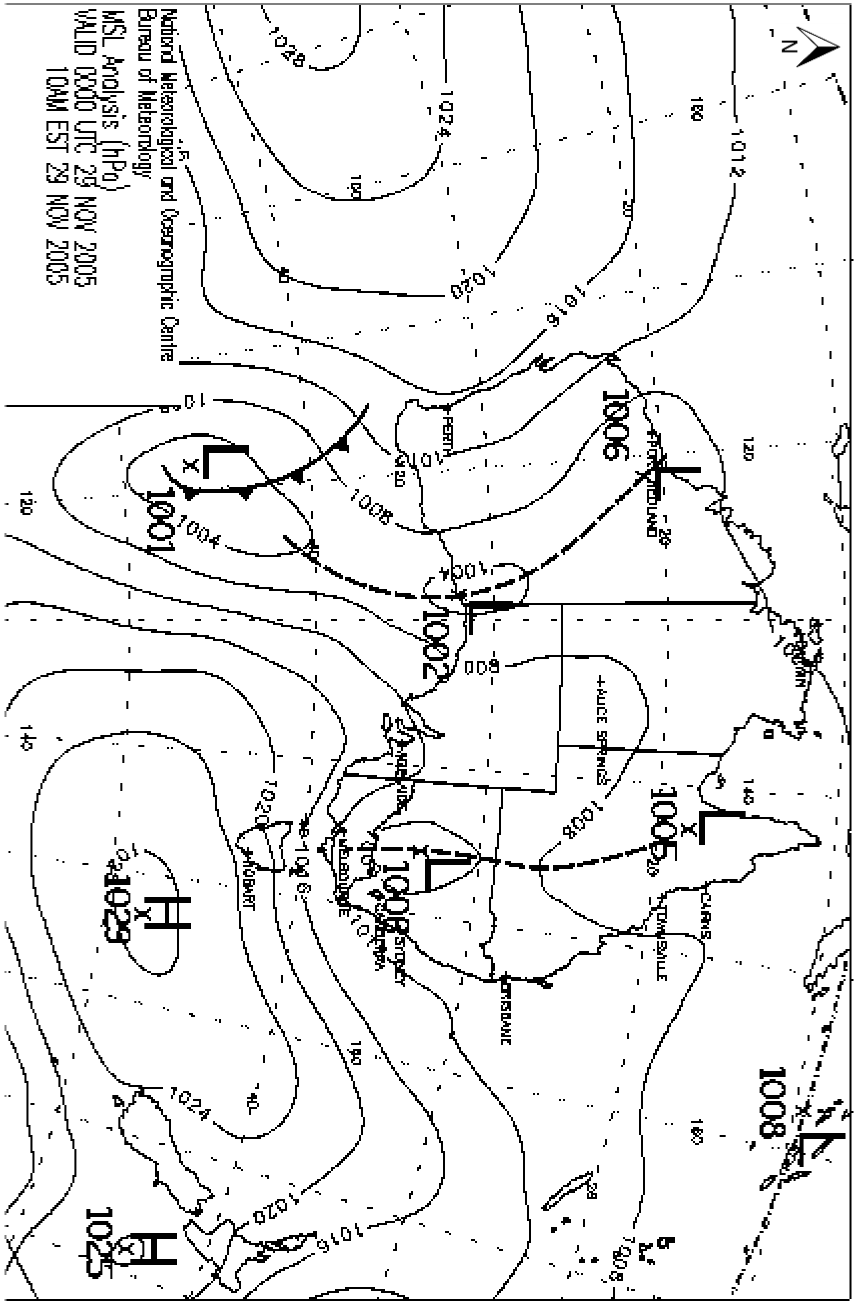
National Meteorological and Oceanographic Centre
Bureau of Meteorology
MSL Analysis (hPa)
VALID 0000 UTC 29 NOV 2005
10AM EST 29 NOV 2005

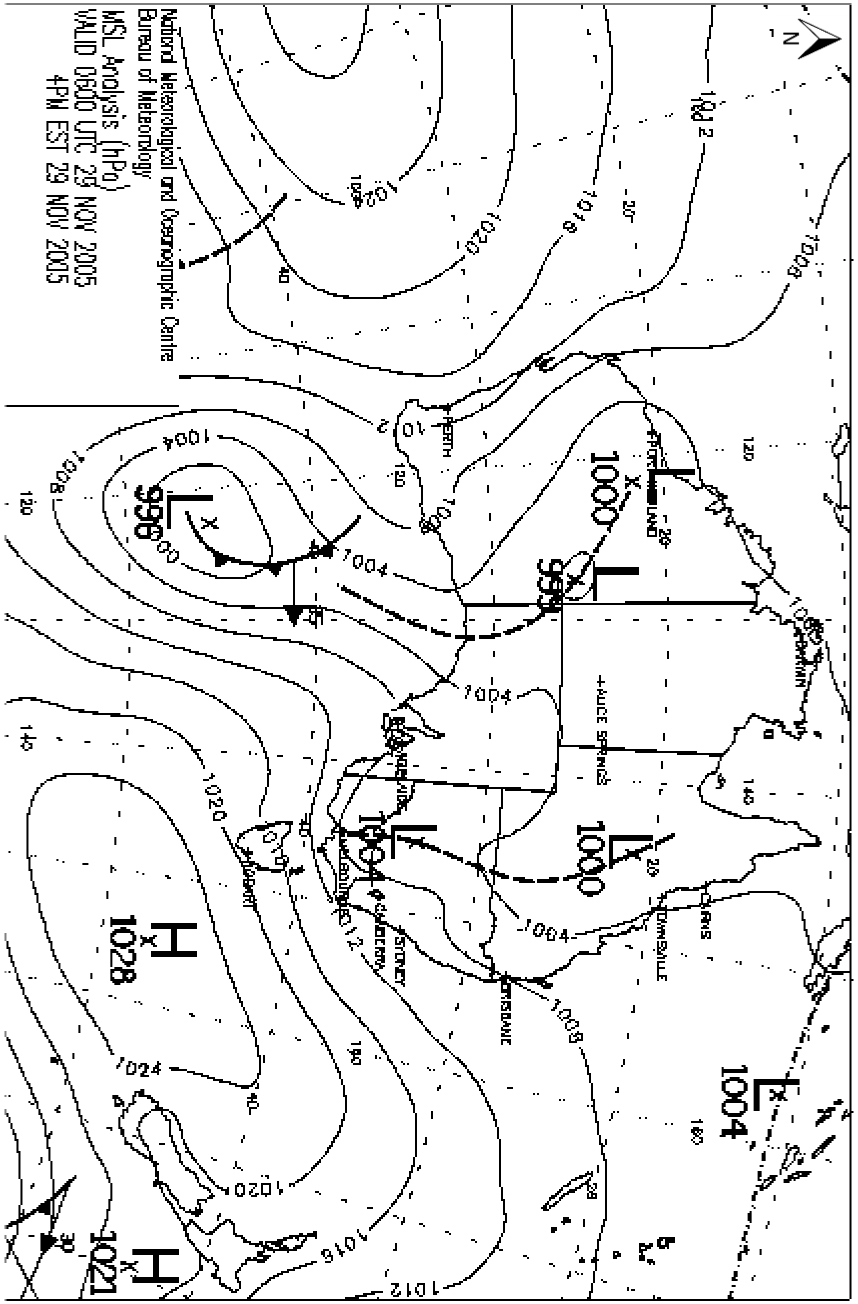
National Meteorological and Oceanographic Centre
Bureau of Meteorology
MSL Analysis (hPa)
VALID 0600 UTC 29 NOV 2005
4PM EST 29 NOV 2005

24/11/2013

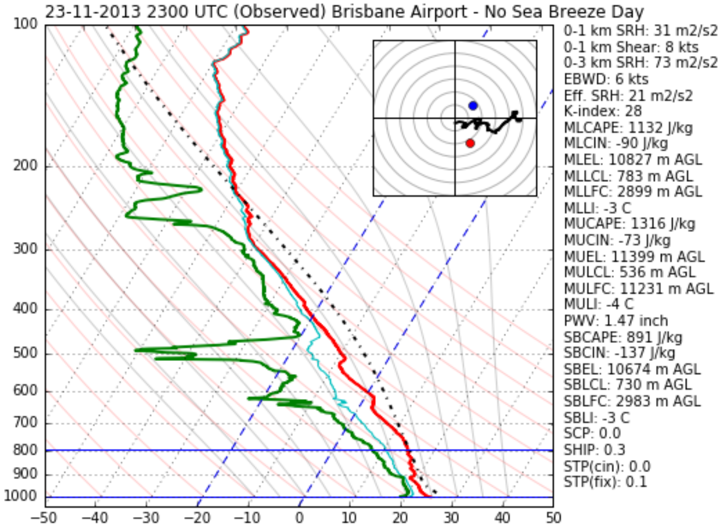
23-11-2013 2300 UTC (Observed) Brisbane Airport - No Sea Breeze Day
0-1 km SRH: 31 m2/s2
0-1 km Shear: 8 kts
0-3 km SRH: 73 m2/s2
EBWD: 6 kts
Eff. SRH: 21 m2/s2
K-index: 28
MLCAPE: 1132 J/kg
MLCIN: -90 J/kg
MLEL: 10827 m AGL
MLLCL: 783 m AGL
MLLFC: 2899 m AGL
MLLI: -3 C
MUCAPE: 1316 J/kg
MUCIN: -73 J/kg
MUEL: 11399 m AGL
MULCL: 536 m AGL
MULFC: 11231 m AGL
MULI: -4 C
PWV: 1.47 inch
SBCAPE: 891 J/kg
SBCIN: -137 J/kg
SBEL: 10674 m AGL
SBLCL: 730 m AGL
SBLFC: 2983 m AGL
SBLI: -3 C
SCP: 0.0
SHIP: 0.3
STP(cin): 0.0
STP(fix): 0.1

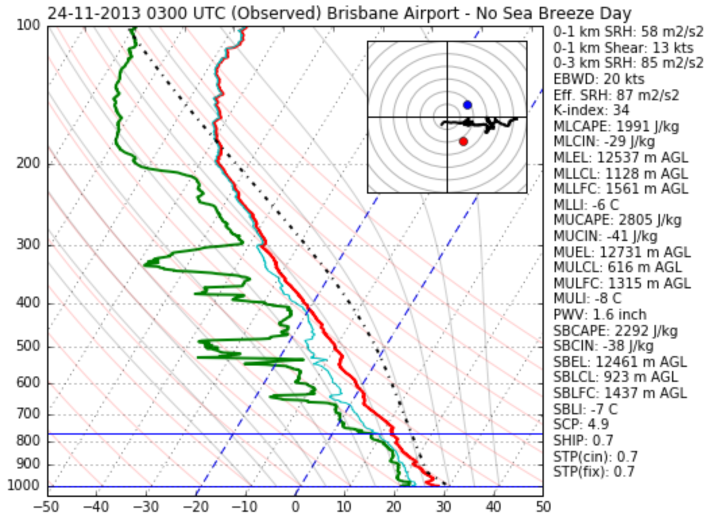
24-11-2013 0300 UTC (Observed) Brisbane Airport - No Sea Breeze Day
0-1 km SRH: 58 m2/s2
0-1 km Shear: 13 kts
0-3 km SRH: 85 m2/s2
EBWD: 20 kts
Eff. SRH: 87 m2/s2
K-index: 34
MLCAPE: 1991 J/kg
MLCIN: -29 J/kg
MLEL: 12537 m AGL
MLLCL: 1128 m AGL
MLLFC: 1561 m AGL
MLLI: -6 C
MUCAPE: 2805 J/kg
MUCIN: -41 J/kg
MUEL: 12731 m AGL
MULCL: 616 m AGL
MULFC: 1315 m AGL
MULI: -8 C
PWV: 1.6 inch
SBCAPE: 2292 J/kg
SBCIN: -38 J/kg
SBEL: 12461 m AGL
SBLCL: 923 m AGL
SBLFC: 1437 m AGL
SBLI: -7 C
SCP: 4.9
SHIP: 0.7
STP(cin): 0.7
STP(fix): 0.7

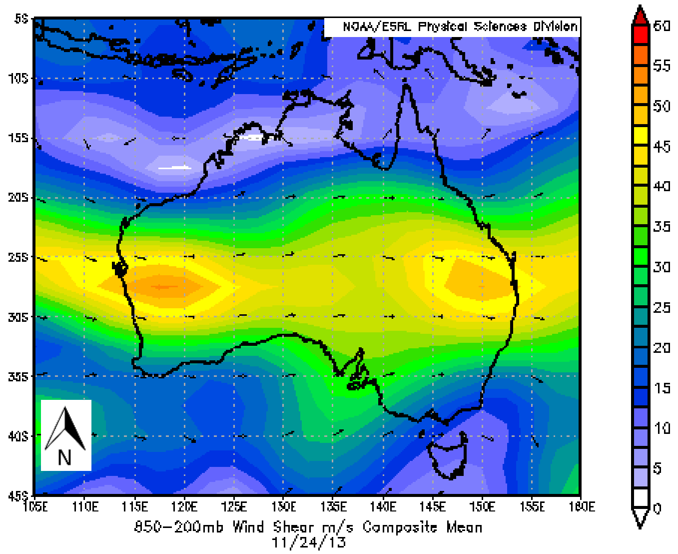
NOAA/ESRL Physical Sciences Division
N
850–200mb Wind Shear m/s Composite Mean
11/24/13

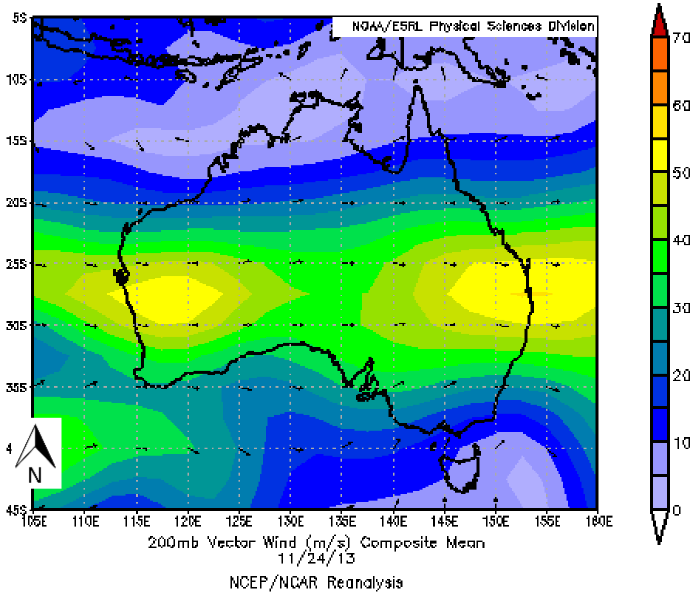
NOAA/ESRL Physical Sciences Division
200mb Vector Wind (m/s) Composite Mean
11/24/13
NCEP/NCAR Reanalysis
0 10 20 30 40 50 60 70

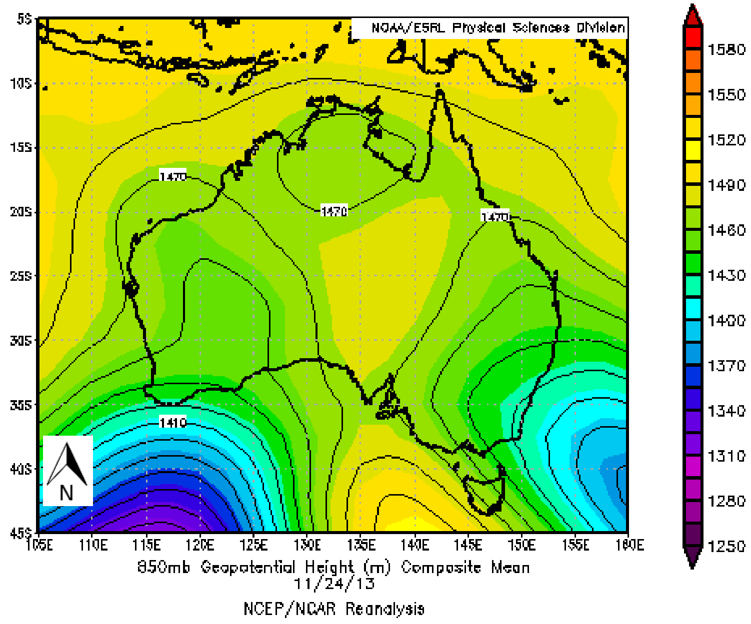
NOAA/ESRL Physical Sciences Division
850mb Geopotential Height (m) Composite Mean
11/24/13
NCEP/NCAR Reanalysis
1250 1280 1310 1340 1370 1400 1430 1460 1490 1520 1550 1580

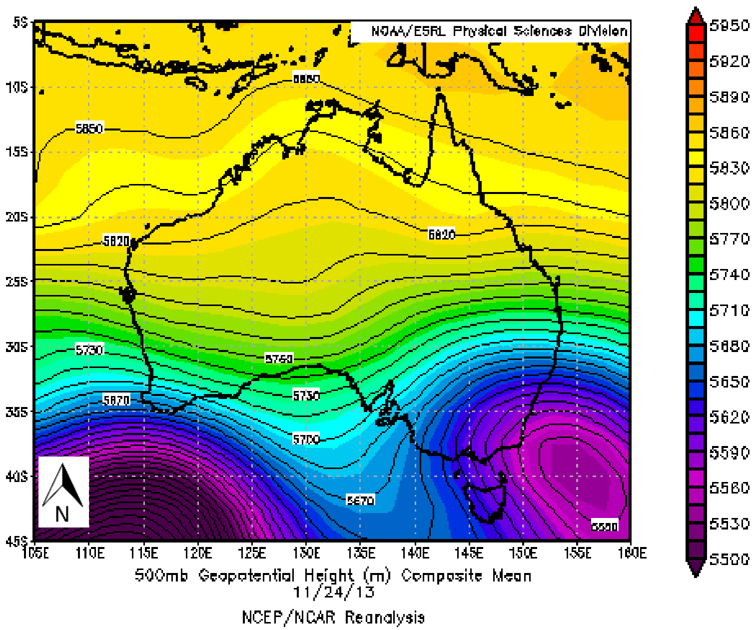
NOAA/ESRL Physical Sciences Division
500mb Geopotential Height (m) Composite Mean
11/24/13
NCEP/NCAR Reanalysis
5500 5530 5560 5590 5620 5650 5680 5710 5740 5770 5800 5830 5860 5890 5920 5950

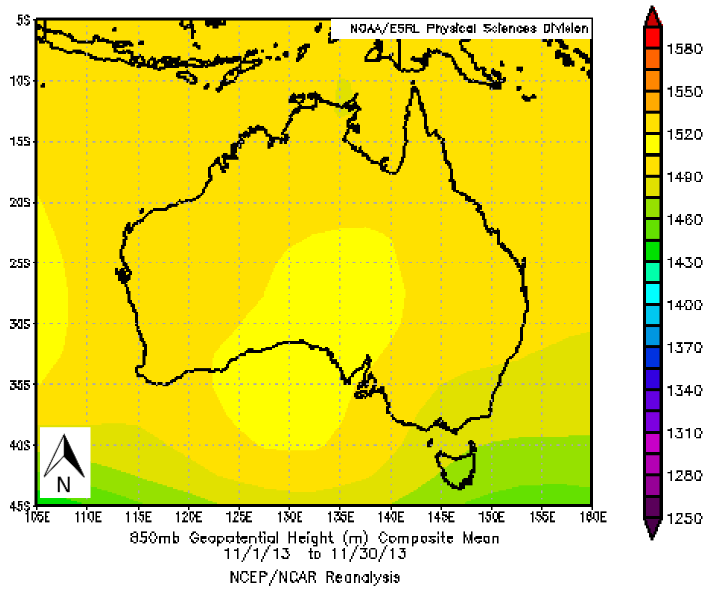
NOAA/ESRL Physical Sciences Division
850mb Geopotential Height (m) Composite Mean
11/1/13 to 11/30/13
NCEP/NCAR Reanalysis
1250 1280 1310 1340 1370 1400 1430 1460 1490 1520 1550 1580

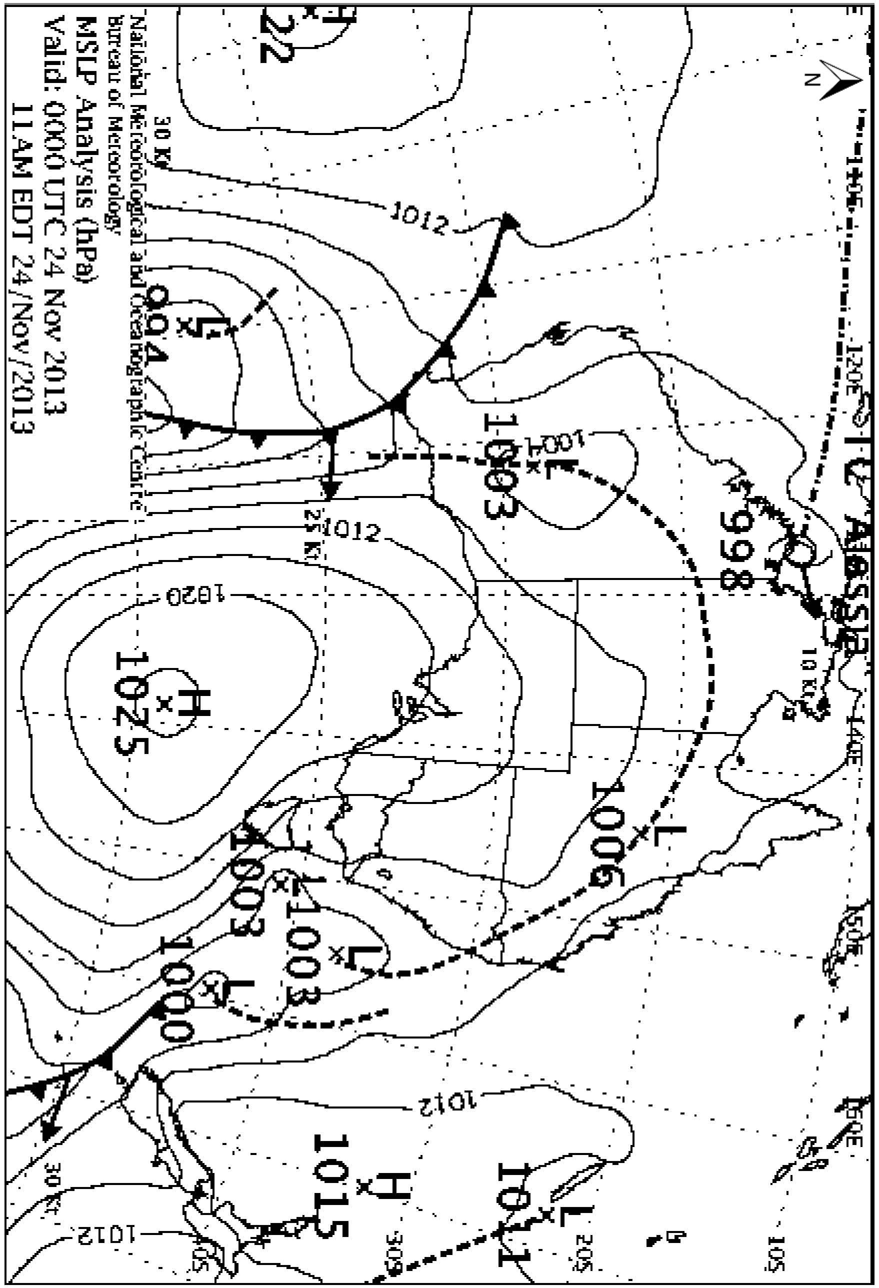
National Meteorological and Oceanographic Centre
Bureau of Meteorology
MSLP Analysis (hPa)
Valid: 0000 UTC 24 Nov 2013
11AM EDT 24/Nov/2013

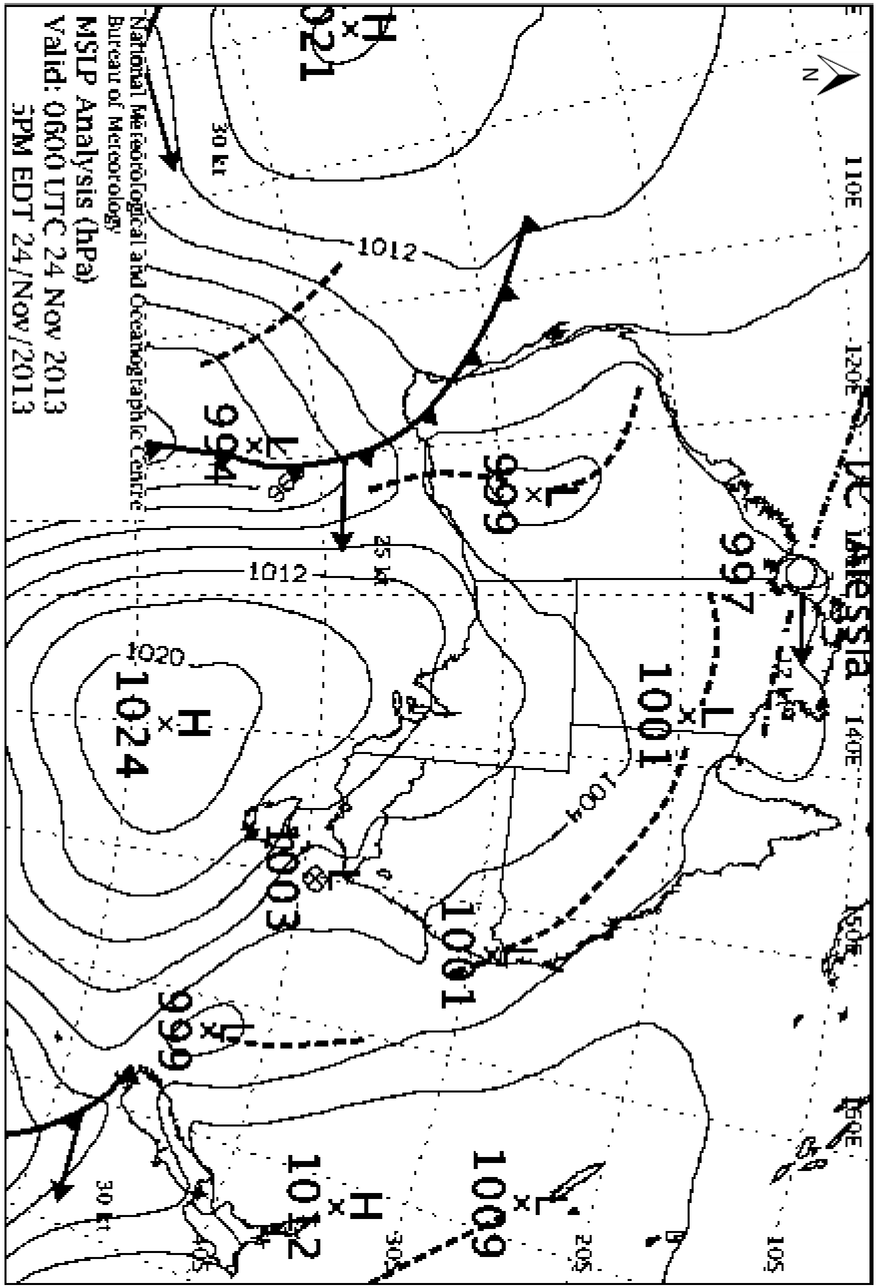
National Meteorological and Oceanographic Centre
Bureau of Meteorology
MSLP Analysis (hPa)
Valid: 0600 UTC 24 Nov 2013
5PM EDT 24/Nov/2013

17/11/2012

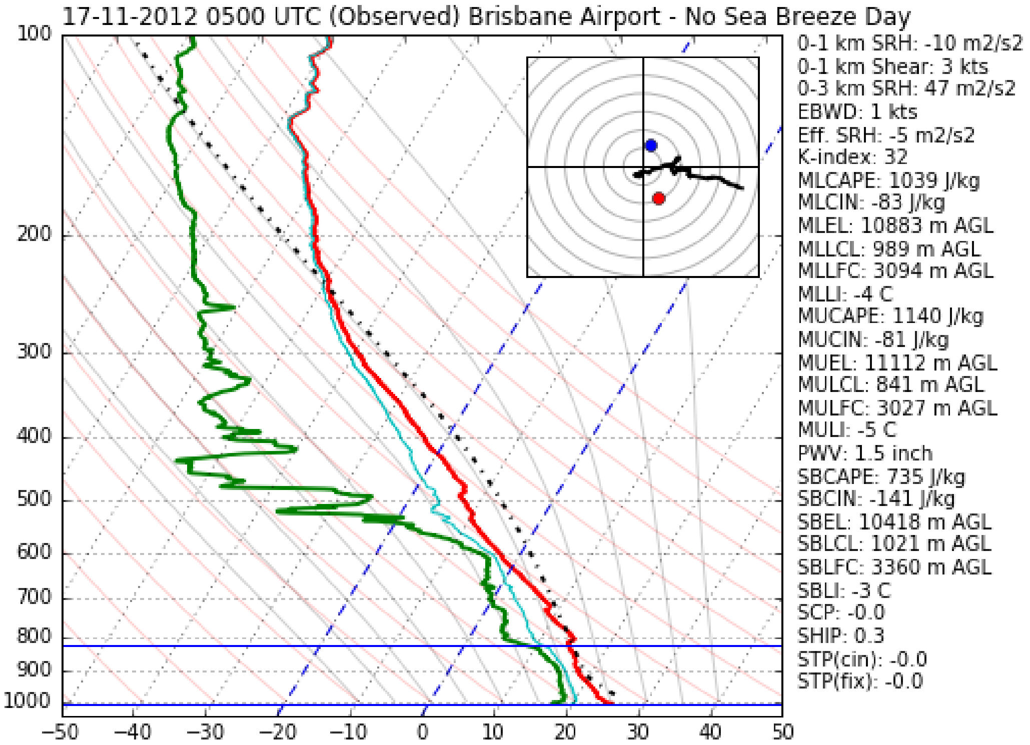
17-11-2012 0500 UTC (Observed) Brisbane Airport - No Sea Breeze Day
0-1 km SRH: -10 m2/s2
0-1 km Shear: 3 kts
0-3 km SRH: 47 m2/s2
EBWD: 1 kts
Eff. SRH: -5 m2/s2
K-index: 32
MLCAPE: 1039 J/kg
MLCIN: -83 J/kg
MLEL: 10883 m AGL
MLLCL: 989 m AGL
MLLFC: 3094 m AGL
MLLI: -4 C
MUCAPE: 1140 J/kg
MUCIN: -81 J/kg
MUEL: 11112 m AGL
MULCL: 841 m AGL
MULFC: 3027 m AGL
MULI: -5 C
PWV: 1.5 inch
SBCAPE: 735 J/kg
SBCIN: -141 J/kg
SBEL: 10418 m AGL
SBLCL: 1021 m AGL
SBLFC: 3360 m AGL
SBLI: -3 C
SCP: -0.0
SHIP: 0.3
STP(cin): -0.0
STP(fix): -0.0

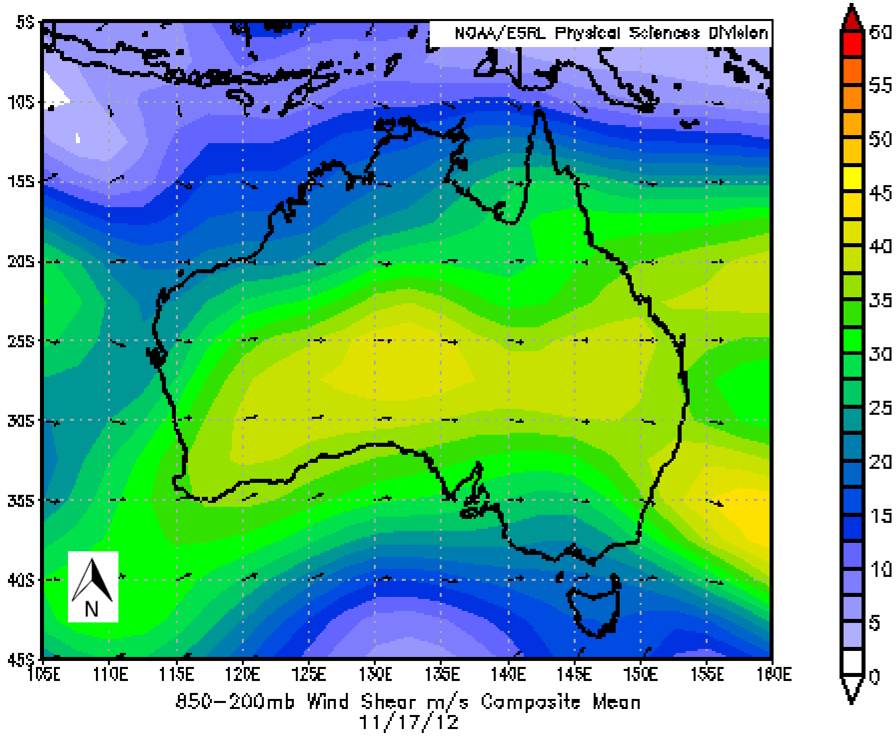
NOAA/ESRL Physical Sciences Division
N
850–200mb Wind Shear m/s Composite Mean
11/17/12

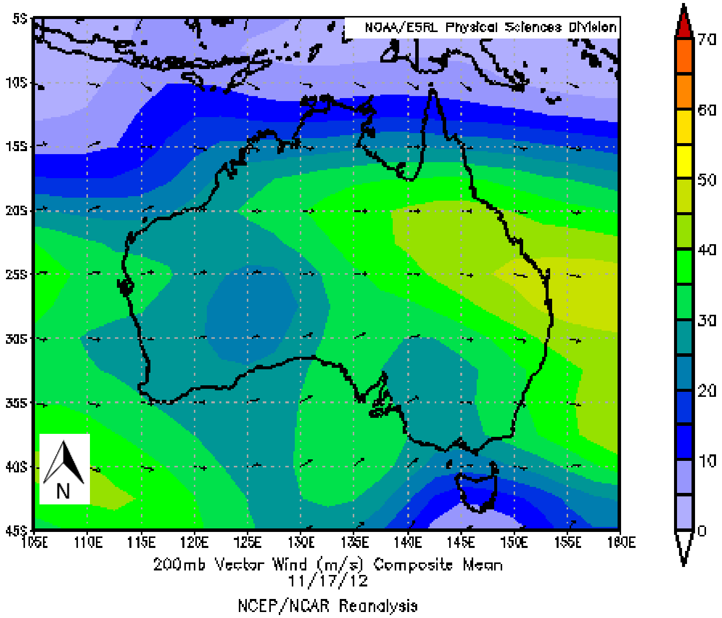
NOAA/ESRL Physical Sciences Division
200mb Vector Wind (m/s) Composite Mean
11/17/12
NCEP/NCAR Reanalysis

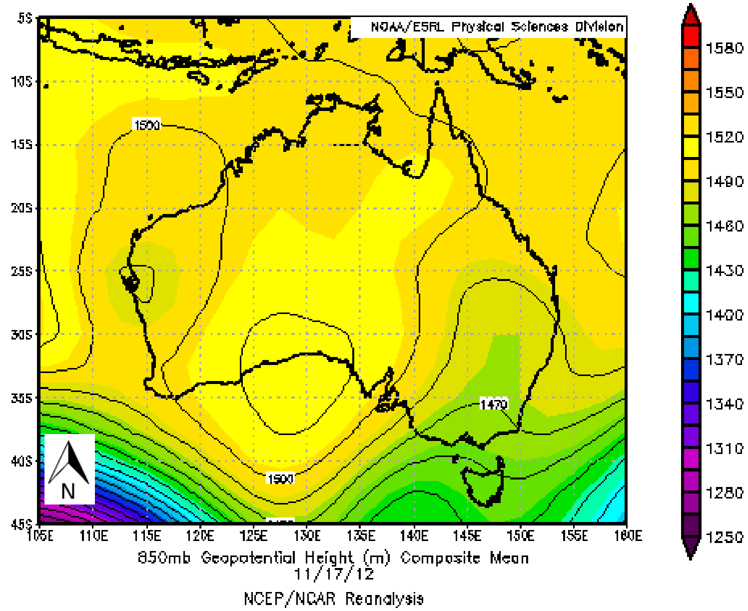
NOAA/ESRL Physical Sciences Division
850mb Geopotential Height (m) Composite Mean
11/17/12
NCEP/NCAR Reanalysis

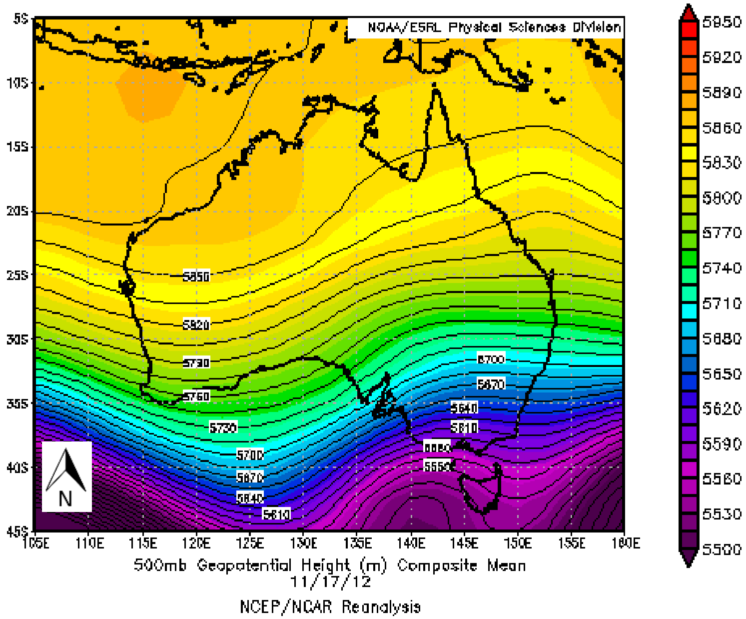
NOAA/ESRL Physical Sciences Division
500mb Geopotential Height (m) Composite Mean
11/17/12
NCEP/NCAR Reanalysis

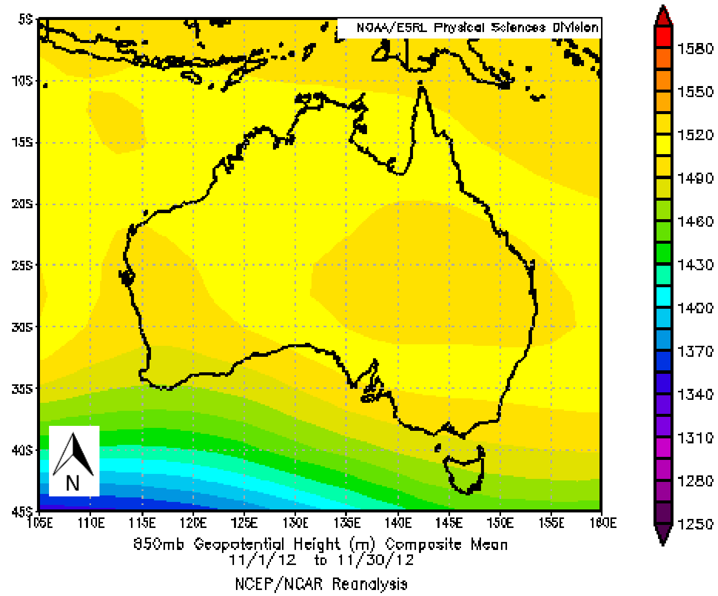
NOAA/ESRL Physical Sciences Division
850mb Geopotential Height (m) Composite Mean
11/1/12 to 11/30/12
NCEP/NCAR Reanalysis

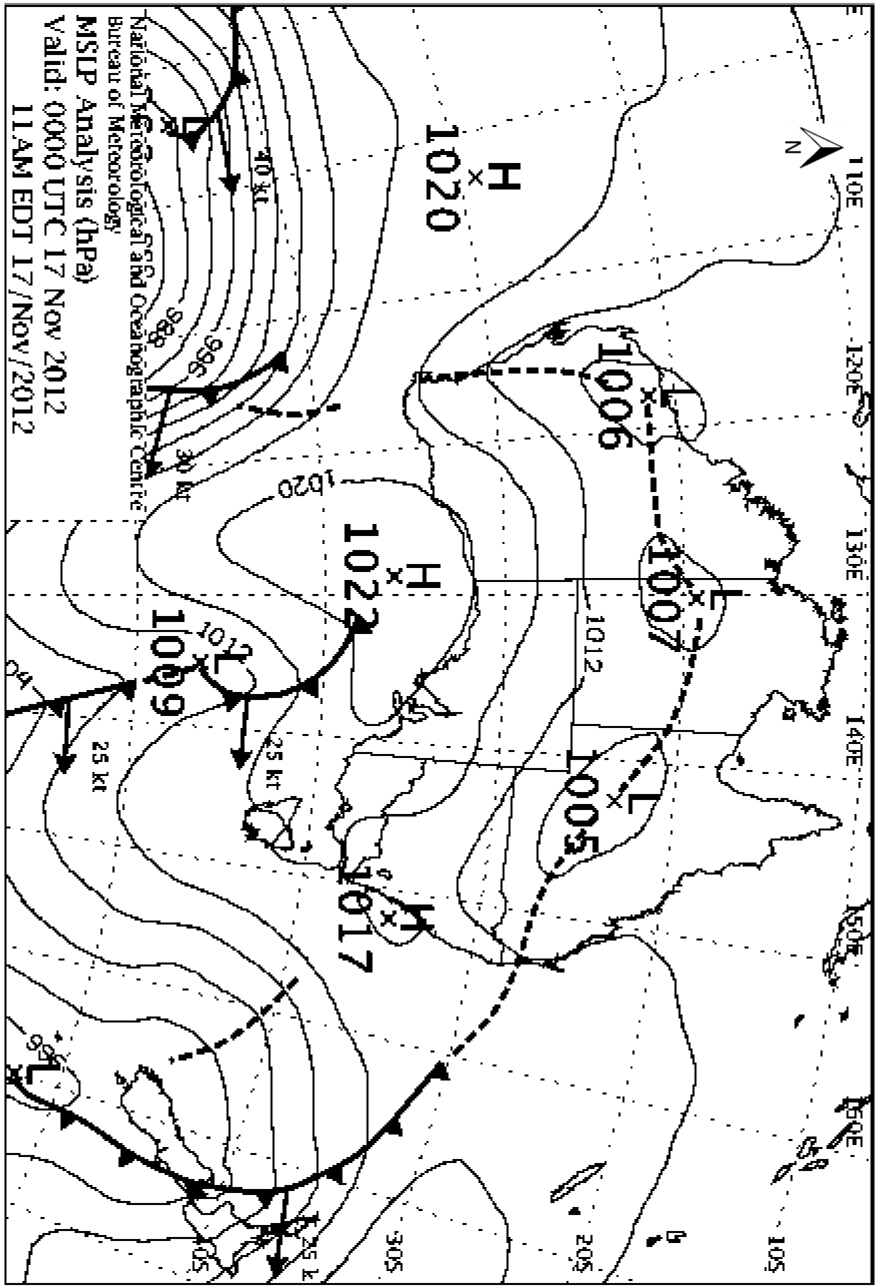
National Meteorological and Oceanographic Centre
Bureau of Meteorology
MSLP Analysis (hPa)
Valid: 0000 UTC 17 Nov 2012
11 AM EDT 17/Nov/2012

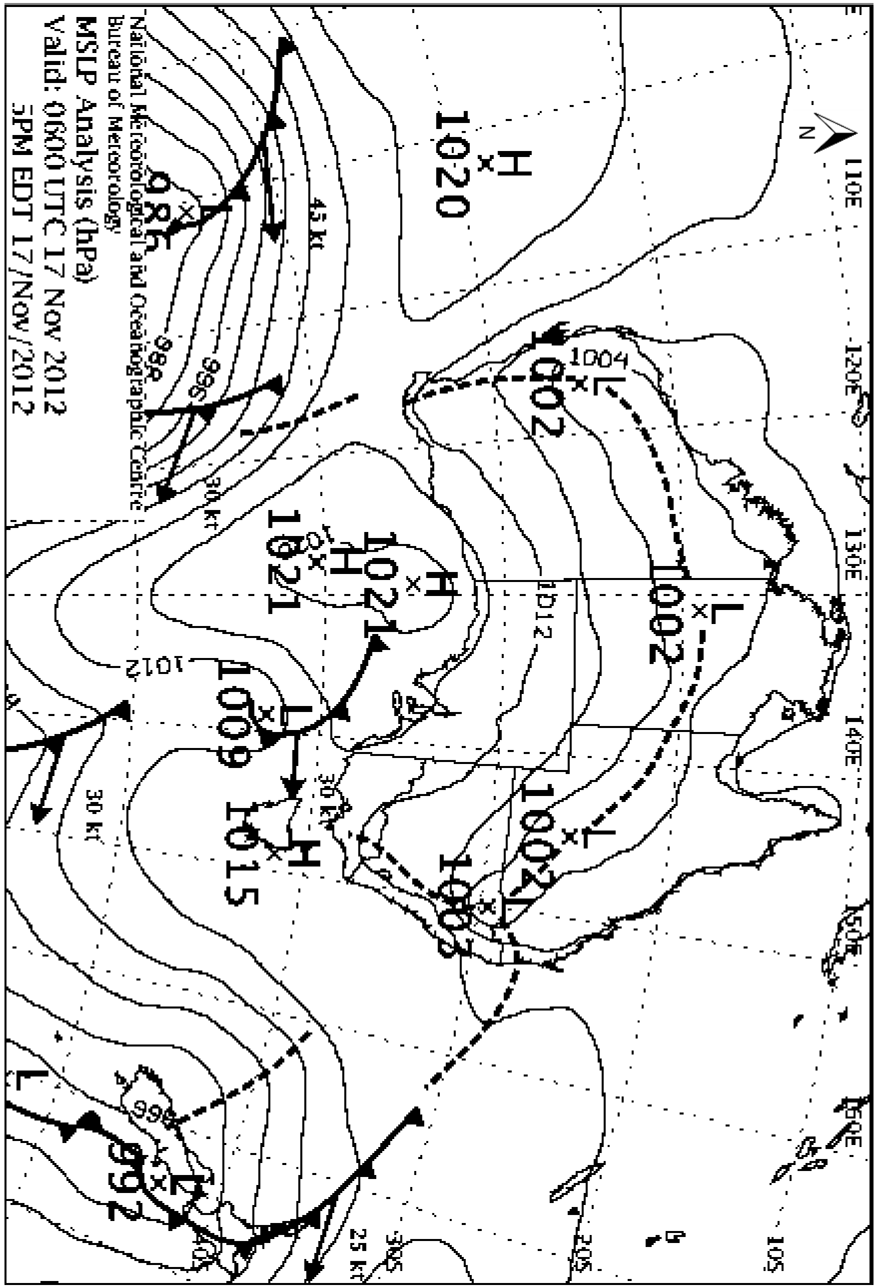
National Meteorological and Oceanographic Centre
Bureau of Meteorology
MSLP Analysis (hPa)
Valid: 0600 UTC 17 Nov 2012
5PM EDT 17/Nov/2012

29/11/2009

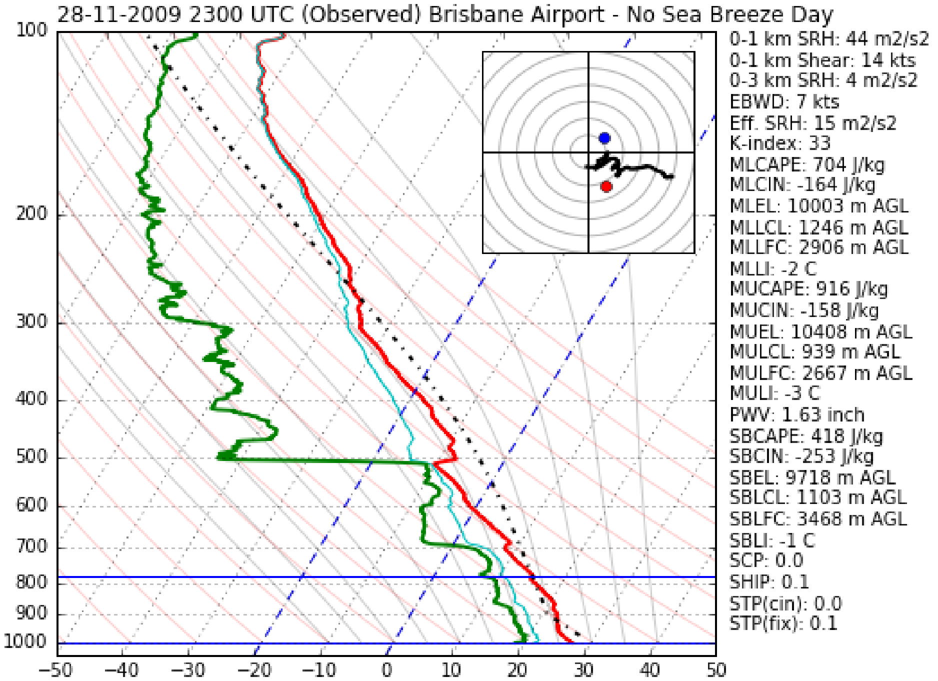
28-11-2009 2300 UTC (Observed) Brisbane Airport - No Sea Breeze Day
0-1 km SRH: 44 m2/s2
0-1 km Shear: 14 kts
0-3 km SRH: 4 m2/s2
EBWD: 7 kts
Eff. SRH: 15 m2/s2
K-index: 33
MLCAPE: 704 J/kg
MLCIN: -164 J/kg
MLEL: 10003 m AGL
MLLCL: 1246 m AGL
MLLFC: 2906 m AGL
MLLI: -2 C
MUCAPE: 916 J/kg
MUCIN: -158 J/kg
MUEL: 10408 m AGL
MULCL: 939 m AGL
MULFC: 2667 m AGL
MULI: -3 C
PWV: 1.63 inch
SBCAPE: 418 J/kg
SBCIN: -253 J/kg
SBEL: 9718 m AGL
SBLCL: 1103 m AGL
SBLFC: 3468 m AGL
SBLI: -1 C
SCP: 0.0
SHIP: 0.1
STP(cin): 0.0
STP(fix): 0.1

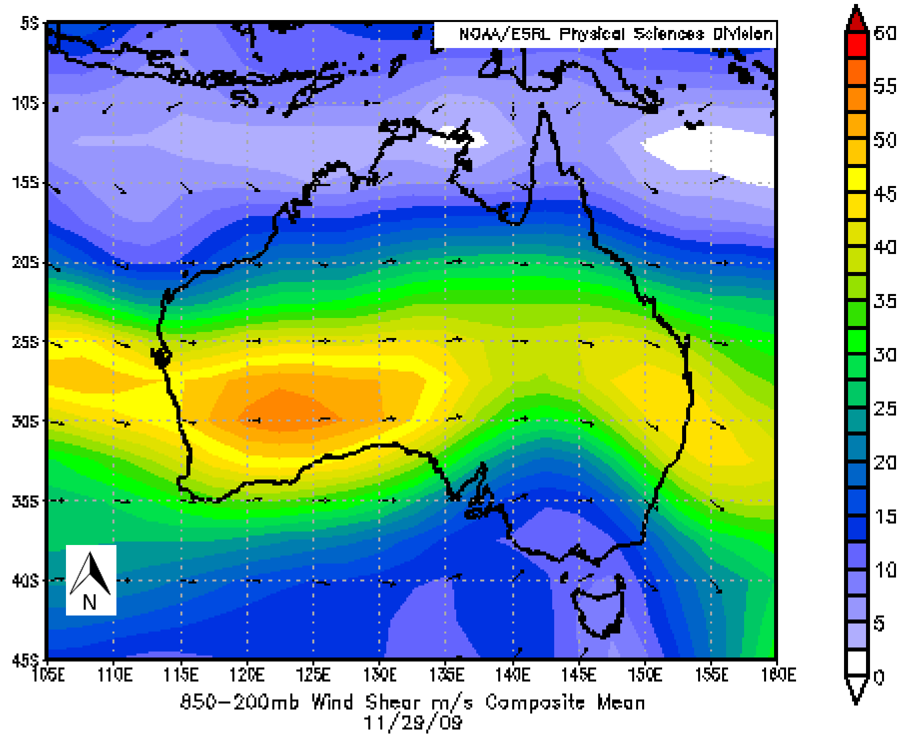
NOAA/ESRL Physical Sciences Division
N
850–200mb Wind Shear m/s Composite Mean
11/29/09

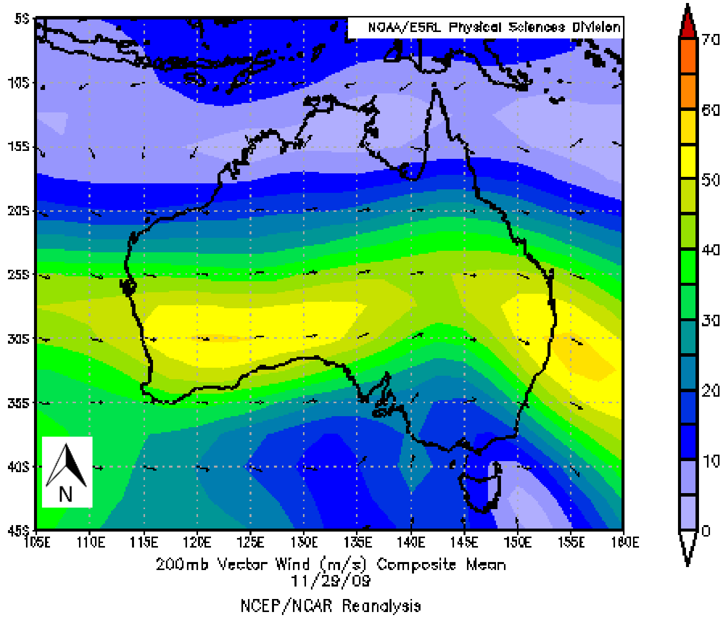
NOAA/ESRL Physical Sciences Division
200mb Vector Wind (m/s) Composite Mean
11/29/09
NCEP/NCAR Reanalysis

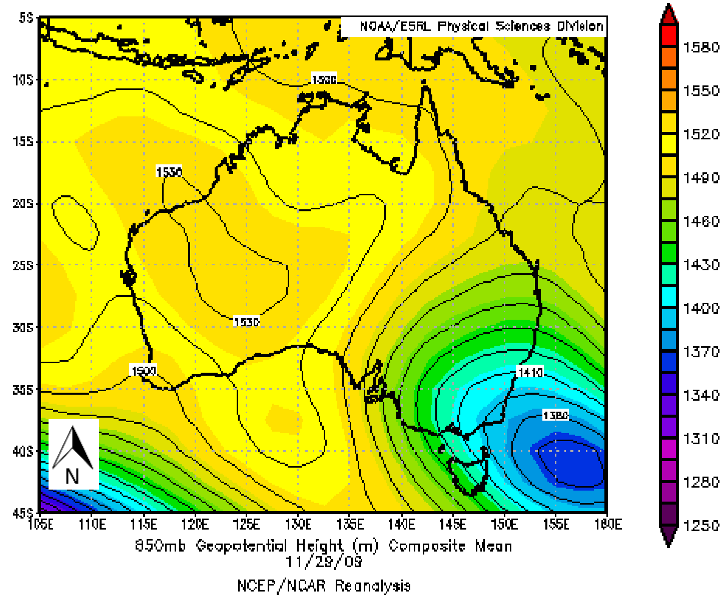
NOAA/ESRL Physical Sciences Division
850mb Geopotential Height (m) Composite Mean
11/29/09
NCEP/NCAR Reanalysis

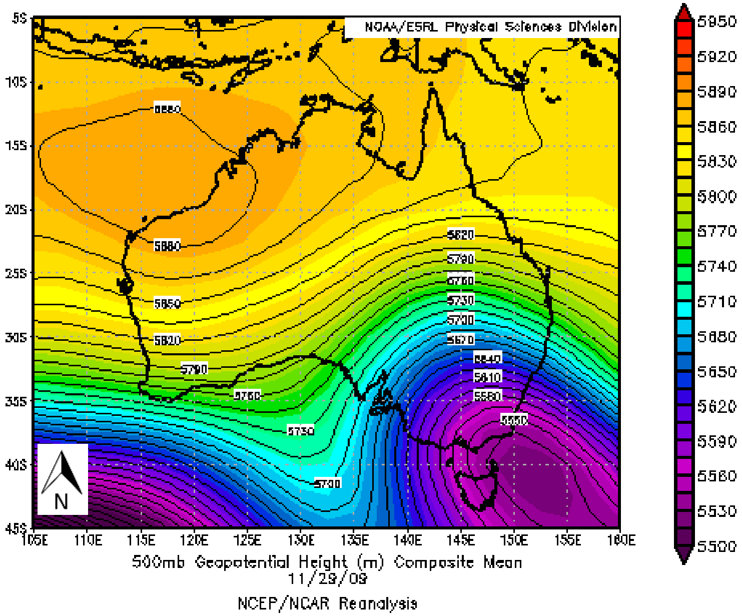
NOAA/ESRL Physical Sciences Division
500mb Geopotential Height (m) Composite Mean
11/29/09
NCEP/NCAR Reanalysis

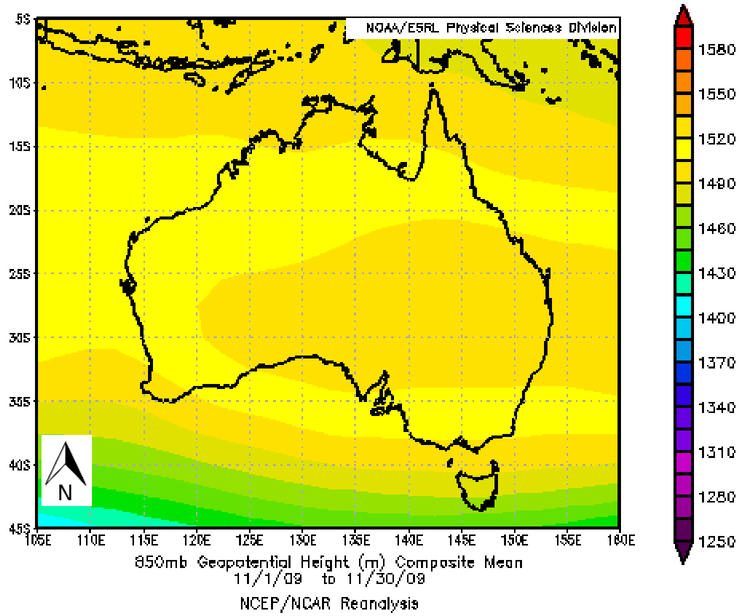
NOAA/ESRL Physical Sciences Division
850mb Geopotential Height (m) Composite Mean
11/1/09 to 11/30/09
NCEP/NCAR Reanalysis

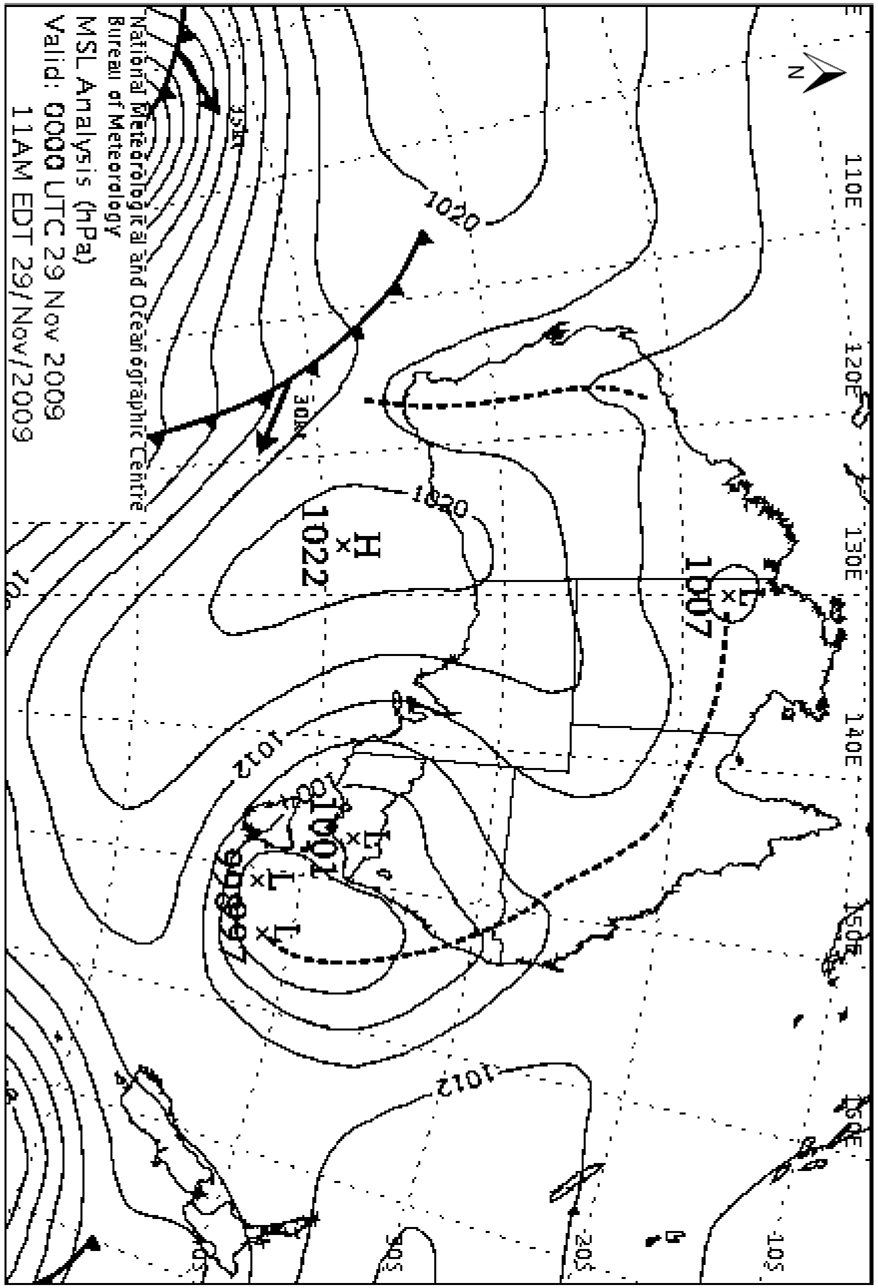
National Meteorological and Oceanographic Centre
Bureau of Meteorology
MSL Analysis (hPa)
Valid: 0000 UTC 29 Nov 2009
11AM EDT 29/Nov/2009
H
1022
L
1007
1020
1012
110E
120E
130E
140E
150E
160E
10S
20S
30S
40S

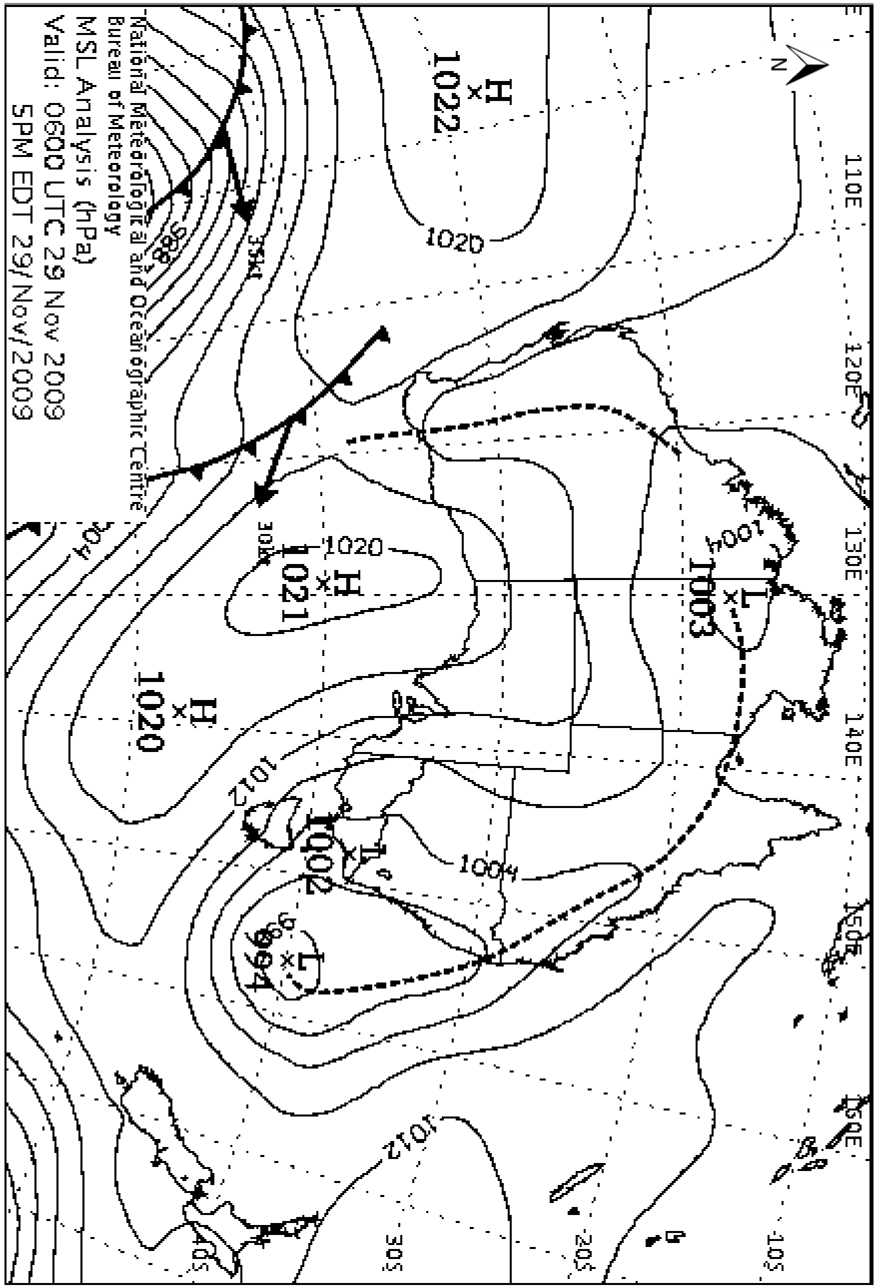
National Meteorological and Oceanographic Centre
Bureau of Meteorology
MSL Analysis (hPa)
Valid: 0600 UTC 29 Nov 2009
5PM EDT 29/Nov/2009
H
1022
H
1021
H
1020
L
1003
L
1002
L
994
1020
1012
1004
110E
120E
130E
140E
150E
160E
10S
20S
30S
40S

17/11/2009

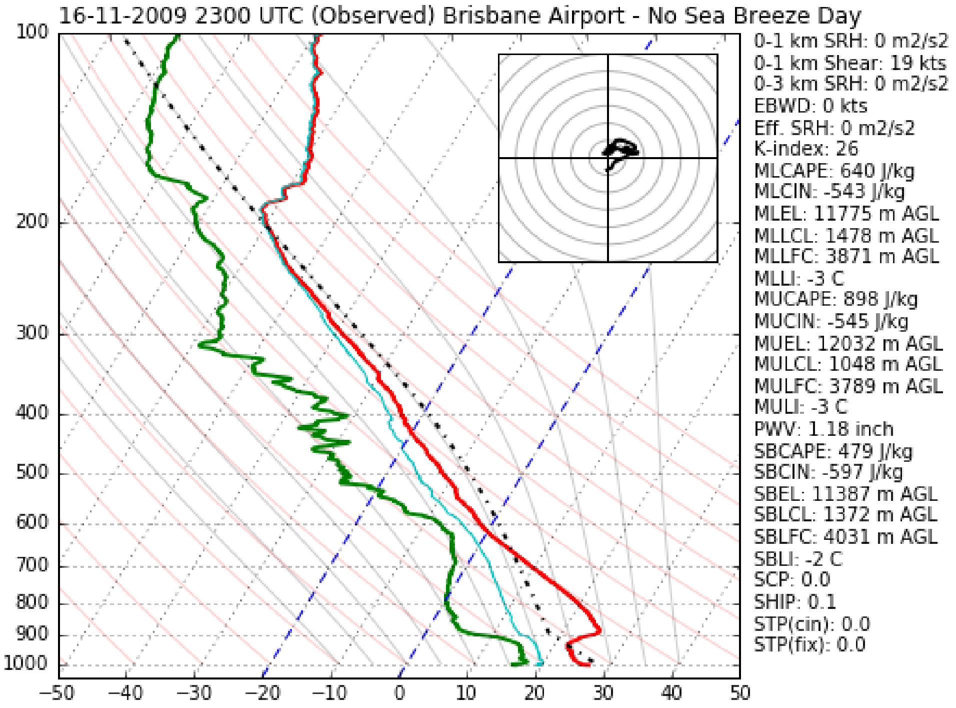
16-11-2009 2300 UTC (Observed) Brisbane Airport - No Sea Breeze Day
0-1 km SRH: 0 m2/s2
0-1 km Shear: 19 kts
0-3 km SRH: 0 m2/s2
EBWD: 0 kts
Eff. SRH: 0 m2/s2
K-index: 26
MLCAPE: 640 J/kg
MLCIN: -543 J/kg
MLEL: 11775 m AGL
MLLCL: 1478 m AGL
MLLFC: 3871 m AGL
MLLI: -3 C
MUCAPE: 898 J/kg
MUCIN: -545 J/kg
MUEL: 12032 m AGL
MULCL: 1048 m AGL
MULFC: 3789 m AGL
MULI: -3 C
PWV: 1.18 inch
SBCAPE: 479 J/kg
SBCIN: -597 J/kg
SBEL: 11387 m AGL
SBLCL: 1372 m AGL
SBLFC: 4031 m AGL
SBLI: -2 C
SCP: 0.0
SHIP: 0.1
STP(cin): 0.0
STP(fix): 0.0

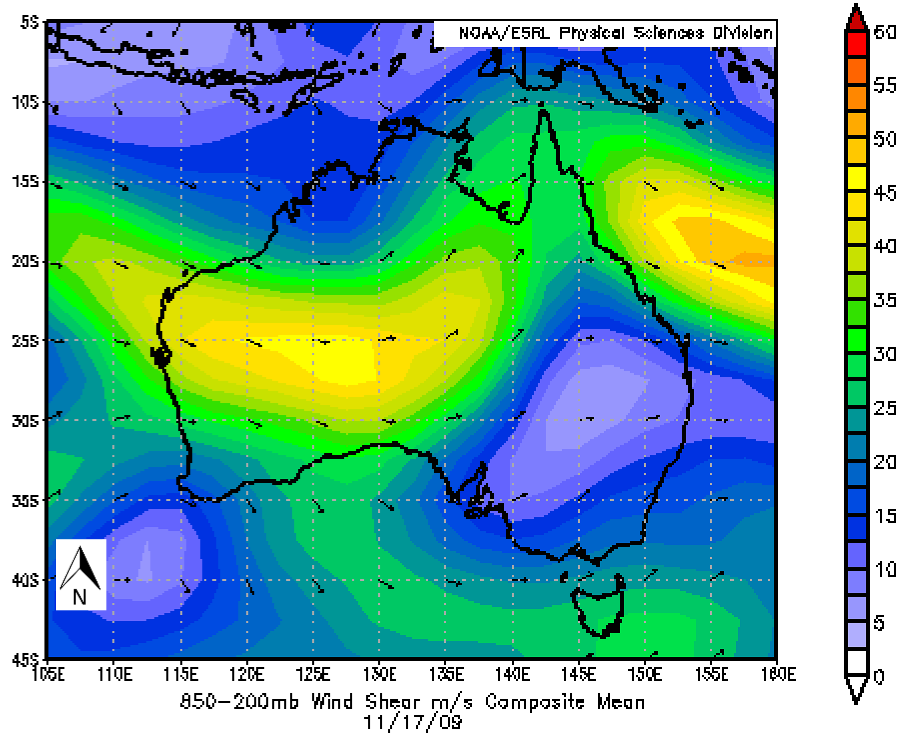
NOAA/ESRL Physical Sciences Division
N
850–200mb Wind Shear m/s Composite Mean
11/17/09

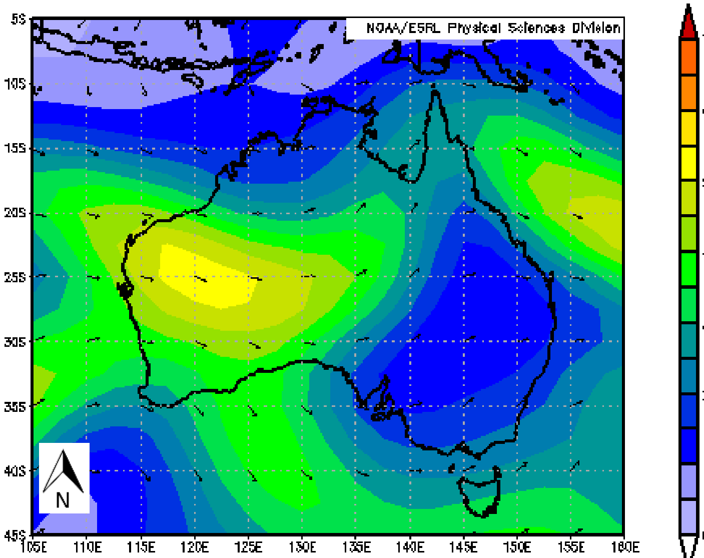

200mb Vector Wind (m/s) Composite Mean
11/17/09
NCEP/NCAR Reanalysis

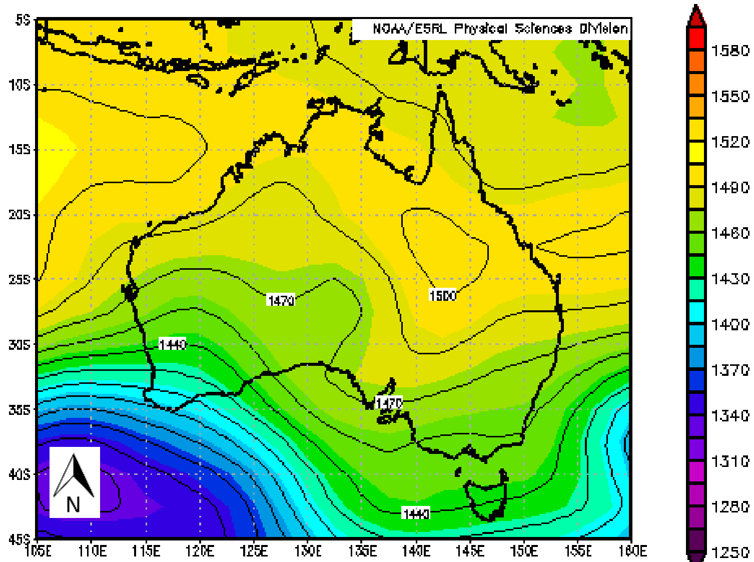

850mb Geopotential Height (m) Composite Mean
11/17/09
NCEP/NCAR Reanalysis

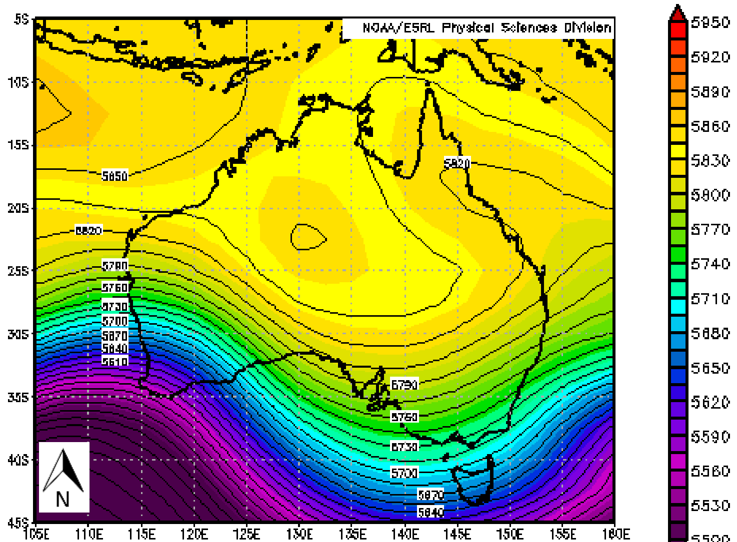

500mb Geopotential Height (m) Composite Mean
11/17/09
NCEP/NCAR Reanalysis

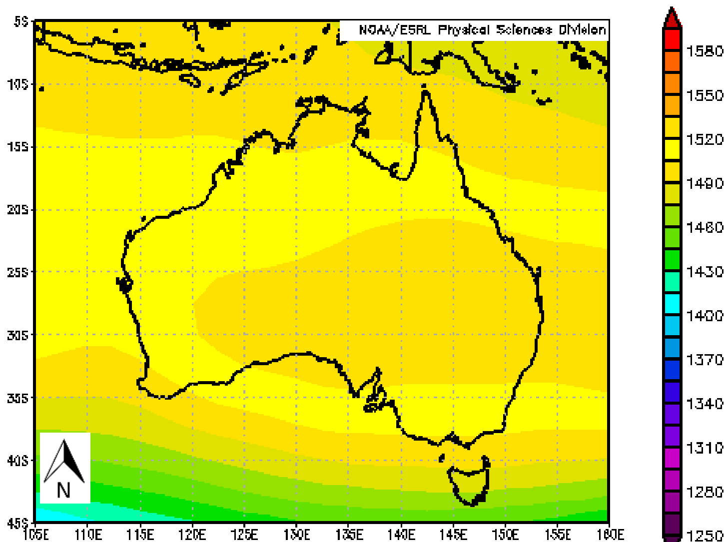

850mb Geopotential Height (m) Composite Mean
11/1/09 to 11/30/09
NCEP/NCAR Reanalysis

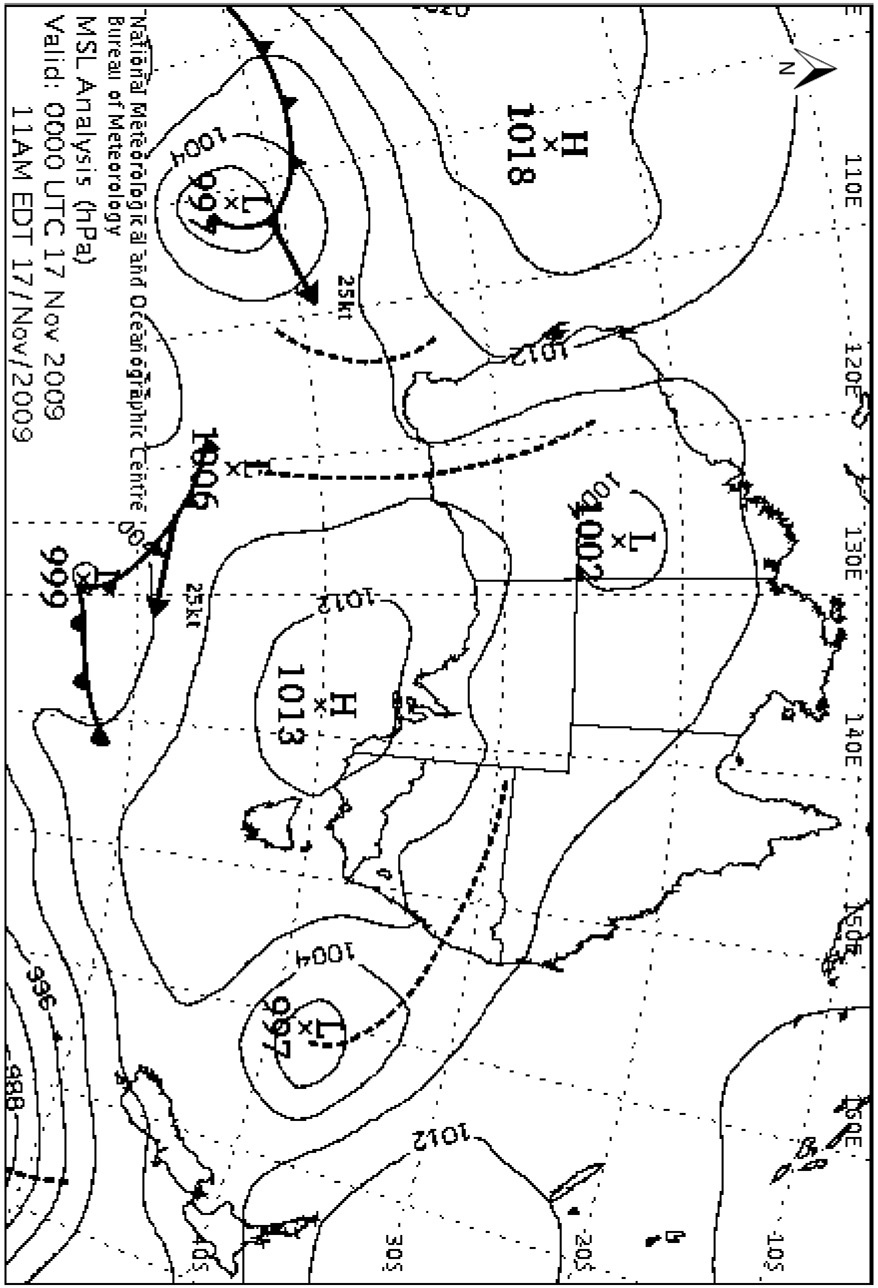
National Meteorological and Oceanographic Centre
Bureau of Meteorology
MSL Analysis (hPa)
Valid: 0000 UTC 17 Nov 2009
11AM EDT 17/Nov/2009

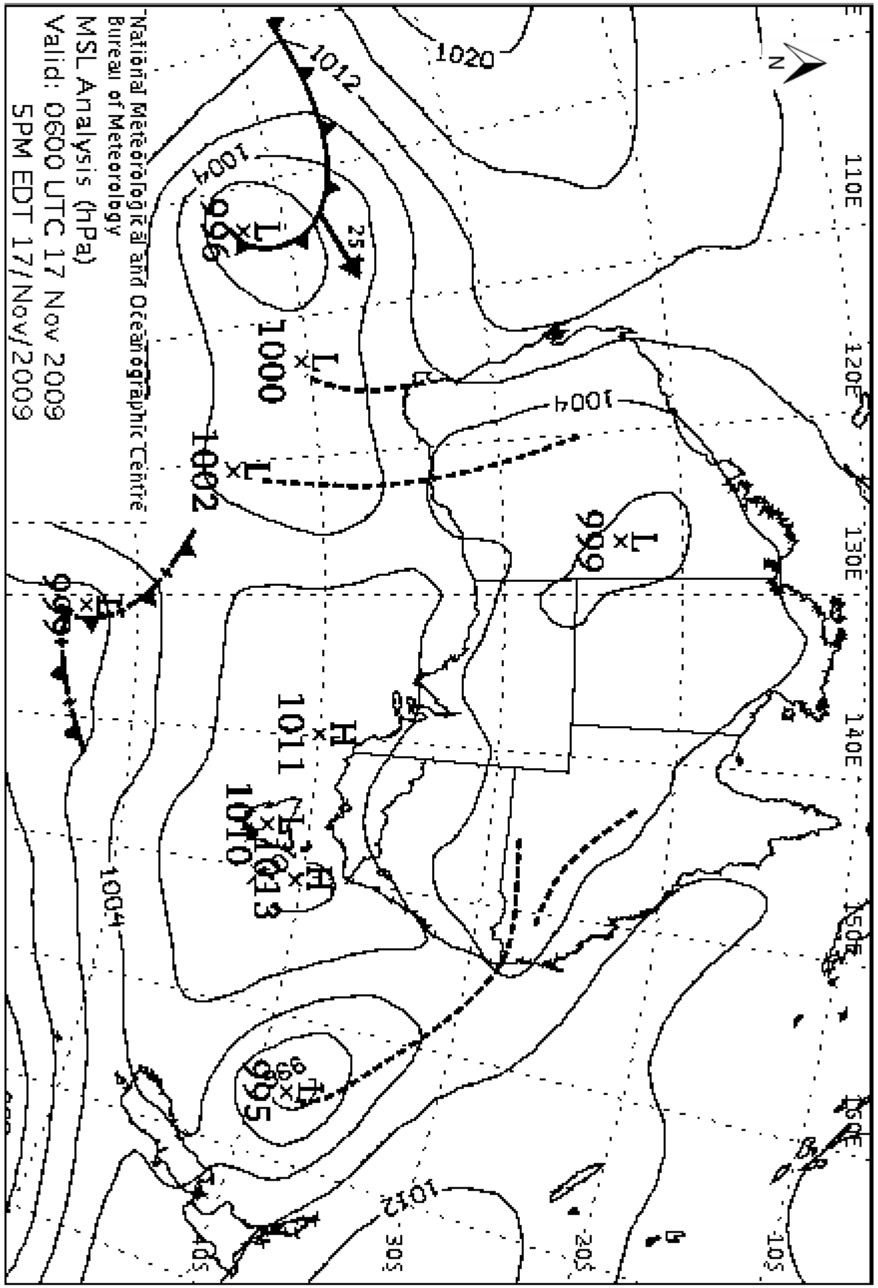
National Meteorological and Oceanographic Centre
Bureau of Meteorology
MSL Analysis (hPa)
Valid: 0600 UTC 17 Nov 2009
5PM EDT 17/Nov/2009

9/11/2004

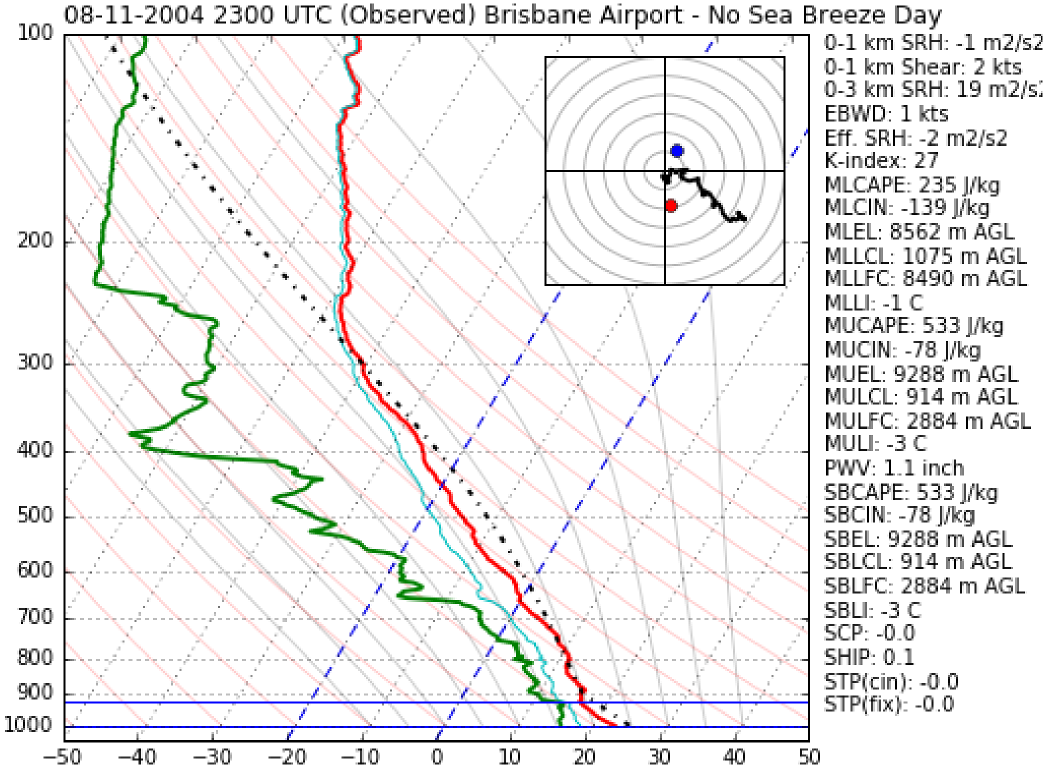
08-11-2004 2300 UTC (Observed) Brisbane Airport - No Sea Breeze Day
0-1 km SRH: -1 m2/s2
0-1 km Shear: 2 kts
0-3 km SRH: 19 m2/s2
EBWD: 1 kts
Eff. SRH: -2 m2/s2
K-index: 27
MLCAPE: 235 J/kg
MLCIN: -139 J/kg
MLEL: 8562 m AGL
MLLCL: 1075 m AGL
MLLFC: 8490 m AGL
MLLI: -1 C
MUCAPE: 533 J/kg
MUCIN: -78 J/kg
MUEL: 9288 m AGL
MULCL: 914 m AGL
MULFC: 2884 m AGL
MULI: -3 C
PWV: 1.1 inch
SBCAPE: 533 J/kg
SBCIN: -78 J/kg
SBEL: 9288 m AGL
SBLCL: 914 m AGL
SBLFC: 2884 m AGL
SBLI: -3 C
SCP: -0.0
SHIP: 0.1
STP(cin): -0.0
STP(fix): -0.0
100
200
300
400
500
600
700
800
900
1000
−50
−40
−30
−20
−10
0
10
20
30
40
50

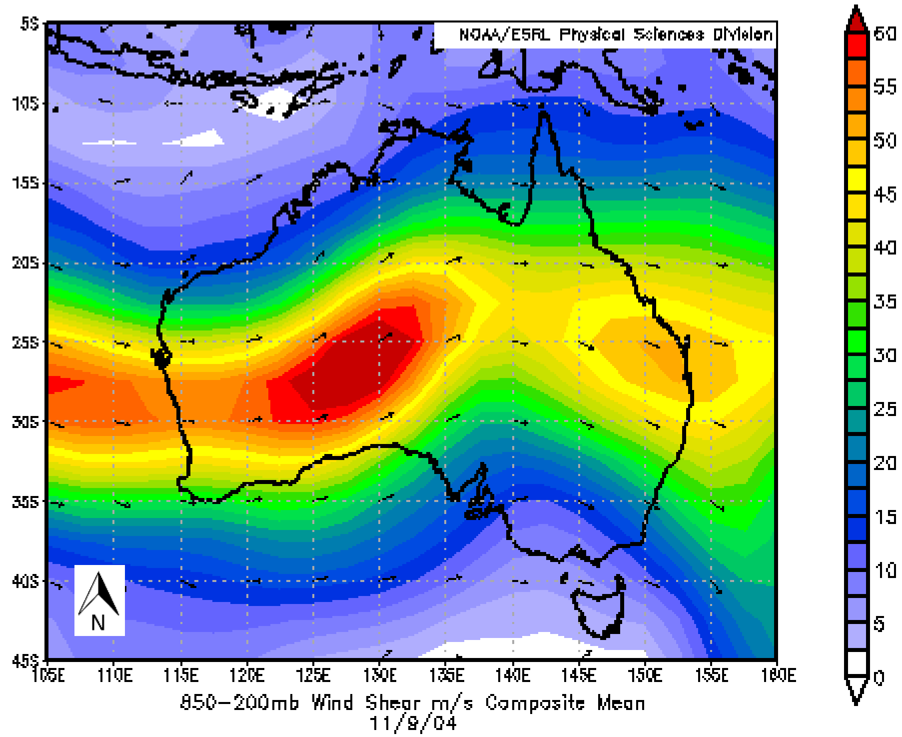
NOAA/ESRL Physical Sciences Division
5S
10S
15S
20S
25S
30S
35S
40S
45S
105E
110E
115E
120E
125E
130E
135E
140E
145E
150E
155E
160E
N
60
55
50
45
40
35
30
25
20
15
10
5
0
850–200mb Wind Shear m/s Composite Mean
11/9/04

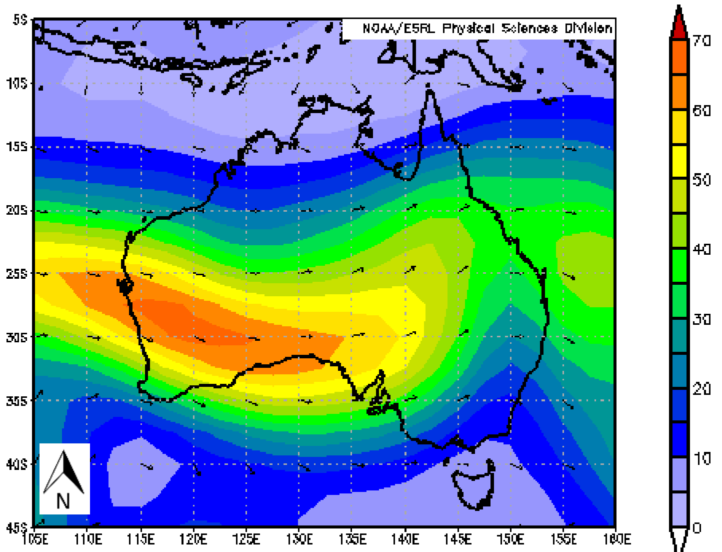

200mb Vector Wind (m/s) Composite Mean
11/9/04
NCEP/NCAR Reanalysis

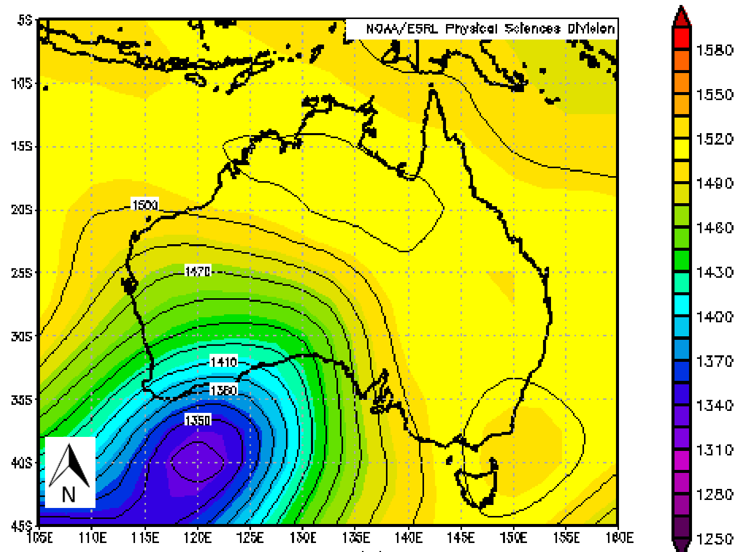

850mb Geopotential Height (m) Composite Mean
11/9/04
NCEP/NCAR Reanalysis

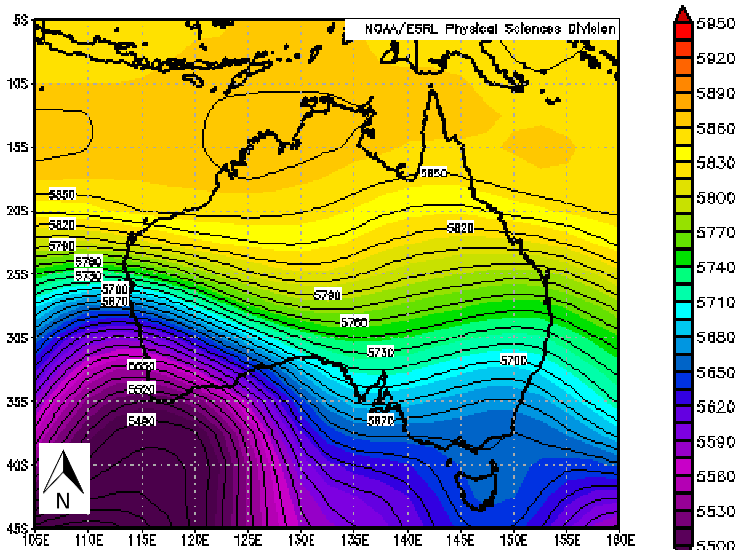

500mb Geopotential Height (m) Composite Mean
11/9/04
NCEP/NCAR Reanalysis

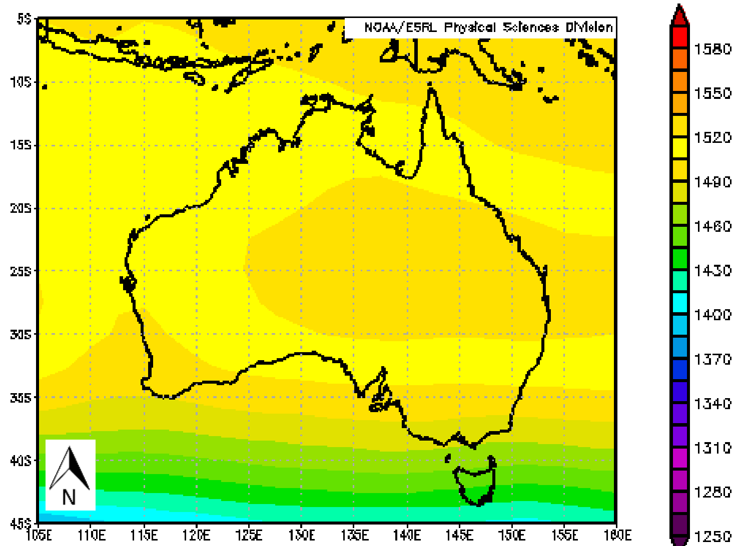

850mb Geopotential Height (m) Composite Mean
11/1/04 to 11/30/04
NCEP/NCAR Reanalysis

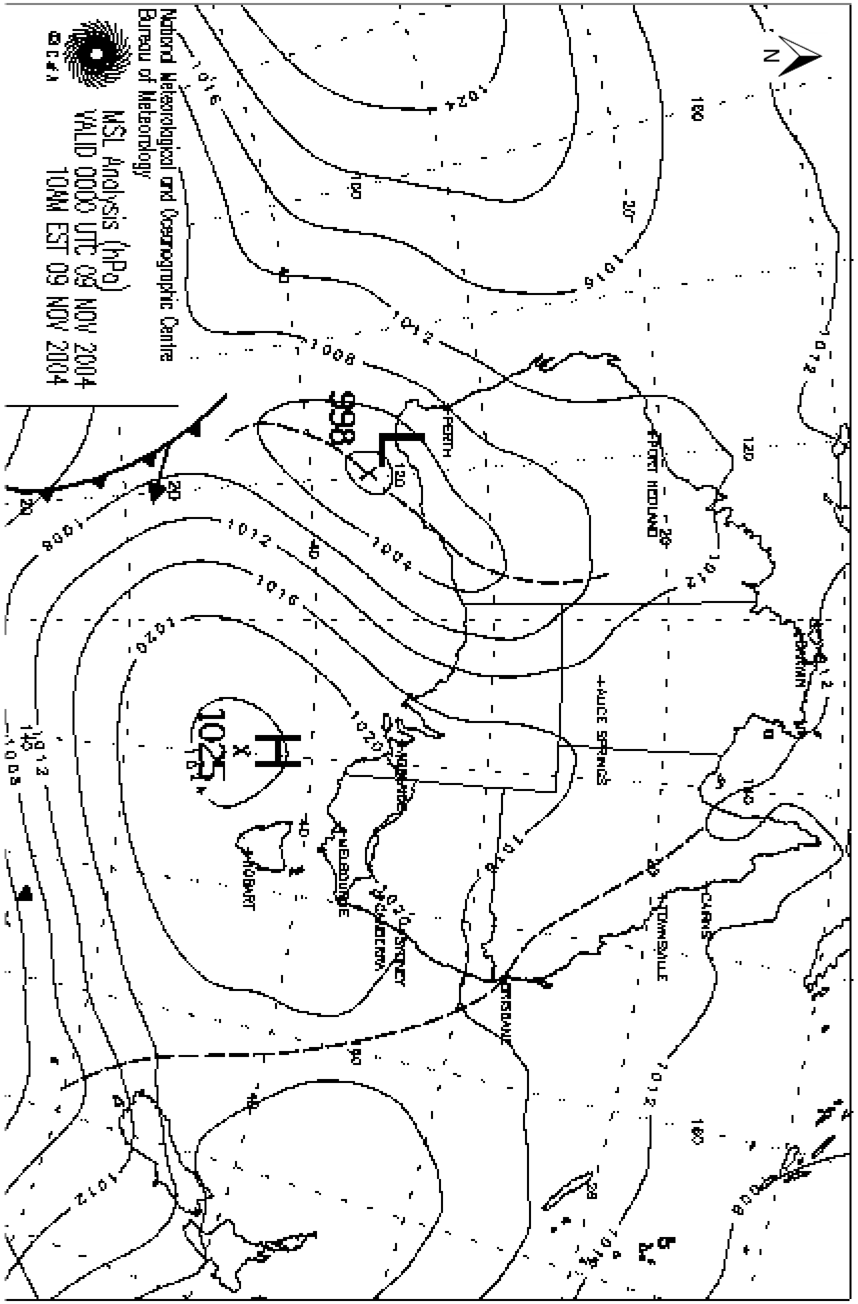
National Meteorological and Oceanographic Centre
Bureau of Meteorology
MSL Analysis (hPa)
VALID 0000 UTC 09 NOV 2004
10AM EST 09 NOV 2004
H
1025
L
998
PERTH
PORT HEDLAND
ALICE SPRINGS
DARWIN
ADELAIDE
MELBOURNE
HOBART
CANBERRA
SYDNEY
BRISBANE
TOWNSVILLE
CAIRNS

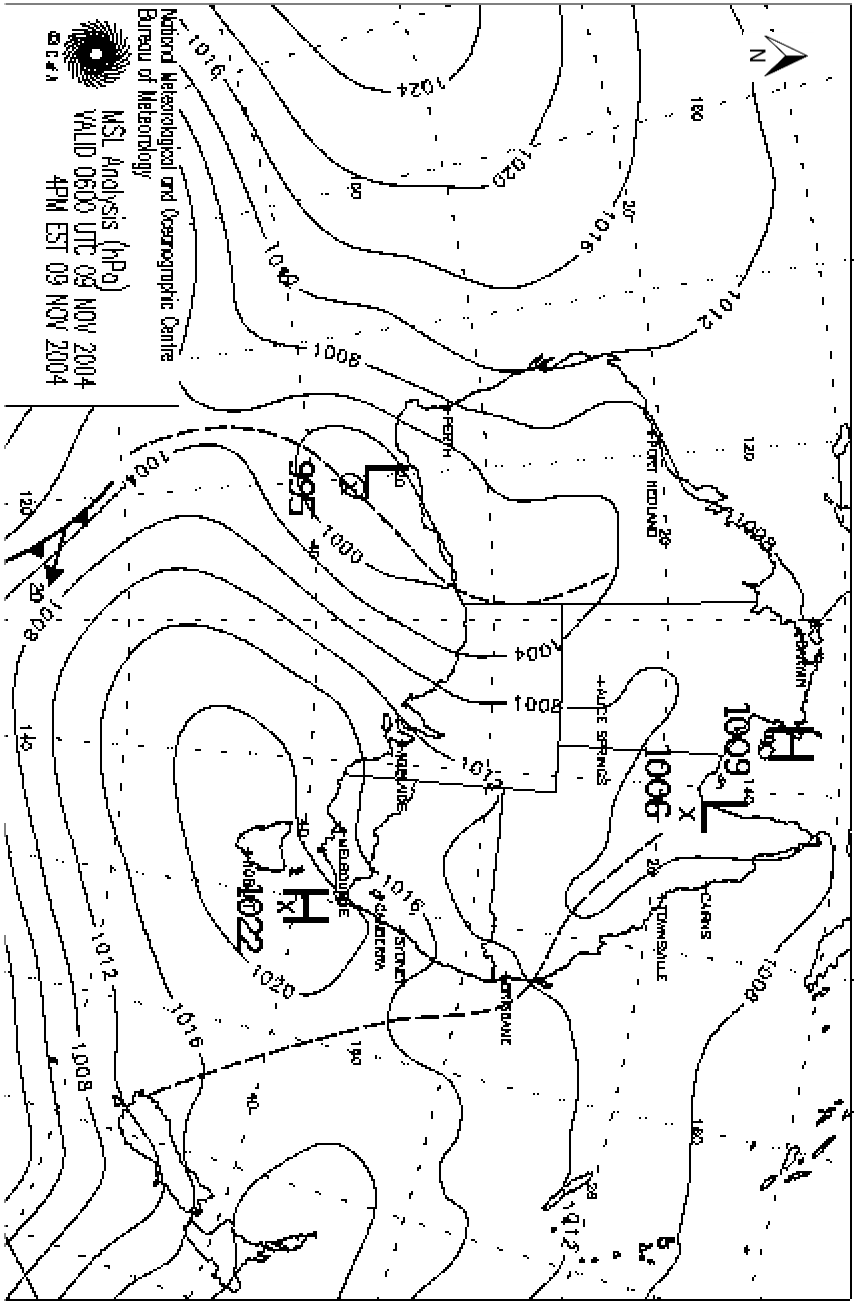
National Meteorological and Oceanographic Centre
Bureau of Meteorology
MSL Analysis (hPa)
VALID 0600 UTC 09 NOV 2004
4PM EST 09 NOV 2004
H
1022
L
995
H
1009
L
1006
PERTH
PORT HEDLAND
ALICE SPRINGS
DARWIN
ADELAIDE
MELBOURNE
HOBART
CANBERRA
SYDNEY
BRISBANE
TOWNSVILLE
CAIRNS

Appendix 5: December

Sea breeze storms

Table 20: Atmospheric conditions for severe storms on non-sea breeze days for December

Date	Time (UTC)	Most-Unstable CAPE	Most-Unstable CIN	Most-Unstable LCL	Most-Unstable LFC	Most-Unstable EL	Most-Unstable LI	0-3 km Pressure-Weighted Mean Wind (kt)	0-6 km Shear (kt)	0-3 km Storm Relative Helicity [m2/s2]	Effective Inflow Layer Bottom Height (m AGL)	Effective Inflow Layer Top Height (m AGL)	Effective Inflow Layer SRH (m2/s2)	Effective Bulk Wind Difference
14/12/2010	2300	165.13	-114.14	1069.31	4842.80	8824.80	-0.58	5.69	15.73	12.95	74.00	86.00	0.40	0.10
28/12/2013	2300	1076.76	-294.47	794.29	3510.89	10215.60	-4.44	4.89	18.33		-16.00	-16.00		
29/12/2013	500	2502.59	-402.94	781.31	12801.00	12982.67	-8.92	3.41	19.88		-24.00	-24.00		
8/12/2014	2300	1015.63	-74.30	664.20	2679.33	11024.00	-3.56	5.41	8.43	52.00		426.00	20.76	5.47
9/12/2014	300	1711.93	-76.42	936.43	2268.41	11164.00	-5.15	3.90	19.19	67.09		2090.00	65.57	14.26
	average	1294.41	-192.45	849.11	5220.49	10842.21	-4.53	4.66	16.31	44.01	11.33	512.40	28.91	6.61

Non-sea breeze storms

Table 21: Atmospheric conditions for severe storms on sea breeze days for December

Date	Time (UTC)	Most-Unstable CAPE	Most-Unstable CIN	Most-Unstable LCL	Most-Unstable LFC	Most-Unstable EL	Most-Unstable LI	0-3 km Pressure-Weighted Mean Wind (kt)	0-6 km Shear (kt)	0-3 km Storm Relative Helicity [m2/s2]	Effective Inflow Layer Bottom Height (m AGL)	Effective Inflow Layer Top Height (m AGL)	Effective Inflow Layer SRH (m2/s2)	Effective Bulk Wind Difference
12/12/2004	2300	416.03	-206.59	690.24	6534.86	9403.00	-1.62	5.26	18.25	32.34		287.00	5.48	1.27
21/12/2009	2300	1172.80	-0.02	1044.78	1062.00	12526.66	-4.45	1.62	10.74	26.62		1108.00	8.22	2.45
15/12/2010	2300	1641.85	-53.03	1289.78	1845.00	12314.00	-5.68	6.33	17.87	24.41	11.00	1959.00	13.59	8.75
	average	1076.90	-86.55	1008.27	3147.29	11414.55	-3.92	4.40	15.62	27.79	11.00	1118.00	9.10	4.15

Non-storm days

Table 22: Atmospheric conditions for non-storm days for December

Date	Time (UTC)	Most-Unstable CAPE	Most-Unstable CIN	Most-Unstable LCL	Most-Unstable LFC	Most-Unstable EL	Most-Unstable LI	0-3 km Pressure-Weighted Mean Wind (kt)	0-6 km Shear (kt)	0-3 km Storm Relative Helicity [m2/s2]	Effective Inflow Layer Bottom Height (m AGL)	Effective Inflow Layer Top Height (m AGL)	Effective Inflow Layer SRH (m2/s2)	Effective Bulk Wind Difference
	average	399.384	-159.966	1275.531	3692.81	6460.874	0.707963	5.274343	13.32114	20.84336	2.549254	260.4934	4.244959	3.929325

9/12/2004

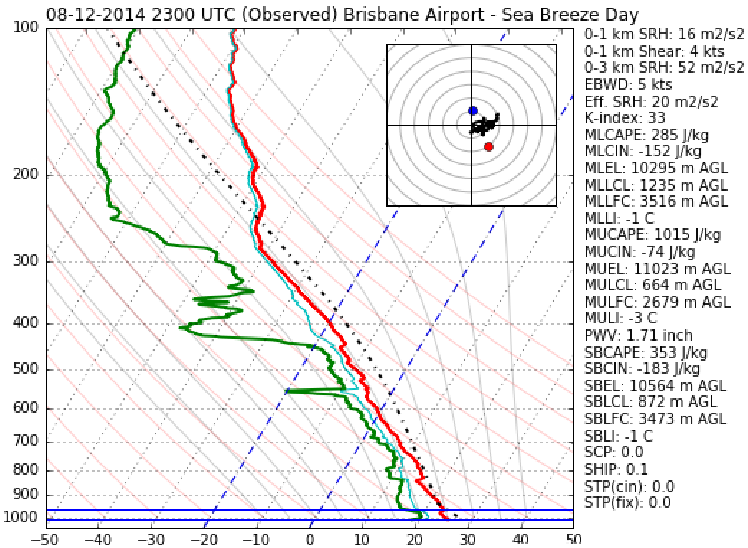
08-12-2014 2300 UTC (Observed) Brisbane Airport - Sea Breeze Day
0-1 km SRH: 16 m2/s2
0-1 km Shear: 4 kts
0-3 km SRH: 52 m2/s2
EBWD: 5 kts
Eff. SRH: 20 m2/s2
K-index: 33
MLCAPE: 285 J/kg
MLCIN: -152 J/kg
MLEL: 10295 m AGL
MLLCL: 1235 m AGL
MLLFC: 3516 m AGL
MLLI: -1 C
MUCAPE: 1015 J/kg
MUCIN: -74 J/kg
MUEL: 11023 m AGL
MULCL: 664 m AGL
MULFC: 2679 m AGL
MULI: -3 C
PWV: 1.71 inch
SBCAPE: 353 J/kg
SBCIN: -183 J/kg
SBEL: 10564 m AGL
SBLCL: 872 m AGL
SBLFC: 3473 m AGL
SBLI: -1 C
SCP: 0.0
SHIP: 0.1
STP(cin): 0.0
STP(fix): 0.0

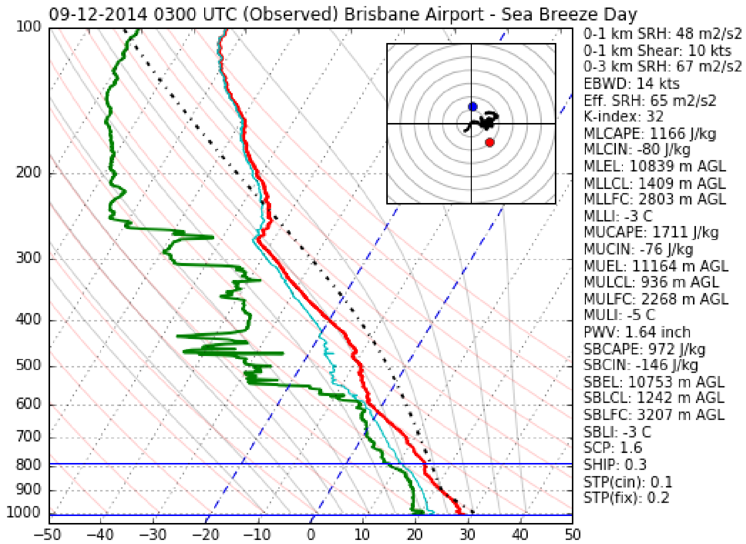
09-12-2014 0300 UTC (Observed) Brisbane Airport - Sea Breeze Day
0-1 km SRH: 48 m2/s2
0-1 km Shear: 10 kts
0-3 km SRH: 67 m2/s2
EBWD: 14 kts
Eff. SRH: 65 m2/s2
K-index: 32
MLCAPE: 1166 J/kg
MLCIN: -80 J/kg
MLEL: 10839 m AGL
MLLCL: 1409 m AGL
MLLFC: 2803 m AGL
MLLI: -3 C
MUCAPE: 1711 J/kg
MUCIN: -76 J/kg
MUEL: 11164 m AGL
MULCL: 936 m AGL
MULFC: 2268 m AGL
MULI: -5 C
PWV: 1.64 inch
SBCAPE: 972 J/kg
SBCIN: -146 J/kg
SBEL: 10753 m AGL
SBLCL: 1242 m AGL
SBLFC: 3207 m AGL
SBLI: -3 C
SCP: 1.6
SHIP: 0.3
STP(cin): 0.1
STP(fix): 0.2

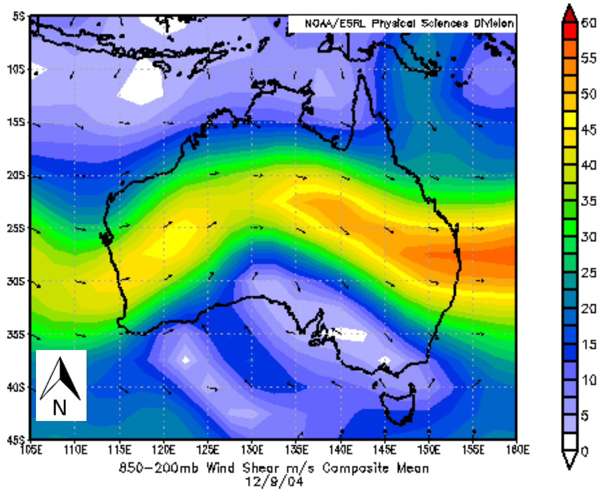
NOAA/ESRL Physical Sciences Division
N
850–200mb Wind Shear m/s Composite Mean
12/9/04

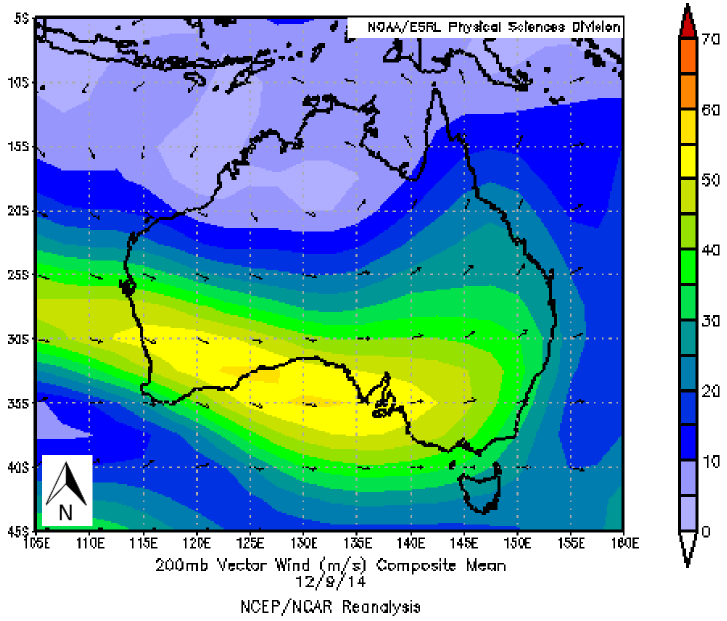
NOAA/ESRL Physical Sciences Division
200mb Vector Wind (m/s) Composite Mean
12/9/14
NCEP/NCAR Reanalysis

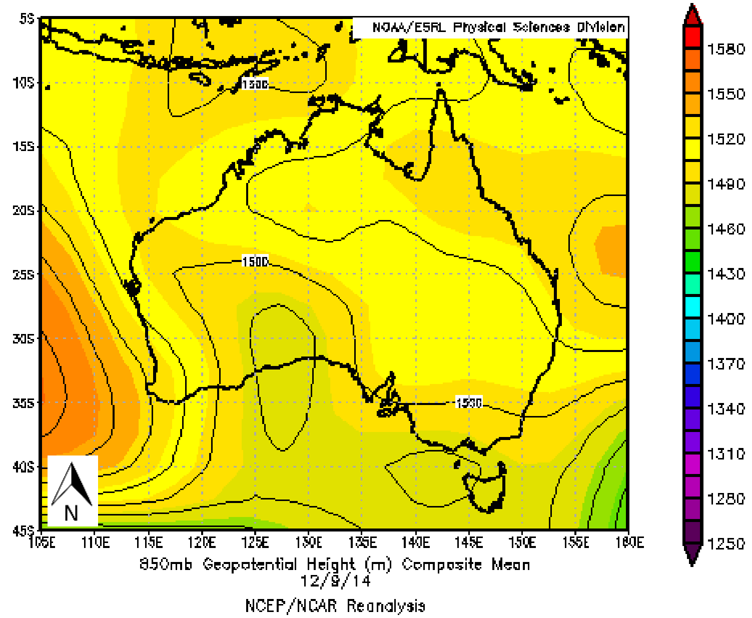
NOAA/ESRL Physical Sciences Division
850mb Geopotential Height (m) Composite Mean
12/9/14
NCEP/NCAR Reanalysis

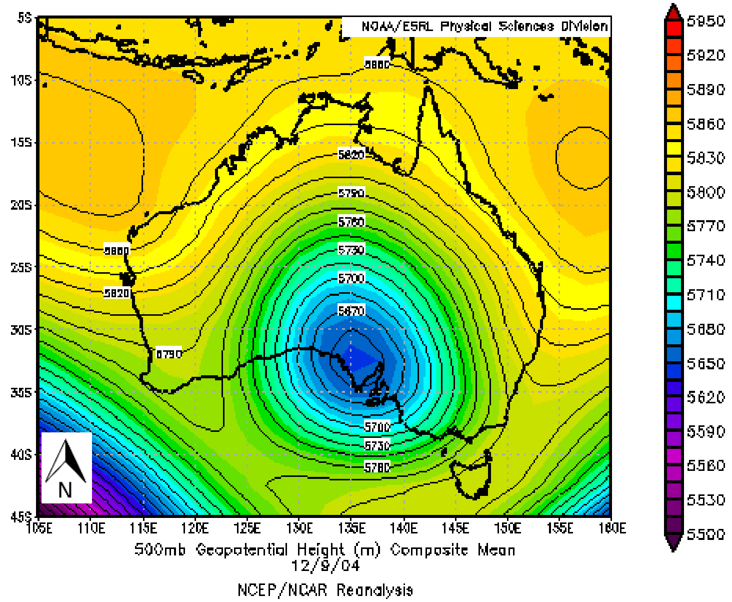
NOAA/ESRL Physical Sciences Division
500mb Geopotential Height (m) Composite Mean
12/9/04
NCEP/NCAR Reanalysis

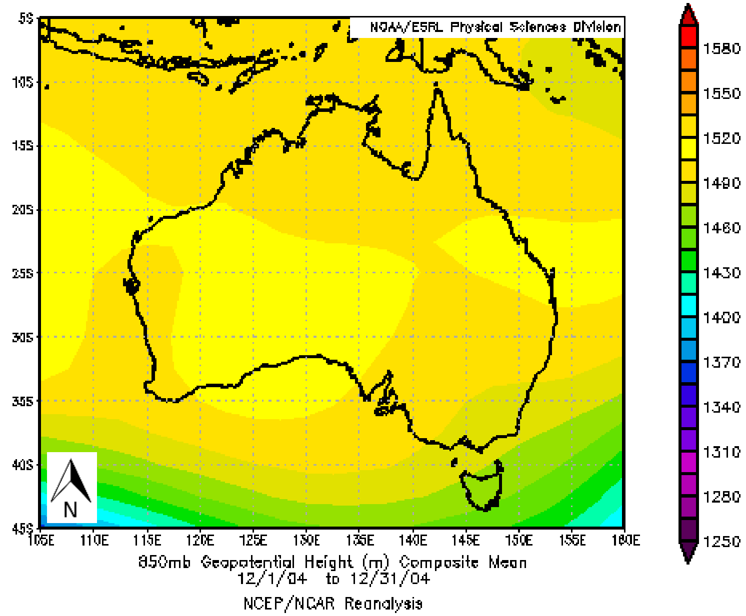
NOAA/ESRL Physical Sciences Division
850mb Geopotential Height (m) Composite Mean
12/1/04 to 12/31/04
NCEP/NCAR Reanalysis

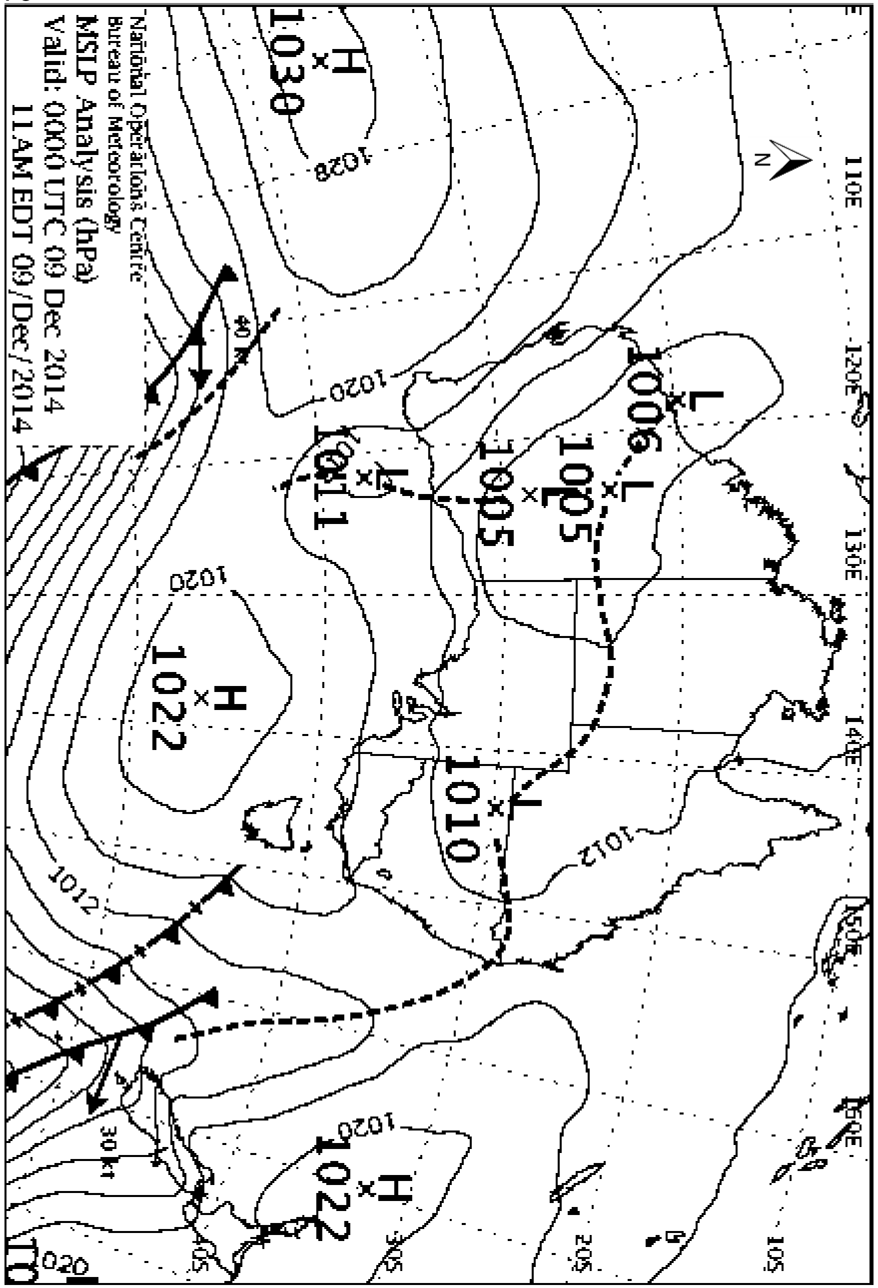
National Operations Centre
Bureau of Meteorology
MSLP Analysis (hPa)
Valid: 0000 UTC 09 Dec 2014
11AM EDT 09/Dec/2014

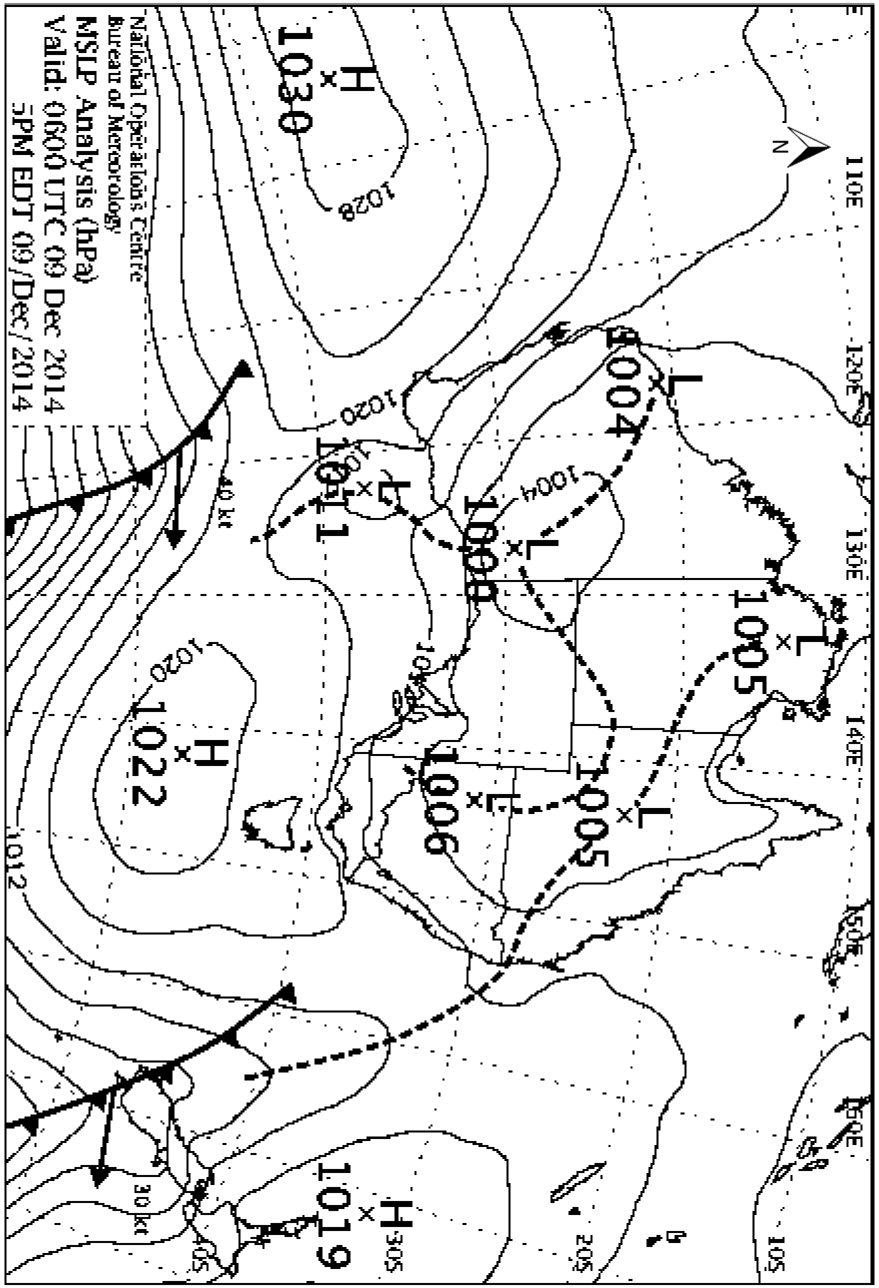
National Operations Centre
Bureau of Meteorology
MSLP Analysis (hPa)
Valid: 0600 UTC 09 Dec 2014
5PM EDT 09/Dec/2014

29/12/2013

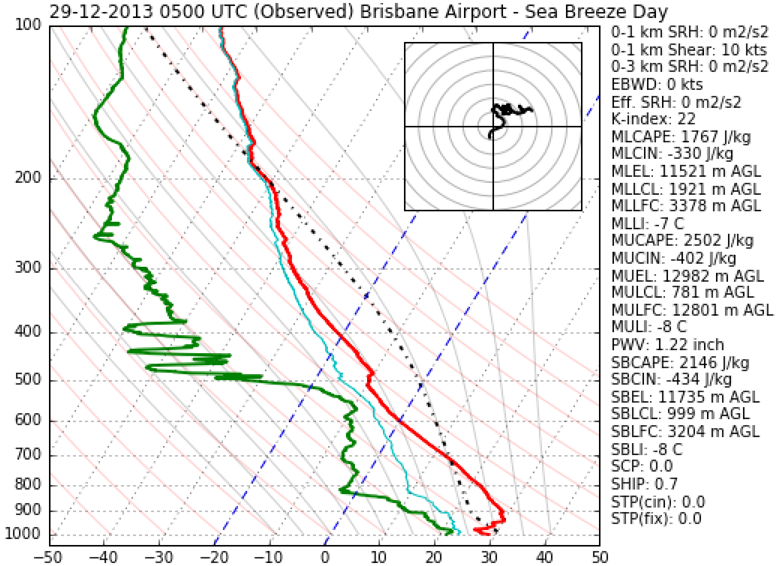
29-12-2013 0500 UTC (Observed) Brisbane Airport - Sea Breeze Day
0-1 km SRH: 0 m2/s2
0-1 km Shear: 10 kts
0-3 km SRH: 0 m2/s2
EBWD: 0 kts
Eff. SRH: 0 m2/s2
K-index: 22
MLCAPE: 1767 J/kg
MLCIN: -330 J/kg
MLEL: 11521 m AGL
MLLCL: 1921 m AGL
MLLFC: 3378 m AGL
MLLI: -7 C
MUCAPE: 2502 J/kg
MUCIN: -402 J/kg
MUEL: 12982 m AGL
MULCL: 781 m AGL
MULFC: 12801 m AGL
MULI: -8 C
PWV: 1.22 inch
SBCAPE: 2146 J/kg
SBCIN: -434 J/kg
SBEL: 11735 m AGL
SBLCL: 999 m AGL
SBLFC: 3204 m AGL
SBLI: -8 C
SCP: 0.0
SHIP: 0.7
STP(cin): 0.0
STP(fix): 0.0

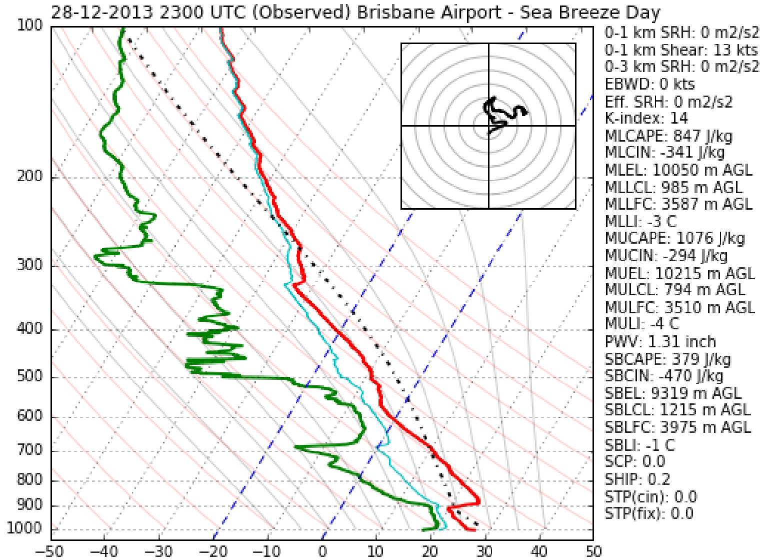
28-12-2013 2300 UTC (Observed) Brisbane Airport - Sea Breeze Day
0-1 km SRH: 0 m2/s2
0-1 km Shear: 13 kts
0-3 km SRH: 0 m2/s2
EBWD: 0 kts
Eff. SRH: 0 m2/s2
K-index: 14
MLCAPE: 847 J/kg
MLCIN: -341 J/kg
MLEL: 10050 m AGL
MLLCL: 985 m AGL
MLLFC: 3587 m AGL
MLLI: -3 C
MUCAPE: 1076 J/kg
MUCIN: -294 J/kg
MUEL: 10215 m AGL
MULCL: 794 m AGL
MULFC: 3510 m AGL
MULI: -4 C
PWV: 1.31 inch
SBCAPE: 379 J/kg
SBCIN: -470 J/kg
SBEL: 9319 m AGL
SBLCL: 1215 m AGL
SBLFC: 3975 m AGL
SBLI: -1 C
SCP: 0.0
SHIP: 0.2
STP(cin): 0.0
STP(fix): 0.0

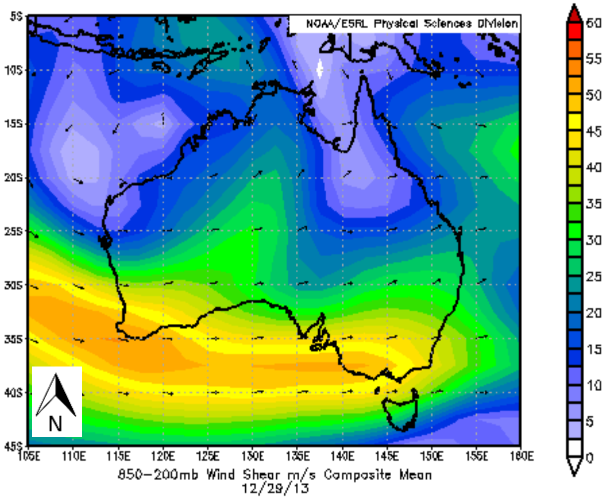
NOAA/ESRL Physical Sciences Division
N
850–200mb Wind Shear m/s Composite Mean
12/29/13

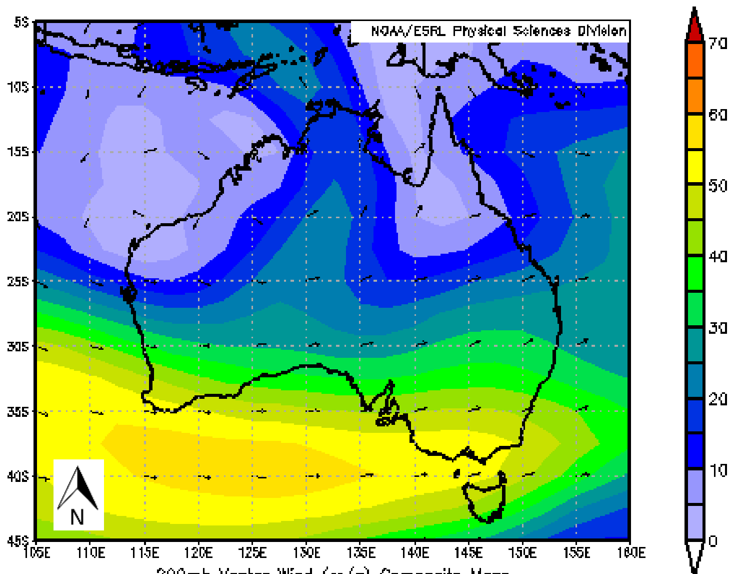

200mb Vector Wind (m/s) Composite Mean
12/29/13
NCEP/NCAR Reanalysis

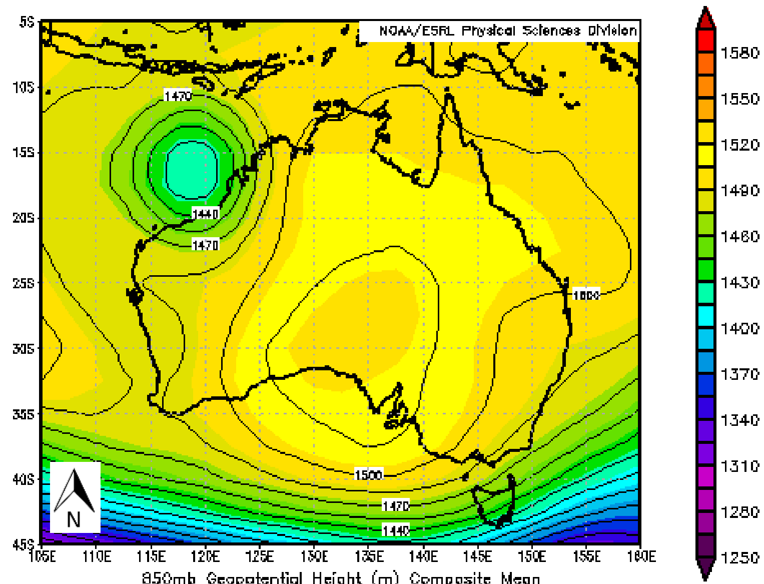

850mb Geopotential Height (m) Composite Mean
12/29/13

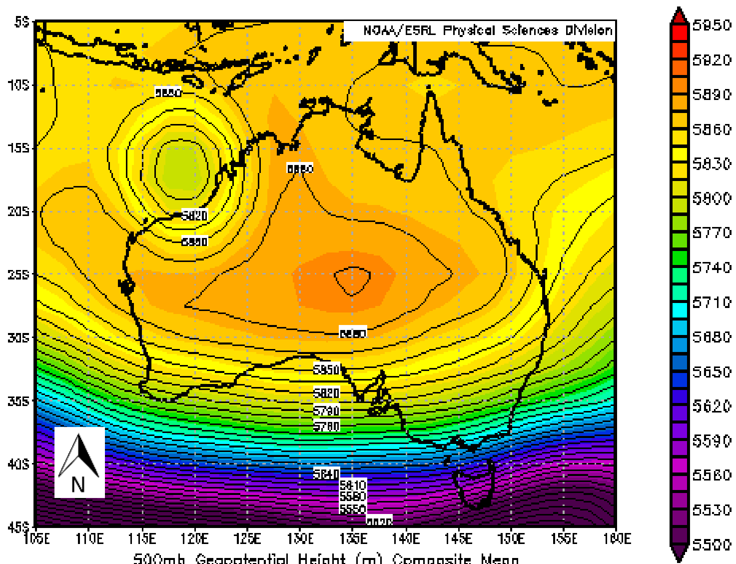

500mb Geopotential Height (m) Composite Mean
12/29/13
NCEP/NCAR Reanalysis

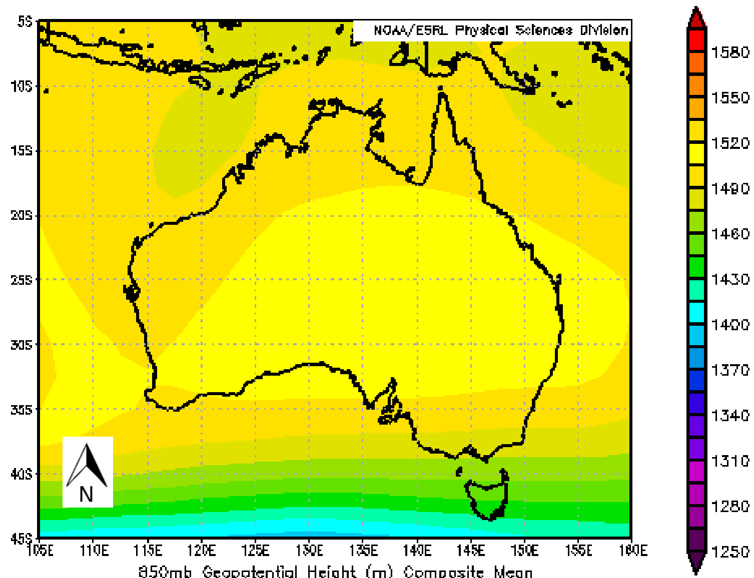

850mb Geopotential Height (m) Composite Mean
12/1/13 to 12/31/13
NCEP/NCAR Reanalysis

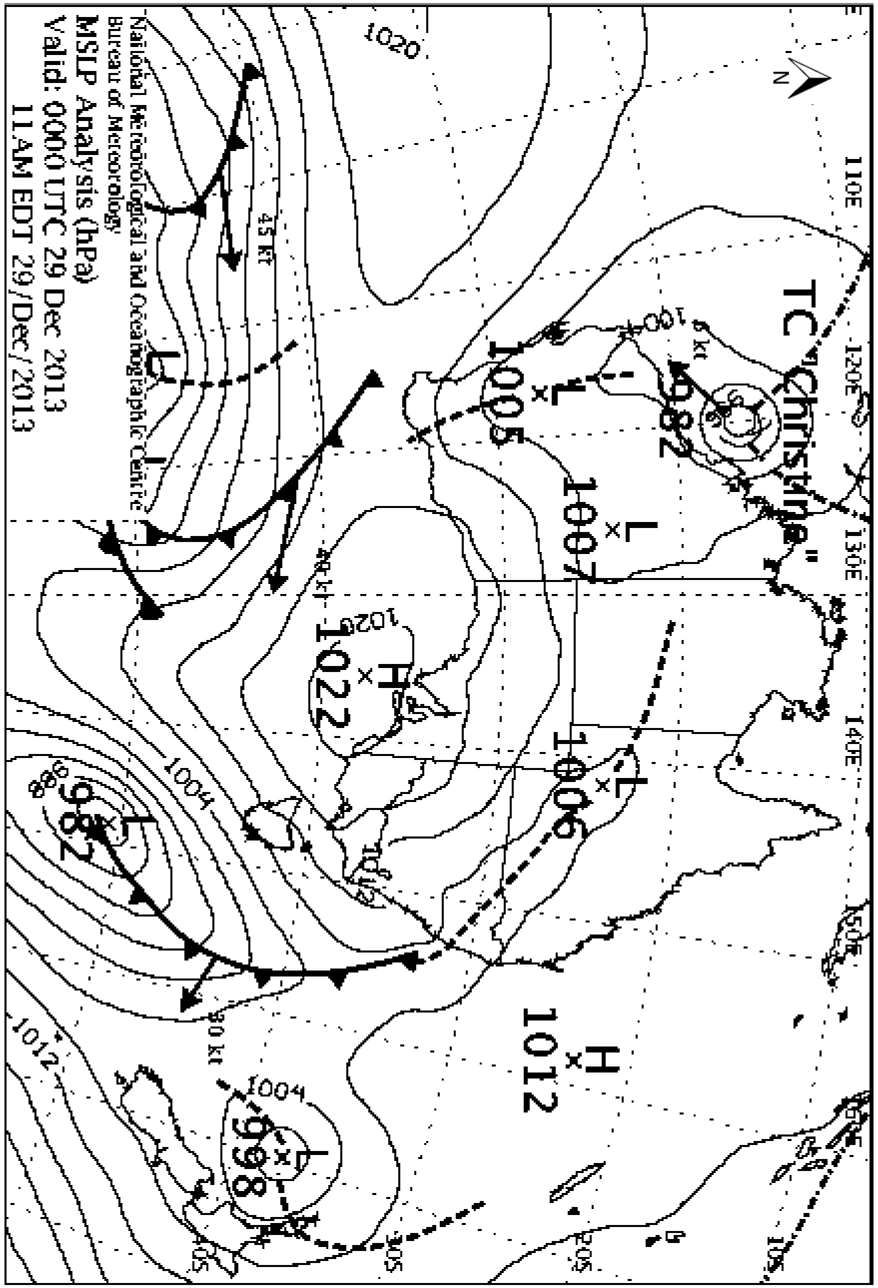
National Meteorological and Oceanographic Centre
Bureau of Meteorology
MSLP Analysis (hPa)
Valid: 0000 UTC 29 Dec 2013
11AM EDT 29/Dec/2013
TC "Christine"

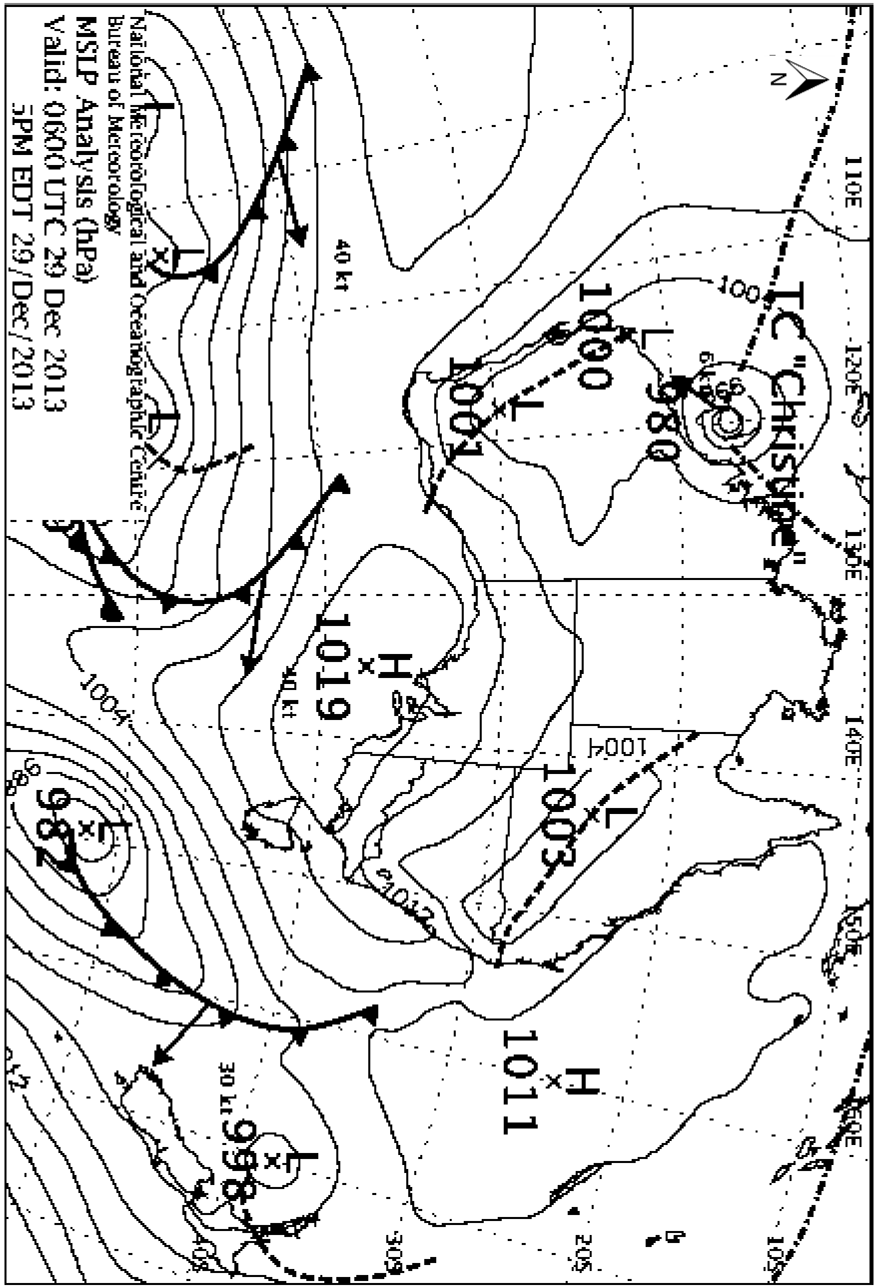
National Meteorological and Oceanographic Centre
Bureau of Meteorology
MSLP Analysis (hPa)
Valid: 0600 UTC 29 Dec 2013
5PM EDT 29/Dec/2013
TC "Christine"

16/12/2010

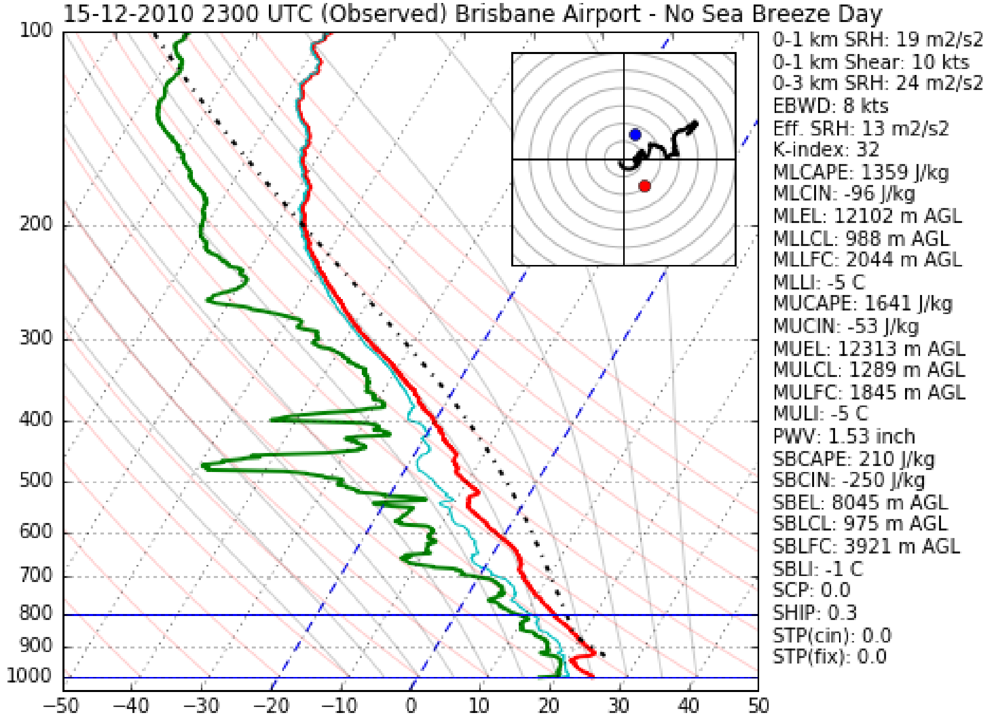
15-12-2010 2300 UTC (Observed) Brisbane Airport - No Sea Breeze Day
100
200
300
400
500
600
700
800
900
1000
−50 −40 −30 −20 −10 0 10 20 30 40 50
0-1 km SRH: 19 m2/s2
0-1 km Shear: 10 kts
0-3 km SRH: 24 m2/s2
EBWD: 8 kts
Eff. SRH: 13 m2/s2
K-index: 32
MLCAPE: 1359 J/kg
MLCIN: -96 J/kg
MLEL: 12102 m AGL
MLLCL: 988 m AGL
MLLFC: 2044 m AGL
MLLI: -5 C
MUCAPE: 1641 J/kg
MUCIN: -53 J/kg
MUEL: 12313 m AGL
MULCL: 1289 m AGL
MULFC: 1845 m AGL
MULI: -5 C
PWV: 1.53 inch
SBCAPE: 210 J/kg
SBCIN: -250 J/kg
SBEL: 8045 m AGL
SBLCL: 975 m AGL
SBLFC: 3921 m AGL
SBLI: -1 C
SCP: 0.0
SHIP: 0.3
STP(cin): 0.0
STP(fix): 0.0

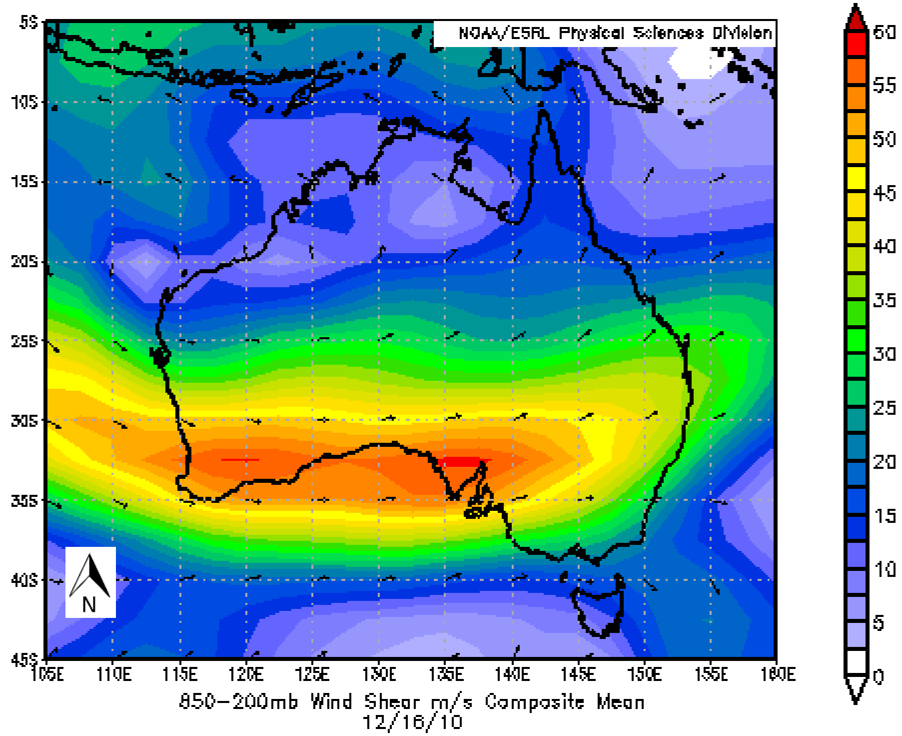
NOAA/ESRL Physical Sciences Division
5S
10S
15S
20S
25S
30S
35S
40S
45S
105E 110E 115E 120E 125E 130E 135E 140E 145E 150E 155E 160E
N
60
55
50
45
40
35
30
25
20
15
10
5
0
850–200mb Wind Shear m/s Composite Mean
12/16/10

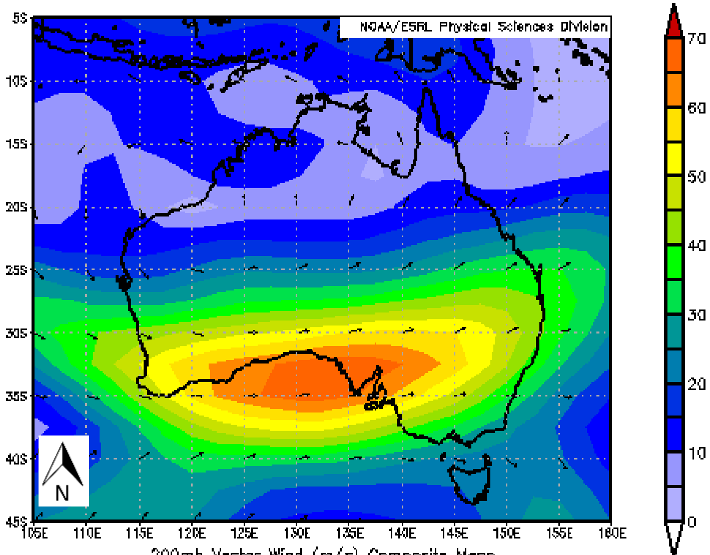

200mb Vector Wind (m/s) Composite Mean
12/16/10
NCEP/NCAR Reanalysis

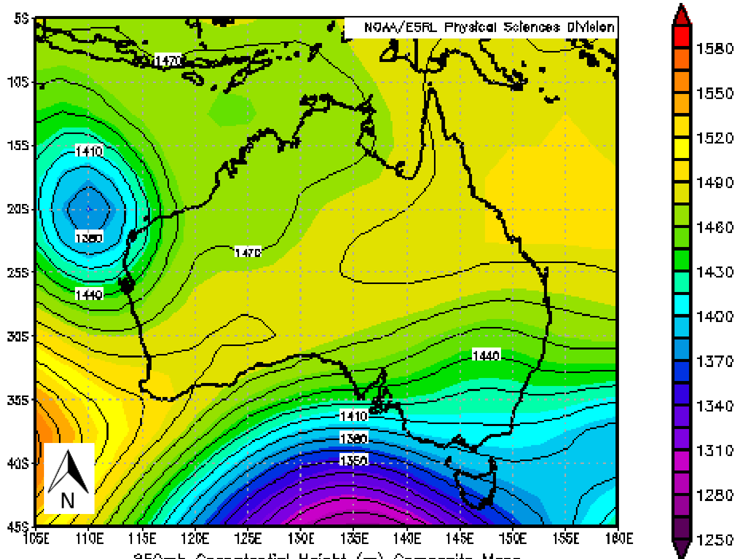

850mb Geopotential Height (m) Composite Mean
12/16/10
NCEP/NCAR Reanalysis

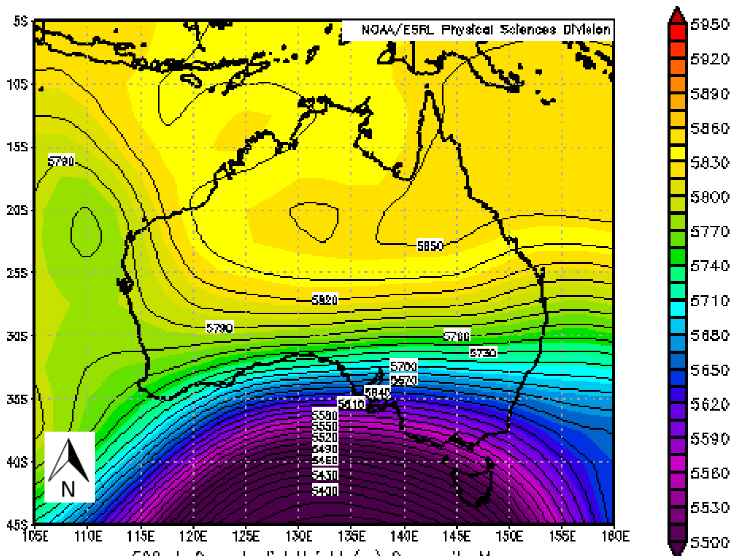

500mb Geopotential Height (m) Composite Mean
12/16/10
NCEP/NCAR Reanalysis

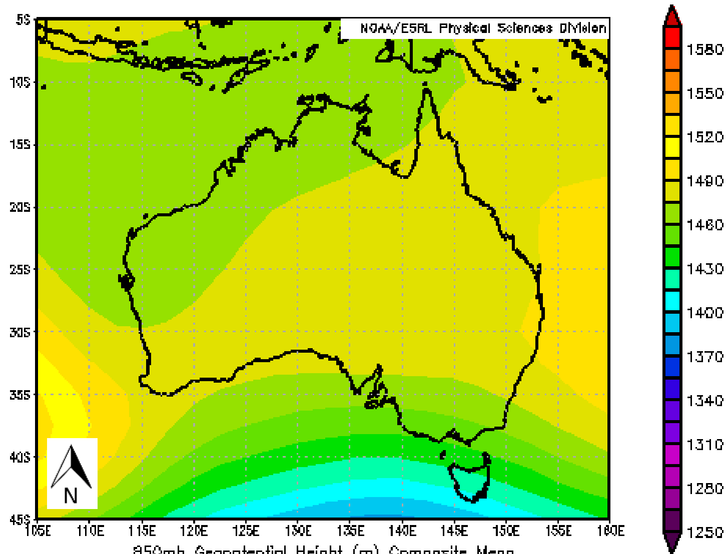

850mb Geopotential Height (m) Composite Mean
12/1/10 to 12/31/10
NCEP/NCAR Reanalysis

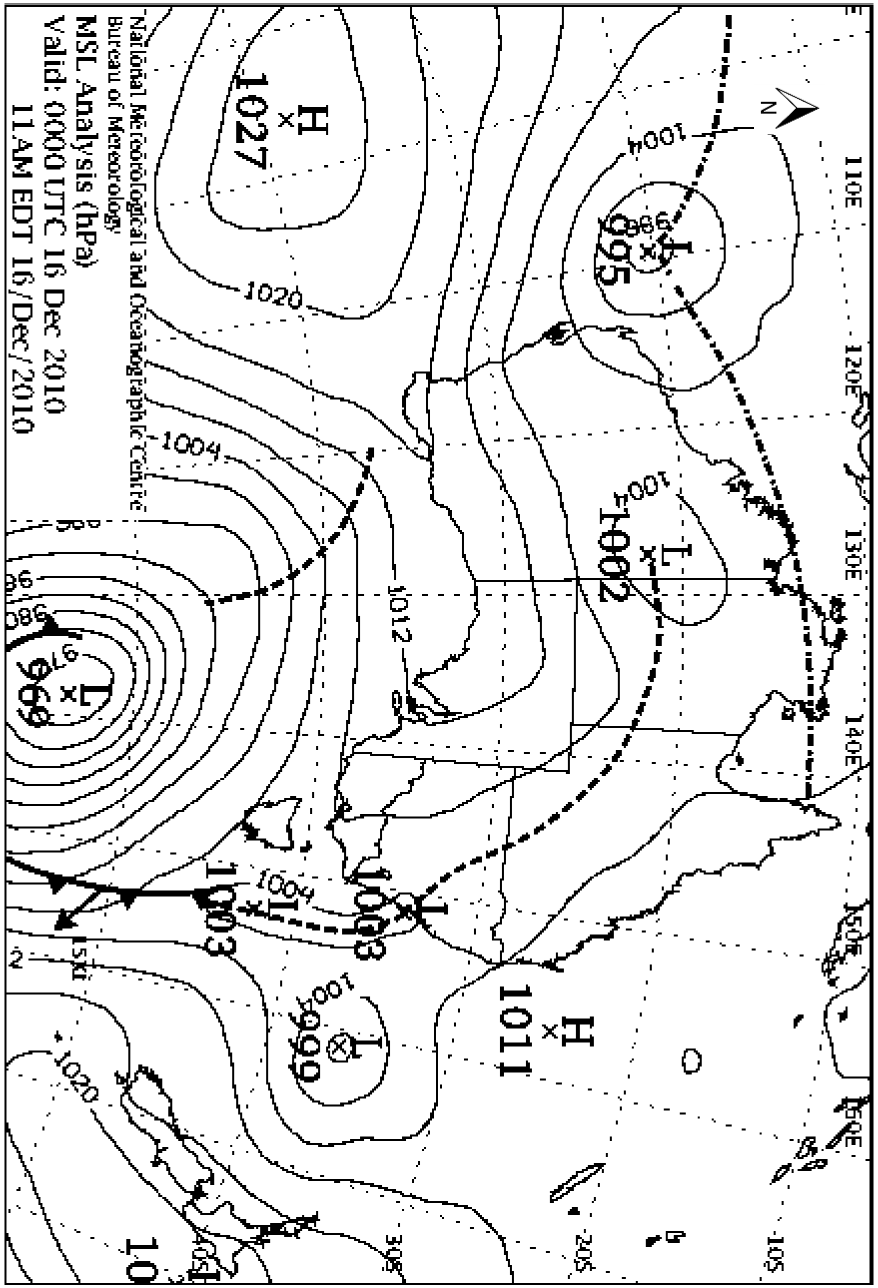
National Meteorological and Oceanographic Centre
Bureau of Meteorology
MSL Analysis (hPa)
Valid: 0000 UTC 16 Dec 2010
11AM EDT 16/Dec/2010

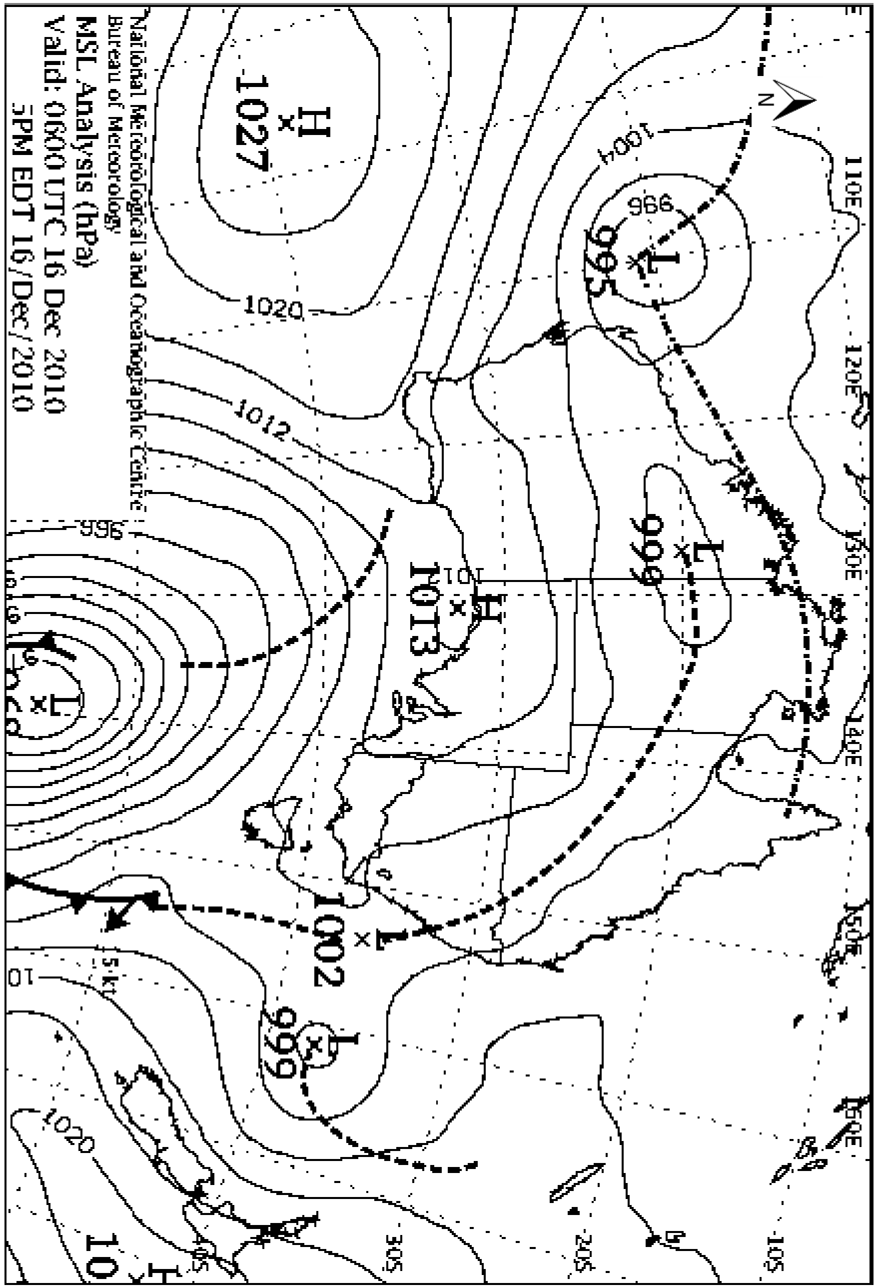
National Meteorological and Oceanographic Centre
Bureau of Meteorology
MSL Analysis (hPa)
Valid: 0600 UTC 16 Dec 2010
5PM EDT 16/Dec/2010

22/12/2009

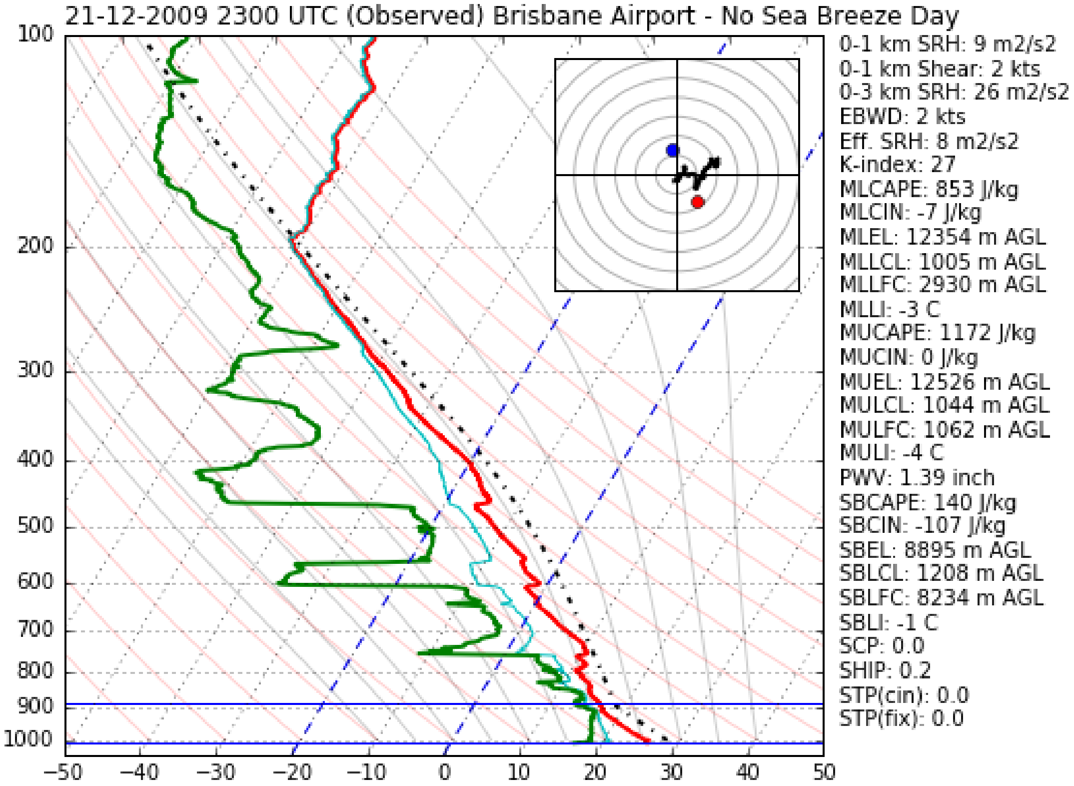
21-12-2009 2300 UTC (Observed) Brisbane Airport - No Sea Breeze Day
0-1 km SRH: 9 m2/s2
0-1 km Shear: 2 kts
0-3 km SRH: 26 m2/s2
EBWD: 2 kts
Eff. SRH: 8 m2/s2
K-index: 27
MLCAPE: 853 J/kg
MLCIN: -7 J/kg
MLEL: 12354 m AGL
MLLCL: 1005 m AGL
MLLFC: 2930 m AGL
MLLI: -3 C
MUCAPE: 1172 J/kg
MUCIN: 0 J/kg
MUEL: 12526 m AGL
MULCL: 1044 m AGL
MULFC: 1062 m AGL
MULI: -4 C
PWV: 1.39 inch
SBCAPE: 140 J/kg
SBCIN: -107 J/kg
SBEL: 8895 m AGL
SBLCL: 1208 m AGL
SBLFC: 8234 m AGL
SBLI: -1 C
SCP: 0.0
SHIP: 0.2
STP(cin): 0.0
STP(fix): 0.0
100
200
300
400
500
600
700
800
900
1000
−50
−40
−30
−20
−10
0
10
20
30
40
50

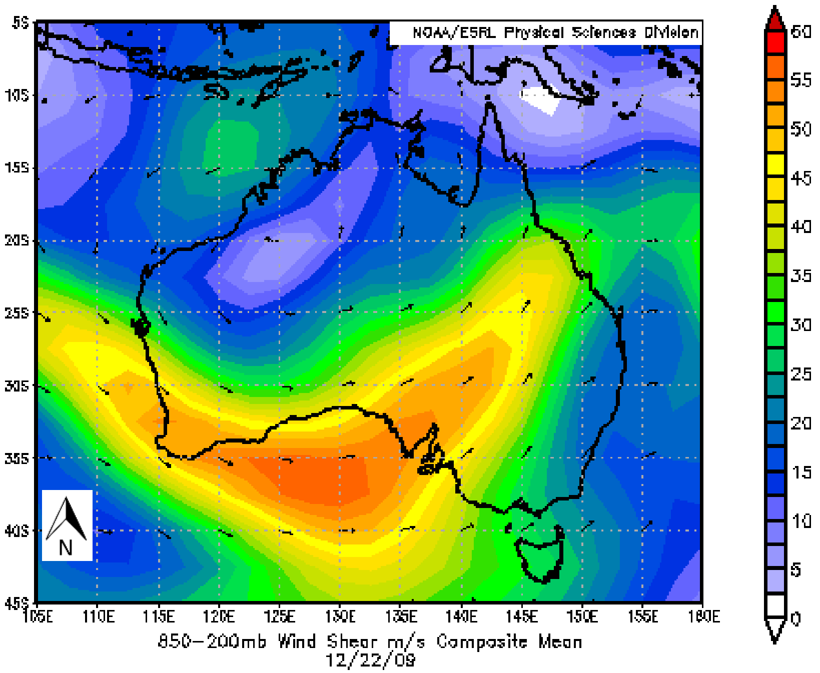
NOAA/ESRL Physical Sciences Division
N
850–200mb Wind Shear m/s Composite Mean
12/22/09

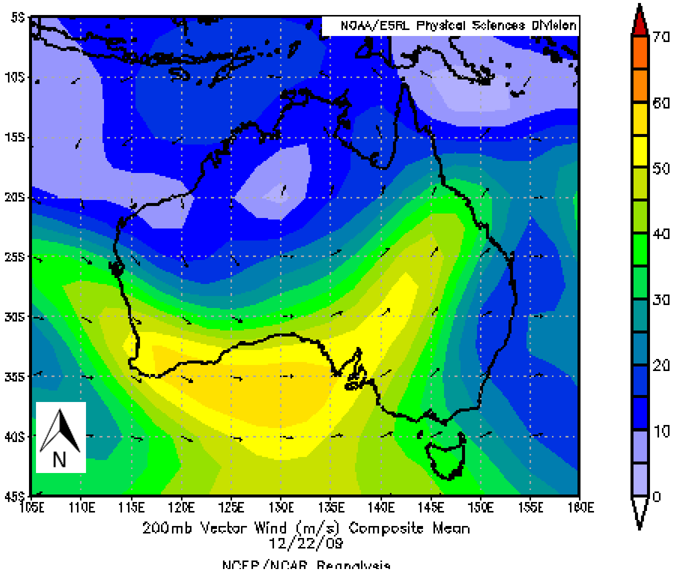
NOAA/ESRL Physical Sciences Division
200mb Vector Wind (m/s) Composite Mean
12/22/09
NCEP/NCAR Reanalysis
N

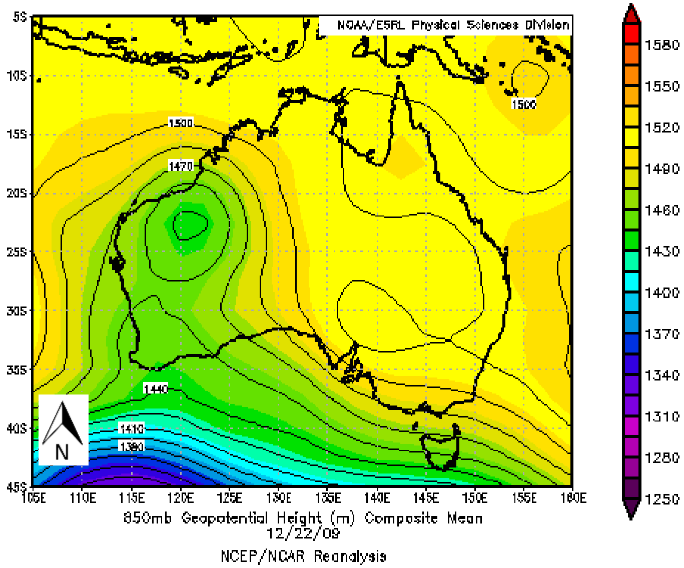
NOAA/ESRL Physical Sciences Division
850mb Geopotential Height (m) Composite Mean
12/22/09
NCEP/NCAR Reanalysis
N

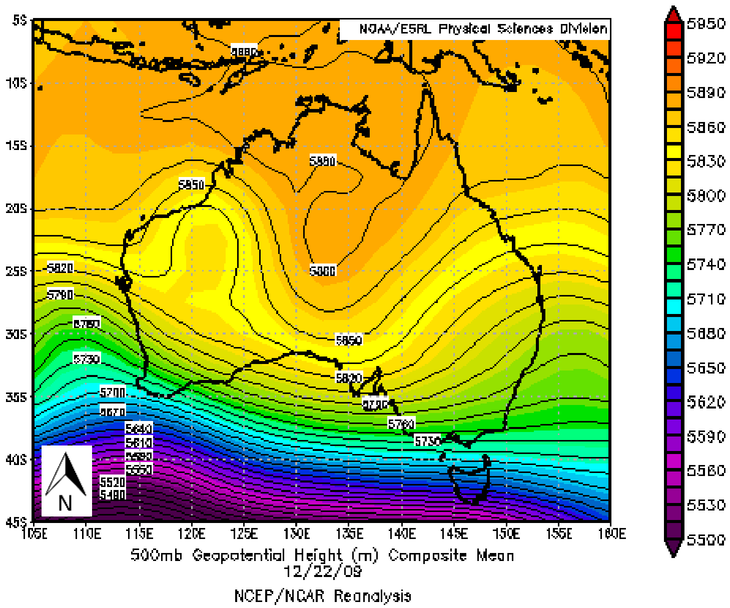
NOAA/ESRL Physical Sciences Division
500mb Geopotential Height (m) Composite Mean
12/22/09
NCEP/NCAR Reanalysis
N

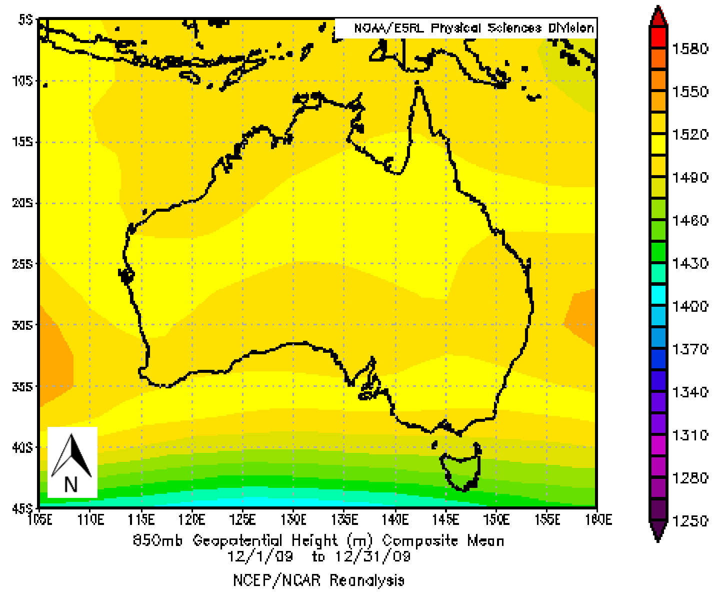
NOAA/ESRL Physical Sciences Division
850mb Geopotential Height (m) Composite Mean
12/1/09 to 12/31/09
NCEP/NCAR Reanalysis
N

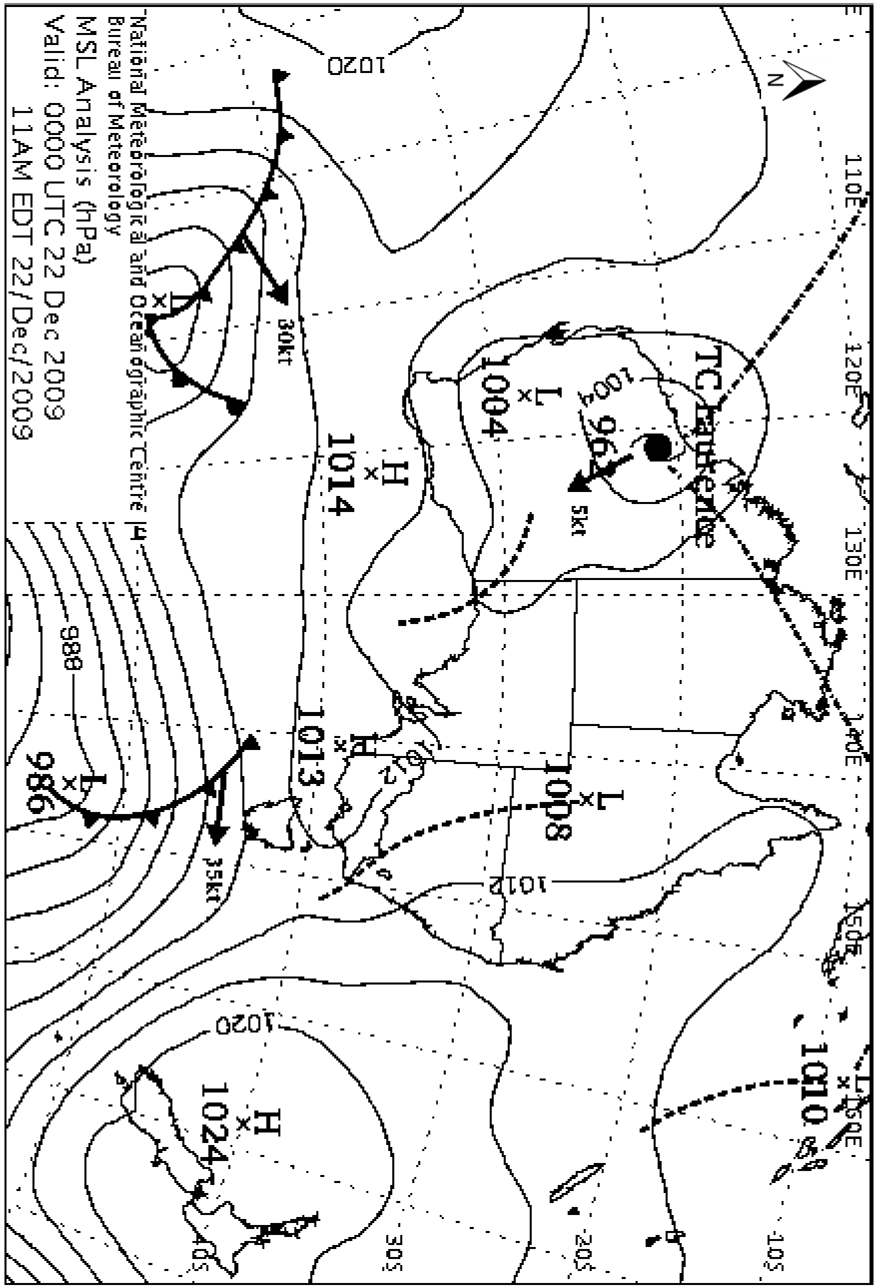
National Meteorological and Oceanographic Centre
Bureau of Meteorology
MSL Analysis (hPa)
Valid: 0000 UTC 22 Dec 2009
11AM EDT 22/Dec/2009
TC Laurence

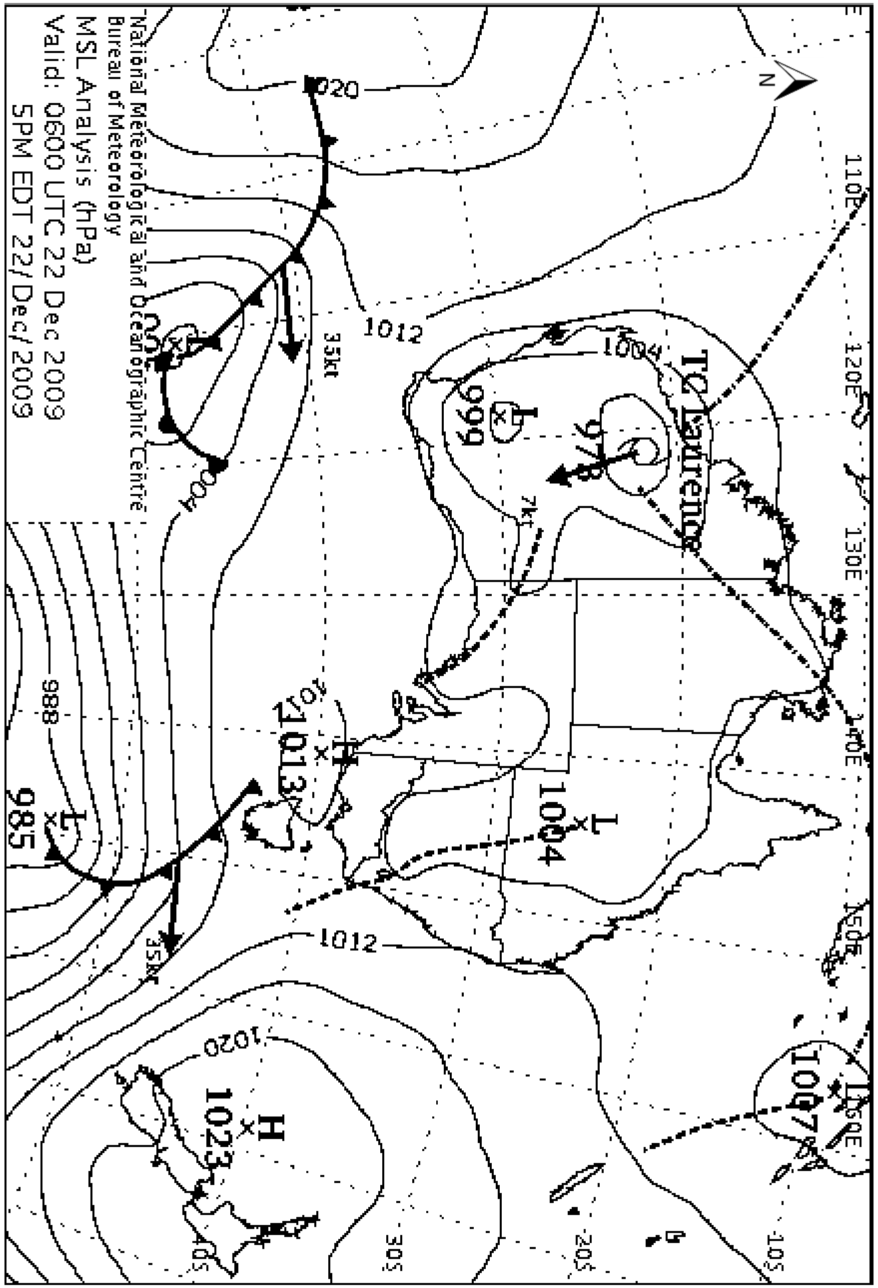
National Meteorological and Oceanographic Centre
Bureau of Meteorology
MSL Analysis (hPa)
Valid: 0600 UTC 22 Dec 2009
5PM EDT 22/Dec/2009
TC Laurence

13/12/2004

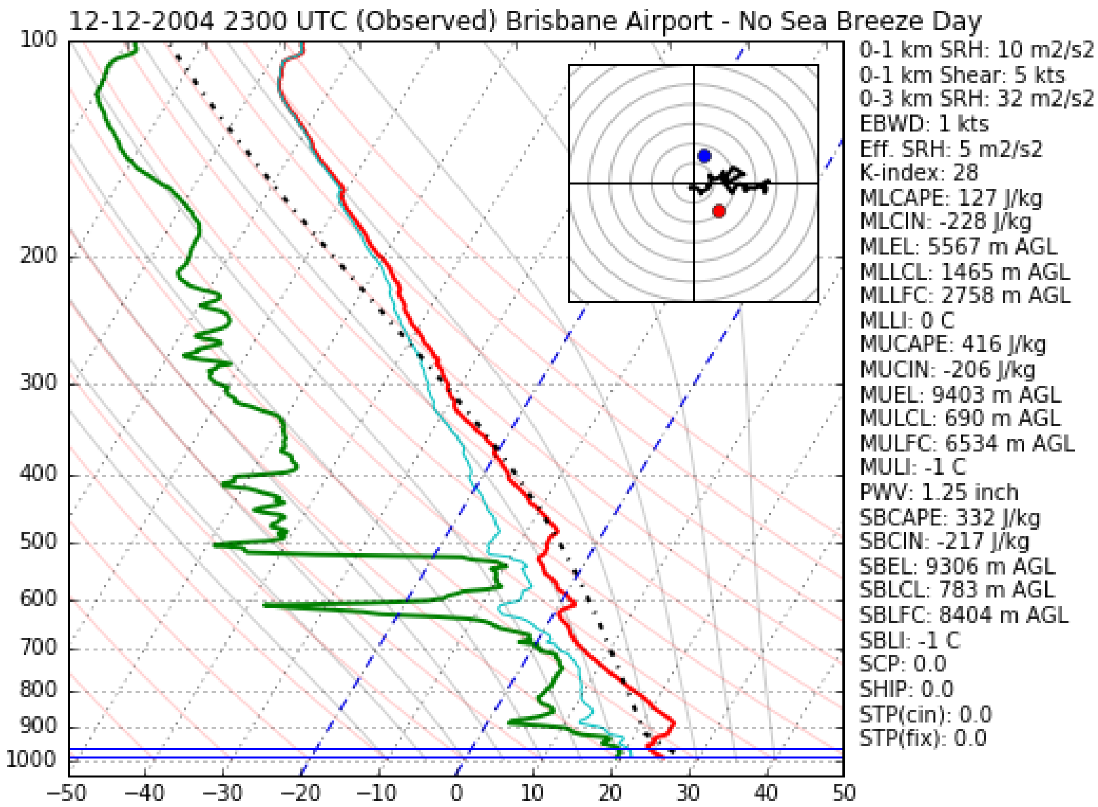
12-12-2004 2300 UTC (Observed) Brisbane Airport - No Sea Breeze Day
0-1 km SRH: 10 m2/s2
0-1 km Shear: 5 kts
0-3 km SRH: 32 m2/s2
EBWD: 1 kts
Eff. SRH: 5 m2/s2
K-index: 28
MLCAPE: 127 J/kg
MLCIN: -228 J/kg
MLEL: 5567 m AGL
MLLCL: 1465 m AGL
MLLFC: 2758 m AGL
MLLI: 0 C
MUCAPE: 416 J/kg
MUCIN: -206 J/kg
MUEL: 9403 m AGL
MULCL: 690 m AGL
MULFC: 6534 m AGL
MULI: -1 C
PWV: 1.25 inch
SBCAPE: 332 J/kg
SBCIN: -217 J/kg
SBEL: 9306 m AGL
SBLCL: 783 m AGL
SBLFC: 8404 m AGL
SBLI: -1 C
SCP: 0.0
SHIP: 0.0
STP(cin): 0.0
STP(fix): 0.0
100
200
300
400
500
600
700
800
900
1000
−50 −40 −30 −20 −10 0 10 20 30 40 50

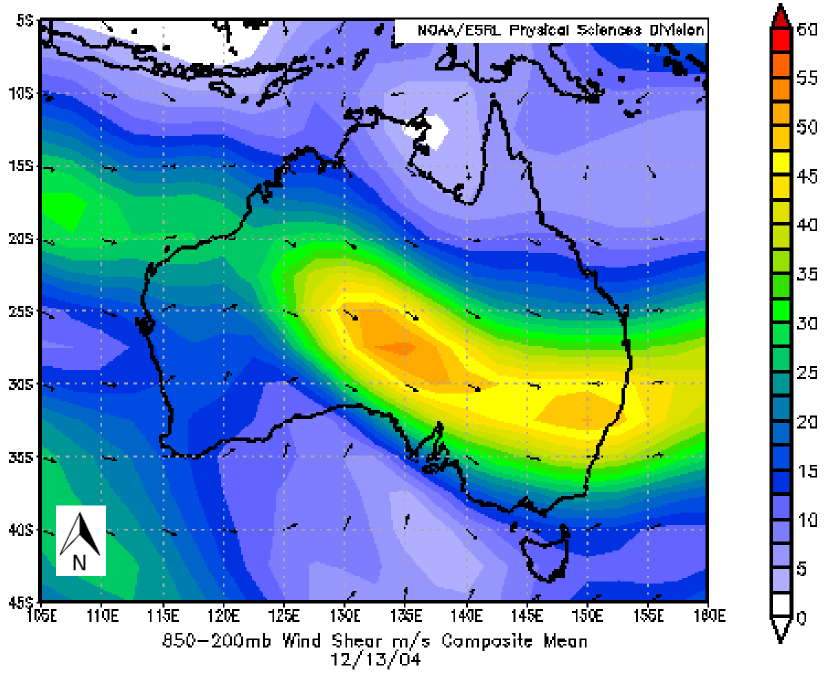
NOAA/ESRL Physical Sciences Division
5S
10S
15S
20S
25S
30S
35S
40S
45S
105E 110E 115E 120E 125E 130E 135E 140E 145E 150E 155E 160E
N
850–200mb Wind Shear m/s Composite Mean
12/13/04
60 55 50 45 40 35 30 25 20 15 10 5 0

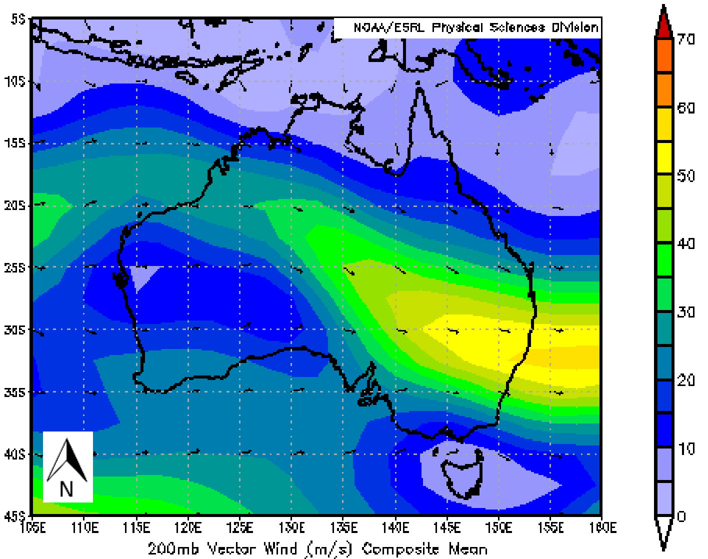

200mb Vector Wind (m/s) Composite Mean
12/13/04
NCEP/NCAR Reanalysis

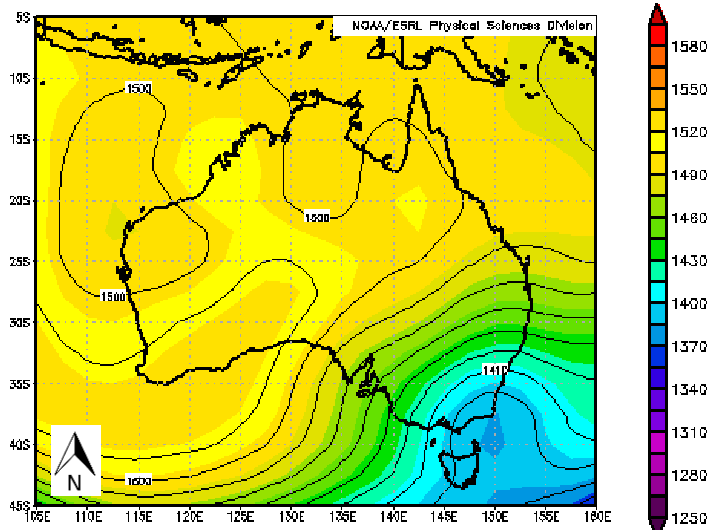

850mb Geopotential Height (m) Composite Mean
12/13/04
NCEP/NCAR Reanalysis

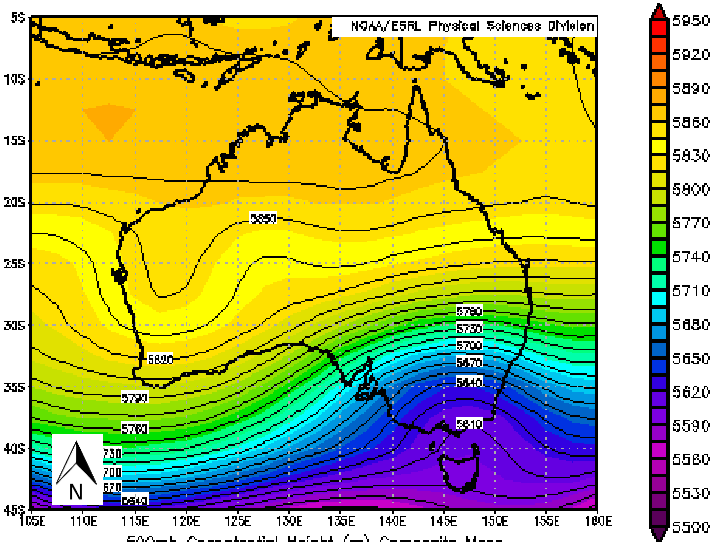

500mb Geopotential Height (m) Composite Mean
12/13/04
NCEP/NCAR Reanalysis

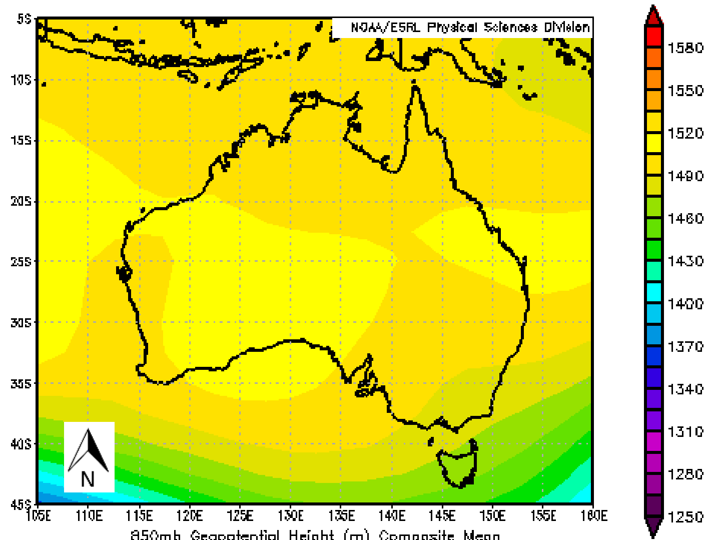

850mb Geopotential Height (m) Composite Mean
12/1/04 to 12/31/04
NCEP/NCAR Reanalysis

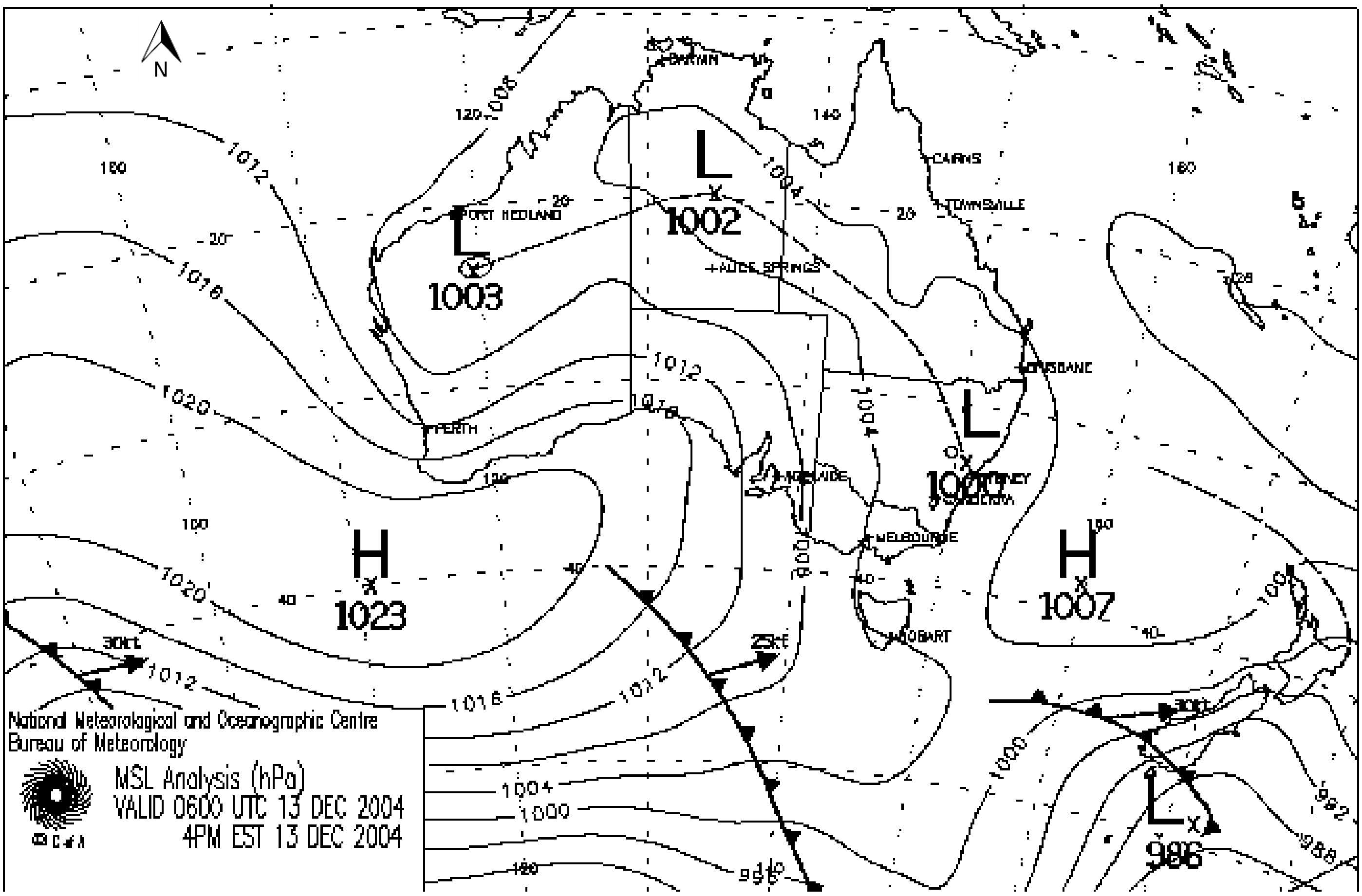
National Meteorological and Oceanographic Centre
Bureau of Meteorology
MSL Analysis (hPa)
VALID 0600 UTC 13 DEC 2004
4PM EST 13 DEC 2004
PERTH
PORT HEDLAND
DARWIN
ALICE SPRINGS
CAIRNS
TOWNSVILLE
BRISBANE
ADELAIDE
MELBOURNE
HOBART
SYDNEY
CANBERRA
H 1023
H 1007
L 1003
L 1002
L 986
30kt
25kt

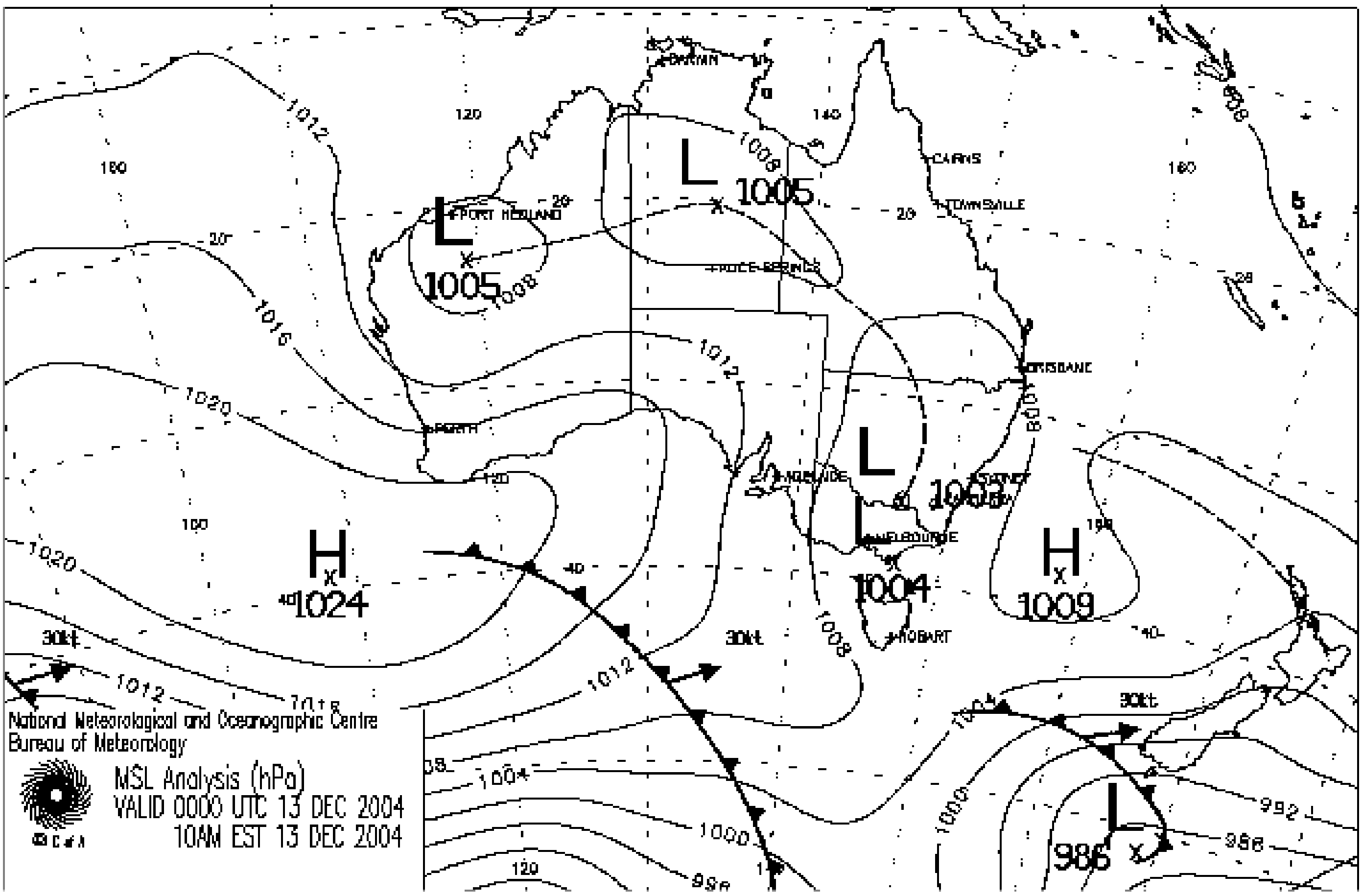
National Meteorological and Oceanographic Centre
Bureau of Meteorology
MSL Analysis (hPa)
VALID 0000 UTC 13 DEC 2004
10AM EST 13 DEC 2004
PERTH
PORT HEDLAND
DARWIN
ALICE SPRINGS
CAIRNS
TOWNSVILLE
BRISBANE
ADELAIDE
MELBOURNE
HOBART
SYDNEY
H 1024
H 1009
L 1005
L 1005
L 1004
L 986
30kt

Appendix 6: Scripts used to perform the analysis

6.5 Scripts created by the author

6.5.1 For implementing the algorithm of Soderholm et al. (2015)

To implement the algorithm of Soderholm et al. (2015) data were parsed through files that filtered the data, with data satisfying the algorithm criteria being accepted and passed to the next filter. Additional data analysis was also perfomed using Microsoft Excel.

6.5.1.1 Wind direction filter

```
import csv


with open("input", "rb") as input, open("output", "ab") as wanted,
open("discarded data", "ab") as unwanted:
    reader = csv.DictReader(input, delimiter=",", skipinitialspace=True)
    fieldnames = reader.fieldnames
    writer_wanted = csv.DictWriter(wanted, fieldnames, delimiter=",")
    writer_unwanted = csv.DictWriter(unwanted, fieldnames, delimiter=",")
    writer_wanted.writeheader()
    writer_unwanted.writeheader()

    for line_number, row in enumerate(reader):
        try:
            if 10.0 <= float(row["Wind (1 minute) direction in degrees
true"]) <= 110.0:
                writer_wanted.writerow(row)
            else:
                writer_unwanted.writerow(row)
        except:
            print "Failed to parse line", line_number
            print row
```

6.5.1.2 Wind speed filter

```
import csv


with open("input") as input, open("output", "wb") as wanted,
open("discarded data", "wb") as unwanted:
    reader = csv.DictReader(input, delimiter=",", skipinitialspace=True)
    fieldnames = reader.fieldnames
    writer_wanted = csv.DictWriter(wanted, fieldnames, delimiter=",")
    writer_unwanted = csv.DictWriter(unwanted, fieldnames, delimiter=",")
    writer_wanted.writeheader()
    writer_unwanted.writeheader()


    for line_number, row in enumerate(reader):
        try:
            if 0.0 <= float(row["Wind (1 minute) speed in km/h"]) <=
40.0:
                writer_wanted.writerow(row)
            else:
                writer_unwanted.writerow(row)
        except:
            print "Failed to parse line", line_number
            print row
```

6.5.1.3 Time filter

```
import csv


with open("input") as input, open("output", "wb") as wanted,
open("discarded data", "wb") as unwanted:
    reader = csv.DictReader(input, delimiter=",", skipinitialspace=True)
    fieldnames = reader.fieldnames
    writer_wanted = csv.DictWriter(wanted, fieldnames, delimiter=",")
    writer_unwanted = csv.DictWriter(unwanted, fieldnames, delimiter=",")
    writer_wanted.writeheader()
    writer_unwanted.writeheader()


    for line_number, row in enumerate(reader):
        try:
            if 11.0 <= float(row["HH24"]) <= 16.0:
                writer_wanted.writerow(row)
            else:
                writer_unwanted.writerow(row)
        except:
            print "Failed to parse line", line_number
            print row
```

6.5.1.4 Duration filter

```
import csv
import datetime

minimum_delta = datetime.timedelta(hours=2)
input_fn = r"X:\weatherresults\sea_breeze_dates_2000_2011.csv"
wanted_fn =
r"X:\weatherresults\sea_breeze_dates_2000_2011_time_filtered.csv"

with open(input_fn, "rb") as input, open(wanted_fn, "wb") as wanted:
    reader = csv.DictReader(input, delimiter=",", skipinitialspace=True)
    fieldnames = reader.fieldnames
    writer_wanted = csv.DictWriter(wanted, fieldnames, delimiter=",")
    try:
        while 1:
            try:
                begin = next(reader)
                begin_dt = datetime.datetime(
                    year=int(begin["Year Month Day Hour Minutes in
YYYY"]),
                    month=int(begin["MM"]), day=int(begin["DD"]),
                    hour=int(begin["HH24"]))
                end = next(reader)
                end_dt = datetime.datetime(
                    year=int(end["Year Month Day Hour Minutes in YYYY"]),
                    month=int(end["MM"]), day=int(end["DD"]),
                    hour=int(end["HH24"]))
                if end_dt - begin_dt > minimum_delta:
                    writer_wanted.writerow(begin)
                    writer_wanted.writerow(end)
            except ValueError as e:
                print "Failed to parse line", line_number
                print row
    except StopIteration:
        pass
```

6.6 For implementing the increasing onshore flow algorithm

To implement the increasing onshore flow algorithm, the gradient of increase in wind speed was calculated using the numpy package of python. Additional data analysis was also perfomed using Microsoft Excel.

6.6.1 Gradient script

```
import glob
import pandas as pd
import numpy as np
from datetime import datetime

for file in glob.glob('X:/brisbaneweatherdata2015/*.txt'):
    df = pd.read_csv(file)

    for col in ['Wind (1 minute) speed in km/h',
                'Wind (1 minute) direction in degrees true']:
        df[col] = pd.to_numeric(df[col], errors='coerce')
        mask = pd.notnull(df[col])
        df = df.loc[mask]

    for date, group in df.groupby([' Year Month Day Hour Minutes in
YYYY', 'MM', 'DD']):
        morning_data = group[group.HH24.between(12, 15)]
        if len(morning_data) == 0: continue
        gradient, intercept = np.polyfit(morning_data['HH24'],
morning_data['Wind (1 minute) speed in km/h'], 1)
        wind_direction = np.average(morning_data['Wind (1 minute)
direction in degrees true'])
        if gradient < 0:
            print("{0:%d, %b %Y}, {1:.2f},
{2:.2f},".format(datetime(*date), gradient, wind_direction))
```

6.7 Scripts created by Halbert (2015) and modified by the author

The SHARPpy package created by Halbert (2015) was used to calculate various indices of atmospheric stability and was used to produce skew-t plots. Additional data analysis was also perfomed using Microsoft Excel.

6.7.1 Calculating indices of atmospheric stability (and writing to csv)

```
import sharppy
import sharppy.sharptab.profile as profile
import sharppy.sharptab.interp as interp
import sharppy.sharptab.winds as winds
import sharppy.sharptab.utils as utils
import sharppy.sharptab.params as params
import sharppy.sharptab.thermo as thermo
import numpy as np
from StringIO import StringIO
import glob
import os



os.chdir('X:/ybbn_snding_data-oax/ybbn_snding_data-oax')
for file in glob.glob("*.oax"):
    spc_file = open(file, 'r').read()
    newName = file[6:8] + '-' + file[4:6] + '-' + file[0:4] + ' ' +
file[8:12]
    try:
        def parseSPC(spc_file):
            ## read in the file
            data = np.array([l.strip() for l in spc_file.split('\n')])
              ## necessary index points
            title_idx = np.where( data == '%TITLE%')[0][0]
            start_idx = np.where( data == '%RAW%' )[0] + 1
            finish_idx = np.where( data == '%END%')[0]
             ## create the plot title
```

```
data_header = data[title_idx + 1].split()
            location = data_header[0]
            time = data_header[1][:11]

            ## put it all together for StringIO
            full_data = '\n'.join(data[start_idx : finish_idx][:])
            sound_data = StringIO( full_data )
            ## read the data into arrays
            p, h, T, Td, wdir, wspd = np.genfromtxt( sound_data,
delimiter=',', comments="%", unpack=True )
            return p, h, T, Td, wdir, wspd


        pres, hght, tmpc, dwpc, wdir, wspd = parseSPC(spc_file)


        prof = profile.create_profile(profile='default', pres=pres,
hght=hght, tmpc=tmpc, \
                                    dwpc=dwpc, wspd=wspd,
wdir=wdir, missing=-9999, strictQC=True)
        msl_hght = prof.hght[prof.sfc] # Grab the surface height value
        #print "SURFACE HEIGHT (m MSL):",msl_hght
        agl_hght = interp.to_agl(prof, msl_hght) # Converts to AGL
        #print "SURFACE HEIGHT (m AGL):", agl_hght
        msl_hght = interp.to_msl(prof, agl_hght) # Converts to MSL
        #print "SURFACE HEIGHT (m MSL):",msl_hght
        sfcpcl = params.parcelx( prof, flag=1 ) # Surface Parcel
        fcstpcl = params.parcelx( prof, flag=2 ) # Forecast Parcel
        mupcl = params.parcelx( prof, flag=3 ) # Most-Unstable Parcel
        mlpcl = params.parcelx( prof, flag=4 ) # 100 mb Mean Layer Parcel
        print ("Cape", mupcl.bplus, ",") # J/kg
        print ("CIN", mupcl.bminus, ",") # J/kg
        print ("LCL", mupcl.lclhght, ",") # meters AGL
        print ("LFC", mupcl.lfchght, ",") # meters AGL
        print ("EL", mupcl.elhght, ",") # meters AGL
        print ("LI", mupcl.li5, ",") # C
        sfc = prof.pres[prof.sfc]
```

```
    p3km = interp.pres(prof, interp.to_msl(prof, 3000.))
            p6km = interp.pres(prof, interp.to_msl(prof, 6000.))
            p1km = interp.pres(prof, interp.to_msl(prof, 1000.))
            mean_3km = winds.mean_wind(prof, pbot=sfc, ptop=p3km)
            sfc_6km_shear = winds.wind_shear(prof, pbot=sfc, ptop=p6km)
            sfc_3km_shear = winds.wind_shear(prof, pbot=sfc, ptop=p3km)
            sfc_1km_shear = winds.wind_shear(prof, pbot=sfc, ptop=p1km)
            print utils.comp2vec(mean_3km[0], mean_3km[1])[1], ","
            print utils.comp2vec(sfc_6km_shear[0], sfc_6km_shear[1])[1], ","
            srwind = params.bunkers_storm_motion(prof)
            #print "Bunker's Storm Motion (right-mover) [deg,kts]:",
utils.comp2vec(srwind[0], srwind[1])
            #print "Bunker's Storm Motion (left-mover) [deg,kts]:",
utils.comp2vec(srwind[2], srwind[3])
            srh3km = winds.helicity(prof, 0, 3000., stu = srwind[0], stv =
srwind[1])
            srh1km = winds.helicity(prof, 0, 1000., stu = srwind[0], stv =
srwind[1])
            print srh3km[0], ","
            stp_fixed = params.stp_fixed(sfcpcl.bplus, sfcpcl.lclhght,
srh1km[0], utils.comp2vec(sfc_6km_shear[0], sfc_6km_shear[1])[1])
            ship = params.ship(prof)
            eff_inflow = params.effective_inflow_layer(prof)
            ebot_hght = interp.to_agl(prof, interp.hght(prof, eff_inflow[0]))
            etop_hght = interp.to_agl(prof, interp.hght(prof, eff_inflow[1]))
            print ebot_hght, ","
            print etop_hght, ","
            effective_srh = winds.helicity(prof, ebot_hght, etop_hght, stu =
srwind[0], stv = srwind[1])
            print effective_srh[0], ","
            ebwd = winds.wind_shear(prof, pbot=eff_inflow[0],
ptop=eff_inflow[1])
            ebwspd = utils.mag( ebwd[0], ebwd[1] )
            print ("Effective bulk wind difference", ebwspd, ",a")
            scp = params.scp(mupcl.bplus, effective_srh[0], ebwspd)
            stp_cin = params.stp_cin(mlpcl.bplus, effective_srh[0], ebwspd,
```

```
mlpcl.lclhght, mlpcl.bminus)
        #print "Supercell Composite Parameter:", scp
        #print "Significant Tornado Parameter (w/CIN):", stp_cin
        #print "Significant Tornado Parameter (fixed):", stp_fixed
        print newName
        f =
open('X:/alldayssatmosphericvaluesallvariablesworkingfile.txt','a')
        f.write(newName)
        f.write(",")
        a=str(mupcl.bplus)
        f.write(a)
        f.write(",")
        b=str(mupcl.bminus)
        f.write(b)
        f.write(",")
        c=str(mupcl.lclhght)
        f.write(c)
        f.write(",")
        n=str(mupcl.lfchght)
        f.write(n)
        f.write(",")
        d=str(mupcl.elhght)
        f.write(d)
        f.write(",")
        e=str(mupcl.li5)
        f.write(e)
        f.write(",")
        g=str(utils.comp2vec(mean_3km[0], mean_3km[1])[1])
        f.write(g)
        f.write(",")
        h=str(utils.comp2vec(sfc_6km_shear[0], sfc_6km_shear[1])[1])
        f.write(h)
        f.write(",")
        i=str(srh3km[0])
```

```
             f.write(i)
            f.write(",")
            j=str(ebot_hght)
            f.write(j)
            f.write(",")
            k=str(etop_hght)
            f.write(k)
            f.write(",")
            l=str(effective_srh[0])
            f.write(l)
            f.write(",")
            m=str(ebwspd)
            f.write(m)
            f.write(",a")
            f.close
        except Exception:
            pass
```

6.7.2 Producing skew-t plots

```
import sharppy
import sharppy.sharptab.profile as profile
import sharppy.sharptab.interp as interp
import sharppy.sharptab.winds as winds
import sharppy.sharptab.utils as utils
import sharppy.sharptab.params as params
import sharppy.sharptab.thermo as thermo
import numpy as np
from StringIO import StringIO
import glob
import os
import matplotlib.pyplot as plt
from matplotlib.axes import Axes
import matplotlib.transforms as transforms
import matplotlib.axis as maxis
import matplotlib.spines as mspines
import matplotlib.path as mpath
from matplotlib.projections import register_projection

os.chdir('X:/seabreezestormdays')
for file in glob.glob("*.oax"):
    spc_file = open(file, 'r').read()
    newName = file[6:8] + '-' + file[4:6] + '-' + file[0:4] + ' ' + 
file[8:12] +  ' UTC (Observed) Brisbane Airport - Sea Breeze Day'
    try:
        def parseSPC(spc_file):
            ## read in the file
            data = np.array([l.strip() for l in spc_file.split('\n')])

            ## necessary index points
            title_idx = np.where( data == '%TITLE%')[0][0]
            start_idx = np.where( data == '%RAW%' )[0] + 1
            finish_idx = np.where( data == '%END%')[0]
```

```
## create the plot title
          data_header = data[title_idx + 1].split()
          location = data_header[0]
          time = data_header[1][:11]

          ## put it all together for StringIO
          full_data = '\n'.join(data[start_idx : finish_idx][:])
          sound_data = StringIO( full_data )

          ## read the data into arrays
          p,  h,  T,  Td,  wdir,  wspd  =  np.genfromtxt(  sound_data,
delimiter=',', comments="%", unpack=True )

          return p, h, T, Td, wdir, wspd

      pres, hght, tmpc, dwpc, wdir, wspd = parseSPC(spc_file)

      prof   =   profile.create_profile(profile='default',   pres=pres,
hght=hght, tmpc=tmpc, \
                                  dwpc=dwpc,         wspd=wspd,
wdir=wdir, missing=-9999, strictQC=True)
      msl_hght = prof.hght[prof.sfc] # Grab the surface height value
      print "SURFACE HEIGHT (m MSL):",msl_hght
      agl_hght = interp.to_agl(prof, msl_hght) # Converts to AGL
      print "SURFACE HEIGHT (m AGL):", agl_hght
      msl_hght = interp.to_msl(prof, agl_hght) # Converts to MSL
      print "SURFACE HEIGHT (m MSL):",msl_hght
      sfcpcl = params.parcelx( prof, flag=1 ) # Surface Parcel
      fcstpcl = params.parcelx( prof, flag=2 ) # Forecast Parcel
      mupcl = params.parcelx( prof, flag=3 ) # Most-Unstable Parcel
      mlpcl = params.parcelx( prof, flag=4 ) # 100 mb Mean Layer Parcel
      sfc = prof.pres[prof.sfc]
      p3km = interp.pres(prof, interp.to_msl(prof, 3000.))
      p6km = interp.pres(prof, interp.to_msl(prof, 6000.))
      p1km = interp.pres(prof, interp.to_msl(prof, 1000.))
```

```
    mean_3km = winds.mean_wind(prof, pbot=sfc, ptop=p3km)
    sfc_6km_shear = winds.wind_shear(prof, pbot=sfc, ptop=p6km)
    sfc_3km_shear = winds.wind_shear(prof, pbot=sfc, ptop=p3km)
    sfc_1km_shear = winds.wind_shear(prof, pbot=sfc, ptop=p1km)
    print "0-3 km Pressure-Weighted Mean Wind (kt):", utils.comp2vec(mean_3km[0], mean_3km[1])[1]
    print "0-6 km Shear (kt):", utils.comp2vec(sfc_6km_shear[0], sfc_6km_shear[1])[1]
    srwind = params.bunkers_storm_motion(prof)
    print "Bunker's Storm Motion (right-mover) [deg,kts]:", utils.comp2vec(srwind[0], srwind[1])
    print "Bunker's Storm Motion (left-mover) [deg,kts]:", utils.comp2vec(srwind[2], srwind[3])
    srh3km = winds.helicity(prof, 0, 3000., stu = srwind[0], stv = srwind[1])
    srh1km = winds.helicity(prof, 0, 1000., stu = srwind[0], stv = srwind[1])
    print "0-3 km Storm Relative Helicity [m2/s2]:",srh3km[0]
    stp_fixed = params.stp_fixed(sfcpcl.bplus, sfcpcl.lclhght, srh1km[0], utils.comp2vec(sfc_6km_shear[0], sfc_6km_shear[1])[1])
    ship = params.ship(prof)
    eff_inflow = params.effective_inflow_layer(prof)
    ebot_hght = interp.to_agl(prof, interp.hght(prof, eff_inflow[0]))
    etop_hght = interp.to_agl(prof, interp.hght(prof, eff_inflow[1]))
    print "Effective Inflow Layer Bottom Height (m AGL):", ebot_hght
    print "Effective Inflow Layer Top Height (m AGL):", etop_hght
    effective_srh = winds.helicity(prof, ebot_hght, etop_hght, stu = srwind[0], stv = srwind[1])
    print "Effective Inflow Layer SRH (m2/s2):", effective_srh[0]
    ebwd = winds.wind_shear(prof, pbot=eff_inflow[0], ptop=eff_inflow[1])
    ebwspd = utils.mag( ebwd[0], ebwd[1] )
    print "Effective Bulk Wind Difference:", ebwspd
    scp = params.scp(mupcl.bplus, effective_srh[0], ebwspd)
    stp_cin = params.stp_cin(mlpcl.bplus, effective_srh[0], ebwspd, mlpcl.lclhght, mlpcl.bminus)
```

```
    print "Supercell Composite Parameter:", scp
  print "Significant Tornado Parameter (w/CIN):", stp_cin
  print "Significant Tornado Parameter (fixed):", stp_fixed
  indices = {'SBCAPE': [int(sfcpcl.bplus), 'J/kg'],\
             'SBCIN': [int(sfcpcl.bminus), 'J/kg'],\
             'SBLCL': [int(sfcpcl.lclhght), 'm AGL'],\
             'SBLFC': [int(sfcpcl.lfchght), 'm AGL'],\
             'SBEL': [int(sfcpcl.elhght), 'm AGL'],\
             'SBLI': [int(sfcpcl.li5), 'C'],\
             'MLCAPE': [int(mlpcl.bplus), 'J/kg'],\
             'MLCIN': [int(mlpcl.bminus), 'J/kg'],\
             'MLLCL': [int(mlpcl.lclhght), 'm AGL'],\
             'MLLFC': [int(mlpcl.lfchght), 'm AGL'],\
             'MLEL': [int(mlpcl.elhght), 'm AGL'],\
             'MLLI': [int(mlpcl.li5), 'C'],\
             'MUCAPE': [int(mupcl.bplus), 'J/kg'],\
             'MUCIN': [int(mupcl.bminus), 'J/kg'],\
             'MULCL': [int(mupcl.lclhght), 'm AGL'],\
             'MULFC': [int(mupcl.lfchght), 'm AGL'],\
             'MUEL': [int(mupcl.elhght), 'm AGL'],\
             'MULI': [int(mupcl.li5), 'C'],\
             '0-1 km SRH': [int(srh1km[0]), 'm2/s2'],\
             '0-1 km Shear': [int(utils.comp2vec(sfc_1km_shear[0],
sfc_1km_shear[1])[1]), 'kts'],\
             '0-3 km SRH': [int(srh3km[0]), 'm2/s2'],\
             'Eff. SRH': [int(effective_srh[0]), 'm2/s2'],\
             'EBWD': [int(ebwspd), 'kts'],\
             'PWV': [round(params.precip_water(prof), 2), 'inch'],\
             'K-index': [int(params.k_index(prof)), ''],\
             'STP(fix)': [round(stp_fixed, 1), ''],\
             'SHIP': [round(ship, 1), ''],\
             'SCP': [round(scp, 1), ''],\
             'STP(cin)': [round(stp_cin, 1), '']}
```

```
# Set the parcel trace to be plotted as the Most-Unstable parcel.
        pcl = mupcl

        # Create a new figure. The dimensions here give a good aspect
ratio
        fig = plt.figure(figsize=(6.5875, 6.2125))
        ax = fig.add_subplot(111, projection='skewx')
        ax.grid(True)

        pmax = 1000
        pmin = 10
        dp = -10
        presvals = np.arange(int(pmax), int(pmin)+dp, dp)

        # plot the moist-adiabats
        for t in np.arange(-10,45,5):
            tw = []
            for p in presvals:
                tw.append(thermo.wetlift(1000., t, p))
            ax.semilogy(tw, presvals, 'k-', alpha=.2)

        def thetas(theta, presvals):
            return  ((theta  +  thermo.ZEROCNK)  /  (np.power((1000.  /
presvals),thermo.ROCP))) - thermo.ZEROCNK

        # plot the dry adiabats
        for t in np.arange(-50,110,10):
            ax.semilogy(thetas(t, presvals), presvals, 'r-', alpha=.2)

        plt.title(newName, fontsize=12, loc='left')
        # Plot the data using normal plotting functions, in this case
using
        # log scaling in Y, as dicatated by the typical meteorological
plot
        ax.semilogy(prof.tmpc,  prof.pres,  'r',  lw=2)  #  Plot  the
temperature profile
```

```
            ax.semilogy(prof.wetbulb, prof.pres, 'c-') # Plot the wetbulb
profile
            ax.semilogy(prof.dwpc, prof.pres, 'g', lw=2) # plot the dewpoint
profile
            ax.semilogy(pcl.ttrace, pcl.ptrace, 'k-.', lw=2) # plot the
parcel trace
            # An example of a slanted line at constant X
            l = ax.axvline(0, color='b', linestyle='--')
            l = ax.axvline(-20, color='b', linestyle='--')

            # Plot the effective inflow layer using blue horizontal lines
            ax.axhline(eff_inflow[0], color='b')
            ax.axhline(eff_inflow[1], color='b')

            #plt.barbs(10*np.ones(len(prof.pres)), prof.pres, prof.u, prof.v)
            # Disables the log-formatting that comes with semilogy
            ax.yaxis.set_major_formatter(plt.ScalarFormatter())
            ax.set_yticks(np.linspace(100,1000,10))
            ax.set_ylim(1050,100)
            ax.xaxis.set_major_locator(plt.MultipleLocator(10))
            ax.set_xlim(-50,50)

            # List the indices within the indices dictionary on the side of
the plot.
            string = ''
            for key in np.sort(indices.keys()):
                string = string + key + ': ' + str(indices[key][0]) + ' ' +
indices[key][1] + '\n'
            plt.text(1.02, 1, string, verticalalignment='top',
transform=plt.gca().transAxes)

            # Draw the hodograph on the Skew-T.
            # TAS 2015-4-16: hodograph doesn't plot for some reason ...
            ax2 = plt.axes([.625,.625,.25,.25])
            below_12km = np.where(interp.to_agl(prof, prof.hght) < 12000)[0]
```

```
                u_prof = prof.u[below_12km]
            v_prof = prof.v[below_12km]
            ax2.plot(u_prof[~u_prof.mask], v_prof[~u_prof.mask], 'k-', lw=2)
            ax2.get_xaxis().set_visible(False)
            ax2.get_yaxis().set_visible(False)
            for i in range(10,90,10):
                # Draw the range rings around the hodograph.
                circle = plt.Circle((0,0),i,color='k',alpha=.3, fill=False)
                ax2.add_artist(circle)
            ax2.plot(srwind[0], srwind[1], 'ro') # Plot Bunker's Storm motion
right mover as a red dot
            ax2.plot(srwind[2], srwind[3], 'bo') # Plot Bunker's Storm motion
left mover as a blue dot

            ax2.set_xlim(-60,60)
            ax2.set_ylim(-60,60)
            ax2.axhline(y=0, color='k')
            ax2.axvline(x=0, color='k')
            plt.savefig('X:/' + newName + '.png', bbox_inches='tight')
            plt.show()
        except Exception:
            pass
```